NTNU – Trondheim
Norwegian University of
Science and Technology

Gold(I) Catalyzed Tandem Cyclization Reactions with Propargyl Acetals

Morten Christian Hogsnes

Chemical Engineering and Biotechnology
Submission date: June 2013
Supervisor: Anne Fiksdahl, IKJ

Norwegian University of Science and Technology
Department of Chemistry

NTNU
Norwegian University of
Science and Technology

Gold(I) catalyzed tandem cyclization reactions with propargyl acetals

Conducted by

Morten Hogsnes

Chemical Engineering and Biotechnology
June 2013
Supervisor: Professor Anne Fiksdahl, IKJ

Norwegian University of Science and Technology
Department of chemistry

Declaration

I hereby declare that the presented work in this master's thesis has been conducted individually. The study has been performed in accordance with the rules and regulations for the integrated master's degree in industrial chemistry and biotechnology (Master of Science degree, 5 years) at the Norwegian University of Science and technology (NTNU). The work has been conducted from February 2013 to June 2013.

Trondheim, June 22th, 2013

Morten Hogsnes

Preface

The presented work has been performed at the Department of Chemistry, Norwegian University of Science and technology (NTNU) from February 2013 until June 2013.

I would like to thank my supervisor, Professor Anne Fiksdahl, for accepting me as a part of her research group and letting me get knowledge in the field of gold chemistry. I would also thank her for her guidance and help throughout my thesis.

I am grateful to PhD student, Melanie Siah, for all the help and advice she gave me both in the laboratory and with solving the stereochemistry of our new molecules. She also contributed to the good atmosphere in the laboratory. I would also like to thank post doc. Naseem Iqbal for his help in the lab.

Thank you very much for providing MS results, Susana Gonzales, and Roger Aarvik for bringing solvents and equipment needed in the lab. Thank you, Oddbjørn Sæther for guidance with NMR devices.

Abstract

The main goal of this thesis has been to further explore gold(I) catalyzed cyclization reactions including propargyl acetals. Gold(I) catalysts have a strong affinity to triple bonds, and alkyne-gold complexes are readily formed.

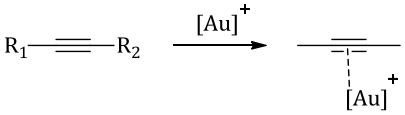

Both propargyl esters and acetals have previously been investigated in gold(I) catalyzed reactions. These propargylic substrates undergo intramolecular rearrangements to form gold carbenoid intermediates **IVa-b**, which exhibit strong electrophilic character and are activated for nucleophillic attacks.

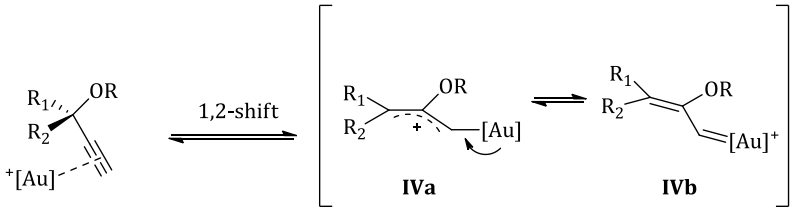

Propargyl esters have previously proven to undergo gold(I) catalyzed [2+1] cyclization reactions with vinyl esters and amides while propargyl acetals have shown to undergo gold(I) catalyzed [3+2] cyclization reactions with the same substrates. The difference in chemoselectivity is due to the electronic properties of the OR-groups in the gold carbenoid intermediates **IVa-b**.

Propargyl acetals have proven to be more reactive than propargyl esters and thus new reactions including these species were investigated further. Propargyl acetals **5a-c** were synthesized in acid catalyzed reactions between propargyl alcohols **3a-c** and 1-methoxy-2-propene. Non-commercial propargyl alcohols **3b-c** were formed in a Grignard reaction with benzylic aldehydes **1a-b**.

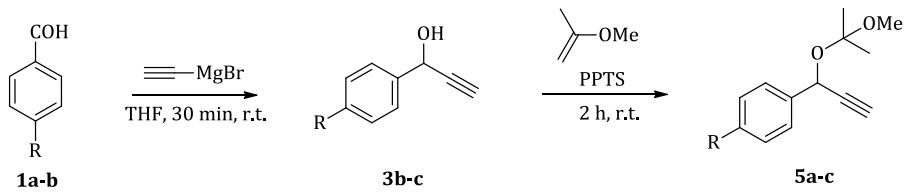

1-Phenylprop-1-yne **6** does not exhibit great nucleophilicity, but in the presence of gold(I) activated propargyl acetals, it has shown to readily undergo cyclization reactions.

In this thesis, propargyl acetals **5a-d** were treated with 1-phenylprop-1-yne **6** in gold(I) catalyzed reactions to readily form different cyclization products **7a-c, 8a-b** and **10a-d** by new tandem cyclization reactions.

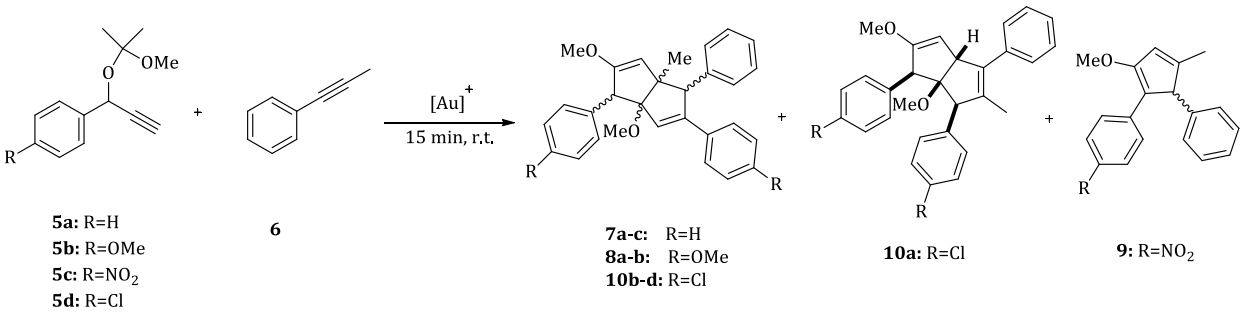

5a: R=H
5b: R=OMe
5c: R=NO_2
5d: R=Cl

6

7a-c: R=H
8a-b: R=OMe
10b-d: R=Cl

10a: R=Cl

9: R=NO_2

Propargyl acetals **5a** and **5d** provided approximately the same product compositions, respectively products **7a-c** and **10b-d**, with each fraction yielding 3-12%. Propargyl acetal **5d** gave one additional product **10a** which was isolated in 7% yield. Product **10a** was generated by following a different reaction mechanism than for the formation of **10b-d**.

The reaction with propargyl acetal **5b** was more regio- and stereospecific as it provided one major product **8a** in 27% yield. Additionally, another stereoisomer **8b** was obtained in 5% yield.

Propargyl acetal **5c** did not provide any tandem cyclization products, but by following a known [3+2] cycloaddition, product **9** was formed in 15% yield.

Possible reaction mechanisms have been proposed for the formation of **7a-c, 8a-b, 10b-d** and **10a** respectively. All products **7-10** were characterized by 1D and 2D NMR experiments, IR and MS. NOESY experiments were of great importance when distinguishing diastereomers.

Sammendrag

Hovedmålet med denne masteroppgaven har vært å utforske nye gullkatalyserte reaksjoner med propargylacetaler. Gull(I)katalysatorer har sterk affinitet til trippelbindinger, og alkyn-gullkomplekser dannes svært raskt.

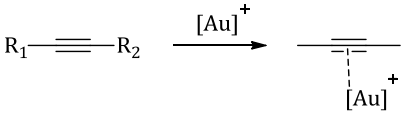

Både propargylestere og -acetaler har tidligere blitt forsket på i gull(I)katalyserte reaksjoner. Disse propargylsubstratene gjennomfører intramolekulære omleiringer for å danne gullkarbenoid-komplekser. Disse kompleksene har en sterk elektrofil karakter og er aktivert for nukleofile angrep.

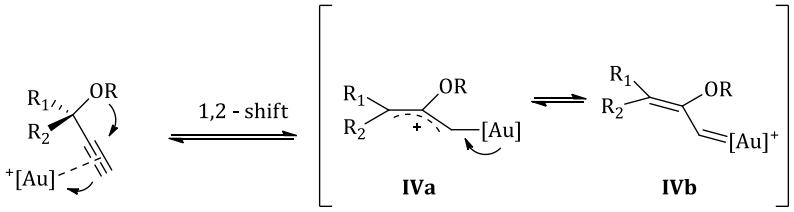

Propargylestere har tidligere bevist at de gjennomgår gull(I)katalyserte [2+1] sykliseringsreaksjoner med vinylestere og -amider. Propargylacetaler har derimot gjennomgått gullkatalyserte [3+2] sykliseringsreaksjoner med de samme substratene. Denne forskjellen i regioselektivitet skyldes elektrontettheten i OR-gruppen og i hvilken grad den kan stabilisere den delokaliserte positive ladningen i intermediatet **IVb**.

Propargylacetaler har vist seg å være mer reaktive enn propargylestere. Derfor er reaksjoner med disse substratene mest interessante å utforske videre. Propargylacetaler **5a-c** ble syntetisert i en syrekatalysert reaksjon mellom propargylalkoholer **3a-c** og 1-metoksy-2-propen. Propargylalkoholene **3b-c** ble dannet i en *Grignardreaksjon* med bensyliske aldehyder.

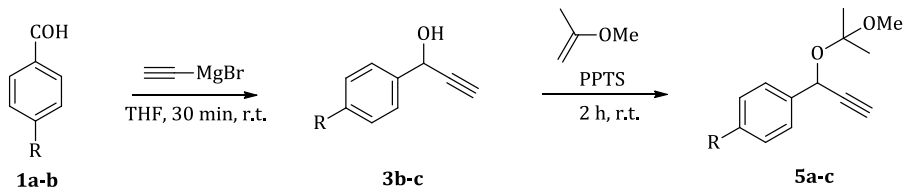

1-Phenylprop-1-yn **6** er ingen sterk nukleofil, men har gjennomgått raske sykliseringsreaksjoner med gullkarbenoider **IVa-IVb**.

I dette studiet har gull(I)katalyserte reaksjoner mellom propargylacetaler **5a-d** og 1-Phenylprop-1-yn **6** blitt gjennomført og flere interessante sykloaddisjonsprodukter **7a-c, 8a-b** og **10a-d** har blitt dannet gjennom nye tandem sykliseringsreaksjoner.

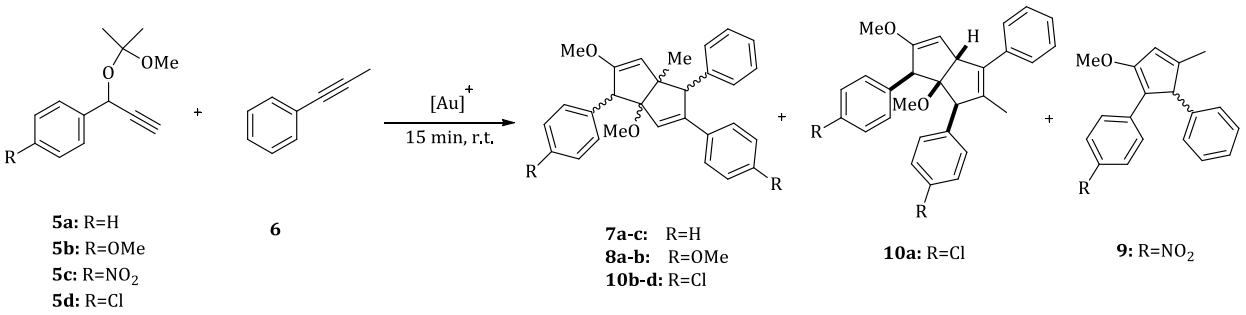

5a: R=H
5b: R=OMe
5c: R=NO_2
5d: R=Cl

6

7a-c: R=H
8a-b: R=OMe
10b-d: R=Cl

10a: R=Cl

9: R=NO_2

Reaksjoner med propargylacetalene **5a** og **5d** ga omtrent samme produktsammensetning, henholdsvis **7a-c** og **10b-d**, hvor hver fraksjon ga utbytte på mellom 3 og 12%. I reaksjonen med propargylacetal **5d** ble i tillegg et annet produkt **10a** isolert i et utbytte på 7%. Produkt **10a** viste seg også å være et tandem sykliseringsprodukt, men ble dannet via en annen reaksjonsmekanisme enn produktene **10b-d**.

Reaksjonen med propargylacetal **5b** var både mer regio- og stereoselektiv enn reaksjonene med de andre acetalene, da den ga et hovedprodukt **8a** i 27% utbytte. I tillegg ble et annet produkt **8b** isolert (5%).

Propargylacetal **5c** ga ingen tandem sykliseringsprodukter i gullkatalysert reaksjon med phenylpropynet **6**, men heller et sykloaddisjonsprodukt **9** (15%) ble dannet ved å følge en kjent [3+2] sykliseringsmekanisme.

Mulige reaksjonsmekanismer har blitt utformet for dannelsen av de nye tandem sykliseringsproduktene **7a-c, 8a-b, 10b-d** samt **10a**. Alle produkter **7-10** ble karakterisert av 1D og 2D NMR eksperimenter, IR og MS. NOESY eksperimenter var til stor hjelp når forskjellige diastereomerer skulle skilles fra hverandre.

Symbols and abbrevations

°C	degrees Celsius
Ac	acyl
Ar	aryl
B_o	Magnetic field
calcd	calculated
C_p	cyclopentadienyl
COSY	Correlated Spectroscopy
δ	chemical shift (ppm)
δ	*partially* induced charge
d	doublet (NMR)
DCD	*Dewar-Chatt-Duncanson (model)*
DCE	dichloroethane
DCM	dichloromethane
e.g.	for example
EI	Electron Impact (MS)
eq	equivalent
ERG	Electron Releasing Group
ESI	Electron Spray Impact (MS)
Et	ethyl
EtOAc	ethyl acetate
EVE	Ethyl Vinyl Ether
EWG	Electron Withdrawing Group
Φ	torsional angle
FID	Flame Ionization Detector
g	gram(s)
GLC	Gas Liquid Chromatography
h	hour(s)
HMBC	Heteronuclear Multi Bond Correlation
HR	High Resolution (MS)
HSQC	Heteronuclear Single Quantum Coherence
Hz	Herz
i-Pr	isopropyl
IR	infrared spectroscopy
J	coupling constant (Hz)
M	Molar
m	multiplet (NMR)
µ	micro
Me	methyl
mg	milligram(s)
MHz	Mega Herz
min	minute(s)
mL	milli Litre(s)
mmol	millimoles
MOP	methoxy propene
MS	Mass Spectrometry
nc	no conversion
NHC	N-heterocyclic carbene
NMR	nuclear magnetic resonance (spectroscopy)
NOE	Nuclear Overhauser Effect

NOESY	Nuclear Overhauser Effect SpectroscopY
obsd	observed
Ph	phenyl
PhD	Doctor of Philosophy
Piv	pivaloyl
ppm	parts per million
PPTS	Pyridinium *p*-toluenesulfonate
PTSA	Pyridinium *p*-toluenesulfonic acid
r.t.	room temperature
R_f	Retardation factor (TLC)
t	triplet
t-Bu	tert butyl
THF	tetrahydrofuran
TLC	Thin Layer Chromatography
TM	transition metal
TMS	TriMethylSilyl
Tol	toluyl
Ts	tosyl
UV	UltraViolet

Content

Chapter 1

Introduction

The research group of Anne Fiksdahl has over the last years explored the field of gold(I) catalyzed cyclization reactions. Propargyl esters treated with vinylic compounds have proven to undergo [2+1] cyclopropanation reactions to form cyclopropane units. Reactions between propargyl acetals and the same substrates followed a [3+2] cyclization mechanism.[18, 48] Tandem cycilization reactions between two propargyl acetal units and one unit of an olefinic ester have recently been discovered in the Fiksdahl group.[21]

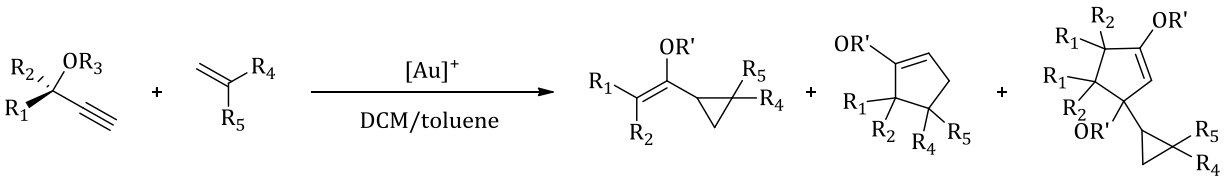

The chemoselectivity of the propargyl substrates is due to the electronic properties of the OR'-group. In the gold carbenoid complex derived from acetals, the delocalized positive charge in intermediate **IVa** is stabilized by the electron donating alkoxy group (OR-group), which allows C-1, C-2 and C-3 to be included in the following cyclization reaction. In the case of propargyl esters, the electron withdrawing O-acyl group deactivates C-1 and C-2, allowing only C-3 to be included in the cyclization reaction.

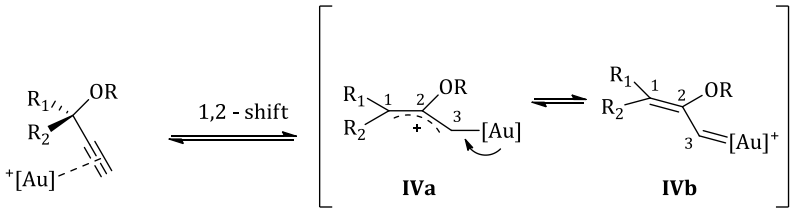

Recently, diarylic imines have proven to give 7-membered benzazepine heterocyclic products[35] in [5+2] cycloaddition reactions with propargyl acetals.

1.1 Aim of project

The propargyl acetals have proven to be more reactive than the propargyl esters,[18] and reactions with these species would therefore be interesting to investigate further. In order to study reactions with other multiple bond reactants, the aim of this project is to investigate new gold(I)

catalyzed reactions between aromatic propargyl acetals and 1-phenylprop-1-yne. By characterizing the stereo- and regiochemistry of the products, the reaction pathways can be determined.

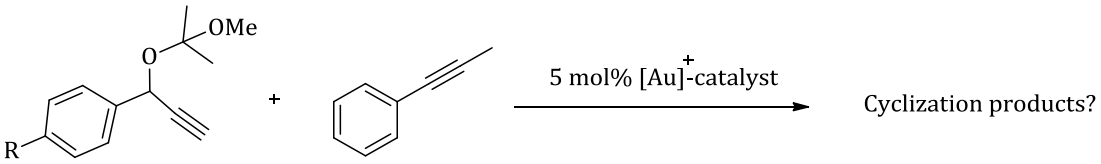

Chapter 2

Theory

2.1 Use of transition metals in organic synthesis

In 1757, *Loius-Claude de Gassicourt*[44] did an experiment in which he was trying to make cobalt-containing inks from arsenic-containing cobalt salts. During this experiment he discovered the ill-smelling *Cadet's liquid* which was synthesized from potassium acetate and arsenic trioxide. This liquid contained a mixture of cacodyl and cacodyl oxide which were the first organometallic substances prepared. Since this discovery, the use of organometallic compounds has been important among chemists.

A key event in organometallic catalysis was the discovery of *Zeise's salt*[56] in 1825. Its inventor, *W. C. Zeise*, was investigating the reaction of $K_2(PtCl_4)$ in boiling ethanol and the product he observed contained ethylene. This was the first π-complex ever discovered.

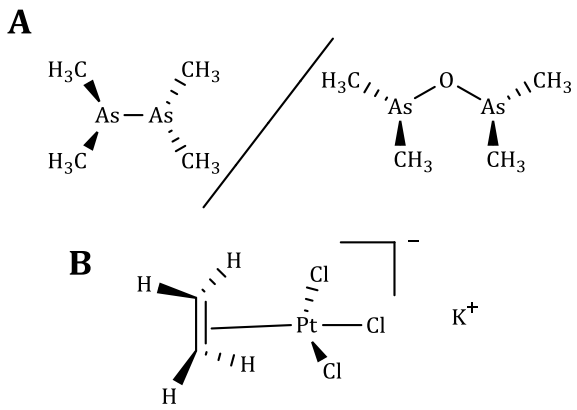

Figure 2.1*: **A**: Cadet's liquid and **B**; Zeise's salt*

Chemists could not properly describe the structure of the salt until the advent of x-ray diffraction in the 20th century.[2] This metal complex with a η^2-ligand was important in the understanding of hapticity in chemistry. *M. J. S. Dewar* [7] described in the 1940s the bonding of an olefin coordinated to copper(I) and silver(I). *J. Chatt* and *L. A. Duncanson*[19] used this model to describe the bonding in Zeise's salt. In transition metal (TM) complexes, the *Dewar-Chatt-Duncanson (DCD) model* describes how the olefin acts as an electron donor and acceptor at the same time.

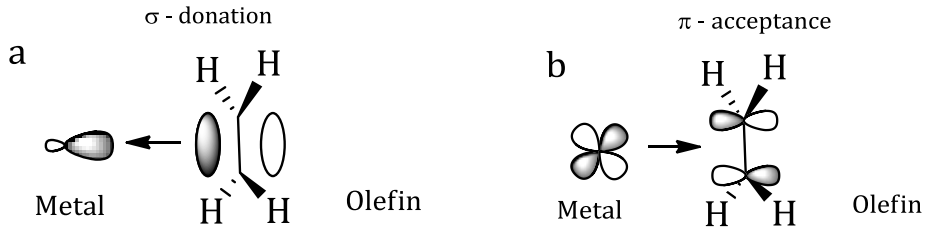

Figure 2.2*: Interactions between a TM and its ηη2 ligand*

Figure 2.2a shows, according to the DCD–model, how the olefin ligand donates electrons from from its occupied π-bonding orbital to the free d_{z^2}-orbital of the metal. In the complex this orbital interaction has a σ–character. The metal acceptor is mainly the d_{z^2}-orbital of the metal. The back-donation from the TM to the ligand (Figure 2.2b) takes place via a d-π* interaction between the filled *d*-orbital of the metal and the empty *π**-orbital of the olefin. All together these interactions weakens the C-C bond in the olefin. The main problem for describing the nature of the bonding between a TM and an unsaturated ligand, where a C–C double bond is included, is to determine if the complex should be described by the *DCD–model* or as a metallo-cyclopropane derivate (Figure 2.3).

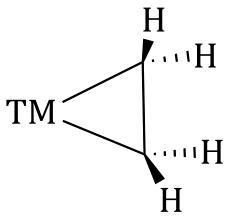

Figure 2.3*: Metallo-cyclopropane*

The first reliable studies of this problem were published by *Steigerwald* and *Goddard* in 1985.[50] They concluded, by investigating C–C bond lengths of the ligand, that there are three factors that determine if a donor–acceptor complex is formed; the metal has low–lying electronic states with doubly occupied *d*–orbitals, the C=C *π*-bond is strong and the *σ*–bond between the TM and the ligand is strong.

In 1912, *F. Grignard* received the Nobel Prize in chemistry[15] for his discovery of the *Grignard reaction* and reagents. In the reaction, aryl-or alkyl–magnesium halides react with an aldehyde or a ketone[29] to form alcohols. The reaction is important in organic synthesis for formation of new C-C bonds. The *Grignard* reagents have also been proven to undergo transmetallation in cross coupling reactions including palladium[52] among other TMs.

In the 1950s, two individual groups[22, 32] reported that they had obtained a product with light orange powder and "remarkable stability". The structure of the compound was determined by R. *B. Woodward* and *G. Wilkinson*[55] in 1952 and later confirmed by NMR and X-ray crystallography.[9] What was discovered was *ferrocene* (Figure 2.4), a very stable organometallic compound with a sandwich structure consisting of an Iron(II) cation and two anionic cyclopentadienyl (*Cp*) rings.

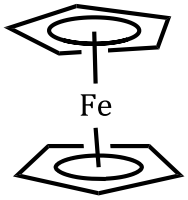

Figure 2.4*: Ferrocene*

In order for the compound to be neutral, the *Cp* rings have one negative charge each, making both of them donate 6 π-electrons. Combined with the 6 *d*–electrons on Fe^{2+} the complex attains an 18-electron configuration. The general name for these sandwich compounds are *metallocenes* and they are used in different reactions such as *Ziegler Natta polymerizat*ion[43] and as an agent in cancer treatment.[25]

In 1961, *L. Vaska* et.al. reported a new organometallic compound[54] which was given the name *Vaska's complex*. It's known for the reversible addition of O_2 and series of oxidative addition reactions due its coordinative unsaturation. Studies on this complex; its great reactivity at normal conditions, have contributed to a greater understanding and study of different processes in catalysis.[53]

Throughout the 60s and 70s several homogenous catalysts containing TMs were synthesized. The *Wilkinson's catalyst*[38] was the first homogeneous olefin hydrogenation catalyst, *H. Kagan* reported the first efficient enantioselective asymmetric Rh(I) hydrogenation catalyst.[20] Today organometallic catalysis is still popular and one of the fastest growing areas in this field is the organogold compounds.[1, 16, 49, 57]

2.2 Organogold chemistry

Since the first organogold compound, the gold carbene Au_2C_2, was discovered in 1900,[31] the use of gold in organometallic chemistry has been a popular field, especially during the last years.[1, 16, 49, 57] Gold(I)–and gold(III)–complexes are the most attractive due to their electron configuration. Use of these catalysts in synthesis is popular because of the mild reaction conditions required and their product selectivity.

In the beginning of the 20th century, organogold complexes including dialkyl substituents were prepared, but they were very unstable. *G. E. Coates* managed later to prepare stable derivatives by addition of tertiary phosphine ligands.[4] The phosphine ligand acts as a π-acceptor and a σ-donor through its lone pair electrons as shown in Figure 2.5.

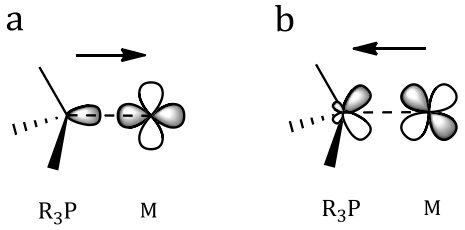

Figure 2.5*: Figure a shows the* σ*–bond between the lone pair on phosphorus and the empty orbital on the metal. Figure b shows the* π*–backdonation from the metal to the* σ^* *orbitals on Phosphorus* [37]

Use of tertiary phosphine ligands on gold(I)–and gold(III) complexes are attractive due to the thermal stability of the gold-phosphorus bond.[41]

The bonding between TMs and π–ligands such as alkenes and alkynes is usually described by the *DCD–model*. Four different principle components can contribute to the bonding of alkynes as ligands as seen in Figure 2.6.

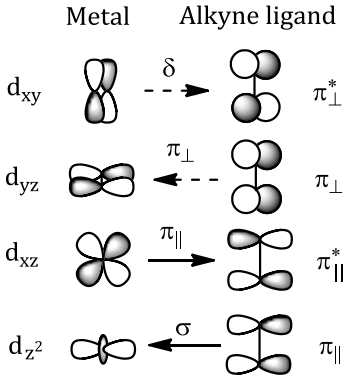

Figure 2.6*: The four principles of bonding between a TM and an alkyne ligand.*[12] *The σ–and the π–interactions are the main contributors to the bonding.*

For the gold(I)–acetylene complex ($[Au^+\text{-}C_2H_2]$), σ–bonding contributes 65% to the bond strength while the π–bonding only contributes 25%. This makes the alkyne mainly a σ–donor and not so great a π–acceptor towards gold(I). For this reason, alkynes are easily activated by gold(I)–catalysts and the gold–alkyne complex gains an electrophilic character.

Addition reactions to alkynes with a *Brønsted acid* as catalyst requires harsh conditions and many by-products may be formed from the carbocation intermediate. By replacing the proton with a softer isolobal catalyst, such as LAu^+, formation of the desired product is much easier to achieve. The Au(I)–catalyst has high affinity to the π–system of the alkyne but has the advantage of being easily cleaved off at the labile metal-carbon bond.[12]

Gold(I) catalysts are not very sensitive towards air because of the high oxidation potential from +I to +III. In addition, water, alcohols and oxygen are better tolerated during the reaction due to gold carbenoid intermediates. The gold carbenoid is stabilized by backbonding from the metal/ligands.

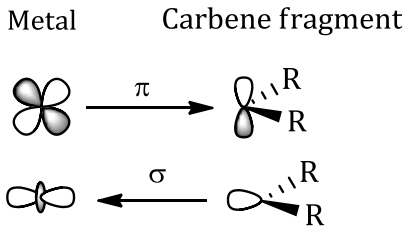

Figure 2.7*: Dominant bonding in a Fischer–type carbene complex* [12]

These carbenoid and non-classical carbocation intermediates, which are involved in gold catalyzed reactions, often lead to high product selectivity. In addition, the carbon-gold bond is labile towards protodeauration, which regenerates the catalyst.

Some of the most popular gold catalyst includes phosphines and N-heterocyclic carbene (NHC) ligands and examples of these are presented in Figure 2.8.

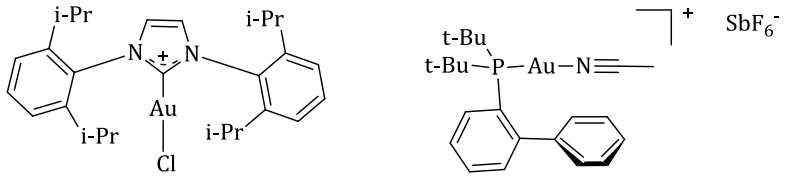

Ia **Ib**

Figure 2.8: Some homogenous gold catalysts[14]

2.3 Gold(I) catalyzed cyclization reactions

Several research groups have demonstrated that propargyl esters can, in presence of gold(I), undergo an intramolecular transformation to generate gold complex intermediates.[5, 6, 27, 48] Additionally, the *Fiksdahl group* has studied the reactivity of propargyl acetals.[18, 21] The propargyl acetals generate similar intermediates as propargyl esters as shown in Scheme 2.1.

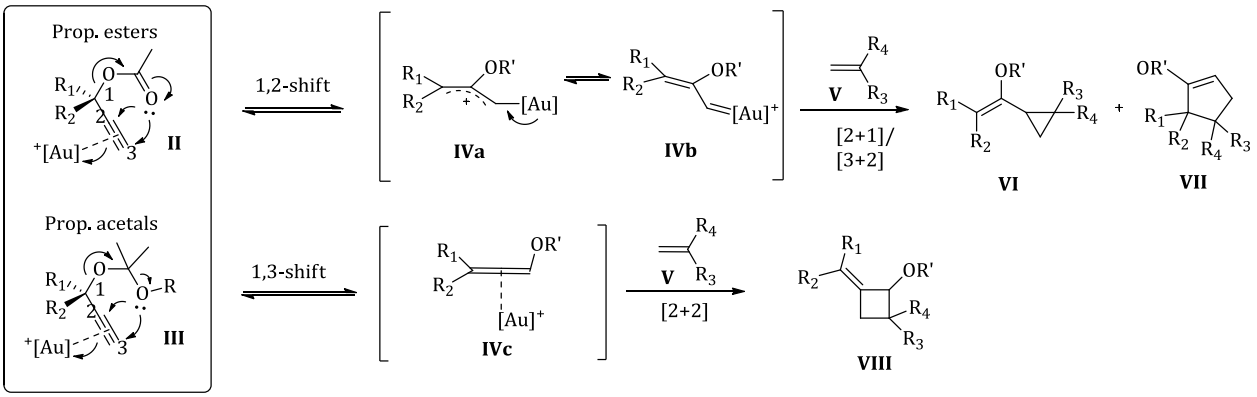

Scheme 2.1: *Gold(I) activation of propargyl esters and acetals*[18]

By performing a 1,2 O-acyl (for esters)/O-alkyl (for acetals) shift, the gold carbenoid complex **IVa-b** is generated. The positive charge is highly delocalized, but can be stabilized by an electron releasing OR' group as in the case of propargyl acetals. Allene-gold complexes **IVc** are formed by an intramolecular 1,3 shift in the propargyl ester/acetal.

Depending on the propargyl substrate, the gold complex intermediates **IVa-c** can undergo cycloadditions with different vinylic substrates **V** such as vinyl ethers and amides[48] and different interesting cyclic products **VI-VIII** can be formed.

2.3.1 [2+1] Cycloaddition reactions

Formal [2+1] cycloaddition reactions generate cyclopropane units, as seen in Scheme 2.1. These units can be found in several naturally occurring products with different biological properties[8] and are also used in a number of interesting chemical transformations.[28, 34, 51] Gold(I) catalyzed cyclopropanations between propargyl esters and vinyl esters have previously been reported by the group of *Fiksdahl*.[48] Reactions between propargyl esters and vinyl acetates were catalyzed with 5 mol% of catalyst **Ib**. The product showed formation of cyclopropane derivatives.

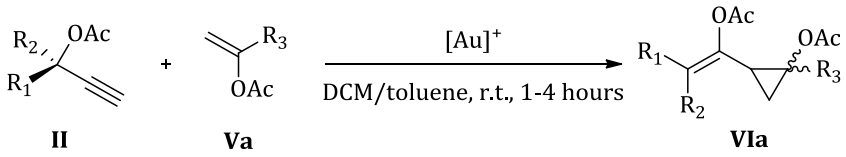

Scheme 2.2*: Formation of a cyclopropane compound.*

The reaction presented in Scheme 2.2 is an example of a [2+1] cycloaddition reaction and the mechanism appears to go via the gold carbenoid intermediate **IVb**[26] and is described in Scheme 2.3. The stereochemical conformations of the cyclopropane compound **VIa** were dependent on the bulkiness of the substituents on the vinyl esters **Va**.

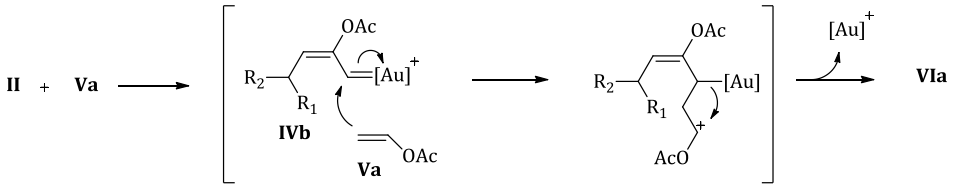

Scheme 2.3*: Mechanism of [2+1] cycloaddition via a gold(I) carbenoid intermediate **IVb**.*

It is known that aryl propargyl esters **IIa** can undergo intramolecular cyclization reactions with a gold allene **IVc** or a gold carbenoid **IVa-b** intermediate to form indenes **IX**.[36] The reactions performed by the group of *Fiksdahl*, presented in Scheme 2.2, also showed formation of these compounds, but only in the range of 10% [48]

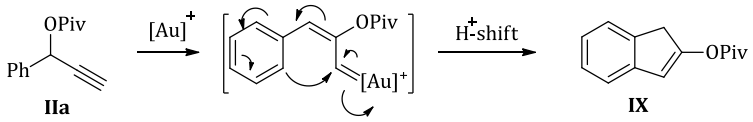

Scheme 2.4: *Intramolecular cyclization reaction to form indenes* ***IX*** [48]

2.3.2 [3+2] Cycloaddition reactions

Different propargyl esters **II** were treated with a variety of both vinyl-esters and sulfonamides by the group of *Fiksdahl*[48] as mentioned in the last Section. An unexpected result was observed in a few of the cases with vinyl sulfamides **Vb**. The reaction did not provide cyclopropanes but rather cyclopentenes **X** instead. One of the examples is shown in Scheme 2.5.

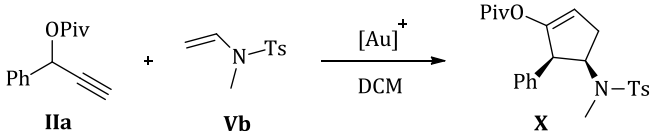

Scheme 2.5*: Gold(I) catalyzed [3+2] cycloaddition*

Nevado have reported a phosphate-gold catalyzed cyclopentaannulation of olefins with propargyl esters. The initially formed cyclopropylvinyl esters appared to undergo a ring expansion at higher temperatures to provide *trans*-cyclopentenyl esters.[13] However, further investigation done by the group of *Fiksdahl* indicated that the cyclopentene products produced in her group did not go through a ring expansion, but rather a direct [3+2] cycloaddition.[48] These diverse observations indicate that the positive charge on the gold carbenoid **IVa-b** is highly delocalized and that the mechanism is controlled by steric and electronic factors. The resonance is shown in Scheme 2.1.

Propargyl acetals **III** are also known to undergo an intramolecular rearrangement to provide gold carbenoid complexes **IVaa-ab**.[57] This rearrangement follows approximately the same mechanism as in the case of esters (Scheme 2.1), but during the internal rearrangement in propargyl acetals, one unit of acetone is cleaved off during the activation with the gold. This mechanism is described in Scheme 2.6.

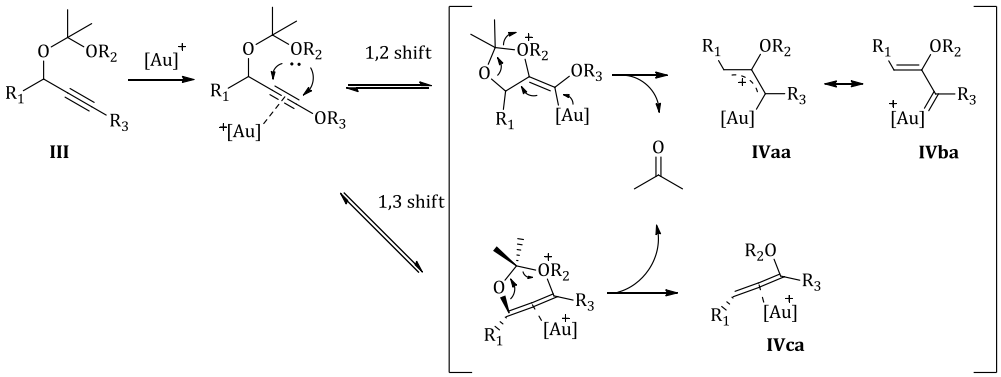

Scheme 2.6*: Gold(I) activation of a propargyl acetal.*

By changing from propargyl esters **II** to propargyl acetals **III**, the reactivity of the propargyl moiety increased drastically, resulting in a reduction of reaction times. The high reactivity of the propargyl acetal may be due to the electron releasing alkoxy (OR_2) substituent which can stabilize the positive charge in the gold carbenoid intermediate **IVaa.**[18]

Reactions between propargyl acetals **IIIa** and vinyl compounds **Vc** mainly undergo a direct [3+2] cycloaddition to form cyclopentenes **XI**.[18] The difference in chemoselectivity for propargyl acetals is probably due to the methoxy group which activates the double bond to take part in the cyclization reaction as described in Scheme 2.7. In the field of gold chemistry, propargyl acetals are exclusively studied by the group of *A. Fiksdahl.*

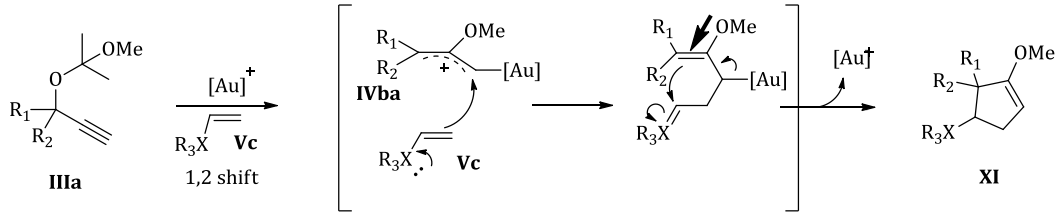

Scheme 2.7*: Gold(I) catalyzed [3+2] cycloaddition reaction via intermediate **IVb**.[18]*

Recent investigation performed by *Gung et.al.* includes reactions between propargyl esters **IIb** and cyclic vinyl ethers **Vd**.[5] Dependent on the ring size of the vinyl ether, different amounts of both the cyclopentenation and cyclopropanation products were formed. One of their reactions is presented in Scheme 2.8.

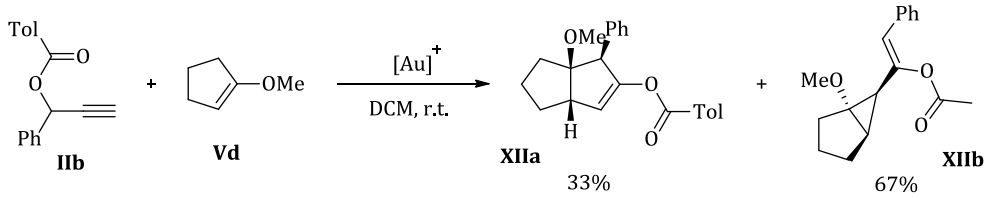

Scheme 2.8*: Reaction performed by Gung et.al.. Both the [3+2] cycloaddition product and [2+1] cycloaddition product was obtained.*

The ratio between the products in Scheme 2.8 was 33:67. The [3+2] cycloaddition product **XIIa** was observed only as the *cis* isomer with respect to the methoxy- and the phenyl group. In other reactions the *cis*/*trans* ratio would vary.

Another interesting point mentioned in the paper by *Gung et.al*[5] is the *ring current effects* which influences the ^1H chemical shift values of substituents located nearby phenyl rings in the molecule. In the case of the [3+2] cyclization product in Scheme 2.8, the methoxy group and the phenyl ring is located *syn* to each other and hence the methoxy group gets an increased δ-value relative to its normal chemical shift. The induced ring currents[11] occur when a molecule with delocalized π–electrons is placed in a magnetic field, such as in a NMR device. The ring current generates an additional magnetic field as described in Figure 2.9. This leads to regions of increased and reduced shielding in the vicinity of the aromatic ring. For this reason the aromatic

hydrogen atoms, which are in a position where the lines of force increase the B_o field, will have increased shift values relative to e.g. hydrogen atoms in an alkene.

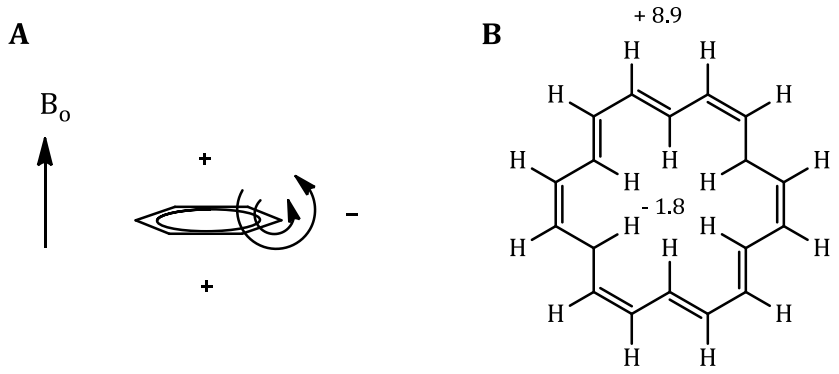

Figure 2.9: ***A:*** *Zones of increased (+) and decreased (-) shielding in an external magnetic field B_o caused by ring current effects.* ***B:*** *In [18]-annulene the six inner hydrogen atoms are highly shielded by the ring current effects and hence their shifts (ppm) are very low*

2.3.3 [5+2] cyclization reactions

Gold-activated alkynes are good electrophiles for both sp^2- and sp^3-hybridized heteroatom nucleophiles, which allow a diversity of heterocycles to be formed.[45] Gold(I) catalyzed reactions between propargyl acetals **IIIa** and diarylic imines **XII** are currently proven, by the *Fiksdahl group,* to give benzazepine heterocycle derivatives **XIII** in 60-80% yields (Scheme 2.9).[35] The formation of product **XIII** appears to go via the gold carbenoid intermediate **IVba**.

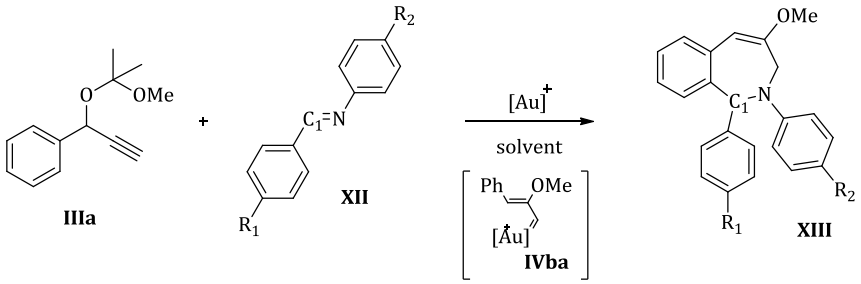

Scheme 2.9: *[5+2] cyclization reaction between propargyl acetals and diaryl imines to form benzazepine heterocycle derivatives.*

The benzazepine heterocycles **XIII** contain a framework which is observed in bioactive natural products and pharmaceuticals.[17, 47] Syntheses of these types of compounds are consequently of great interest.

Several gold(I) catalyzed experiments with propargylic acetals and diaryl imines were conducted to find the optimized catalyst for the [5+2] cyclization reaction.[35] The most efficient catalyst **Ic** is presented in Scheme 2.10. The active catalyst **Ic** is generated in situ by counter ion exchange.

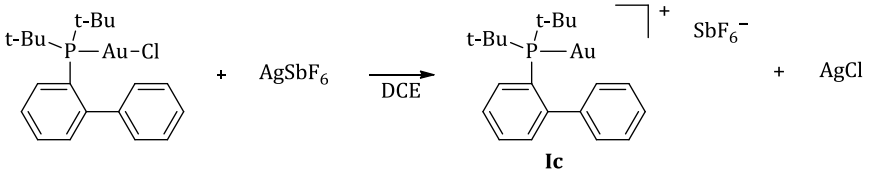

Scheme 2.10*: Generation of the optimized gold(I) catalyst for [5+2] cycloadditions*

Until now, no research has been done on the gold(I) catalyzed [5+2] cycloaddition between propargyl acetals and imines, but a proposed mechanism has been developed be the *Fiksdahl group* and is presented in Scheme 2.11.[35]

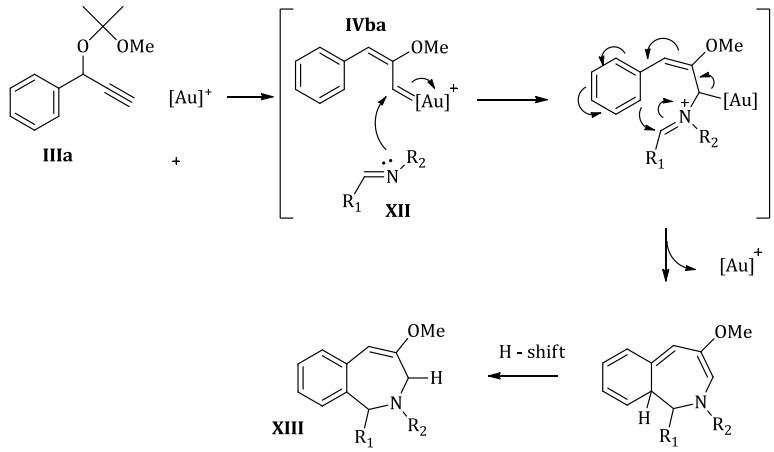

Scheme 2.11*: Proposed reaction mechanism of the [5+2] cyclization reaction between propargylic acetals and imines.*

Scheme 2.12 shows a deuterium labeling experiment[35] in which incorporation of one deuterium on the 3-position of the 7–membered heterocycle **d_5-XIII** is shown. This is in accordance with an *o*–phenyl proton shift after the protodeauration step. Cyclization through an electrophilic aromatic Mannich–type reaction occurs and the benzene–ring regains its aromaticity.

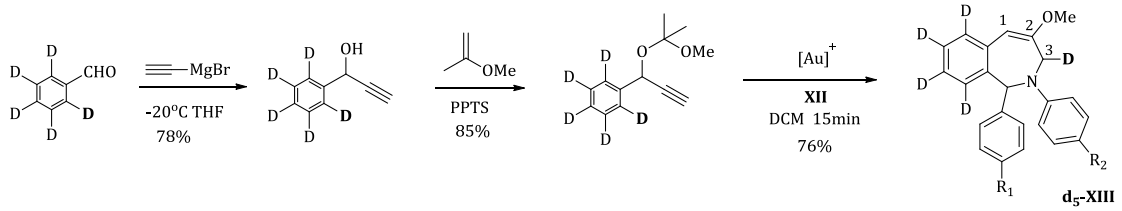

Scheme 2.12*: Deuterium labeling experiment to determine the proton shift in the [5+2] cyclization reaction*

2.4 Synthesis of propargyl alcohols and acetals

As previously stated, propargyl acetals are much more reactive than the corresponding ester, and are therefore more interesting to use in further research on gold(I) catalyzed cyclization reactions. Propargyl acetals are synthesized from propargyl alcohols and not many of them are

commercially available. One efficient reaction to form propargyl alcohols is a through a *Grignard reaction* with aldehydes[42] as presented in Scheme 2.13. Aryl substituted propargyl alcohols and acetals have shown to control the stereoselectivity[18] and are hence of the greatest interest.

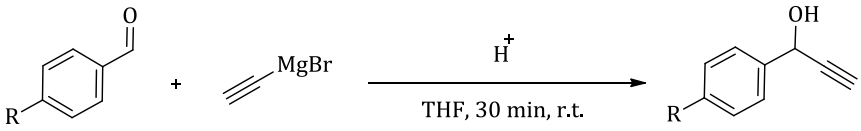

Scheme 2.13*: Synthesis of propargyl alcohols*

As mentioned in Section 2.2, the *Grignard reaction* is an important tool for the formation of C–C bonds. THF is often used as a solvent in these reactions, as it forms a more stable complex with the Grignard reagent than e.g. diethyl ether.[3] THF is also preferred due to its hygroscopic properties, which excludes side reactions between the *Grignard* reagent and water. The mechanism of the *Grignard reaction* is presented in Scheme 2.14.

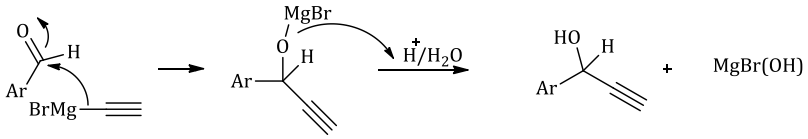

Scheme 2.14*: Mechanisms of the Grignard reaction[3]*

The reactions between propargyl alcohols and vinyl ethers to form propargyl acetals **III** are shown in Scheme 2.15.

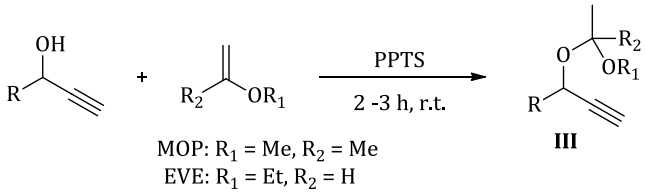

Scheme 2.15*: Synthesis of propargyl acetals.[57]*

This reaction is acid catalyzed by pyridinium *p*-toluensulfonate (PPTS) which is found to be weaker and can be used in milder conditions than the corresponding *p*–toluensulfonic acid (PTSA).[33] Propargyl acetals derived from methoxy propene (MOP) have been shown to favor cyclization reactions more than in the case of ethyl vinyl ether (EVE).[18] The reaction mechanism for the synthesis of propargyl acetals is described in Scheme 2.16:

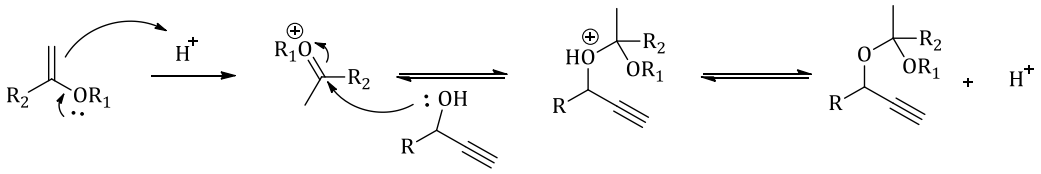

Scheme 2.16*: Mechanism for the acid catalyzed formation of acetals.*[10]

2.5 NMR applications [11]

In 1946 two research groups independently observed nuclear magnetic resonance signals for the first time. Respectively *F. Bloch* and *E.M. Purcell* were awarded the Nobel Prize for Physics in 1952 for their discovery. During the first three decades all NMR spectroscopy measurements relied on *one-dimensional* (1D) modes of observation. *Two-dimensional* (2D) NMR experiments were developed during the 1970's and started a new area in NMR spectroscopy. The advantage of 2D NMR spectra is that they show ^{1}H vs. ^{1}H or ^{1}H vs. ^{13}C chemical shift correlations, which are great tools when solving regio- and stereochemistry of organic molecules.

2D NMR experiments include COSY, HSQC, HMBC and NOESY among others. Both COSY and NOESY spectra show ^{1}H vs. ^{1}H interactions. The difference between them is that COSY shows correlations via spin-spin coupling in the molecule, while NOESY spectra show protons that are close through space. HSQC shows C-H correlations via one-bond carbon-proton coupling and HMBC shows C-H correlations via long-range C-H coupling.

NOESY experiments are important tools when solving stereochemistry in molecules. The [3+2] cyclization product **XIIa** in Scheme 2.8 is a bicyclic compound with three stereogenic centers. The compound can potentially have four different diastereoisomers (with corresponding enantiomers). Two enantiomers dissolved in an achiral solvent will have identical NMR spectra and can't be distinguished.

Scalar couplings between nuclei are indirect couplings transmitted through chemical bonds. Vicinal couplings, ^{3}J(H,H), show couplings between protons separated by three bonds. They are influenced by e.g. substituents and the torsional angle φ. A greater understanding of vicinal couplings was made by *M. Karplus.* The *Karplus curve* shows the relationship between $^{3}J(H,H)$ (Hz) and the torsional angle φ, and is presented in Figure 2.10. The plot describes how the coupling constants are largest for φ = 0° or 180°, and smallest for φ = 90°.

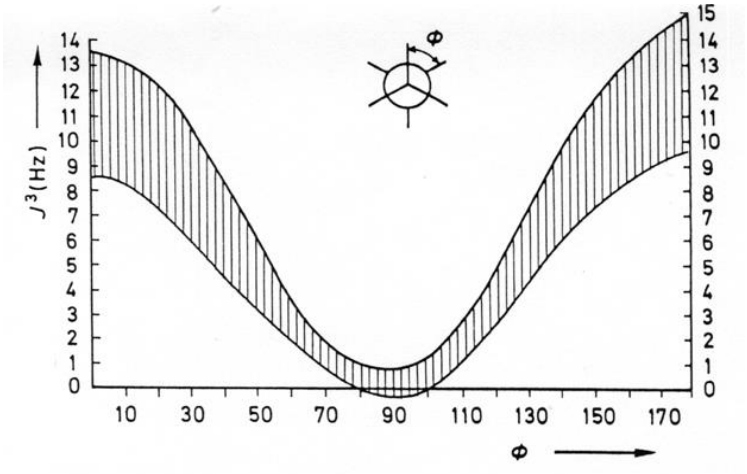

Figure 2.10: *The Karplus curve*

In saturated systems couplings through more than three bonds are often less than 1 Hz. However, in allylic compounds, the $^4J(H,H)$ couplings can become quite large. These couplings are highly dependent on the angle φ between the C-H bond and the axis of the π-orbital in the double bond as shown in Figure 2.11

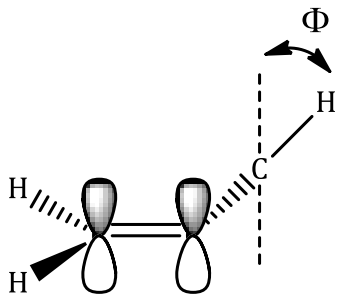

Figure 2.11*: The angle φ between the C-H bond and the axis of the π-orbital in the double bond determines the couplings in allylic systems.*

The closer the angle φ is to 0°, the larger will the coupling be. Couplings through five or more bonds can rarely be seen.

Chapter 3

Results and discussion

This chapter is divided in three parts. The first part covers the synthesis of starting materials and is presented in Section 3.1. This part consists of synthesis of propargyl alcohols and acetals. The major work is presented in Section 3.2, where details of all the gold(I) catalyzed cyclization reactions are presented. Finally, in Section 3.3, suggestions for further development in this field are given.

All new compounds have been fully characterized by NMR, IR and MS. Different stereoisomers were distinguished by 2D NOESY experiments and are presented in this chapter. The shift values of ^{1}H and ^{13}C are given in blue and red, respectively. Experimental data and characterization details are given in Chapter 5.

3.1 Synthesis of starting materials

3.1.1 Synthesis of propargyl alcohols

The propargyl alcohols **3b-c** were synthesized according to a similar procedyre.[42] Propargyl alcohol **3a** was commercially available. All details and results of these syntheses are given in Table 3.1.

Table 3.1*: Synthesis of propargyl alcohols*

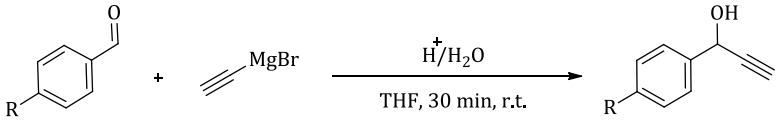

1a-b **2** **3b-c**

Entry	Aldehyde	Propargyl alcohol	Yield [%]
1	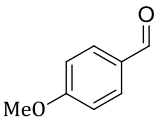 **1a**	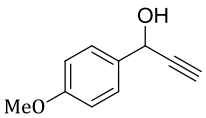 **3b**	54
2	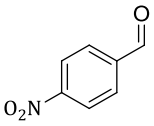 **1b**	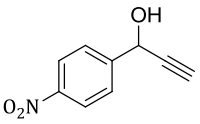 **3c**	-

The substituted benzaldehydes **1a**-**b** were treated with a 0.5 M solution of the Grignard reagent **2** in THF. This Grignard reaction was described in Section 2.4. Since this is an exothermic reaction,[39] the temperature was kept low while adding the benzaldehyde **1a**-**b** to the Grignard reagent. A saturated solution of ammonium chloride was added to quench the reaction.

The literature based procedure proved not to work as well for aldehyde **1b** (Entry 2). The solid *p*-nitrobenzaldehyde **1b** did not dissolve easily in THF. Fortunately, this did not seem to affect the conversion of aldehyde **1b** or the reaction time (monitored by GLC). However, in the work up of the product crude, the extraction proved to be difficult with the literature procedure. The product was probably less soluble in diethyl ether than the literature substrate. A more polar solvent, such as ethyl acetate or dichloromethane, should be used for this substrate. No flash chromatography was performed for purification of the product **3c**, as the proton NMR analysis of the crude product indicated that the correct product **3c** had been obtained.[23] The crude product was used in further synthesis.

3.1.2 Synthesis of propargyl acetals

All details and results of the syntheses of propargyl acetals **5a-c** are given in Table 3.2.

Table 3.2*: Synthesis of propargyl acetals*

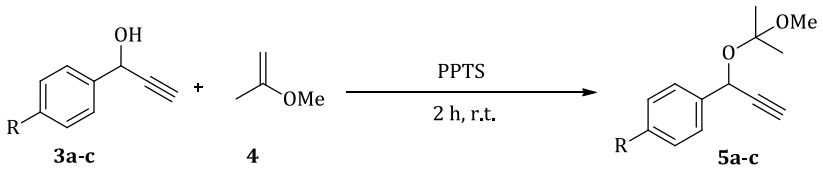

Entry	Propargyl alcohol	Propargyl acetal	Yield [%]
1	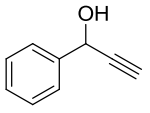 **3a**	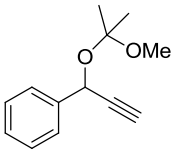 **5a**	77
2	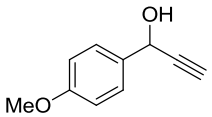 **3b**	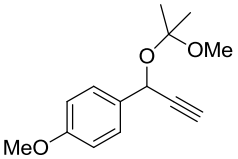 **5b**	63
3	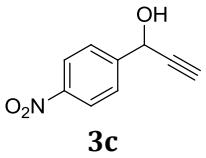 **3c**	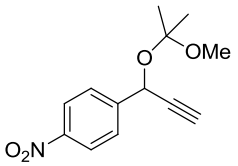 **5c**	31[i]

[i] Yield over two steps from aldehyde **1b**.

Syntheses of propargyl acetals **5a**-**b** have previously been reported and these compounds have been used in gold(I) catalyzed reactions.[21] The reaction mechanism for the acid catalyzed formation of propargyl acetals was described in Section 2.4. Due to the unstability of the acetals **5a**-**c**, which tended to decompose to alcohols **3a**-**c** at room temperature, these reactions had to be performed under inert conditions. The observed yields of propargyl acetals **5a**-**b** are in accordance with, or better than literature.[21]

Synthesis of propargyl acetal **5c** was performed according to the same procedure as for propargyl acetals **5a**-**b**. The low total yield of **5c** may be due to the challenges in the work-up of propargyl alcohol **1b** and also that the impurities in the product crude of **1b** have affected the reaction and formation of **5c**. Due to time limitations the reaction was not repeated. However, sufficient amount of the product **5c** was produced to continue with further syntheses.

3.2 Gold(I) catalyzed reactions

All details and results of the gold(I) catalyzed reactions are summerized in Table 3.3. Due to optimization studies previously carried out in this group regarding gold(I) catalyzed [2+1] and [3+2] cycloaddition reactions, gold catalyst **Ib** was used in Entries I-IV (Figure 3.1).[18] Counter ions such as hexafluorantimonate(V) or bis(trifluoromethylsulfonyl)amide combined with the gold(I) complexes seemed to be important, as no reaction took place where they were not present.

All experiments showed immediate and full conversion of the propargyl acetals **5a-d**, with a corresponding color change in the reaction flask. All the reactions were allowed to stir for 15 minutes before being quenched with triethylamine.

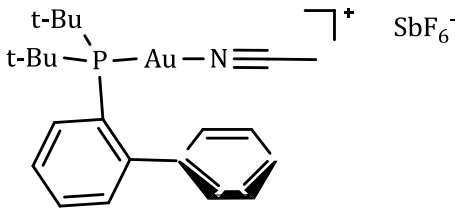

Figure 3.1*: Gold catalyst **Ib***

All the gold(I) catalyzed reactions were carried out with three equivalents of 1-phenyl-prop-1-yne **6**. Recent research in the group indicates that some of the propargyl acetals undergo a dimerization in the presence of gold(I) catalysts, hence, an excess of the phenyl propyne is desirable to use.

All assignments of stereo- and regiochemistry of products **7-10** are based on ^{1}H, ^{13}C and 2D correlation NMR spectroscopy. The low yields observed of many of the products, and the fact that these reactions were conducted in small scale (100 mg), gave challenges due to weak NMR spectra. Due to the low natural abundance of ^{13}C, some spectra were difficult to analyze. Hence, full characterization of some of the products was not possible at this time.

Once the identity of the products formed had been established, a screening of different gold(I) and gold(III) catalysts was carried out. These reactions are described in Subsection 3.2.6 in this Chapter.

Table 3.3*: Gold(I) catalyzed reactions*

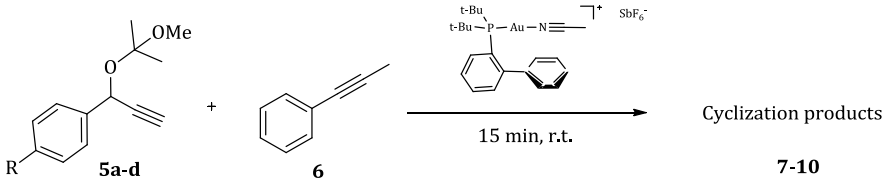

	Propargyl acetal	Cyclization product	Yield [%]
Reaction I	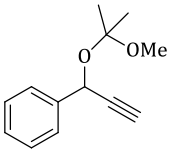 **5a**	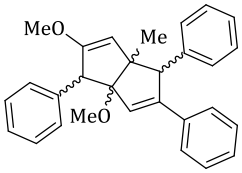 **7a**	3
		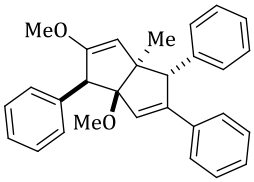 **7b**	3
		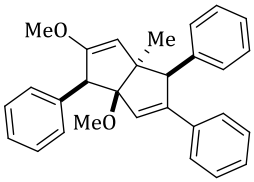 **7c**	10
Reaction II	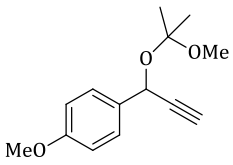 **5b**	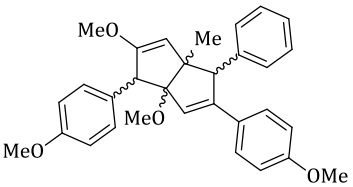 **8a**	27
		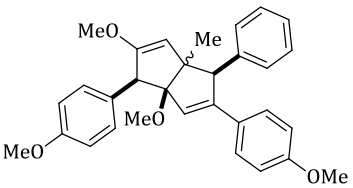 **8b**	5

Table 3.3 continuation: *Gold(I) catalyzed reactions*

	Propargyl acetal	Cyclization product	Yield [%]
Reaction III	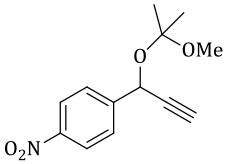 **5c**	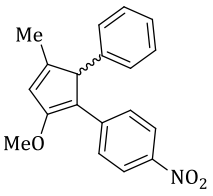 **9**	15
Reaction IV	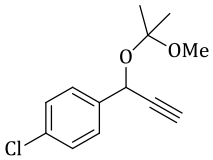 **5d**	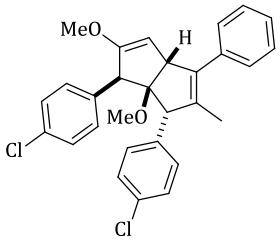 **10a**	7
		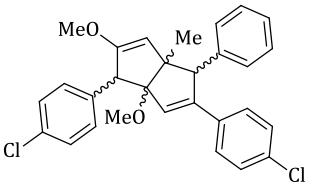 **10b**	6
		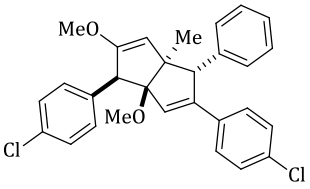 **10c**	4
		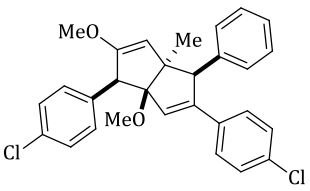 **10d**	12

3.2.1 Reaction I

The reaction between the unsubstituted propargyl acetal **5a** and phenylpropyne **6** was the first reaction conducted in this thesis and is presented in Scheme 3.1.

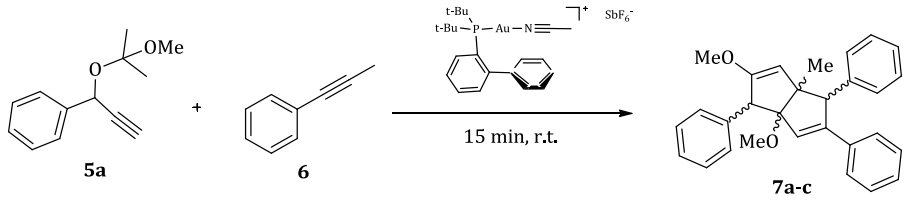

Scheme 3.1*: Reaction I.*

Monitored by GLC, it was clear that the reaction was complete after 15 minutes. Both TLC and GLC showed several products. A sketch of the TLC is presented in Figure 3.2

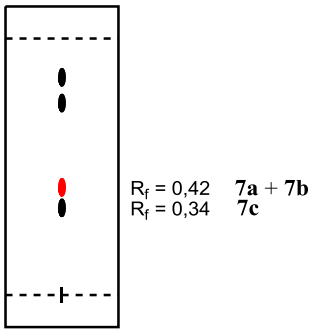

Figure 3.2*: TLC of product crude in reaction I. Eluent 15:1 pentane:ethyl acetate*

The two lower spots on the TLC in Figure 3.2 were given our attention, as they gave the purest ^{1}H NMR spectra after isolation. The spot with R_f = 0.42 appeared to consist of two isomers but the lowest spot (R_f = 0.34) consisted of one, pure compound. It became clear after ^{1}H NMR, ^{13}C NMR, 2D correlation NMR (Appendix H) and mass spectrometry that the product **7c** was a result of a tandem cyclization reaction containing two units of the propargyl acetal **5a** and one unit of the phenylpropyne **6**. None of the previous tandem cyclization reactions proposed by this group, presented in section 2.3, could describe the formation of the new tandem cyclization product **7c**.

A new reaction mechanism was proposed and is presented in Scheme 3.2.

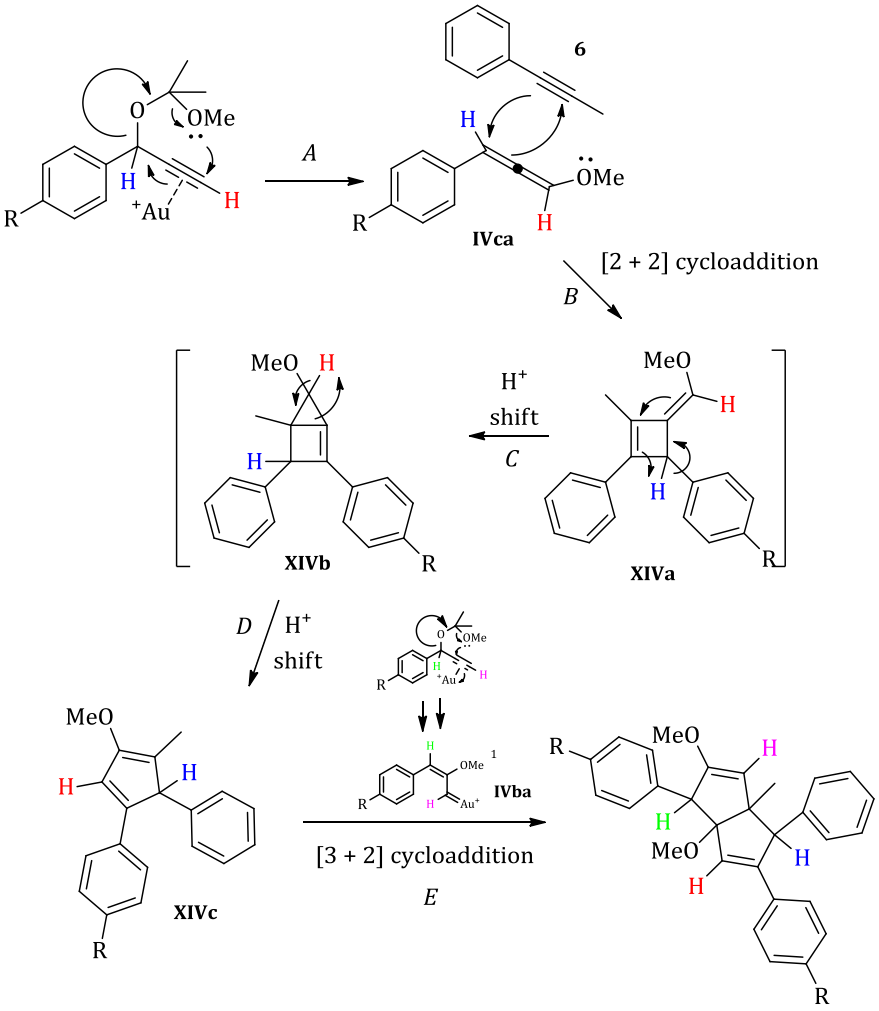

Scheme 3.2*: Proposed reaction mechanism of the tandem cyclization reactions resulting in several products presented in Table 3.3*

In the first step (*A*) the gold catalyst activates the propargylic acetal into the allenic intermediate **IVca**, which is described in Scheme 2.6, by a 1,3 intramolecular alkoxy shift. This is followed by a [2+2] cycloaddition reaction (*B*) with the phenyl propyne **6** by activation from the terminal methoxy group. A similar four membered ring (as **XIVa**) was previously formed and isolated by this group.[18] In the next steps (*C, D*) a intramolecular rearrangement, including a double proton shift, occurs, induced by the formation of a substituted 1,3 pentadiene, due to less ring strain. In the final step (*E*) of the tandem cyclization process, there is a [3+2] cycloaddition between the five membered ring **XIVc** and the gold-complex **IVba** which follows the reaction mechanism presented in Scheme 2.7.

This mechanism was proposed by Prof. Anne Fiksdahl and Post Doc. Naseem Iqbal, and 1D and 2D NMR experiments of product **7c** support the proposed regiochemistry. It was established that two protons were attached to sp^3 hybridized carbon atoms, and two benzylic protons were attached to sp^2 hybridized carbon atoms because of the correlated ^{13}C shift values observed in HSQC (Appendix H-3). HMBC- and COSY spectra (Appendices H-4, H-5) was very helpful when solving the structure of the molecule skeleton. HMBC and COSY correlations of compound **7c** are presented in Figure 3.3.

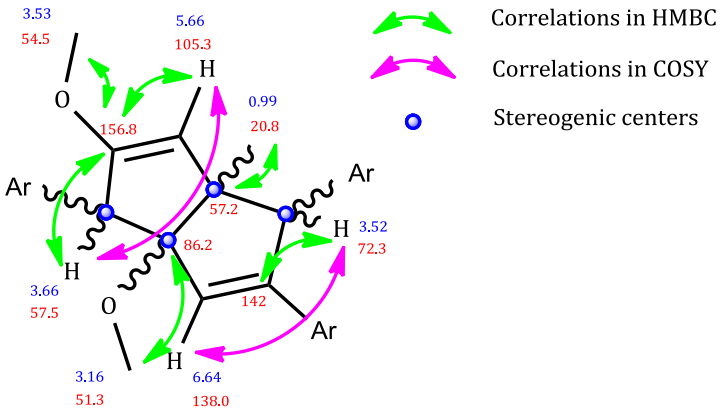

Figure 3.3*: Chemical shifts and HMBC/COSY correlations in the skeleton of compound* ***7c****.*

The strong COSY correlations between the protons shown in Figure 3.3 are a bit surprising as they are separated by four bonds, but it may be due to long range couplings which were described in Section 2.5. In some of the products, a splitting between these protons was observed in the proton specter as well.

The isomers **7a-b** with R_f=0.42 in Figure 3.2 proved to be more difficult to separate from each other, but was accomplished after extensive testing of several eluent systems. The final eluent system was 50:1 pentane:THF. Both isomers **7a-b** showed similarities with **7c** in ^{13}C NMR and in the 2D correlation NMR spectra, so it was established that they both were different stereoisomers of product **7c.** Though the ^{1}H shifts seemed to differ, but this is probably due to the stereochemistry and ring current effects as described in the latter part of Section 2.3.

The proposed product in Figure 3.3 has four stereogenic centers, and the stereochemistry of the isolated products (enantiomers are not desired to distinguish in this synthetic field, hence the relative stereochemistry in the figures) were determined by NOESY experiments. What was obvious from NOESY of all three compounds **7a-c** was that there was no correlation between the methyl group (^{1}H δ = 1.05 ppm) and the methoxy group (^{1}H δ = 3.08 ppm). Hence, they had to have a *trans* configuration relatively to each other. Figures 3.4-3.6 show the different isomers obtained from Reaction I.

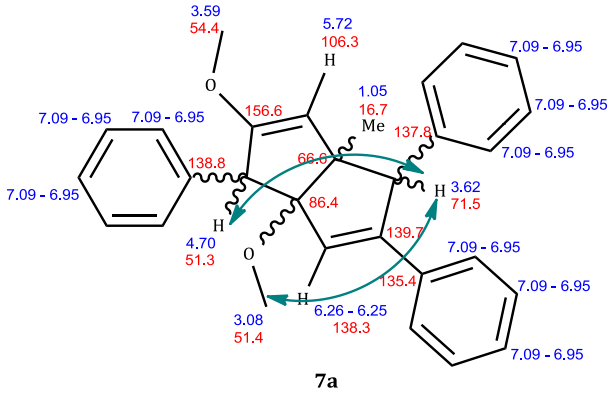

Figure 3.4*: Chemical shifts and NOE correlations of compound* ***7a***

The NOESY specter (Appendix H-7) of compound **7a** showed clear correlation between the two benzylic protons as well as a strong signal between the methoxy group (^{1}H δ = 3.08 ppm) and the benzylic proton (^{1}H δ = 3.62 ppm). From 3D projections of the molecule, all these three groups should have *cis* configuration relative to each other. This is a possible isomer, but the reason for the uncertainty about the stereochemistry in **7a** will be discussed later in this Chapter (Subsection 3.2.2).

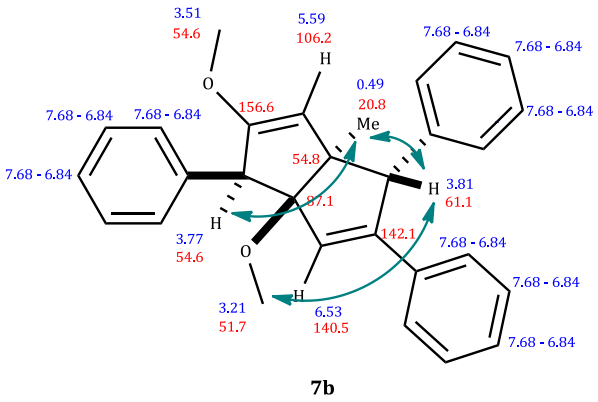

7b

Figure 3.5*: Chemical shifts and NOE correlations of compound **7b***

The NOESY specter (Appendix H-7) of compound **7b** showed clear correlation between the methyl group (^{1}H δ = 0.49 ppm) and the benzylic proton (^{1}H δ = 3.77 ppm), and also between the methoxy group (^{1}H δ = 3.21 ppm) and the other benzylic proton (^{1}H δ = 3.81 ppm). Additionally, no signal between the two benzylic protons was observed. Hence, the stereochemistry presented in Figure 3.5 seemed appropriate. There was observed a small correlation between the methyl group (^{1}H δ = 0.49 ppm) and the benzylic proton (^{1}H δ = 3.81 ppm), but this can be due to their neighboring positions. The low shift of the methyl group in **7b** compared to **7a** and **7c** may be due to the ring current effects caused by the neighboring phenyl group.

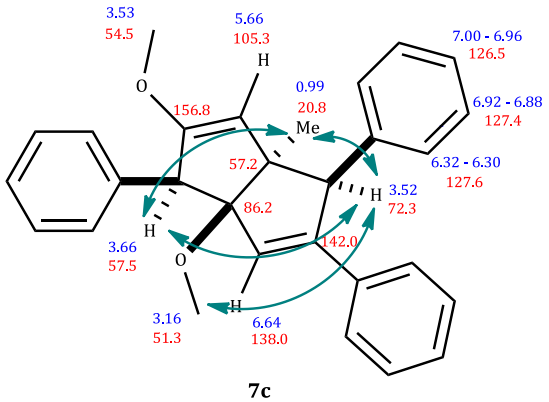

7c

Figure 3.6*: Chemical shifts and NOE correlations of compound **7c***

The NOESY specter (Appendix H-6) of compound **7c** showed clear correlation between the methyl group (^{1}H δ = 0.99 ppm) and both of the benzylic protons, hence *cis* configuration between these three groups was interpreted. The NOESY also indicated correlation between the

methoxy group (^{1}H δ = 3.16 ppm) and the benzylic proton (^{1}H δ = 3.52 ppm), even though they are proposed to be *trans* to each other, but due to the flexibility of the molecule and free rotation of the methoxy group, this seems possible. In the other two isomers **7a-b**, the aromatic shifts were difficult to distinguish. However, in product **7c** five aromatic protons stood out and clearly belonged to the same aromatic system. 2D COSY and NOESY experiments confirmed this (Appendices H-4, H-6). These deviations may also be due to the ring current effects.

The different stereochemistry of the complex bicyclic molecules is hard to understand from 2D drawings, hence, better understanding was achieved by building the different stereoisomers. A 3D model (from ChemDraw Ultra 12.0) of product **7c** is shown in Figure 3.7.

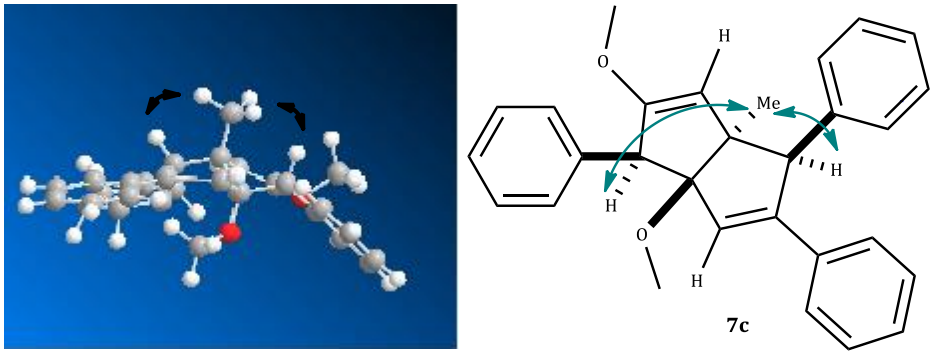

Figure 3.7*: A 3D model of compound* ***7c****, showing NOE correlations between the methyl group and the two benzylic protons.*

It was desirable to repeat Reaction I, but with different substituents on the aromatic part of the propargylic acetal (**5b-d**), to see if similar products were produced. To easier recognize each isomer in later reactions, some unique features were focused on in every one of them; In **7a** one benzylic proton had a higher shift than in the other isomers (^{1}H δ = 4.70 ppm), in **7b** the methyl group was assigned a very low proton shift (^{1}H δ = 0.49 ppm) and in **7c** a unique doublet (with a minor splitting) was observed (^{1}H δ = 6.31 ppm).

3.2.2 Reaction II

With a greater understanding of what kind of products to expect, Reaction II (Scheme 3.3) was conducted. Propargyl acetal **5b** and phenylpropyne **6** were mixed with the gold(I) catalyst and the reaction was monitored by GLC and TLC.

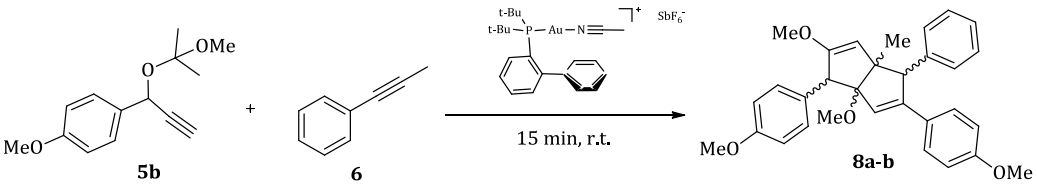

Scheme 3.3*: Reaction II.*

Unlike Reaction I, one major peak (and several minor) was observed in GLC. After column chromatography, it became clear that there was one major product **8a** in this reaction, which yielded 27 %. Only this product was successfully isolated, but a mixture containg 61% of product **8b** was pure enough to recognize some familiar features in the ^{1}H NMR spectrum.

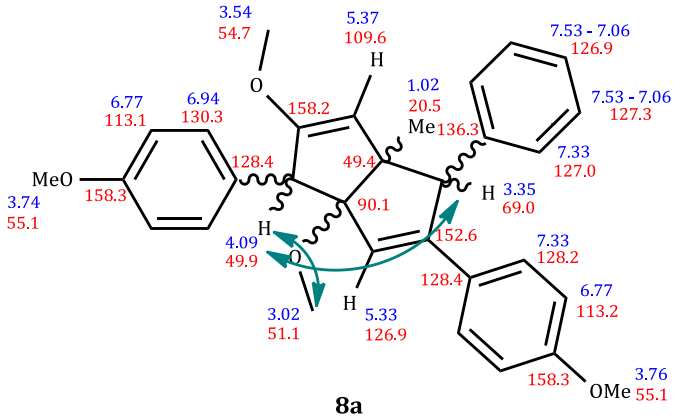

8a

Figure 3.8*: Chemical shifts and NOE correlations of compound **8a.***

The structure and NOE correlations of the major product **8a** (Appendix I) is presented in Figure 3.8. By comparing ^{13}C NMR shifts and 2D correlation NMR with compounds **7a-c**, it was established that product **8a** shared their regiochemistry. Nevertheless, ^{1}H NMR did not match any of the three products **7a-c**, indicating formation of a new isomer. With the assumption of the bridged methoxy- and the methyl group having *trans* configuration relatively to each other, four different isomers are possible. As mentioned in the previous section, the stereochemistry of compound **7a** could not be determined. This is because, by interpretation of NOESY spectra (Appendices H-7. I-6), the stereochemistry of isomers **8a** and **7a** can not be distinguished. In both cases strong correlations between the benzylic protons are observed. There is no possibility for this in both of the two possible remaining isomers.

By introducing a methoxy group in the para position on the phenylic propargyl acetal, the electron density of the acetal increases. This apparently affects the stereoselectivity of the reaction (as product **8a** yielded 27%). The final cycloaddition (step *E* in Scheme 3.2) in the tandem cyclization process is believed to go through a direct [3+2] cyclization reaction. The additional *p*-OMe group on the phenyl ring of the intermediate **IVa** increases its electron density, which may increase the speed in the final step (*E*). For this reason, one major product **8a** is formed.

In addition, one other product **8b** was isolated in a mixture of different compounds. A PhD student[46] in the group managed to isolate the compound with a much greater grade of purity, which is shown in the 1D and 2D NMR spectra taken. These spectra were of great help when assigning ^{1}H and ^{13}C NMR shifts of this product. Figure 3.9 shows stereochemistry and chemical shifts of product **8b**.

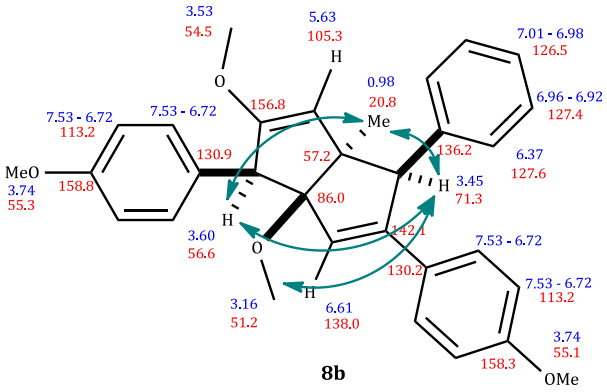

Figure 3.9*: Chemical shifts and NOE correlations of compound **8b.***

It was readily established that compound **8b** was an analogue of compound **7c** by recognition of the unique doublet (^{1}H δ = 6.37 ppm) and NOE correlations (Appendices J-1 and J-6).

In the proton and carbon NMR spectra for compounds **8a** and **8b** there can be observed a major impurity (^{1}H δ (ppm) = 6.98, 5.01, 2.27, 1.43, ^{13}C δ (ppm) = 151.5, 135.8, 128.3, 125.5, 34.2, 30.3, 21.2). This was later established as being the stabilizing agent butylhydroxytoluene in THF, which was used in purification chromatography. Once this was realized, dry THF from the MB SPS-800 Solvent Purification System or 2-methyl tetrahydrofuran was used instead.

3.2.3 Reaction III

Scheme 3.4 shows Reaction III.

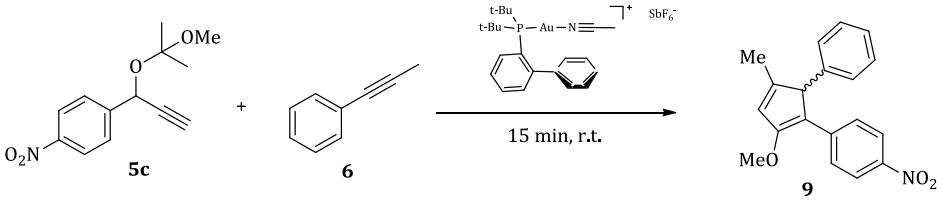

Scheme 3.4*: Reaction III.*

The electron releasing *p*-OMe substituent seemed to affect the stereoselectivity of the reaction, and, thus, it was considered to be interesting to introduce a strong electron withdrawing group on the aromatic part of the propargyl acetal. The propargylic acetal **5c** was treated with phenylpropyne **6** in a gold(I) catalyzed reaction. GLC of the product mixture did not show similar pattern as the two previous reactions. There were indications of a much smaller molecule **9** being the major product. Figure 3.10 shows the structure of the proposed pentadiene product.

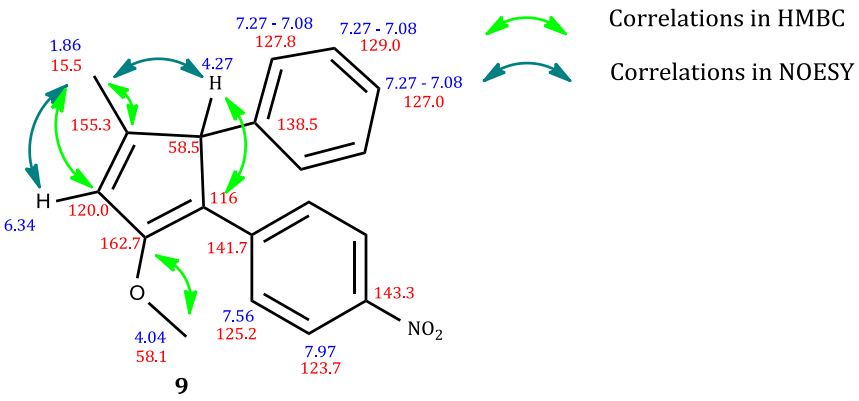

Figure 3.10*: Chemical shifts and 2D NMR correlations of compound* ***9.***

The structure of product **9** seemed similar to the five membered ring intermediate **XIVc** from the reaction mechanism presented in Scheme 3.2. However, after interpreting HMBC and NOESY spectra (Appendices K-4, K-5), it was established that the formation of product **9** went by intermediate **XVIb**. Intermediate **XVIb** was formed by a [3+2] cyclization reaction between gold carbenoid complex **IVbb** and phenylpropyne **6**. The presented mechanism (Scheme 3.5) is similar to the one presented in Scheme 2.7 in Subsection 2.3.2 in the theory part.

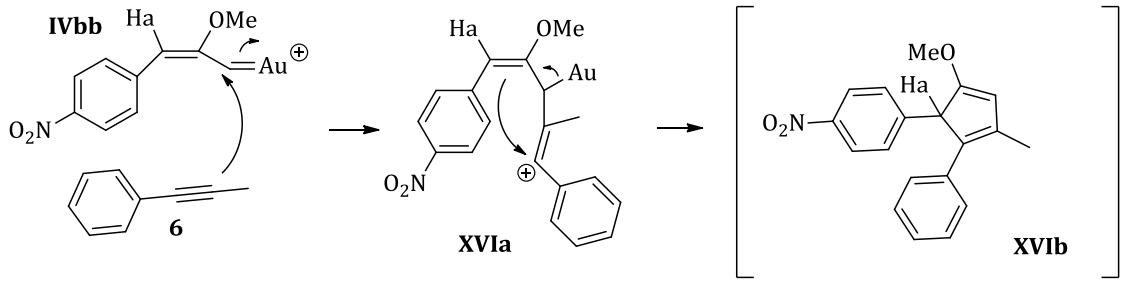

Scheme 3.5*: 1. Step of the reaction pathway for product* ***9***

From studies of the NOESY and HMBC 2D correlation NMR spectra, it became obvious that there was a proton shift of the benzylic proton **Ha**. This proton shift and the proposed underlying forces for this mechanism are shown in Scheme 3.6.

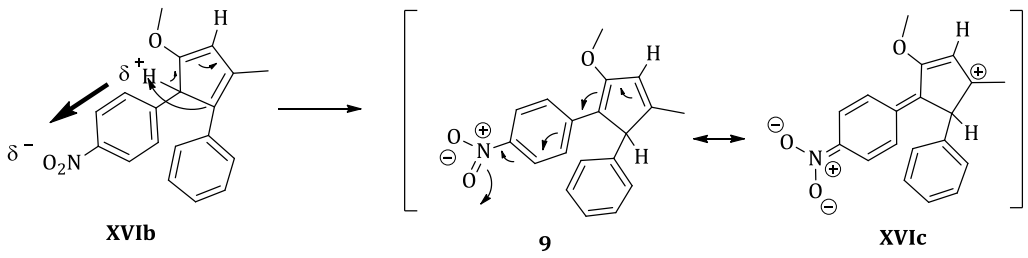

Scheme 3.6*: Mechanism of the intramolecular H-shift in product* ***9*** *and resonance due to the conjugated system.*

The reason for the proton shift in product **9** may be due to the electron withdrawing nitro group which makes the proton more acidic. The *p*-nitro phenyl group is now in direct conjugation with the quaternary carbon that the methyl group is attached to. This explains the high shift of the quaternary carbon (^{13}C δ = 155.3 ppm) in resonance structure **XVIc**.

In an attempt to see if a tandem cyclization product could be generated, the electron deficient product **9** was mixed with the electron rich propargyl acetal **5b**. However, no further cyclization took place, as no such products were observed. Current research, done by a PhD student in the group,[46] indicates that product **9** undergoes further cyclization with the electron deficient propargyl acetal **5c**. However, no products have been characterized yet. This result can be explained by the fact that the electron deficient nucleophile **9** needs an even stronger electrophilic reactant such as propargyl acetal **5c** for cyclization to occur.

The reaction with the propargyl acetal **5c** did not undergo the same tandem cyclization reactions as acetals **5a** and **5b**. This can be explained by the electron-withdrawing nature of the *p*-nitro phenyl group, which deactivates compound **9** sufficiently to favor formation of this "intermediate" rather than products similar to Reactions I and II.

This reaction shows that, even by using highly deactivated propargyl acetals, cyclization still occurs. This is an interesting evidence of the strong ability of the gold(I) catalyst to activate even less reactive substrates.

3.2.4 Reaction IV

The divergent results of Reaction III made it interesting to introduce other electron withdrawing groups on the propargyl acetal reagent. The *p*-Cl substituted propargyl acetal **5d** was mixed with phenylpropyne **6** in the gold(I) cayalyzed reaction as presented in Scheme 3.7.

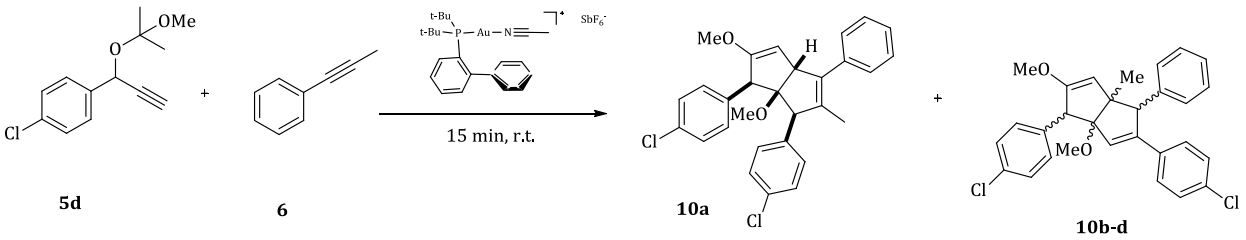

Scheme 3.7*: Reaction IV.*

The reaction was monitored by GLC and TLC and showed a quite similar product composition as observed in Reaction I. The TLC is presented in Figure 3.11.

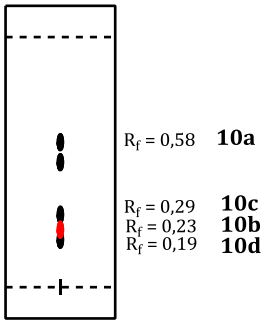

Figure 3.11*: TLC of product crude in reaction I. Eluent 10:1 pentane:ethyl acetate*

Four different products **10a-d** were isolated and characterized in this reaction. **10b-d** appeared to be analogous to compounds **7a-c.** The unique features, which were explained in the latter part of Subsection 3.2.1, were recognized in these three products. Chemical shifts and proposed stereochemistry of compounds **10b-d** are presented in Figures 3.12-3.14.

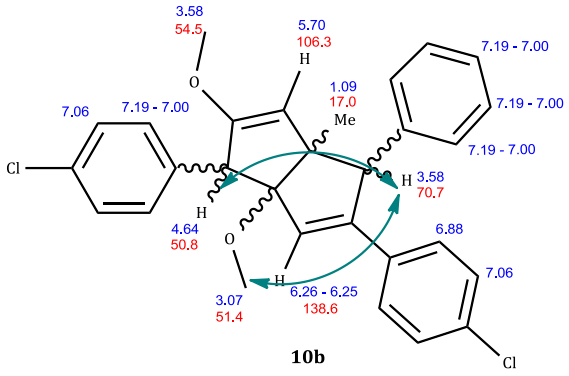

Figure 3.12*: Chemical shifts and NOE correlations of compound **10b.***

The stereochemistry of compound **10b** could not be determined, as was the case for compound **7a**, due to insufficient data to distinguish these two compounds from product **8a**.

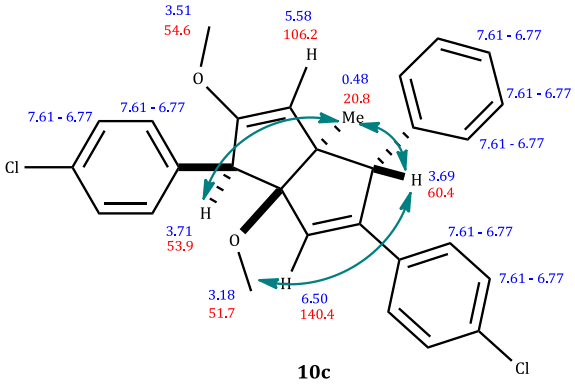

Figure 3.13*: Chemical shifts and NOE correlations of compound **10c.***

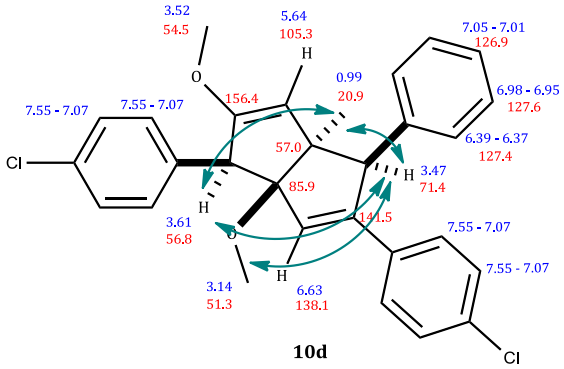

Figure 3.14*: Chemical shifts and NOE correlations of compound **10d.***

Products **10b** and **10d** were successfully isolated, but product **10c** could only be obtained in a mixture with product **10b**. Compound **10c** could still be partially characterized by comparison of NMR data of the mixture of **10b** and **10c** and NMR data of the pure compound **10b** (Appendices M, N).

Much effort was spent on elucidating the regio- and stereochemistry of products **7a-c** and **10b-d.** With this work accomplished, the new focus was on the upper spots observed on the TLC in Figure 3.11. Product **10a** was isolated in a relatively good yield (7%) compared to the other products. From ^{1}H and ^{13}C NMR experiments (Appendices L-1, L-2) it could be concluded that product **10a** also was a result of a tandem cyclization reaction. However, this product seemed to have a different regiochemistry than the previous products **10b-d**.

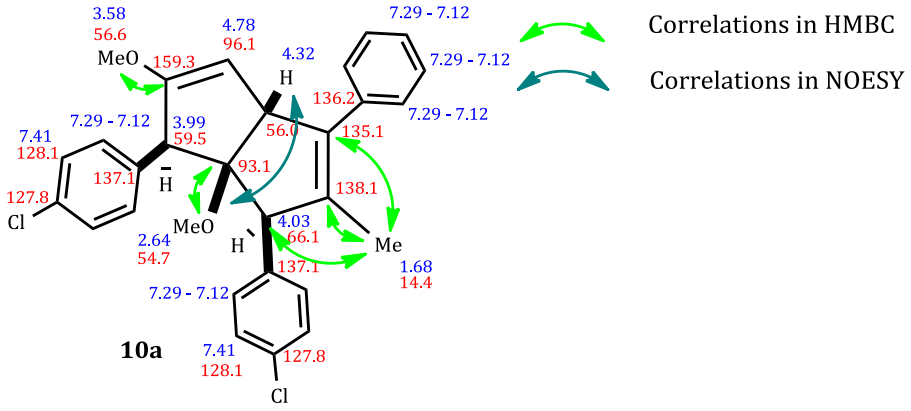

Figure 3.15*: Chemical shifts and NOE correlations of compound **10a.***

In the HSQC (Appendix L-3) of product **10a** it was observed that three protons were attached to sp^3-hybridized carbon atoms, which differed from products **10b-d**. By analyzing 2D correlation NMR spectra, Prof. A. Fiksdahl proposed the structure presented in Figure 3.15. Product **10a** is most likely produced through a [3+2] cycloaddition to form the five membered intermediate **XVIb** similar to Step 1 in the formation product **9** (Scheme 3.5). Then a second [3+2] cyclization reaction, similar to the last step *(E)* of the tandem cyclization reaction presented in Scheme 3.1, occurs to form product **10a**.

The stereochemistry in product **10a** seems to be quite similar to the compound synthesized by Gung et.al[5] which was described in Scheme 2.8 in Subsection 2.3.2 in the Theory part.

3.2.5 Deuterium labeled experiment

As a mechanism for the formation of compounds **7a-c**, **8a-b** and **10b-d** was proposed, it was appropriate to perform a deuterium labeled experiment to confirm it. A rough sketch of the complete syntheses is presented in Scheme 3.8.

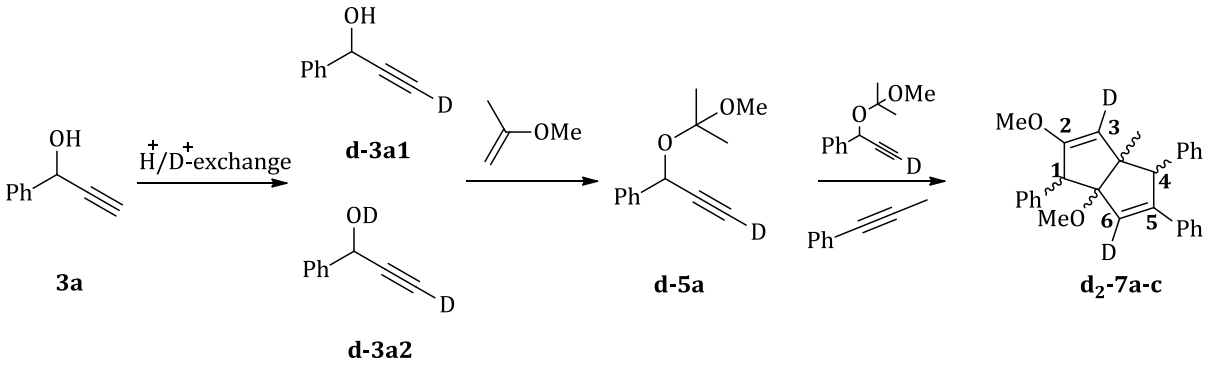

Scheme 3.8*: Deuterium labeled experiment*

The deutarated propargyl alcohols **d-3a1** and **d-3a2** were prepared in accordance to literature. [30] From ^{1}H and ^{13}C NMR spectra it was obvious that a mixture of these two compounds was obtained (Appendices P-1, P-2). Full conversion of the propargylic alcohol **3a** was not achieved; hence, small traces of undeuterated products would occur throughout the following syntheses. The observed triplets in the ^{13}C NMR spectrum of **d-3a1-2** (^{13}C δ (ppm) = 83.0, 74.5) (which also are observed in the ^{13}C NMR spectrum of **d-5a**) are due to the splitting between ^{13}C and ^{2}D, as the carbon NMR experiment is not decoupled regarded to deuterium. This is explained in Figure 3.16.

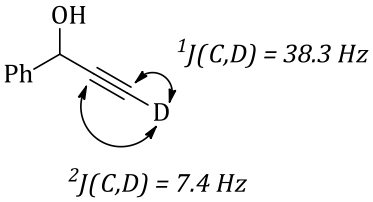

Figure 3.16: *Coupling constants of triplets observed in ^{13}C NMR spectrum for deuterated compounds* ***d-3a1-2.***

The coupling between deuterium and the non-terminal carbon in compounds ***d-3a1-2*** (^{13}C δ = 83.0 ppm), $^{2}J(C,D)$=7.4 Hz, occurs probably due to the tight triple bond, which allows the distance between the two nuclei to be shorter.

The deuterated propargylic acetal **d-5a** was synthesized following a known procedure [21] and was used in the synthesis of **d_2-7a-c**. It would be interesting to see if the ^{1}H NMR signals of the methine protons in products **7a-c** would be absent. The ^{1}H NMR spectrum of **d_2-7c** (Appendix R-1) shows only traces of the actual ^{1}H NMR signals of H-3 and H-6 (^{1}H δ (ppm) = 6.64, 5.66) for compound **7c**. Similar observations were made for compounds **d_2-7a** and **d_2-7b**. This supports the proposed reaction mechanism presented in Scheme 3.2.

3.2.6 Optimization reactions

Several gold(I) catalyzed cyclization reactions involving propargyl acetals and esters have been performed by the group of *Fiksdahl.*[21,18] Optimization reactions considering both the catalyst and solvents has previously been conducted on different cyclization reactions.[18, 35] Based on these results, catalyst **Ib** was used in Reactions I-IV in this thesis as well. After isolation and characterization of the unexpected complex products had been carried out to the best of our abilities, a range of different catalysts were screened to see if this could have an effect on yields and stereo-/regioselectivity. The results of these screening reactions are presented in Table 3.4.

Table 3.4*: Optimization studies of gold(I) catalyzed cyclization reactions*

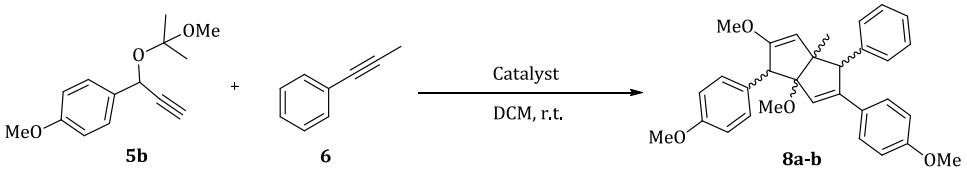

Entry	Catalyst		Time	Conversion[a]
1	Au(I)[P(*t*-Bu)$_2$(*o*-biphenyl)CH$_3$CN]SbF$_6$	**Ib**	15 min	99%
2	Au(I)[P(*t*-Bu)$_2$(*o*-biphenyl)Cl	**Id**	24 h	nc
3	Au(I)[P(*t*-Bu)$_2$(*o*-biphenyl)Cl+AgSbF$_6$	**Ic**	1 h	80%
4	Au(I)[P(*t*-Bu)$_2$(*o*-biphenyl)Cl+AgNTf$_2$	**Ie**	15 min	99%
5	Au(I)(PPh$_3$)Cl+AgSbF$_6$	**If**	15 min	nc[b]
6	Au(I)(PPh$_3$)Cl	**Ig**	24 h	nc
7	PicAu(III)Cl$_2$	**Ih**	15 min	99%
8	AgSbF$_6$	**Ii**	15 min	nc[b]
9	AgNTf$_2$	**Ij**	15 min	nc[b]

[a]Observed by GLC, [b]full conversion of propargyl acetal **5b**, but not to desired products.

Gold(I) catalyst **Ib** is used in all cyclization reactions in this thesis. Additionally, gold(I) catalysts **Ic** and **Ie** provided high yields of the tandem cyclization products **8a-b**. The active gold(I) catalysts **Ic** and **Ie** are formed by an ion exchange reaction which was presented in Scheme 2.10 in Subsection 2.3.3. What is common for the three catalysts **Ib**, **Ic** and **Ie** is the presence of counter ions. Counter ions appeared to be important in order of cyclization reactions take place. In the case of gold(I) catalyst, where no counter ion is present, no conversion was observed. Similar results have previously been observed in the *Fiksdahl group*[18, 35].

The high activity of gold(III) catalyst **Ih** was a bit surprising, as it previously had only given moderate yields in cyclization reactions reported by the group. Silver(I) catalysts **Ii** and **Ij** gave

full conversion of the propargyl acetal **5b** in 15 minutes, but the desired products **8a-b** were not formed. A PhD student in the group[46] carried out the reaction with silver(I) catalyst **Ii** in a bigger scale and isolated the major product **XVII** in 25% yield.

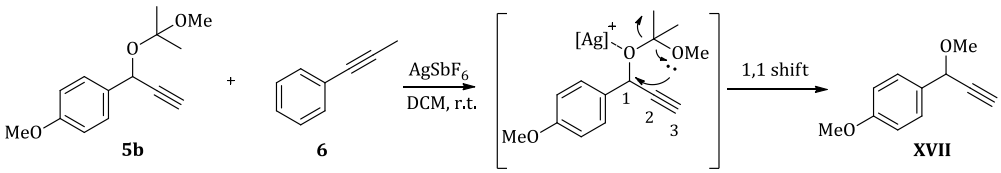

Scheme 3.9*: Mechanism for the silver(I) catalyzed formation of product **XVII***

The silver(I) catalyst have higher affinity to the oxygen atom rather than to the triple bond and will function as a Lewis acid towards oxygen. C-1 is then activated for nucleophile attack and a 1,1 shift of the alkoxy (OMe) occurs to form product **XVII.** Silver(I) activation of propargyl alcohols to form propargyl ethers have previously been reported[40].

Gold(I) catalyst **If** gave full conversion after 15 minutes, but desired products were not observed. By comparison of peaks in GLC, a product similar to **XVII** may have been produced.

3.3 Further work

The experimental work in the present project was quite time consuming and the main focus was to purify and characterize the new obtained products from Reactions I-IV. Real yields may be higher since the objective was to obtain sufficiently pure products for characterization. Product isolation and purification was at times challenging and due to time limitations, all reactions and the following purifications could not be repeated.

In Reaction I, there are indications of the formation of analogues to both product **8a**, which was observed in Reaction II, and product **10a**, which was observed in Reaction IV. The analogue to product **8a** was also observed (but not isolated) in Reaction IV. A repetition of Reaction I and IV, perhaps with bigger amounts of starting materials **5a-c** and **6**, should be conducted, as the product compositions in these two reactions seems to be quite complex.

It may be desirable to introduce other ERG or EWG on the propargyl acetal to see if similar regio- and stereoselectivity, as observed in respectively Reaction II and III, will occur. It may also be of interest to polarize the phenylpropyne **6** with both EWG and ERG to see if that may affect the product selectivity. Additionally, introduction of bulky substituents on the aromatic part of the propargyl acetals or phenylalkyne **6** may contribute to higher chemoselectivity.

Chapter 4

Conclusion

Propargyl alcohols **3b-c** were synthesized through a *Grignard reaction.* Propargyl alcohol **3b** was isolated in 54% yield.

Propargyl acetals **5a-c** were synthesized in acid catalyzed reactions from propargyl alcohols **3a-c**. Propargyl acetals **5a** and **5b** were isolated in 63% and 77% yields, respectively.

Previously, gold(I) catalyzed [2+1], [3+2] and [5+2] cyclization reactions have been performed. Propargyl acetals and esters have proven to undergo intramolecular rearrangements to form gold carbenoid and allene intermediates **IVa-c**. Depending on the nature of the substrates, these intermediates undergo different cyclization reactions to form cyclic products. In this thesis, further investigation on gold(I)-catalyzed reactions of propargyl acetals has been done.

Propargyl acetals **5a-d** were treated with 1-phenylprop-1-yne **6** in the presence of gold(I) catalyst **Ib**, and, depending on the electronic character of the propargyl acetal, a number of cyclization products **7-10** were formed.

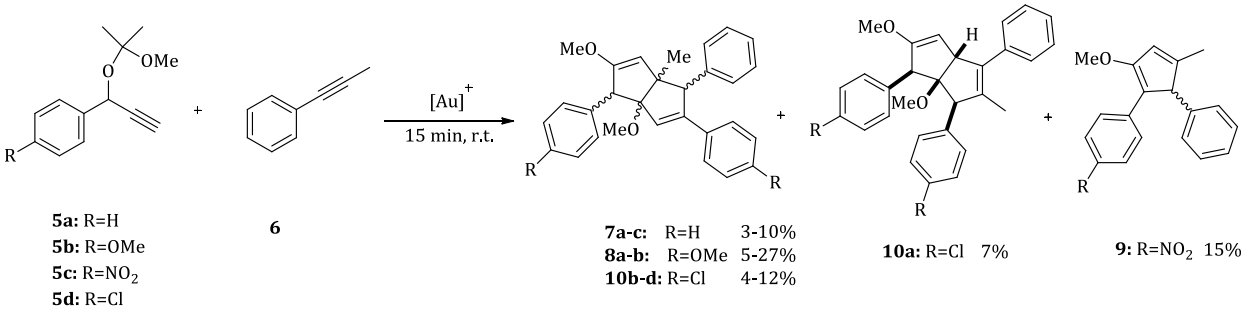

5a: R=H
5b: R=OMe
5c: R=NO_2
5d: R=Cl

6

7a-c: R=H 3-10%
8a-b: R=OMe 5-27%
10b-d: R=Cl 4-12%

10a: R=Cl 7%

9: R=NO_2 15%

The hypothesis that the gold(I)-activated intermediates **IVa-c**, generated from propargyl acetals, seem to be highly reactive towards unsaturated species was confirmed, as they would undergo cyclization reactions even with the poor nucleophillic 1-phenylprop-1-yne **6**.

The chemoselectivity of the reactions proved to vary. In reactions I and IV, products with different regio- and stereochemistry were formed. Tandem cyclization products **7a-c** and **10b-d**, respectively, were diastereomers and followed the same reaction mechanism. Tandem cyclization product **10a** contained a different regiochemistry and followed a different cyclization mechanism.. The analogue compounds **7c** and **10d** were the major products, yielding 10% and 12% respectively, in both reactions. This was also confirmed by GLC of the crude product mixture.

There were indications of several tandem cyclization products being produced in the reaction with propargyl acetal **5b** as well, but in this case, only one major product **8a**, which yielded 27%, and a minor product **8b**, which yielded 5%, were isolated. The introduction of an electron donating substituent on the aromatic part of the propargyl acetal, appeared to drastically increase the product selectivity of the reaction.

The highly deactivated propargyl acetal **5c** did not undergo a tandem cyclization reaction, but rather a single [3+2] cycloaddition. The formation of this product did not follow the same mechanism as some of the major products in the other reactions.

In conclusion, there is still more to be investigated in this exciting area of chemistry.

Chapter 5

Experimental

5.1 General methods

All reactions were performed under inert atmosphere. Solvents and reagents were of synthetic grade and were used directly as supplied from the manufacturer. Dry DCM and THF were obtained from a MB SPS-800 Solvent Purification System (MBraun), and were used directly in the experiments. Thin layer chromatography (TLC) was performed on Merck TLC aluminium sheets, Silica gel 60 F254. The TLC plates were developed by UV-light and a solution of *p*-anisaldehyde stain (5 ml conc. H2SO4, 1.5 ml absolute acetic acid and 3.7 ml *p*-anisaldehyde in 137 ml absolute ethanol) with heating. Gas liquid chromatography (GLC) was performed on a Varian CP-3800 with a FID detector to monitor reactions and observe product selectivity. Supelco VersaFlash system with Versaflash cartridges with 20-45 or 45-75 μm spherical silica based on porous (70 °A) particles was used for flash chromatography.

Infrared spectrometry (IR) was performed on a Nicolet 20SXC FT-IR spectrometer. The spectra were analyzed using EZ OMNIC software. Mass spectrometry (MS) with electron ionization (EI) was performed on a MAT 95XL instrument (TermoQuest Finnigan). Mass spectra with electron spray ionization (ESI) were recorded by Sintef on an Agilent O-ToF instrument. All mass spectra are high resolution (HR-MS).

1D NMR spectra were recorded on Avance DPX 300 MHz and 400 MHz (Bruker) spectrometers. 2D spectra were recorded on the Avance DPX 400 (Bruker) spectrometer. All samples were dissolved in deuterated chloroform with an internal standard of TMS. Spectra were analyzed using TopSpin NMR software (Version 3.0.b.8). Chemical shifts (δ) are given as parts per million (ppm) and coupling constants (J) are given in Hertz (Hz). The peaks are given as singlets (s), doublets (d), triplets (t), quintets (quin), multiplets (m), or as a combination of these. 2D experiments were used to determine the chemical shifts and the configuration of the obtained products.

5.2 Preparation of starting materials

5.2.1 General procedure A: Synthesis of propargyl alcohols

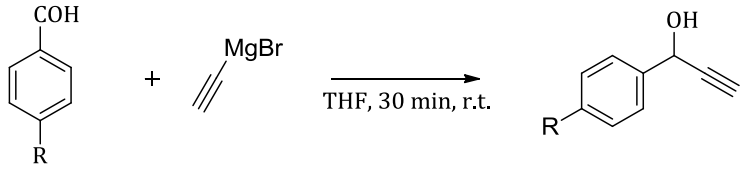

1a: R=OMe
1b: R=NO_2

2

3b: R=OMe
3c: R=NO_2

Propargyl alcohols **3b-c** were synthesized according to known procedure[42]

Ethynylmagnesium bromide **2** (0.5 M in THF) was cooled to -20 ˚C and the relevant aldehyde **1a-b** was dissolved in THF (10 ml) and added drop wise. The reaction was stirred for 30 minutes at room temperature, monitored by TLC and GLC. A saturated solution of NH_4Cl in water was added to the reaction flask. The mixture was filtered, diluted with diethyl ether (20 ml) and the water phase was extracted with diethyl ether (20 ml). The combined organic phases were dried over anhydrous sodium sulfate and concentrated *in vacuo*. The alcohol **3b-c** was isolated by flash chromatography using an appropriate eluent system.

1-(4-Methoxyphenyl)prop-2-yn-1-ol

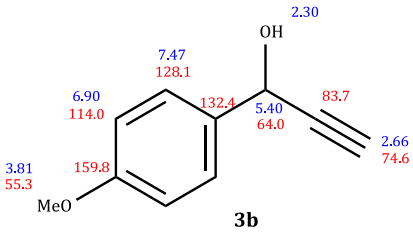

3b

Compound **3b** was synthesized according to General procedure A, using 1-4-methoxybenzaldehyde **1a** (1.0 g, 7.3 mmol) and ethynylmagnesium bromide **2** (18.4 ml, 0.5 M). Flash chromatography with an isocratic eluent of 3:1 pentane:ethyl acetate was used to isolate 1-(4-methoxyphenyl)prop-2-yn-1-ol **3b** (650 mg, 54 %) as a yellow oil.

^{1}H NMR (400 MHz, $CDCl_3$-TMS) (Appendix A-1) δ (ppm) 7.47 (d, 2H, *J* = 8.7 Hz), 6.90 (d, 2H, *J* = 8.7 Hz), 5.40 (s, 1H), 3.81 (s, 3H), 2.66 (d, 1H, *J* = 2.2 Hz), 2.30 (d, 1H, *J* = 4.1 Hz);
^{13}C NMR (400 MHz, $CDCl_3$-TMS) (Appendix A-2) δ (ppm) 159.8 (1C), 132.4 (1C), 128.1 (2C), 114.0 (2C), 83.7 (1C), 74.6 (1C), 64.0 (1C), 55.3 (1C).
Both ^{1}H – and ^{13}C – NMR shifts are consistent with literature.[24]

1-(4-Nitrophenyl)prop-2-yn-1-ol

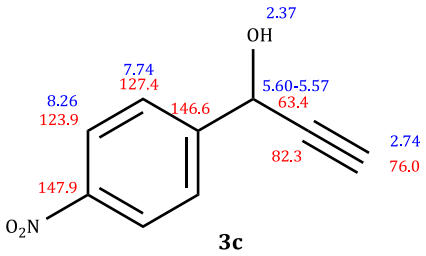

3c

Compound **3c** was synthesized according to General procedure A, using 4-nitrobenzaldehyde **1b** (1.0 g, 6.6 mmol) and ethynylmagnesium bromide **2** (16.5 ml, 0.5 M). The crude product was used further without purification via chromatography after NMR analysis (741 mg) as a yellow solid.

^{1}H NMR (400 MHz, $CDCl_3$-TMS) (Appendix B-1) δ (ppm) 8.26 (d, 2H, *J* = 8.8 Hz), 7.74 (d, 2H, *J* = 8.6 Hz), 5.60-5.57 (m, 1H), 2.74 (d, 1H, *J* = 2.3 Hz), 2.37 (d, 1H, *J* = 5.8 Hz);
^{13}C NMR (400 MHz, $CDCl_3$-TMS) (Appendix B-2) δ (ppm) 147.9 (1C), 146.6 (1C), 127.4 (2C), 123.9 (2C), 82.3 (1C), 76.0 (1C), 63.4 (1C).
Both ^{1}H – and ^{13}C – NMR shifts are consistent with literature.[23]

5.2.2 General procedure B: Synthesis of propargyl acetals[21]

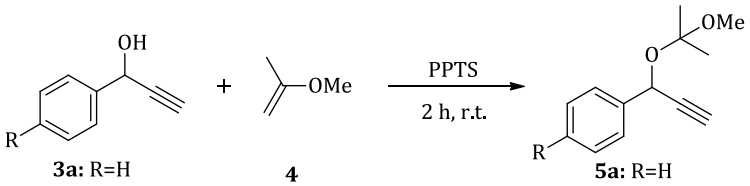

3a: R=H
3b: R=OMe
3c: R=NO_2

4

5a: R=H
5b: R=OMe
5c: R=NO_2

The required propargyl acetal **5a-c** was synthesized according to literature.[21]

A mixture of the relevant propargyl alcohol **3a-c** and the 2-methoxyprop-1-ene **4** was cooled to 0 °C. Catalytic amounts of Pyridinium *p*-toluenesulfonate were added and the reaction mixture was stirred for 2 hours at room temperature, monitored by TLC and GLC. The crude was diluted with diethyl ether (20 ml) and washed with water (3 x 20 ml) and brine (20 ml). The combined organic phases were dried over anhydrous sodium sulfate, filtered and concentrated in *vacuo*. The propargyl acetal **5a-c** was isolated by flash chromatography using an appropriate eluent system.

(1-((2-Methoxypropan-2-yl)oxy)prop-2-yn-1-yl)benzene

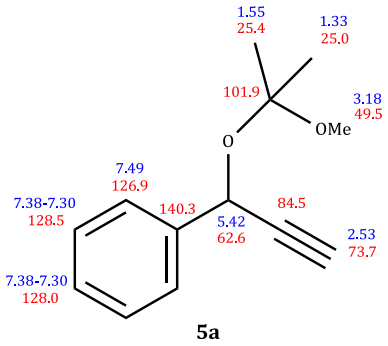

5a

Compound **5a** was synthesized according to General procedure B, using 1-phenylprop-2-yn-1-ol **1a** (513 mg, 3.88 mmol) and 2-methoxyprop-1-ene **4** (5 mL, 52.21 mmol). Flash chromatography with an isocratic eluent of 80:1 pentane:ethyl acetate was used to isolate (1-((2-methoxypropan-2-yl)oxy)prop-2-yn-1-yl)benzene **5a** (601 mg, 77%) as a clear oil.

^{1}H NMR (400 MHz, $CDCl_3$-TMS) (Appendix C-1) δ (ppm) 7.49 (d, 2H, *J* = 7.2 Hz), 7.38-7.28 (m, 3H), 5.42 (d, 1H, *J* = 2.1), 3.18 (s, 3H), 2.53 (d, 1H, *J* = 2.2 Hz), 1.55 (s, 3H), 1.33 (s, 3H);
^{13}C NMR (400 MHz, $CDCl_3$-TMS) (Appendix C-2) δ (ppm) 140.3 (1C), 128.5 (2C), 128.0 (1C), 126.9 (2C), 101.9 (1C), 84.5 (1C), 73.7 (1C), 62.6 (1C), 49.5 (1C), 25.4 (1C), 25.0 (1C).
Both ^{1}H – and ^{13}C – NMR shifts are consistent with literature.[21]

1-Methoxy-4-(1-((2-methoxypropan-2-yl)oxy)prop-2-yn-1-yl)benzene

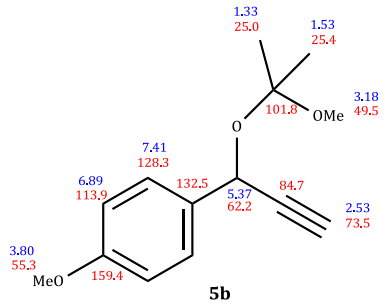

5b

Compound **5b** was synthesized according to General procedure B, using 1-(4-methoxyphenyl)prop-2-yn-1-ol **3b** (506 mg, 3.12 mmol) and 2-methoxyprop-1-ene **4** (5 mL, 52.21 mmol). Flash chromatography with an isocratic eluent of 40:1 pentane:ethyl acetate was used to isolate 1-methoxy-4-(1-((2-methoxypropan-2-yl)oxy)prop-2-yn-1-yl)benzene **5b** (454 mg, 63%) as a clear oil.

^{1}H NMR (400 MHz, $CDCl_3$-TMS) (Appendix D-1) δ (ppm) 7.41 (d, 2H, *J* = 8.6 Hz), 6.89 (d, 2H, *J* = 8.7 Hz), 5.37 (d, 1H, *J* = 2.1 Hz), 3.80 (s, 3H), 3.18 (s, 3H), 2.53 (d, 1H, *J* = 2.2 Hz), 1.53 (s, 3H), 1.33 (s, 3H);
^{13}C NMR (400 MHz, $CDCl_3$-TMS) (Appendix D-2) δ (ppm) 159.4 (1C), 132.5 (1C), 128.3 (2C), 113.9 (2C), 101.8 (1C), 84.7 (1C), 73.5 (1C), 62.2 (1C), 55.3 (1C), 49.5 (1C), 25.4 (1C), 25.0 (1C).
Both ^{1}H- and ^{13}C NMR shifts are consistent with literature.[21]

1-(1-((2-Methoxypropan-2-yl)oxy)prop-2-yn-1-yl)-4-nitrobenzene

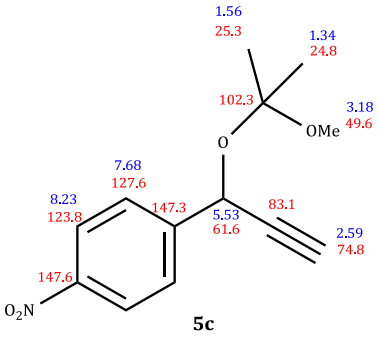

5c

Compound **5c** was synthesized according to General procedure B, using 1-(4-nitrophenyl)prop-2-yn-1-ol **3c** (519 mg, 2.93 mmol) and 2-methoxyprop-1-ene **4** (5 mL, 52.21 mmol). Flash chromatography with an isocratic eluent of 50:1 pentane:ethyl acetate was used to isolate the product **5c** (523 mg, over two steps from **1c**: 31%) as an off white oil.

R_f = 0.38 (10:1 Pentane:EtOAc);
HRMS (EI) calcd for $[M\text{-}CH_3O]^+$ 218.0817, obsd 218.0815;
^{1}H NMR (400 MHz, $CDCl_3$-TMS) (Appendix E-1) δ (ppm) 8.23 (d, 2H, *J* = 8.8 Hz), 7.68 (d, 2H, *J* = 8.7 Hz), 5.53 (d, 1H, *J* = 2.1 Hz), 3.18 (s, 3H), 2.59 (d, 1H, *J* = 2.2 Hz), 1.56 (s, 3H), 1.34 (s, 3H);
^{13}C NMR (400 MHz, $CDCl_3$-TMS) (Appendix E-2) δ (ppm) 147.6 (1C), 147.3 (1C), 127.6 (2C), 123.8 (2C), 102.3 (1C), 83.1 (1C), 74.8 (1C), 61.6 (1C), 49.6 (1C), 25.3 (1C), 24.8 (1C);
IR (thin film, cm^{-1}) (Appendix E-4) 3257, 2992, 2940, 2857, 1517, 1343, 1211, 1186, 1145, 1030, 852, 701.

5.3 Gold catalyzed reactions

5.2.3 General procedure C: Gold catalyzed tandem cyclization reactions

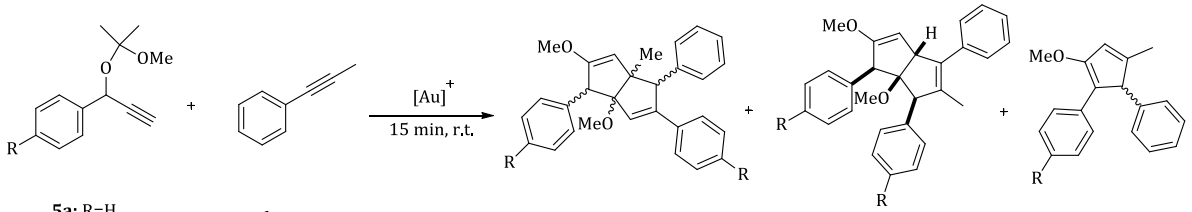

5a: R=H
5b: R=OMe
5c: R=NO_2
5d: R=Cl

6

7a-c: R=H
8a-b: R=OMe
10b-d: R=Cl

10a: R=Cl

9: R=NO_2

The relevant propargyl acetal **5a-d** (1 eq.) and prop-1-yn-1-ylbenzene **6** (3 eq.) were separately dissolved in dichloromethane (1.7mL each) and added to a solution of the catalyst (**Ib**) (5 mol%) in dichloromethane (1.7mL) simultaneously. The reaction was stirred for 15 min at room temperature, monitored by TLC and GLC. The reaction mixture was filtered through celite and concentrated *in vacuo*. The products **7-10** were isolated by flash chromatography using an appropriate eluent system.

Reaction I

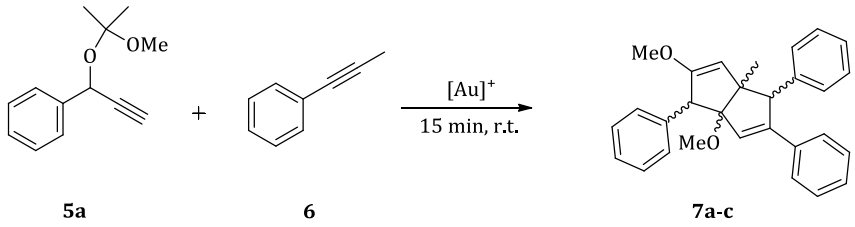

5a **6** **7a-c**

Compounds **7a-c** were synthesized according to General procedure C, using propargylic acetal **5a** (108 mg, 0.53 mmol) and prop-1-yn-1-ylbenzene **6** (185 mg, 1.59 mmol). Flash chromatographies with isocratic eluents of 100:1 pentane:ethyl acetate/50:1 pentane:tetrahydrofuran were used to isolate the products **7a-c**.

2,6a-Dimethoxy-3a-methyl-1,4,5-triphenyl-1,3a,4,6a-tetrahydropentalene

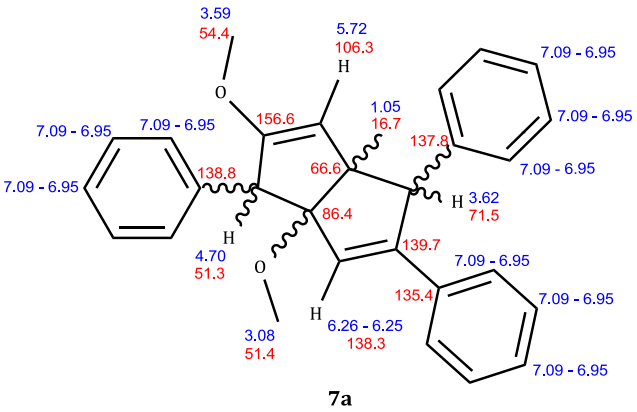

7a

2,6a-Dimethoxy-3a-methyl-1,4,5-triphenyl-1,3a,4,6a-tetrahydropentalene **7a** (3 mg, 3 %) was isolated as an off white liquid.

R_f = 0.29 (20:1 Pentane:THF);
HRMS (EI) calcd for $C_{29}H_{28}O_2$ [M^{*+}] 408.2089, obsd 408.2090;
^{1}H NMR (400 MHz, $CDCl_3$-TMS) (Appendix F-1) δ (ppm) 7.09-6.95 (m, 15H), 6.26-6.25 (m, 1H), 5.72 (s, 1H), 4.70 (s, 1H), 3.62 (s, 1H), 3.59 (s, 3H), 3.08 (s, 3H), 1.05 (d, 3H, J = 1.4 Hz);
^{13}C NMR (400 MHz, $CDCl_3$-TMS) (Appendix F-2) δ (ppm) 156.6 (1C), 139.7 (1C), 138.8 (1C), 138.3 (1C), 137.8 (1C), 135.4 (1C), 129.6 (2C), 128.8 (2C), 127.6 (4C) 127.2 (4C), 126.5 (1C), 125.9 (1C), 125.7 (1C), 106.3 (1C), 86.4 (1C), 71.5 (1C), 66.6 (1C), 54.4 (1C), 51.4 (1C), 51.3 (1C), 16.7 (1C);
IR (cm^{-1}) (thin film, cm^{-1}) (Appendix F-6): 2987, 2955, 2925, 2587, 1490, 1454, 1376, 1183, 1147, 1068, 1013, 872.

(1S,3aR,4R,6aS)-2,6a-Dimethoxy-3a-methyl-1,4,5-triphenyl-1,3a,4,6a-tetrahydropentalene

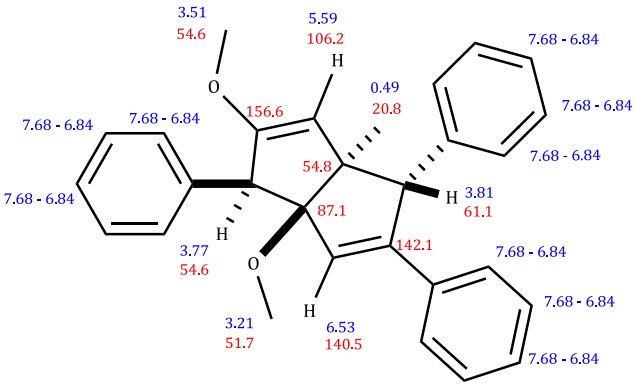

7b

(1S,3aR,4R,6aS)-2,6a-Dimethoxy-3a-methyl-1,4,5-triphenyl-1,3a,4,6a-tetrahydropentalene **7b** (3 mg, 3 %) was isolated as an off white liquid.

R_f = 0.23 (20:1 Pentane:THF);
HRMS (EI) calcd for $C_{29}H_{28}O_2$ [M^{*+}] 408.2089, obsd 408.2086;
^{1}H NMR (400 MHz, $CDCl_3$-TMS) (Appendix G-1) δ (ppm) 7.68-6.84 (m, 15H), 6.53 (m, 1H), 6.59 (s, 1H), 3.81 (s, 1H), 3.77 (s, 1H), 3.51 (s, 3H), 3.21 (s, 3H), 0.49 (s, 3H);
^{13}C NMR (400 MHz, $CDCl_3$-TMS) (Appendix G-2) δ (ppm) 156.6 (1C), 142.1 (1C), 140.5 (1C), 139.5, 137.6, 128.2, 127.9, 127.6, 127.1, 127.0, 126.4, 106.2 (1C), 100.0, 87.1 (1C), 61.1 (1C), 54.8 (1C), 54.6 (1C), 54.6 (1C), 51.7 (1C), 20.8 (1C);
^{13}C NMR does not give sufficient information to assign all the carbon shifts
IR (cm^{-1}) (thin film, cm^{-1}) (Appendix G-4): 2954, 2924, 2869, 2853, 1492, 1453, 1230, 1097, 699, 581, 570.

(1S,3aR,4S,6aS)-2,6a-dimethoxy-3a-methyl-1,4,5-triphenyl-1,3a,4,6a-tetrahydropentalene

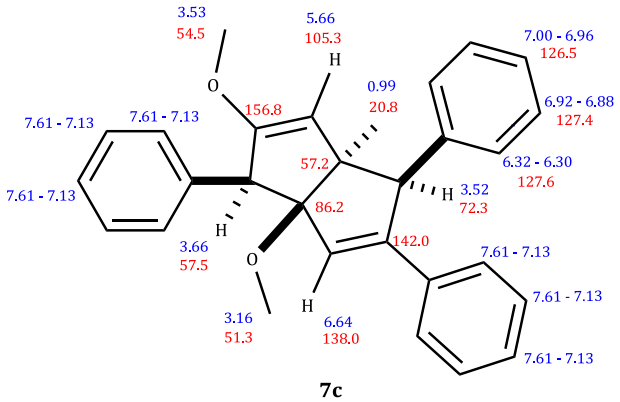

7c

(1S,3aR,4S,6aS)-2,6a-dimethoxy-3a-methyl-1,4,5-triphenyl-1,3a,4,6a-tetrahydropentalene **7c** (10 mg, 10 %) was isolated as an off white liquid.

R_f = 0.34 (15:1 Pentane:EtOAc)
HRMS (EI) calcd for $C_{29}H_{28}O_2$ [M^{*+}]

^{1}H NMR (400 MHz, $CDCl_3$-TMS) (Appendix H-1) δ (ppm) 7.61-7.13 (m, 10H), 7.00-6.96 (m, 1H), 6.92-6.88 (m, 2H), 6.64 (s, 1H), 6.32-6.30 (m, 2H), 5.66 (s, 1H), 3.66 (s, 1H), 3.53 (s, 3H), 3.52 (s, 1H), 3.16 (s, 3H), 0.99 (s, 3H);
^{13}C NMR (400 MHz, $CDCl_3$-TMS) (Appendix H-2) δ (ppm) 156.8 (1C), 142.0 (1C), 138.7 (1C), 138.1 (1C), 138.0 (1C), 136.1 (1C), 132.0 (2C), 128.2 (2C), 128.1 (2C) 127.8 (2C), 127.6 (2C), 127.4 (2C), 127.0 (1C), 126.7 (1C), 126.5 (1C), 105.3 (1C), 86.1 (1C), 72.3 (1C), 57.5 (1C), 57.2 (1C), 54.5 (1C), 51.2 (1C), 20.8 (1C);
IR (cm^{-1}) (thin film, cm^{-1}) (Appendix H-8): 3012, 2952, 2925, 1646, 1490, 1453, 1231, 1096, 1032, 751.

MS data was lost due to unknown reasons.

Reaction II

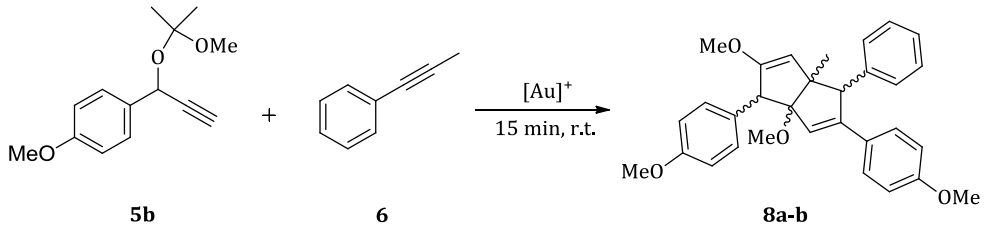

5b **6** **8a-b**

Compounds **8a-b** were synthesized according to General procedure C, using propargylic acetal **5b** (154 mg, 0.64 mmol) and prop-1-yn-1-ylbenzene **6** (224 mg, 1.92 mmol). Flash chromatography with an isocratic eluent of 20:1 pentane:ethyl acetate was used to isolate the products **8a-b**.

2,6a-Dimethoxy-1,5-bis(4-methoxyphenyl)-3a-methyl-4-phenyl-1,3a,4,6a-tetrahydropentalene

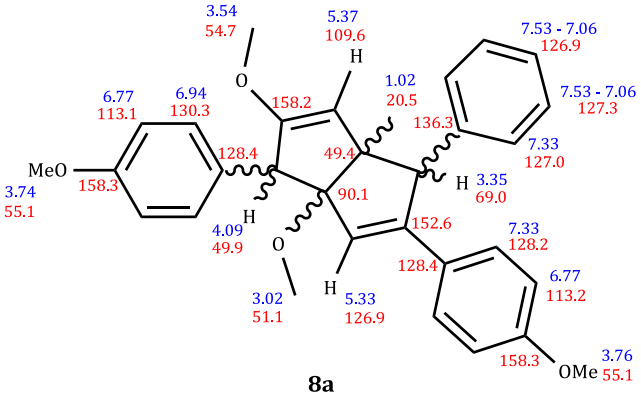

8a

2,6a-Dimethoxy-1,5-bis(4-methoxyphenyl)-3a-methyl-4-phenyl-1,3a,4,6a-tetrahydropentalene **8a** (41 mg, 27%) was isolated as an off white liquid.

R_f = 0.24 (10:1 Pentane:EtOAc);
HRMS (EI) calcd for $C_{31}H_{32}O_4$ [M^{*+}] 468.2301, obsd 468.2299;

^{1}H NMR (400 MHz, $CDCl_3$-TMS) (Appendix I-1) δ (ppm) 7.53-7.06 (m, 3H), 7.33 (d, 4H, *J* = 4.3 Hz), 6.94 (d, 2H, *J* = 8.6 Hz), 6.77 (d, 4H, *J* = 8.6 Hz), 5.37 (s, 1H), 5.33 (s, 1H), 4.09 (s, 1H), 3.76 (s, 3H), 3.74 (s, 3H), 3.54 (s, 3H), 3.35 (s, 1H), 3.02 (s, 3H), 1.02 (s, 3H);
^{13}C NMR (400 MHz, $CDCl_3$-TMS) (Appendix I-2) δ (ppm) 158.3 (1C), 158.2 (1C), 158.2 (1C), 152.6 (1C), 136.3 (1C), 130.3 (2C), 128.4 (2C), 128.2 (2C), 127.3 (2C), 127.0 (2C), 126.9 (1C), 113.2 (2C), 113.1 (2C), 109.6 (1C), 90.1 (1C), 69.0 (1C), 55.1 (1C), 55.1 (1C), 54.6 (1C), 51.1 (1C), 49.9 (1C), 49.4 (1C), 25.6 (1C), 20.5 (1C);
IR (cm^{-1}) (thin film, cm^{-1}) (Appendix I-7): 2919, 2824, 1644, 1610, 1509, 1243, 1177, 1124, 1034, 903, 826, 730, 699.

(1S,3aR,4S,6aS)-2,6a-Dimethoxy-1,5-bis(4-methoxyphenyl)-3a-methyl-4-phenyl-1,3a,4,6a-tetrahydropentalene

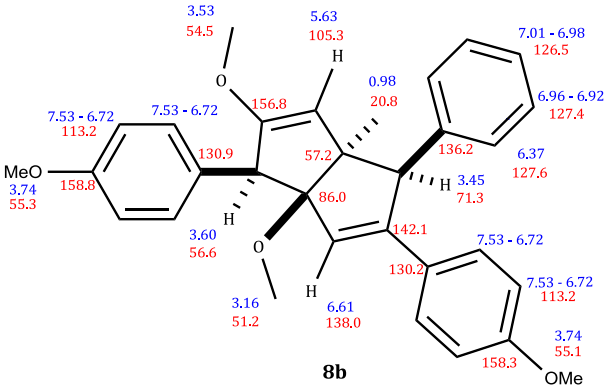

8b

(1S,3aR,4S,6aS)-2,6a-Dimethoxy-1,5-bis(4-methoxyphenyl)-3a-methyl-4-phenyl-1,3a,4,6a-tetrahydropentalene **8b** (12 mg, 61% purity, 5%) was isolated as an off white liquid.

R_f = 0.14 (10:1 Pentane/EtOAc);
HRMS (EI) calcd for $C_{31}H_{32}O_4$ [M^{*+}] 468.2301, obsd 468.2299;
^{1}H NMR (400 MHz, $CDCl_3$-TMS) (Appendix J-1) δ (ppm) 7.53-6.72 (m, 8H), 7.01-6.98 (m, 1H), 6.96-6.92 (m, 2H), 6.61 (s, 1H), 6.37 (d, 2H, *J* = 7.2 Hz), 5.63 (s, 1H), 3.74 (s, 3H), 3.74 (s, 3H), 3.60 (s, 1H), 3.53 (s, 3H), 3.45 (s, 1H), 3.16 (s, 3H), 0.98 (s, 3H);
^{13}C NMR (400 MHz, $CDCl_3$-TMS) (Appendix J-2) δ (ppm) 158.8 (1C), 158.3 (1C), 156.8 (1C) 142.1 (1C), 138.0 (1C), 136.2 (1C), 132.9 (2C), 130.9 (1C), 130.2 (1C), 128.9 (2C), 127.6 (2C) 127.4 (2C), 126.5 (1C), 113.2 (4C), 105.3 (1C), 86.0 (1C), 71.4 (1C), 57.2 (1C), 56.6 (1C), 55.4 (1C), 55.1 (1C), 54.5 (1C), 51.2 (1C), 20.8 (1C);
IR (cm^{-1}) (Appendix J-7)

Reaction III

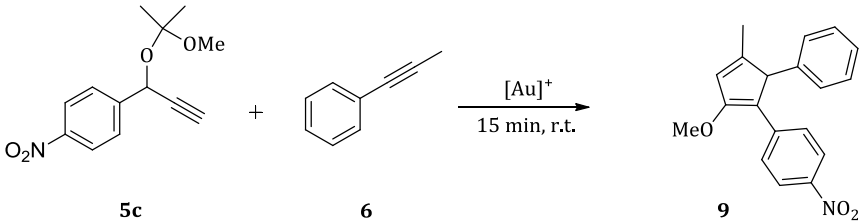

5c **6** **9**

Compound **9** was synthesized according to General procedure C, using propargylic acetal **5c** (202 mg, 0.81 mmol) and prop-1-yn-1-ylbenzene **6** (284 mg, 2.43 mmol). Flash chromatography with an isocratic eluent of 60:1 pentane:ethyl acetate was used to isolate product **9**.

1-(3-Methoxy-4-methyl-5-phenylcyclopenta-1,3-dien-1-yl)-4-nitrobenzene

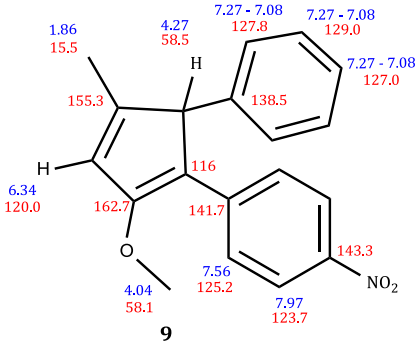

9

1-(3-Methoxy-4-methyl-5-phenylcyclopenta-1,3-dien-1-yl)-4-nitrobenzene **9** (18 mg, 15 %) was isolated as an orange solid.

R_f = 0.43 (5:1 Pentane:EtOAc);
HRMS (EI) calcd for $C_{19}H_{17}NO_3$ [M^{*+}] 308.1287, obsd 308.1287;
^{1}H NMR (400 MHz, $CDCl_3$-TMS) (Appendix K-1) δ (ppm) 7.97 (d, 2H, *J* = 9.2 Hz), 7.56 (d, 2H, *J* = 9.1 Hz), 7.27-7.08 (m, 5H), 6.34 (s, 1H), 4.27 (s, 1H), 4.04 (s, 3H), 1.86 (d, 3H, *J* = 1.3 Hz)
^{13}C NMR (400 MHz, $CDCl_3$-TMS) (Appendix K-2) δ (ppm) 162.7 (1C), 155.3 (1C), 143.3 (1C), 141.7 (1C), 138.5 (1C), 129.0 (2C), 127.8 (2C), 127.0 (1C), 125.2 (2C), 123.7 (2C), 120.0 (1C), 116.5 (1C), 58.5 (1C), 58.1 (1C), 15.5 (1C);
IR (cm^{-1}) (thin film, cm^{-1}) (Appendix K-6): 2924, 2841, 1589, 1515, 1331, 1315, 1107, 852, 752, 735, 699.

Reaction IV

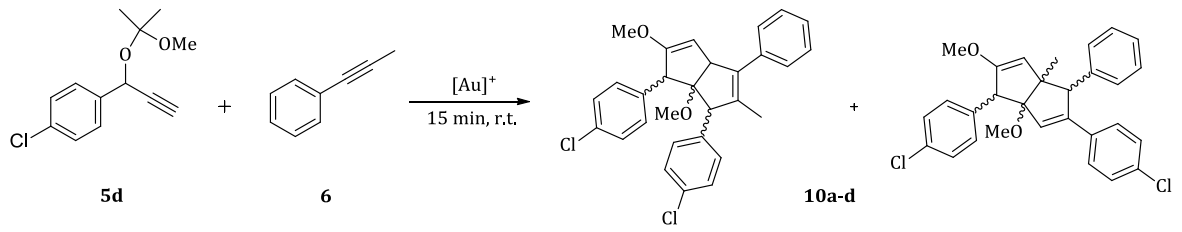

5d **6** **10a-d**

Compounds **10a-d** were synthesized according to General procedure C, using propargylic acetal **5d** (110 mg, 0.46 mmol) and prop-1-yn-1-ylbenzene **6** (161 mg, 1.38 mmol). Flash chromatography with an isocratic eluent of 100:1 pentane:ethyl acetate was used to isolate the products **10a-d**.

(1S,3aR,6S,6aS)-1,6-bis(4-Chlorophenyl)-5,6a-dimethoxy-2-methyl-3-phenyl-1,3a,6,6a-tetrahydropentalene

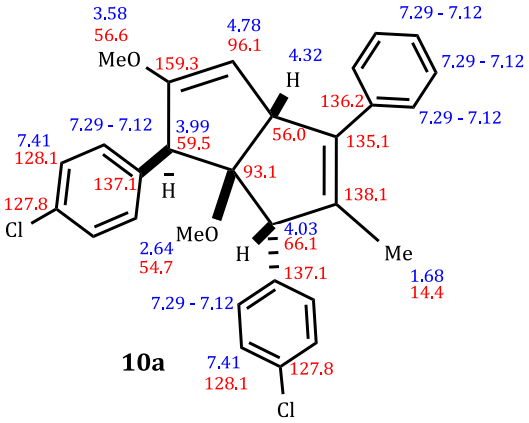

(1S,3aR,6S,6aS)-1,6-bis(4-Chlorophenyl)-5,6a-dimethoxy-2-methyl-3-phenyl-1,3a,6,6a-tetrahydropentalene **10a** (7 mg, 7 %) was isolated as an off white liquid.

R_f = 0.58 (10:1 Pentane:EtOAc)
HRMS (EI) calcd for $C_{29}H_{26}Cl_2O_2$ [M^{*+}] 477.1385, obsd 477.1388;
^{1}H NMR (400 MHz, $CDCl_3$-TMS) (Appendix L-1) δ (ppm) 7.41 (d, 4H, *J* = 4.3 Hz), 7.29-7.12 (m, 9H), 4.78 (s, 1H), 4.32 (s, 1H), 4.03 (s, 1H), 3.99 (s, 1H), 3.58 (s, 3H), 2.64 (s, 3H), 1.68 (s, 3H);
^{13}C NMR (400 MHz, $CDCl_3$-TMS) (Appendix L-2) δ (ppm) 159.3 (1C), 138.1 (1C), 137.1 (1C), 137.1 (1C), 136.2 (1C), 135.1 (1C), 132.5 (1C), 131.4 (2C), 130.8 (2C), 128.3 (2C), 128.2 (2C), 128.2 (2C), 128.1 (2C), 127.8 (2C), 96.1 (1C), 93.1 (1C), 66.1 (1C), 59.5 (1C), 56.6 (1C), 56.0 (1C), 54.7 (1C), 14.4 (1C);
IR (cm^{-1}) (thin film, cm^{-1}) (Appendix L-7): 2950, 2919, 1646, 1490, 1340, 1225, 1090, 1014, 701.

1,5-bis(4-Chlorophenyl)-2,6a-dimethoxy-3a-methyl-4-phenyl-1,3a,4,6a-tetrahydropentalene

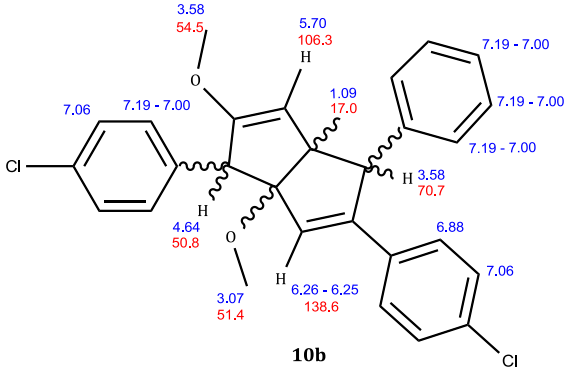

A mixture of products **10b** and **10c** (10 mg, 64% of **10b** and 36% of **10c**) were isolated as an off white liquid.

R_f = 0.23 (10:1 Pentane:EtOAc);
HRMS (EI) calcd for $C_{29}H_{28}O_2Cl_2$ [M^{*+}] 476.1310, obsd 476.1309;
^{1}H NMR (400 MHz, $CDCl_3$-TMS) (Appendix M-1 and N-1) δ (ppm) 7.19-7.00 (m, 7H), 7.06 (d, 4H, *J* = 8.4 Hz), 6.88 (d, 2H, *J* = 8.6 Hz), 6.26-6.25 (m, 1H), 5.70 (s, 1H), 4.64 (s, 1H), 3.58 (s, 3H), 3.07 (s, 3H), 1.09 (d, 3H, *J* = 1.3 Hz);

^{13}C NMR (400 MHz, $CDCl_3$-TMS) (Appendix M-2) δ (ppm) 138.6 (1C), 106.3 (1C), 70.7 (1C), 54.5 (1C), 51.5 (1C), 50.8 (1C), 17.0 (1C);
^{13}C NMR does not give sufficient information to assign all the carbon shifts
IR (cm^{-1}) (thin film, cm^{-1}) (Appendix M-7): 2955, 2923, 2867, 1490, 1257, 1091, 1014, 817, 742, 703, 568.

(1S,3aR,4R,6aS)-2,6a-dimethoxy-3a-methyl-1,4,5-triphenyl-1,3a,4,6a-tetrahydropentalene

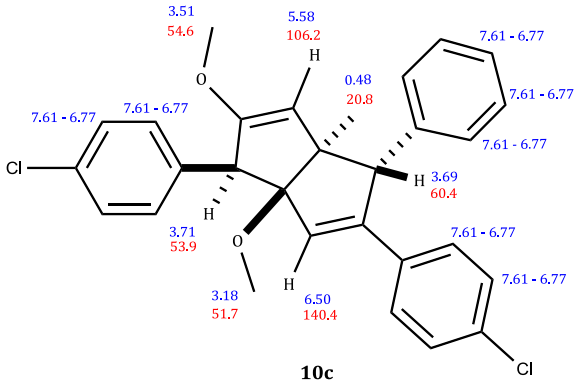

10c

A mixture of products **10b** and **10c** (10 mg, 64% of **10b** and 36% of **10c**) were isolated as an off white liquid.

R_f = 0.29 (10:1 Pentane:THF)
HRMS (EI) calcd for $C_{29}H_{26}O_2Cl_2$ [M^{*+}] 476.1310, obsd 476.1310;
^{1}H NMR (400 MHz, $CDCl_3$-TMS) (Appendix M-1) δ (ppm) 7.68-6.84 (m, 15H), 6.53 (m, 1H), 6.59 (s, 1H), 3.81 (s, 1H), 3.77 (s, 1H), 3.51 (s, 3H), 3.21 (s, 3H), 0.49 (s, 3H)
^{13}C NMR (400 MHz, $CDCl_3$-TMS) (Appendix M-2) δ (ppm) 156.6 (1C), 142.1 (1C), 140.5 (1C), 139.5, 137.6, 128.2, 127.9, 127.6, 127.1, 127.0, 126.4, 106.2 (1C), 100.0, 87.1 (1C), 61.1 (1C), 54.8 (1C), 54.6 (1C), 54.6 (1C), 51.7 (1C), 20.8 (1C);
^{13}C NMR does not give sufficient information to assign all the carbon shifts.
IR (cm^{-1}) (thin film, cm^{-1}) (Appendix M-7): 2955, 2923, 2867, 1490, 1257, 1091, 1014, 817, 742, 703, 568.

(1S,3aR,4S,6aS)-1,5-bis(4-Chlorophenyl)-2,6a-dimethoxy-3a-methyl-4-phenyl-1,3a,4,6a-tetrahydropentalene

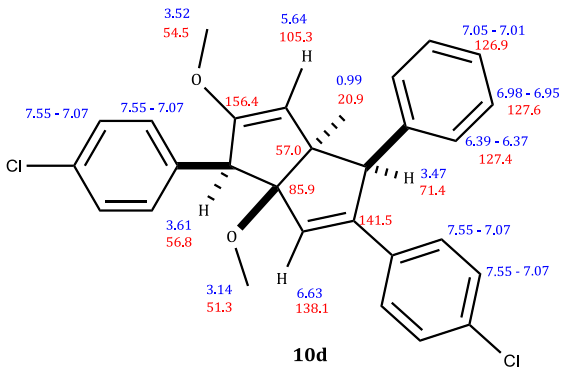

10d

(1S,3aR,4S,6aS)-1,5-bis(4-Chlorophenyl)-2,6a-dimethoxy-3a-methyl-4-phenyl-1,3a,4,6a-tetrahydropentalene **10d** (12 mg, 12%) was isolated as an off white liquid.

R_f = 0.19 (10:1 Pentane/EtOAc);
HRMS (EI) calcd for $C_{29}H_{26}O_2Cl_2$ [$M^{\cdot+}$] 476.1310, obsd 476.1309;
^{1}H NMR (400 MHz, $CDCl_3$-TMS) (Appendix O-1) δ (ppm) 7.55-7.07 (m, 8H), 7.05-7.01 (m, 1H), 6.98-6.95 (m, 2H), 6.63 (s, 1H), 6.39-6.37 (m, 2H), 5.64 (d, 1H, *J* = 1.1 Hz), 3.61 (s, 1H), 3.52 (s, 3H), 3.47 (s, 1H), 3.14 (s, 3H), 0.99 (s, 3H)
^{13}C NMR (400 MHz, $CDCl_3$-TMS) (Appendix O-2) δ (ppm) 156.4 (1C), 141.5 (1C), 138.1 (1C), 137.1 (1C), 136.4 (1C), 135.7 (1C), 133.2 (2C), 133.0 (1C), 132.6 (1C) 129.5 (2C), 128.2 (2C), 128.1 (2C), 127.6 (2C), 127.4 (2C), 126.9 (1C), 105.3 (1C), 85.9 (1C), 71.4 (1C), 57.0 (1C), 56.8 (1C), 54.5 (1C), 51.3 (1C), 20.9 (1C);
IR (cm^{-1}) (thin film, cm^{-1}) (Appendix O-7): 2919, 2839, 1639, 1490, 1445, 1226, 1091, 1014, 838, 813, 741, 702.

5.4 Deuterated experiment

Proton-deuterium exchange on propargyl alcohol 3a

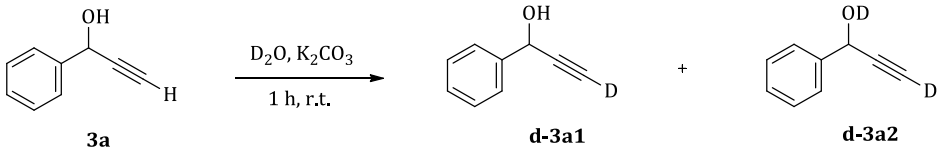

The propargyl alcohol **3a** (511 mg, 3.87 mmol) was added to a solution of D_2O (10 ml) and K_2CO_3 (548 mg, 3.97 mmol) and the reaction mixture was stirred for one hour. The water phase was extracted with dichloromethane (3*10 ml) and the combined organic phases were dried over anhydrous sodium sulfate and concentrated *in vacuo*. An unpurified mixture of the products **d-3a1-2** (454 mg) was obtained as a yellow oil.

Both ^{1}H- and ^{13}C NMR shifts (Appendix P-1, P-2) are consistent with literature.[30]

Deuteurated propargyl acetal

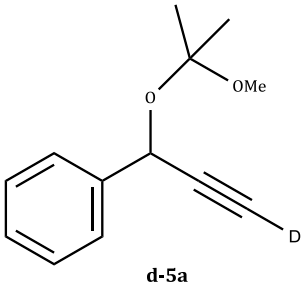

Compound **d-5a** was synthesized according to General procedure B, using the mixture of propargyl alcohols **d-3a1-2** (430 mg, 3.25 mmol) and 2-methoxyprop-1-ene (**4**) (5 mL, 52.21 mmol). The unpurified product **d-5a** (353 mg) was obtained as a yellow oil.

^{1}H NMR (400 MHz, $CDCl_3$-TMS) (Appendix Q-1) δ (ppm) 7.49 (d, 2H, *J* = 7.2 Hz), 7.37-7.27 (m, 3H), 5.42 (s, 1H), 3.18 (s, 3H), 1.54 (s, 3H), 1.33 (s, 3H);
^{13}C NMR (400 MHz, $CDCl_3$-TMS) (Appendix Q-2) δ (ppm) 140.2 (1C), 128.5 (2C), 127.9 (1C), 126.8 (2C), 101.8 (1C), 84.0 (1C), 73.4 (1C), 62.5 (1C), 49.4 (1C), 25.4 (1C), 24.9 (1C);
Both ^{1}H- and ^{13}C NMR shifts are consistent with literature.[21]

Gold(I) catalyzed cyclization reaction with deutirized propargyl acetal d-5a

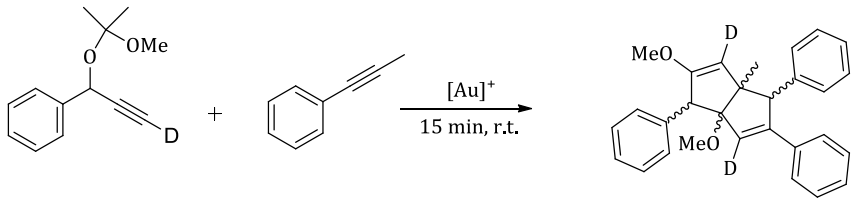

d-5a **6** **d_2-7a-c**

Compounds **d_2-7a-c** were synthesized according to General procedure C, using the propargylic acetal **d-5a** (160 mg, 0.78 mmol) and prop-1-yn-1-ylbenzene **6** (274 mg, 2.35 mmol). Flash chromatography with an isocratic eluent of 70:1 pentane:methyl tetrahydrofuran was used to isolate the products **d_2-7a-c**.

^{1}H NMR data for compound **d_2-7c:**

^{1}H NMR (400 MHz, $CDCl_3$-TMS) (Appendix H-1) δ (ppm) 7.61-7.13 (m, 10H), 7.00-6.96 (m, 1H), 6.92-6.88 (m, 2H), 6.32-6.30 (m, 2H), 3.66 (s, 1H), 3.53 (s, 3H), 3.52 (s, 1H), 3.16 (s, 3H), 0.99 (s, 3H);

Only traces of the two peaks (^{1}H δ (ppm) = 6.64, 5.66) in product **7c** can be observed in the ^{1}H NMR spectrum for the deuterated product **d_2-7c.**

Bibliography

1 Philippe Belmont, and Evelyne Parker, 'Silver and Gold Catalysis for Cycloisomerization Reactions', *European Journal of Organic Chemistry,* 2009 (2009), 6075-89.

2 M. Black, R. H. B. Mais, and P. G. Owston, 'The Crystal and Molecular Structure of Zeise's Salt, Kptcl3.C2h4.H2o', *Acta Crystallographica Section B,* 25 (1969), 1753-59.

3 F.A. Carey, *Organic Chemistry*. 7 edn (New York: McGraw Hill Companies, 2008).

4 G. E. Coates, and C. Parkin, '64. Tertiary Phosphine Complexes of Trimethylgold: Infrared Spectra of Complexes of Gold and Some Other Metals', *Journal of the Chemical Society (Resumed)* (1963), 421-29.

5 Ryan C. Conyers, and Benjamin W. Gung, 'Gold(I)-Catalyzed Divergence in the Preparation of Bicyclic Enol Esters: From Exclusively [3c+2c]-Cycloaddition Reactions to Exclusive Formation of Vinylcyclopropanes', *Chemistry – A European Journal,* 19 (2013), 654-64.

6 Andrea Correa, Nicolas Marion, Louis Fensterbank, Max Malacria, Steven P Nolan, and Luigi Cavallo, 'Golden Carousel in Catalysis: The Cationic Gold/Propargylic Ester Cycle', *Angewandte Chemie,* 120 (2008), 730-33.

7 M. J. S. Dewar, 'A Review of Π Complex Theory', *Bull. Soc. Chim. Fr.* (1951), C79.

8 William A. Donaldson, 'Synthesis of Cyclopropane Containing Natural Products', *Tetrahedron,* 57 (2001), 8589-627.

9 J. D. Dunitz, L. E. Orgel, and A. Rich, 'The Crystal Structure of Ferrocene', *Acta Crystallographica,* 9 (1956), 373-75.

10 R. J. Sundberg F. A. Carey, *Advanced Organic Chemistry, Part B: Reactions and Synthesis* (Springer, 2007).

11 H. Friebolin, *Basic One-and Two-Dimensional Nmr Spectroscopy*. 5 edn (Wiley-VCH, 2011).

12 Alois Fürstner, and Paul W Davies, 'Catalytic Carbophilic Activation: Catalysis by Platinum and Gold Π Acids', *Angewandte Chemie International Edition,* 46 (2007), 3410-49.

13 David Garayalde, Karolin Krüger, and Cristina Nevado, 'Gold-Catalyzed Cyclopenta- and Cycloheptannulation Cascades: A Stereocontrolled Approach to the Scaffold of Frondosins a and B', *Angewandte Chemie International Edition,* 50 (2011), 911-15.

14 David J. Gorin, Benjamin D. Sherry, and F. Dean Toste, 'Ligand Effects in Homogeneous Au Catalysis', *Chemical Reviews,* 108 (2008), 3351-78.

15 V. Grignard, 'Sur Quelques Nouvelles Combinaisons Organométaliques Du Magnésium Et Leur Application À Des Synthèses D'alcools Et D'hydrocabures', *Compt. Rend. ,* 130 (1900), 1322-25.

16 A. Stephen K. Hashmi, 'Gold-Catalyzed Organic Reactions', *Chemical Reviews,* 107 (2007), 3180-211.

17 Scott B. Hoyt, Clare London, David Gorin, Matthew J. Wyvratt, Michael H. Fisher, Catherine Abbadie, John P. Felix, Maria L. Garcia, Xiaohua Li, Kathryn A. Lyons, Erin McGowan, D. Euan MacIntyre, William J. Martin, Birgit T. Priest, Amy Ritter, McHardy M. Smith, Vivien A. Warren, Brande S. Williams, Gregory J. Kaczorowski, and William H. Parsons, 'Discovery of a Novel Class of Benzazepinone Nav1.7 Blockers: Potential Treatments for Neuropathic Pain', *Bioorganic & Medicinal Chemistry Letters,* 17 (2007), 4630-34.

18 Naseem Iqbal, Christian A. Sperger, and Anne Fiksdahl, 'Gold(I)-Catalysed Alkene Cycloaddition Reactions of Propargyl Acetals', *European Journal of Organic Chemistry,* 2013 (2013), 907-14.

19 L. A. Duncanson J. Chatt, *J. Chem. Soc.* (1953), 2929.

20 Henri B. Kagan, and Phat Dang Tuan, 'Asymmetric Catalytic Reduction with Transition Metal Complexes. I. Catalytic System of Rhodium(I) with (-)-2,3-0-Isopropylidene-2,3-Dihydroxy-1,4-

Bis(Diphenylphosphino)Butane, a New Chiral Diphosphine', *Journal of the American Chemical Society,* 94 (1972), 6429-33.

21 Maya Kaur, 'Gold(I) Catalyzed Tandem Cyclization Reactions' (Master thesis, Norwegian University of Science and Technology, 2012).

22 T. J. Kealy, and P. L. Pauson, 'A New Type of Organo-Iron Compound', *Nature,* 168 (1951), 1039-40.

23 Andrej Kolarovič, and Zuzana Fáberová, 'Catalytic Decarboxylation of 2-Alkynoic Acids', *The Journal of Organic Chemistry,* 74 (2009), 7199-202.

24 Manyam Praveen Kumar, and Rai-Shung Liu, 'Zn(Otf)2-Catalyzed Cyclization of Proparyl Alcohols with Anilines, Phenols, and Amides for Synthesis of Indoles, Benzofurans, and Oxazoles through Different Annulation Mechanisms', *The Journal of Organic Chemistry,* 71 (2006), 4951-55.

25 Louis Y. Kuo, Mercouri G. Kanatzidis, Michal Sabat, Andrew L. Tipton, and Tobin J. Marks, 'Metallocene Antitumor Agents. Solution and Solid-State Molybdenocene Coordination Chemistry of DNA Constituents', *Journal of the American Chemical Society,* 113 (1991), 9027-45.

26 B. C. G. Söderberg L. S. Hegedus, *Transition Metals in the Synthesis of of Complex Organic Molecules* (University Science Books, 2010).

27 Fernando López, and José L. Mascareñas, 'Recent Developments in Gold-Catalyzed Cycloaddition Reactions', *Beilstein Journal of Organic Chemistry,* 7 (2011), 1075-94.

28 D.J. Gorin M. J. Johansson, S.T. Staben, F.D. Toste *j. Am. Chem. Soc,* 131 (2005), 2056-57.

29 J. March M.B. Smith, *Advanced Organic Chemistry: Reactions, Mechanisms and Structure*. Vol. 6 (New York: Wiley-Interscience, 2007).

30 Andrei V. Malkov, Laure Gouriou, Guy C. Lloyd-Jones, Ivo Starý, Vratislav Langer, Paul Spoor, Victoria Vinader, and Pavel Kočovský, 'Asymmetric Allylic Substitution Catalyzed by C1-Symmetrical Complexes of Molybdenum: Structural Requirements of the Ligand and the Stereochemical Course of the Reaction', *Chemistry – A European Journal,* 12 (2006), 6910-29.

31 J. A. Mathews, and L. L. Watters, 'The Carbide of Gold', *Journal of the American Chemical Society,* 22 (1900), 108-11.

32 Samuel A. Miller, John A. Tebboth, and John F. Tremaine, '114. Dicyclopentadienyliron', *Journal of the Chemical Society (Resumed)* (1952), 632-35.

33 Masaaki Miyashita, Akira Yoshikoshi, and Paul A. Grieco, 'Pyridinium P-Toluenesulfonate. A Mild and Efficient Catalyst for the Tetrahydropyranylation of Alcohols', *The Journal of Organic Chemistry,* 42 (1977), 3772-74.

34 Gary A. Molander, and Cristina Alonso-Alija, 'Opening of Cyclopropyl Ketones with Smi2. Synthesis of Spirocyclic and Bicyclic Ketones by Intramolecular Trapping of an Electrophile', *Tetrahedron,* 53 (1997), 8067-84.

35 A. Fiksdahl N. Iqbal, 'Gold(I) Catalyzed Benzo[C]Azepin-4-Ol Synthesis by Intermolecular [5 + 2] Cycloaddition ', (Norwegian University of Science and Technology).

36 S. Dìez-Gonzàles N. Marion, S. P. Nolan, *Angew. Chem.,* 118 (2006), 3729–32.

37 A. Guy Orpen, and Neil G. Connelly, 'Structural Systematics: The Role of P-A .Sigma.* Orbitals in Metal-Phosphorus .Pi.-Bonding in Redox-Related Pairs of M-Pa3 Complexes (a = R, Ar, or; R = Alkyl)', *Organometallics,* 9 (1990), 1206-10.

38 J. A. Osborn, F. H. Jardine, J. F. Young, and G. Wilkinson, 'The Preparation and Properties of Tris(Triphenylphosphine)Halogenorhodium(I) and Some Reactions Thereof Including Catalytic Homogeneous Hydrogenation of Olefins and Acetylenes and Their Derivatives', *Journal of the Chemical Society A: Inorganic, Physical, Theoretical* (1966), 1711-32.

39 G. S. Silverman P. E. Rakita, *5. Safe Handling Practices of Industrial Scale Grignard Reagents* (1996).

40 Matthew N. Pennell, Peter G. Turner, and Tom D. Sheppard, 'Gold- and Silver-Catalyzed Reactions of Propargylic Alcohols in the Presence of Protic Additives', *Chemistry – A European Journal,* 18 (2012), 4748-58.

41 R. J. Puddephatt, 'Reactivity and Mechanism in Organogold Chemistry', *Gold Bulletin,* 10 (1977), 108-13.
42 Florian Punner, and Gerhard Hilt, 'Regioselective Solvent-Dependent Benzannulation of Conjugated Enynes', *Chemical Communications,* 48 (2012), 3617-19.
43 R. T. Mathers R. Hoff, 'Frontmatter', in *Handbook of Transition Metal Polymerization Catalysts* (John Wiley & Sons, Inc., 2010), pp. i-xxi.
44 D. Seyferth, 'Cadet's Fuming Arsenical Liquid and the Cacodyl Compounds of Bunsen', *Organometallics,* 20 (2001), 1488-98.
45 Hong C. Shen, 'Recent Advances in Syntheses of Heterocycles and Carbocycles Via Homogeneous Gold Catalysis. Part 1: Heteroatom Addition and Hydroarylation Reactions of Alkynes, Allenes, and Alkenes', *Tetrahedron,* 64 (2008), 3885-903.
46 Melanie Siah, (2013).
47 Masahiro So, Tomoko Kotake, Kenji Matsuura, Makoto Inui, and Akio Kamimura, 'Concise Synthesis of 2-Benzazepine Derivatives and Their Biological Activity', *The Journal of Organic Chemistry,* 77 (2012), 4017-28.
48 Christian A. Sperger, Jørn E. Tungen, and Anne Fiksdahl, 'Gold(I)-Catalyzed Reactions of Propargyl Esters with Vinyl Derivatives', *European Journal of Organic Chemistry,* 2011 (2011), 3719-22.
49 Christian Sperger, Lilian H. S. Strand, and Anne Fiksdahl, 'Gold Catalysed Cyclisation Reactions of 1,6-Diynes Triggered by the Addition of Methanol', *Tetrahedron,* 66 (2010), 7749-54.
50 Michael L. Steigerwald, and William A. Goddard, '2s + 2s Reactions at Transition Metals. Part 3. Dichlorotitanacyclopropane. The Structure and Reactivity of a Metallacyclopropane', *Journal of the American Chemical Society,* 107 (1985), 5027-35.
51 Yoshiaki Sugita, Chikasa Kimura, Hiroki Hosoya, Shiori Yamadoi, and Ichiro Yokoe, 'Synthesis of 4-Oxepanones by the Lewis Acid-Promoted Ring-Expansion Reaction of Cyclopropapyranones', *Tetrahedron Letters,* 42 (2001), 1095-98.
52 T. Hayashi T. Kamikawa, *Synlett* (1997), 163.
53 L. Vaska, and J. W. DiLuzio, 'Activation of Hydrogen by a Transition Metal Complex at Normal Conditions Leading to a Stable Molecular Dihydride', *Journal of the American Chemical Society,* 84 (1962), 679-80.
54 L. Vaska, and John W. DiLuzio, 'Carbonyl and Hydrido-Carbonyl Complexes of Iridium by Reaction with Alcohols. Hydrido Complexes by Reaction with Acid', *Journal of the American Chemical Society,* 83 (1961), 2784-85.
55 Geoffrey Wilkinson, M. Rosenblum, M. C. Whiting, and R. B. Woodward, 'The Structure of Iron Bis-Cyclopentadienyl', *Journal of the American Chemical Society,* 74 (1952), 2125-26.
56 W. C. Zeise, 'Von Der Wirkung Zwischen Platinchlorid Und Alkohol, Und Von Den Dabei Entstehenden Neuen Substanzen', *Annalen der Physik,* 97 (1831), 497-541.
57 Guozhu Zhang, and Liming Zhang, 'Au-Containing All-Carbon 1,3-Dipoles: Generation and [3+2] Cycloaddition Reactions', *Journal of the American Chemical Society,* 130 (2008), 12598-99.

A Propargyl alcohol 3b

A-1 ^{1}H NMR of propargyl alcohol **3b**

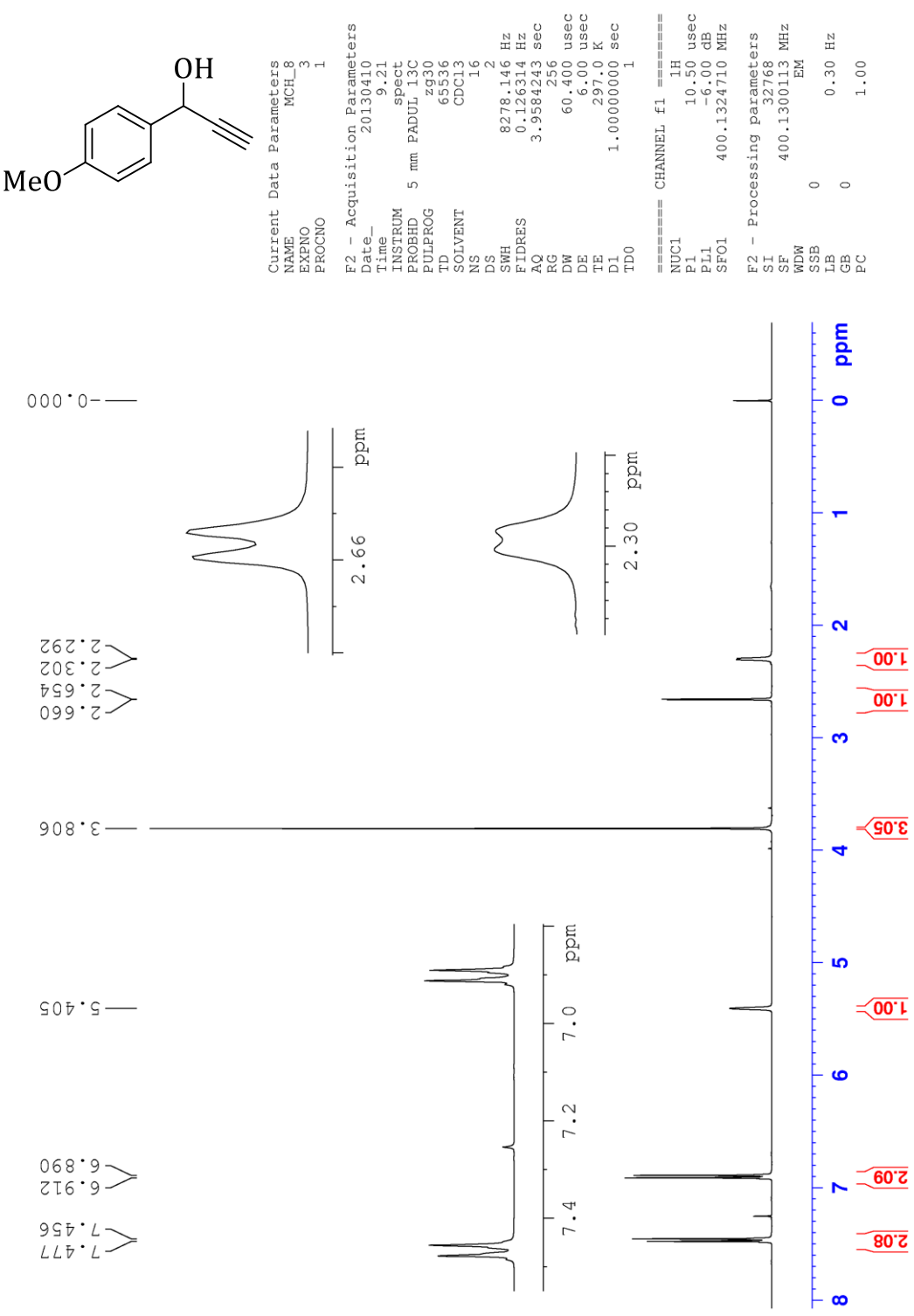

A-2 ^{13}C NMR of propargyl alcohol 3b

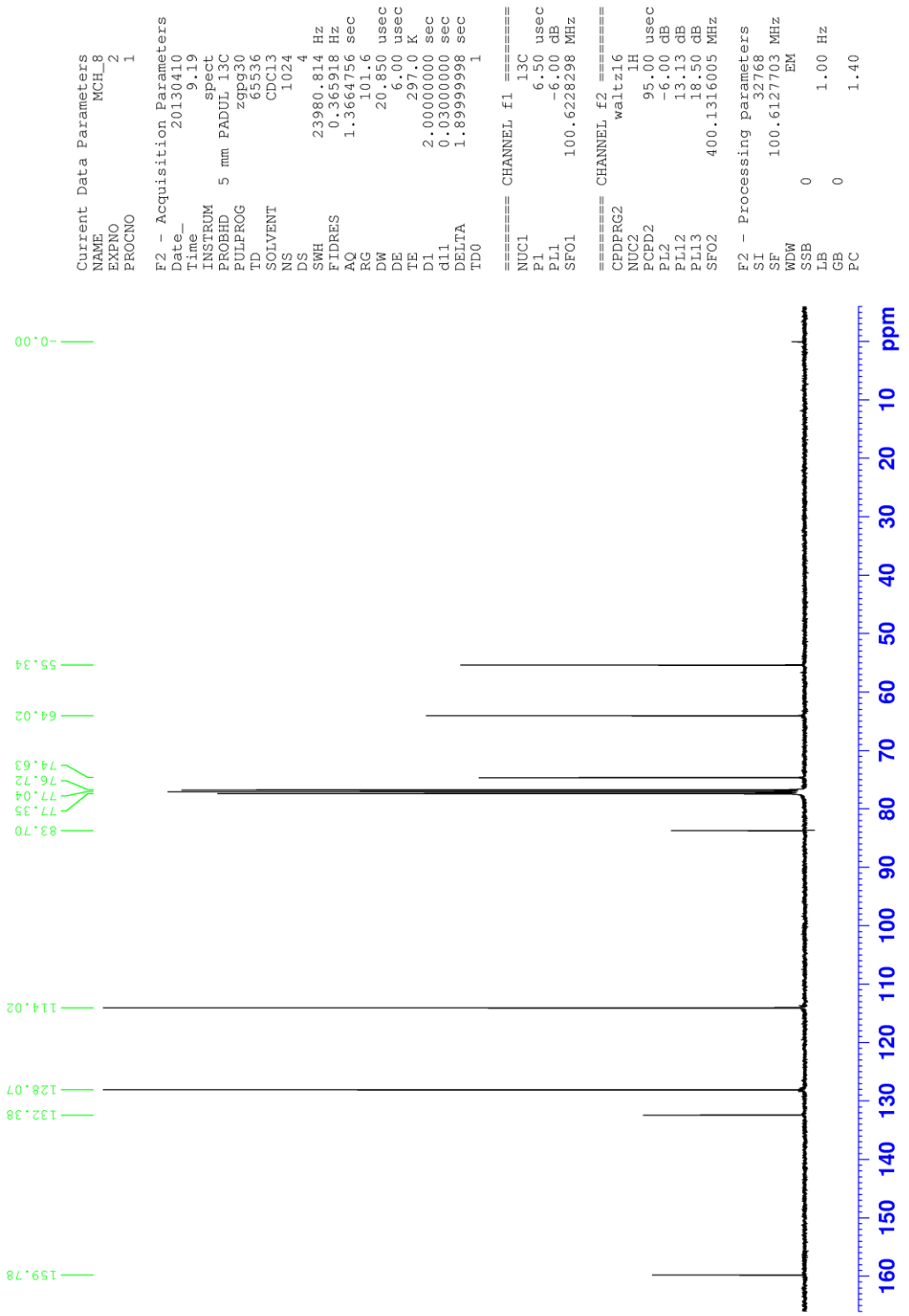

B Propargyl alcohol 3c

B-1 ^{1}H NMR of propargyl alcohol **3c**

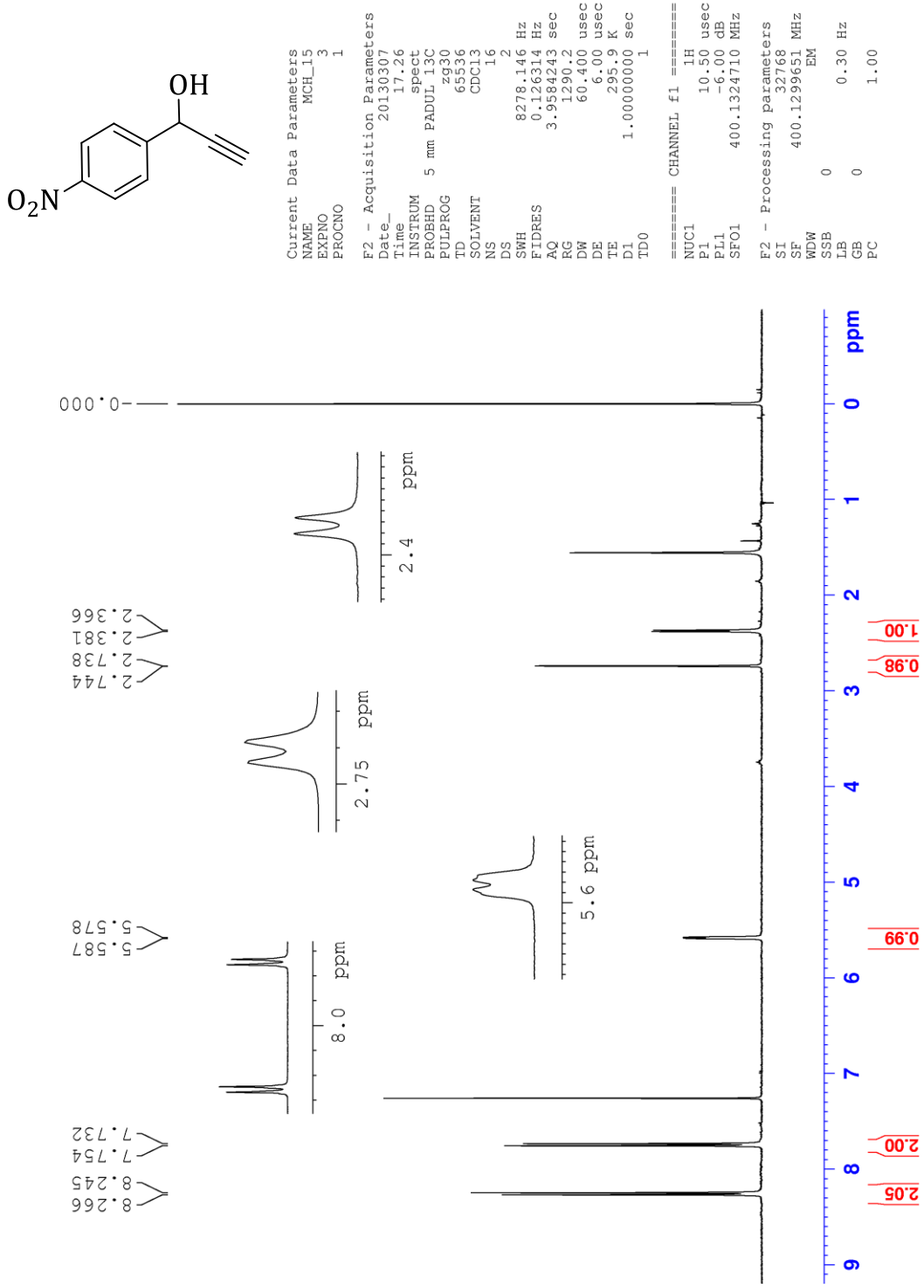

B-2 ^{13}C NMR of propargyl alcohol **3c**

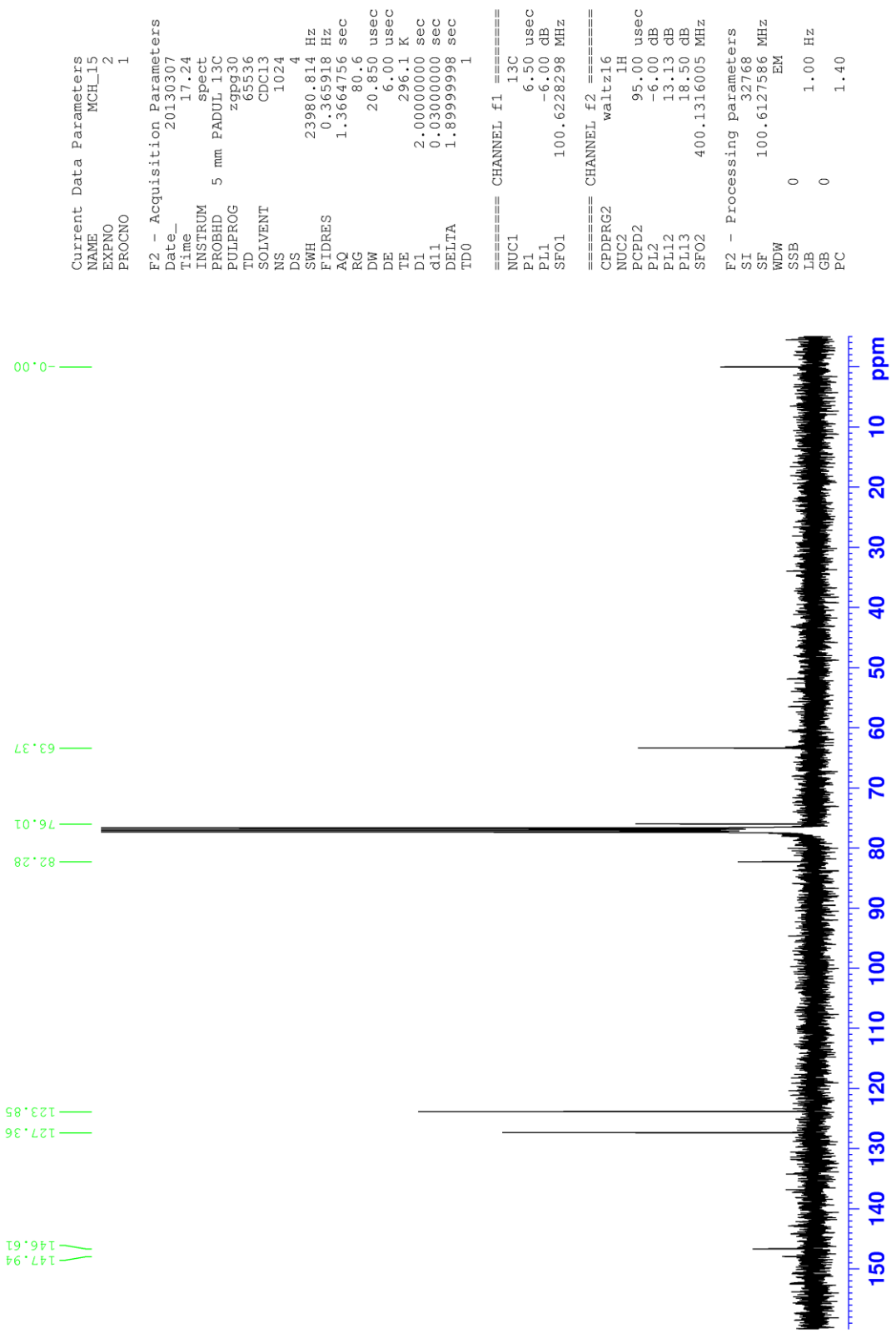

C Propargyl acetal 5a

C-1 ^{1}H NMR of propargyl acetal **5a**

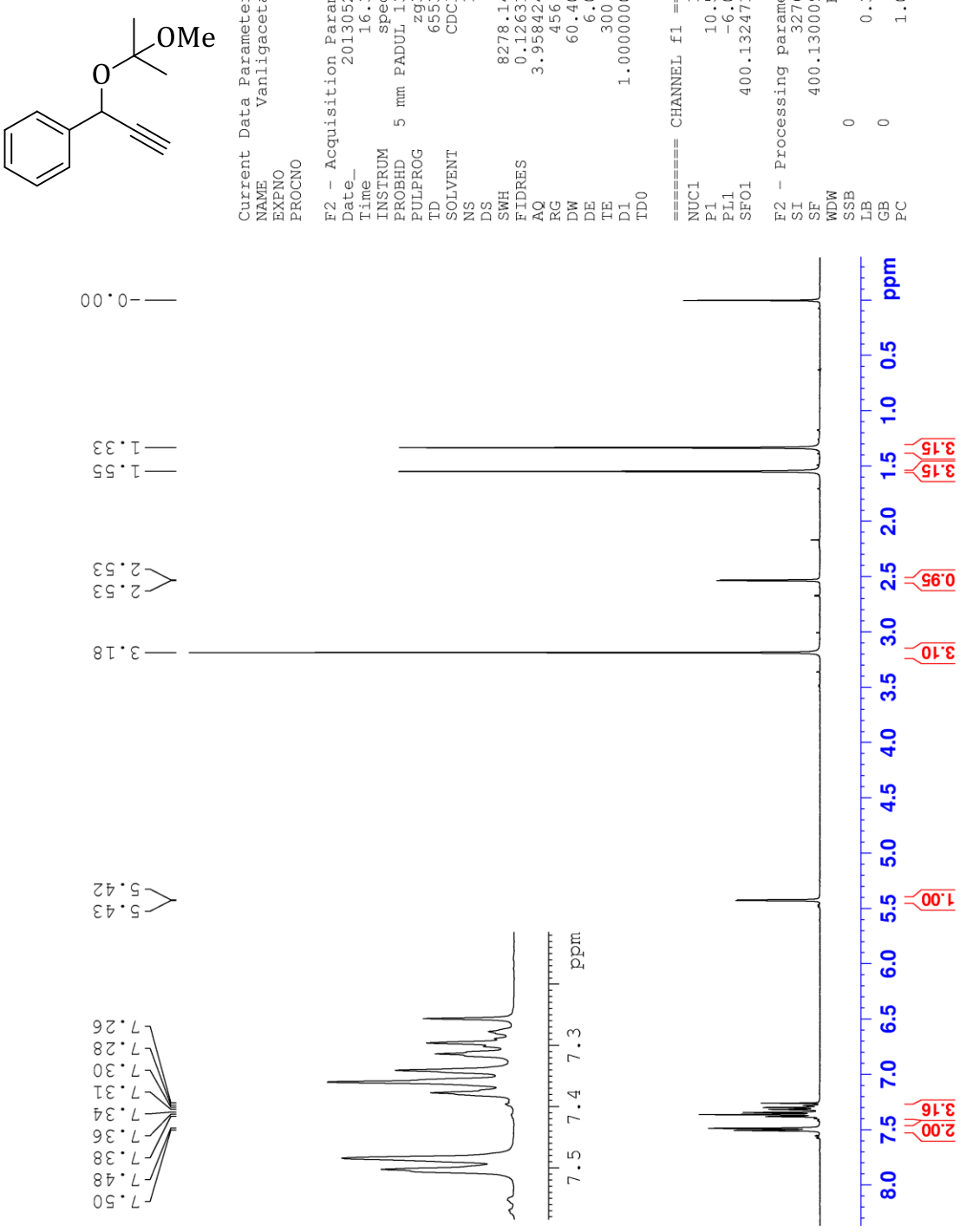

C-2 ^{13}C NMR of propargyl acetal **5a**

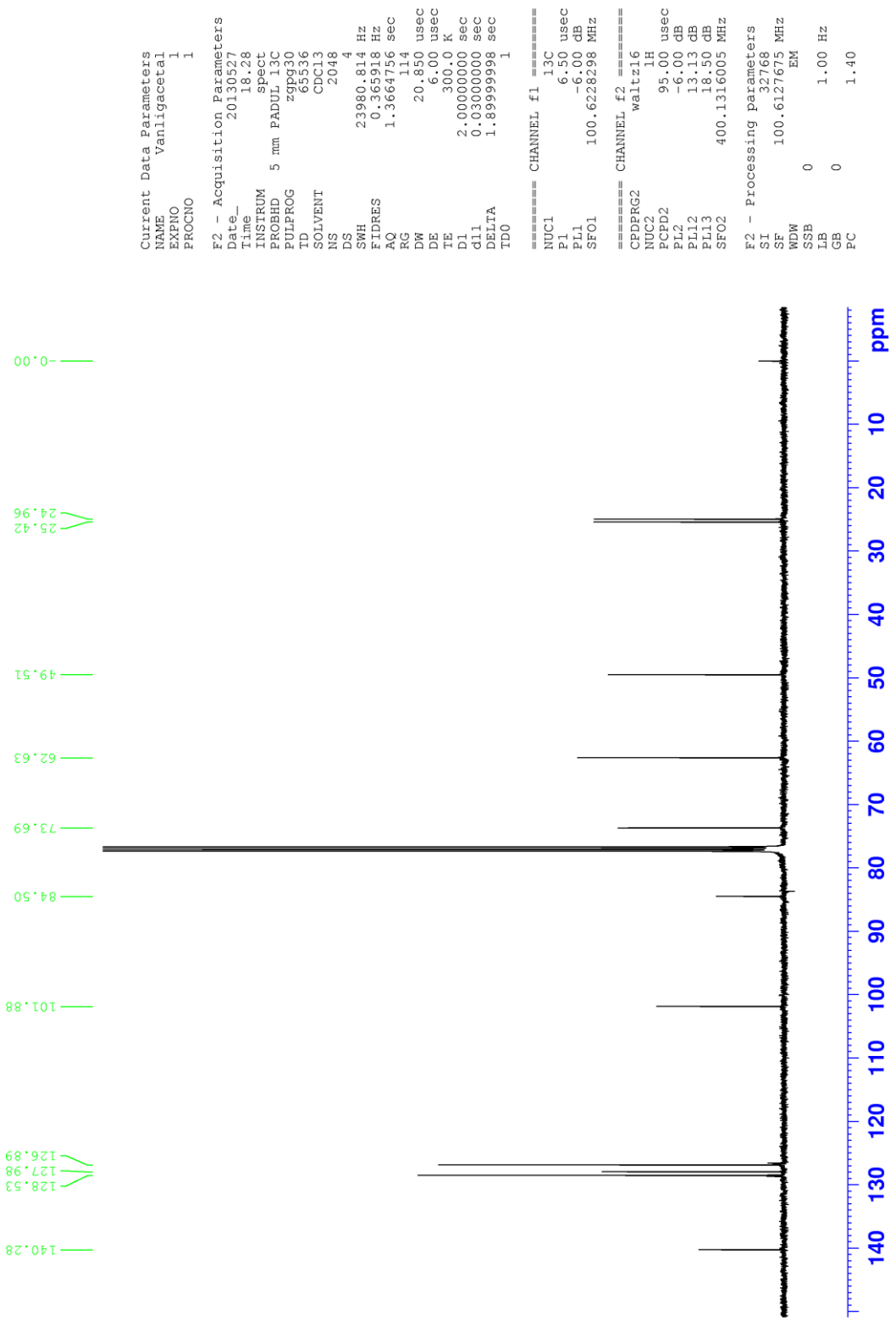

D Propargyl acetal 5b

D-1 ^{1}H NMR of propargyl acetal **5b**

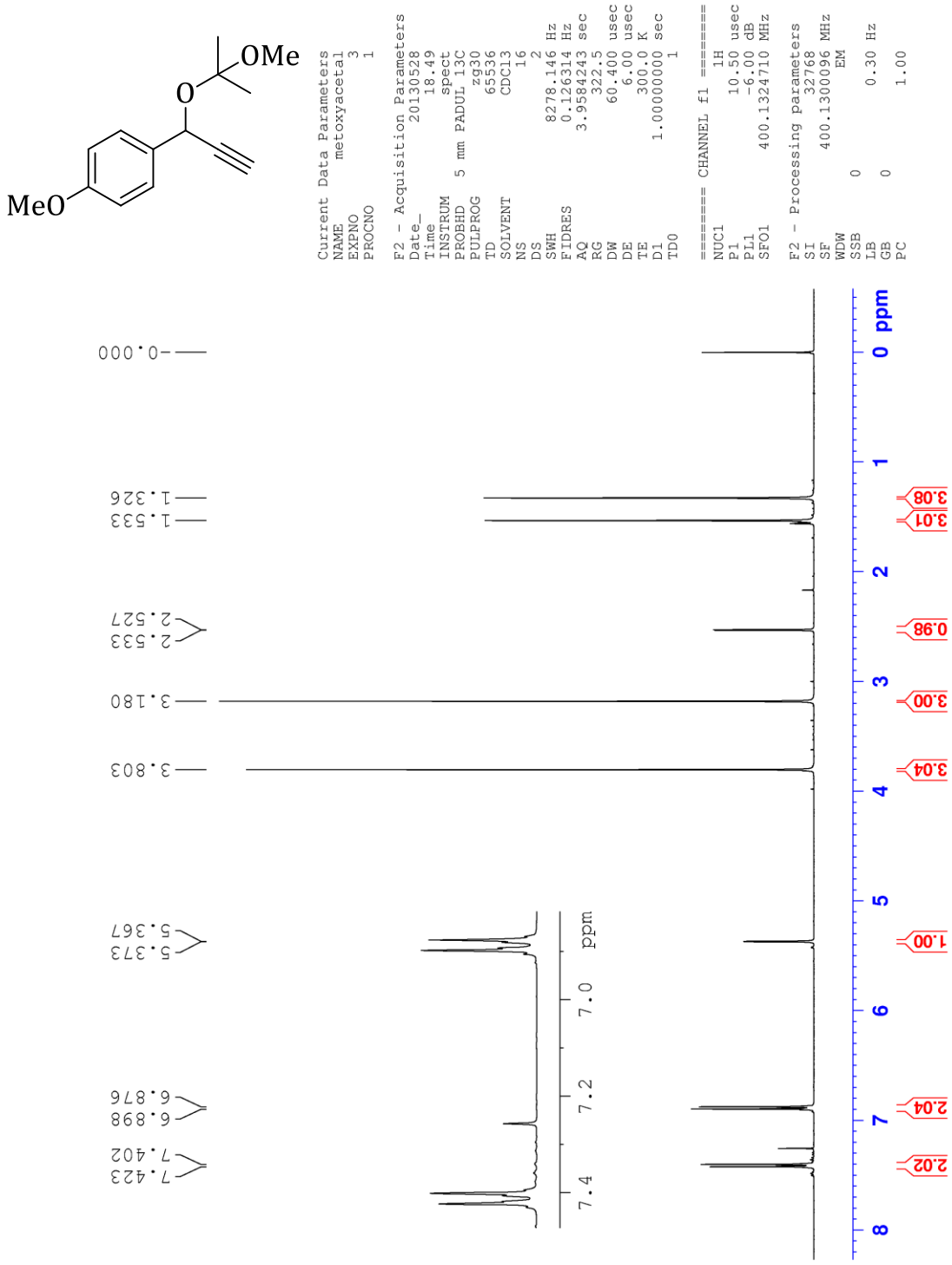

D-2 ^{13}C NMR of propargyl acetal **5b**

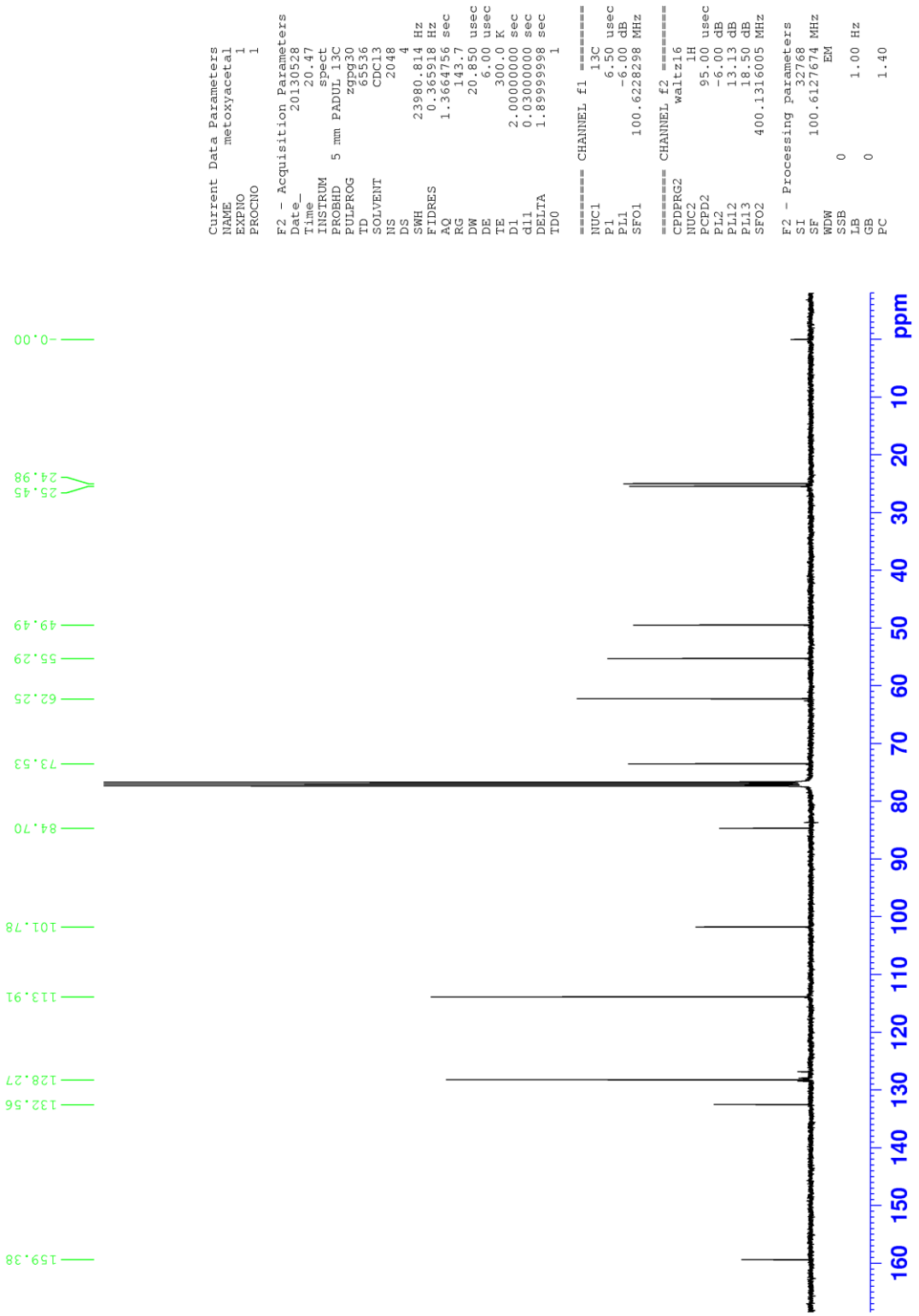

E Propargyl acetal 5c

E-1 ^{1}H NMR of Propargyl acetal **5c**

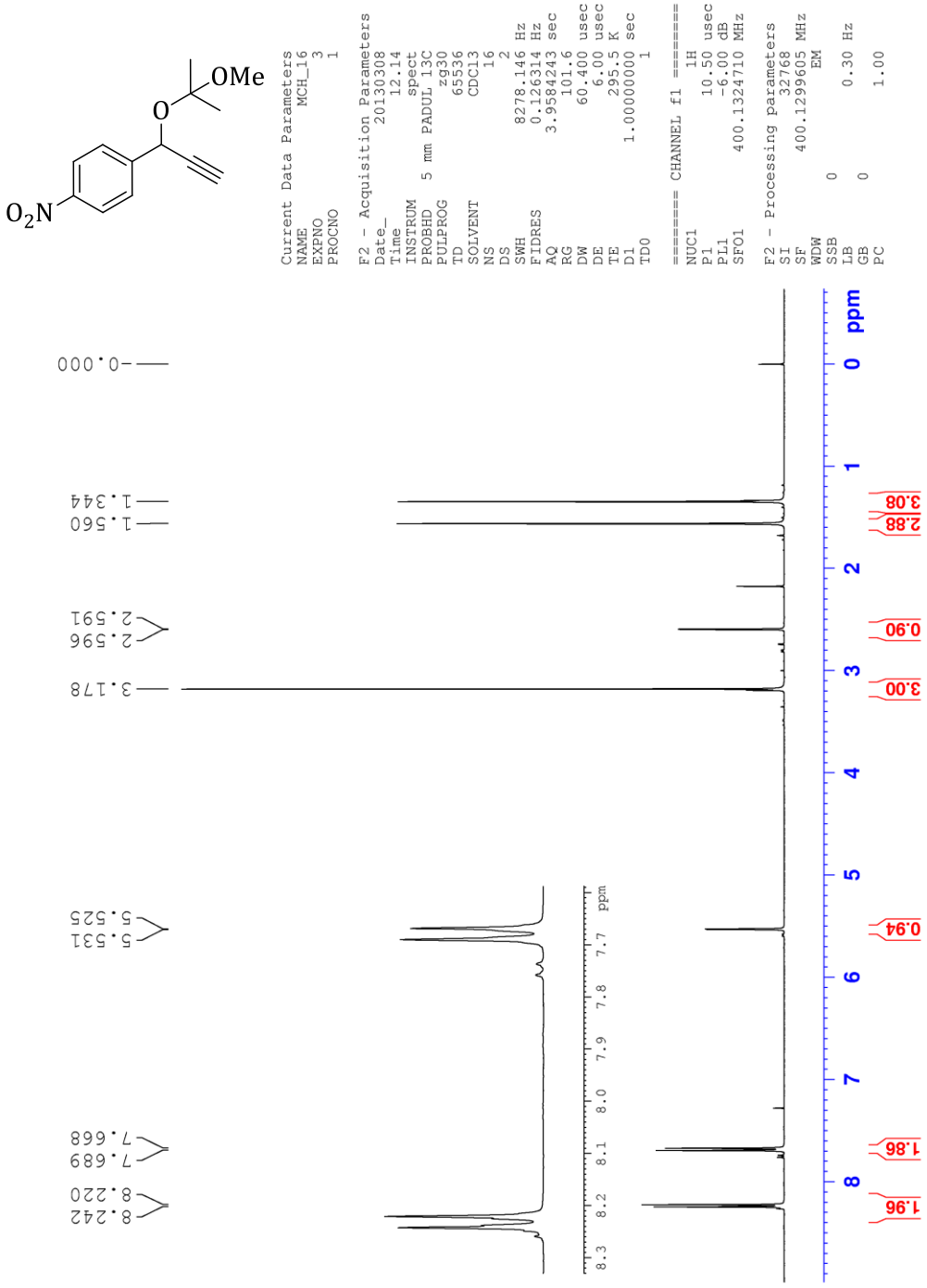

E-2 ^{13}C NMR of propargyl acetal **5c**

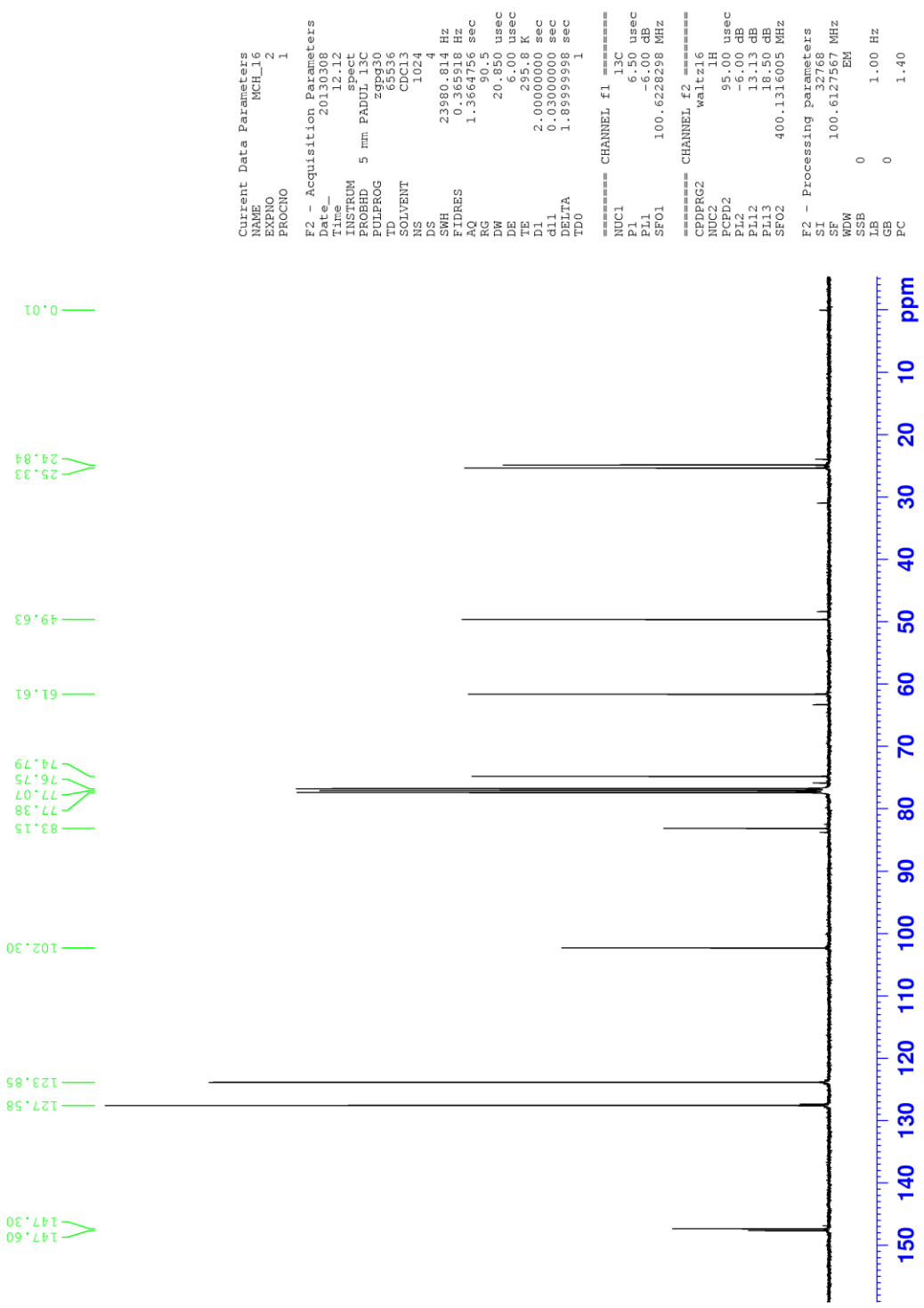

E-3 HSQC of propargyl acetal **5c**

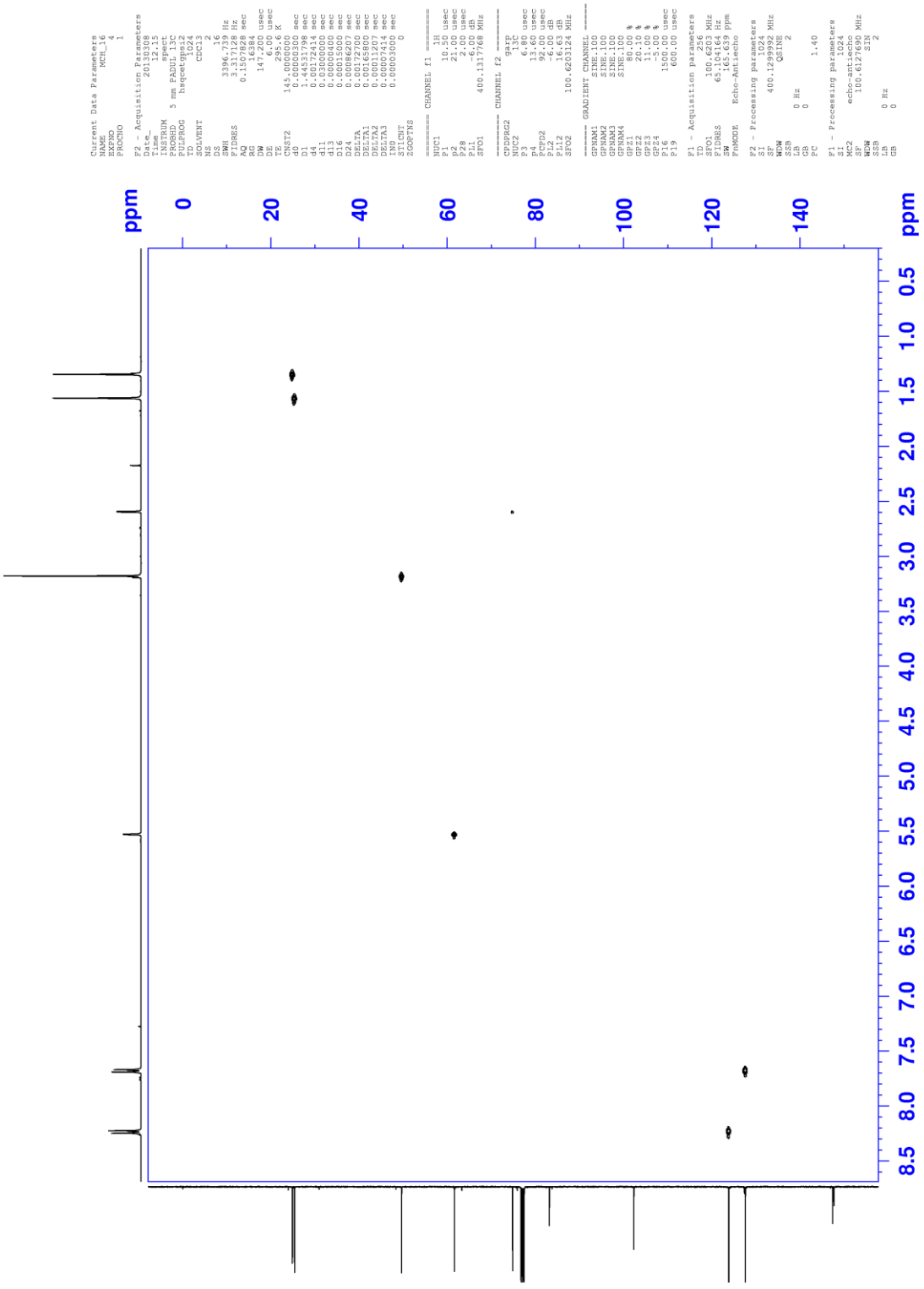

E-4 IR of propargyl acetal **5c**

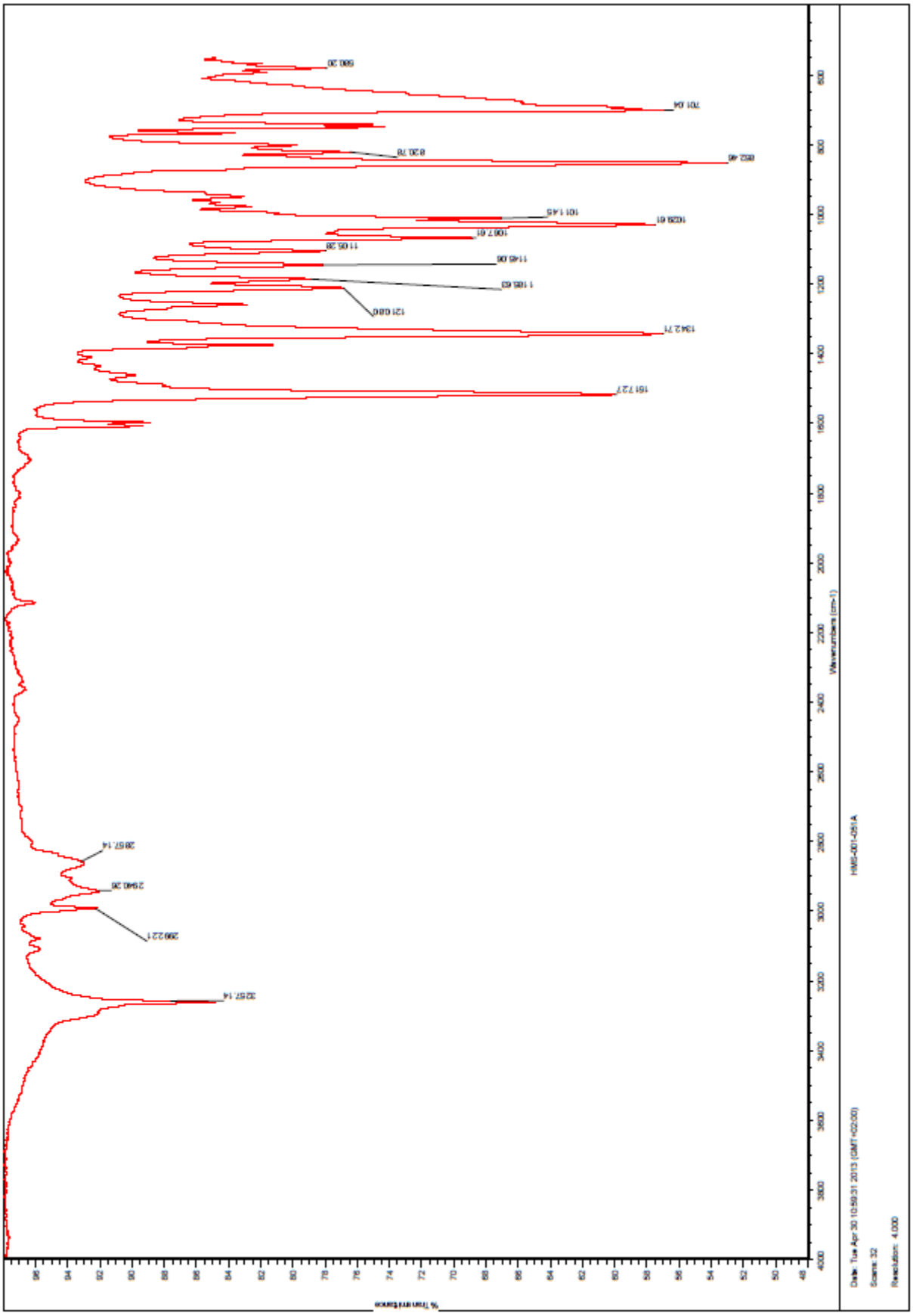

F Cyclization product 7a

F-1 ^{1}H NMR of cyclization product **7a**

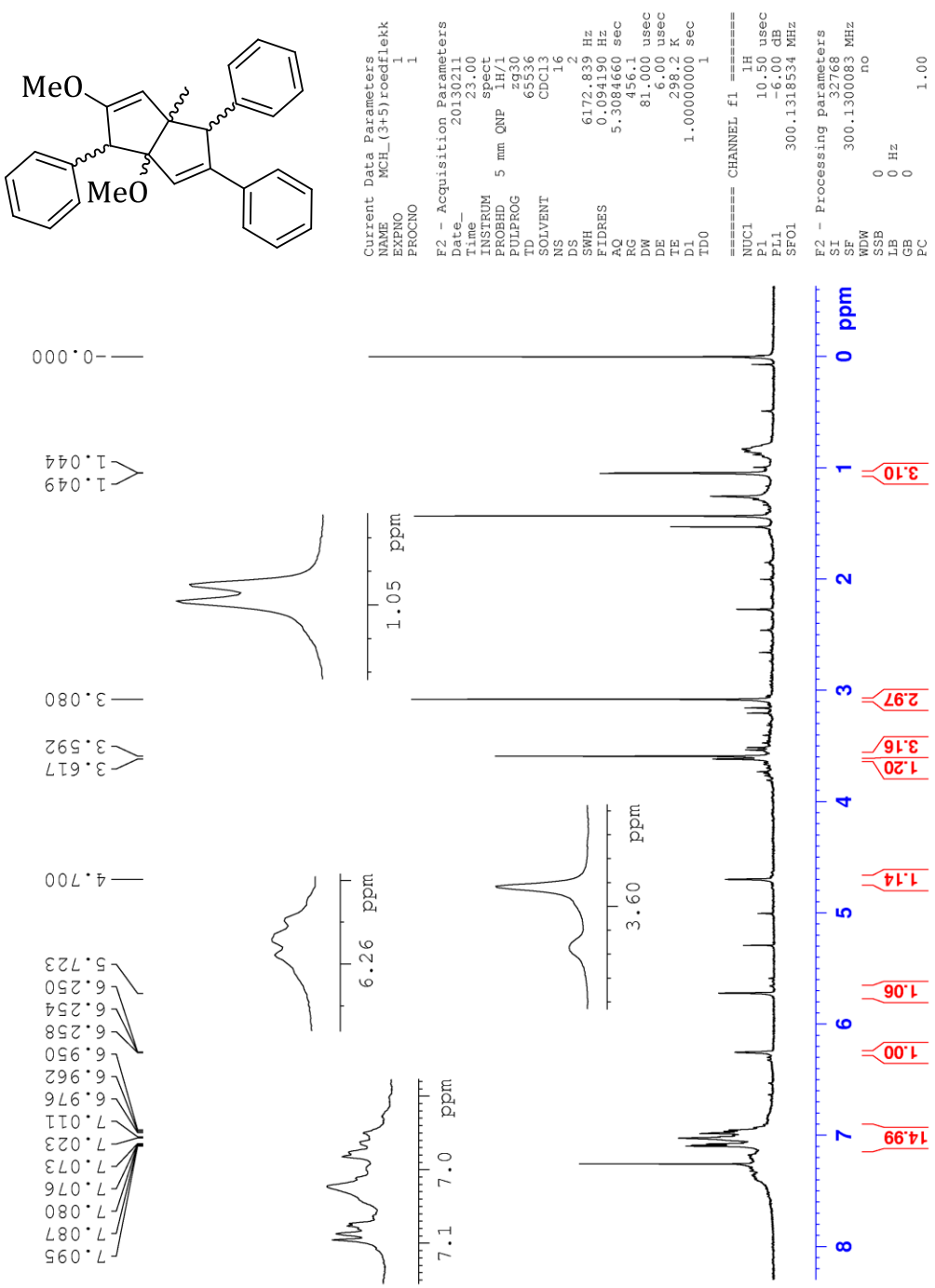

F-2 ^{13}C NMR of cyclization product **7a**

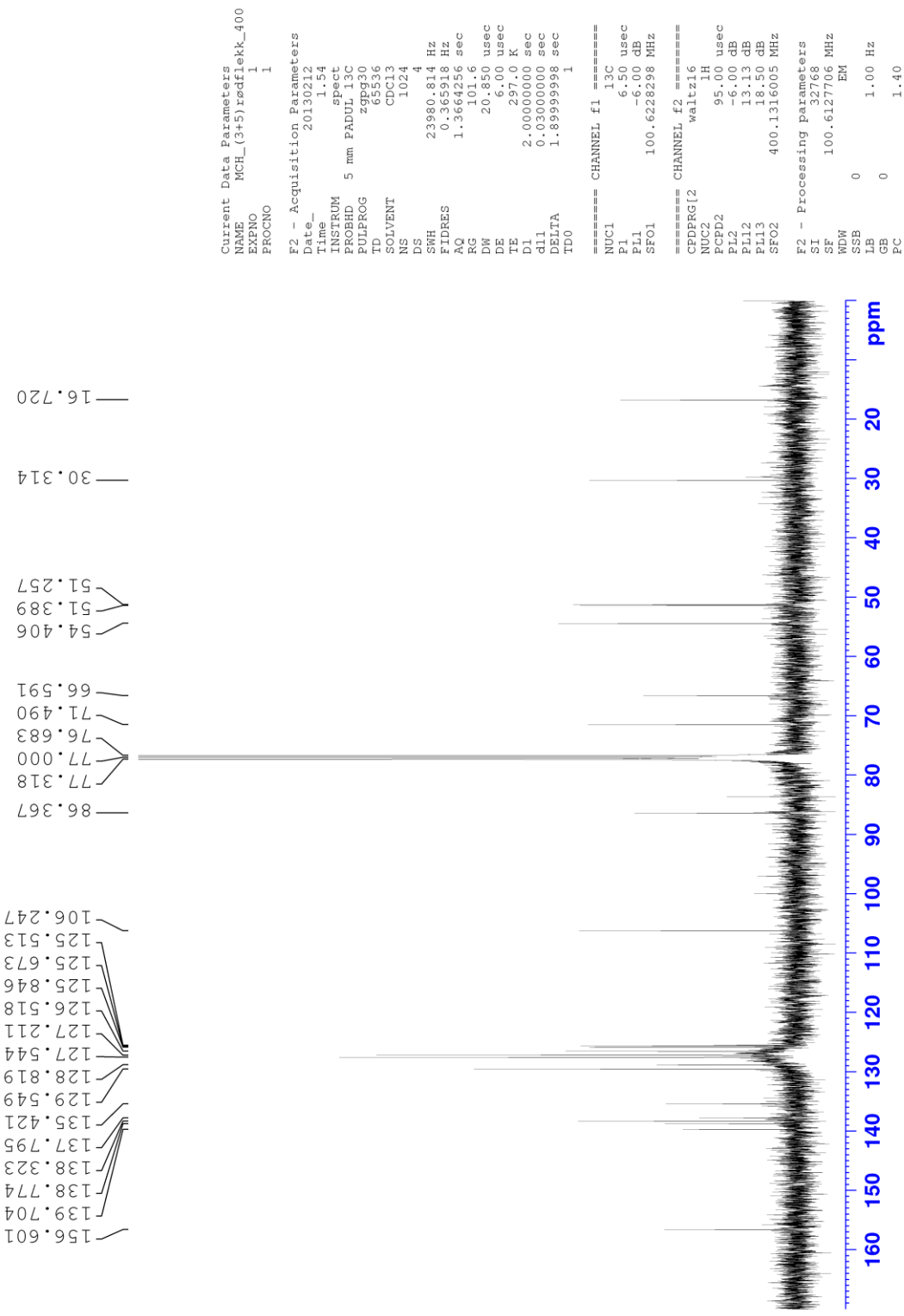

F-3 HSQC of cyclization product **7a**

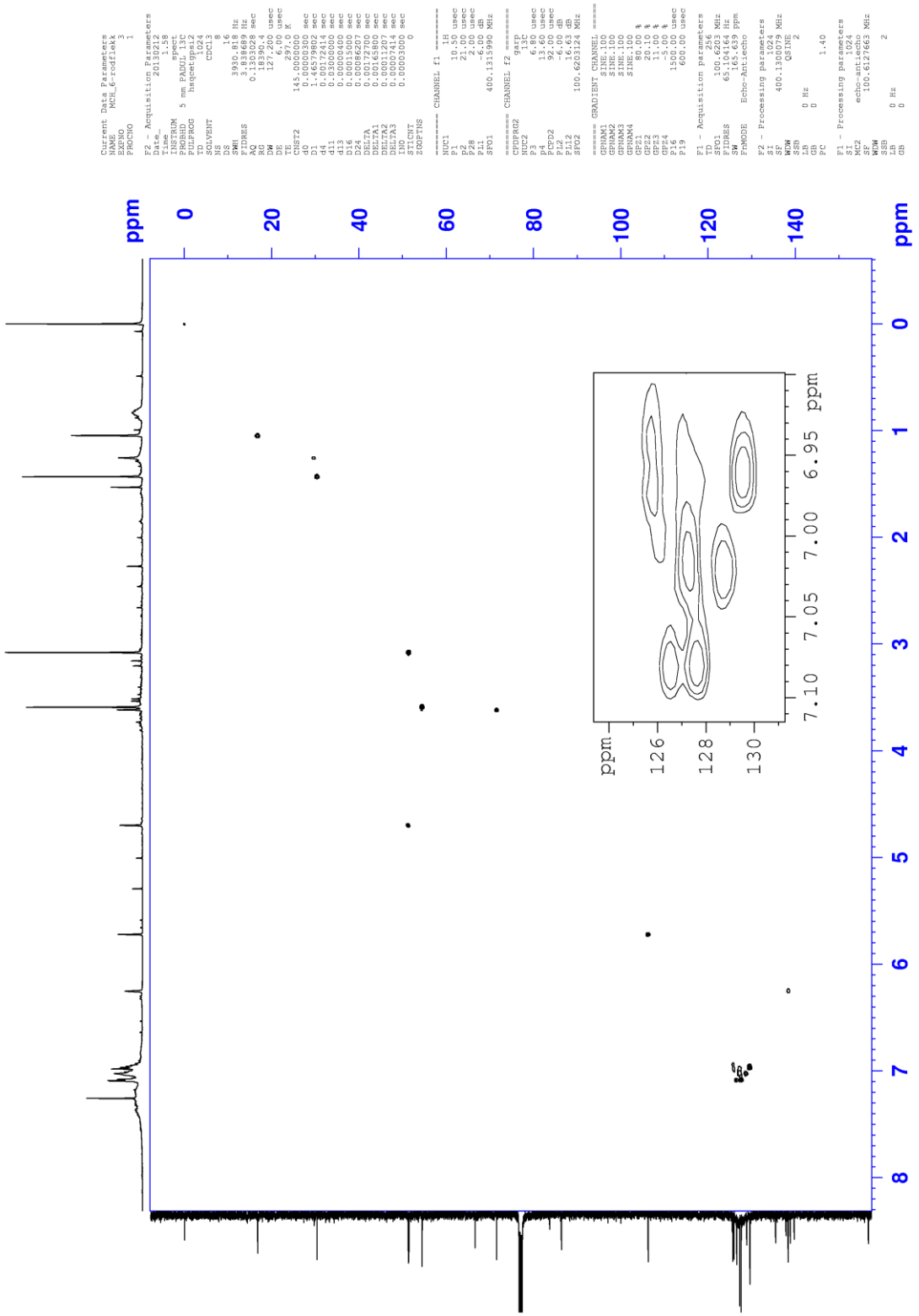

F-4 COSY of cyclization product **7a**

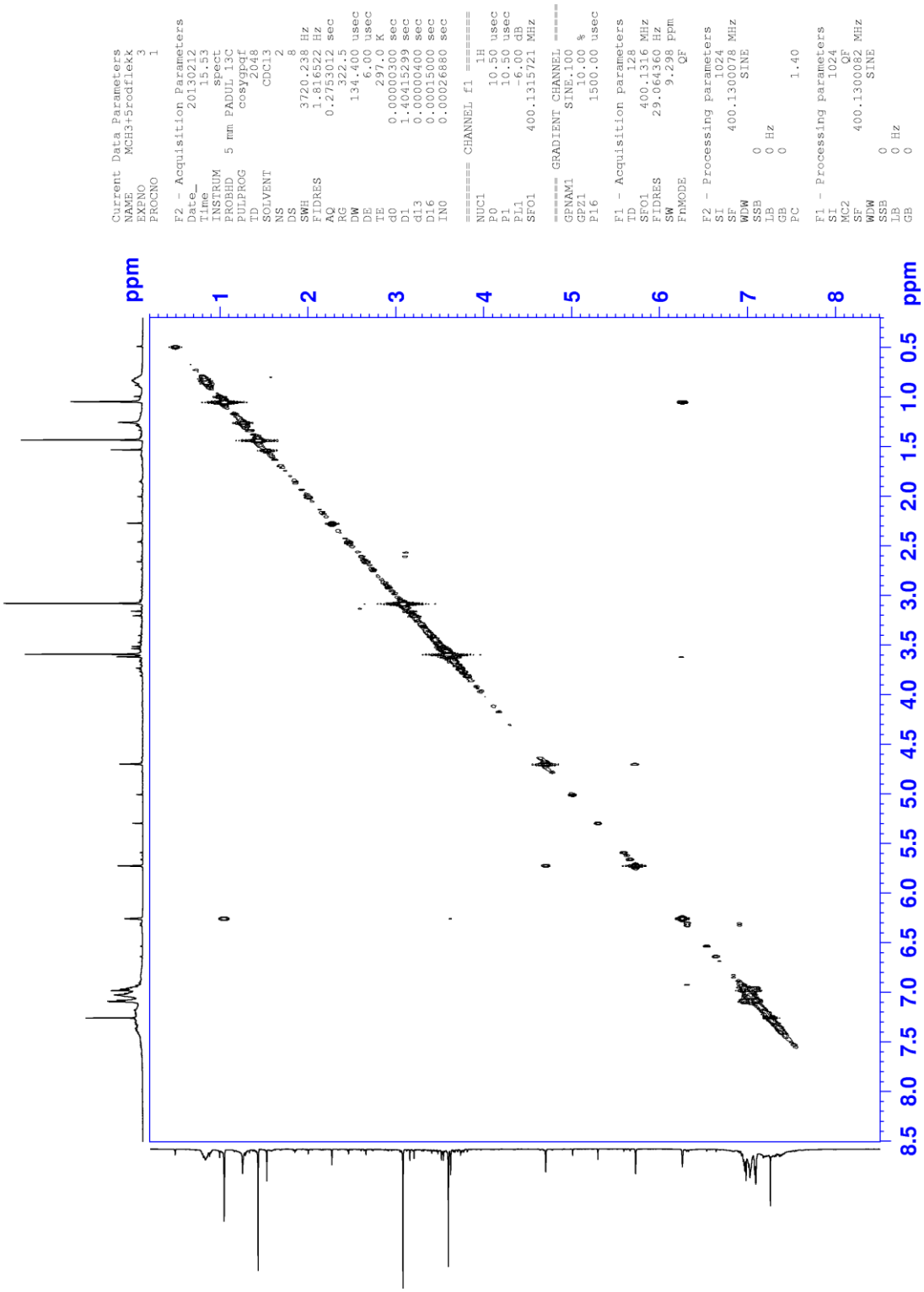

F-5 HMBC of cyclization product **7a**

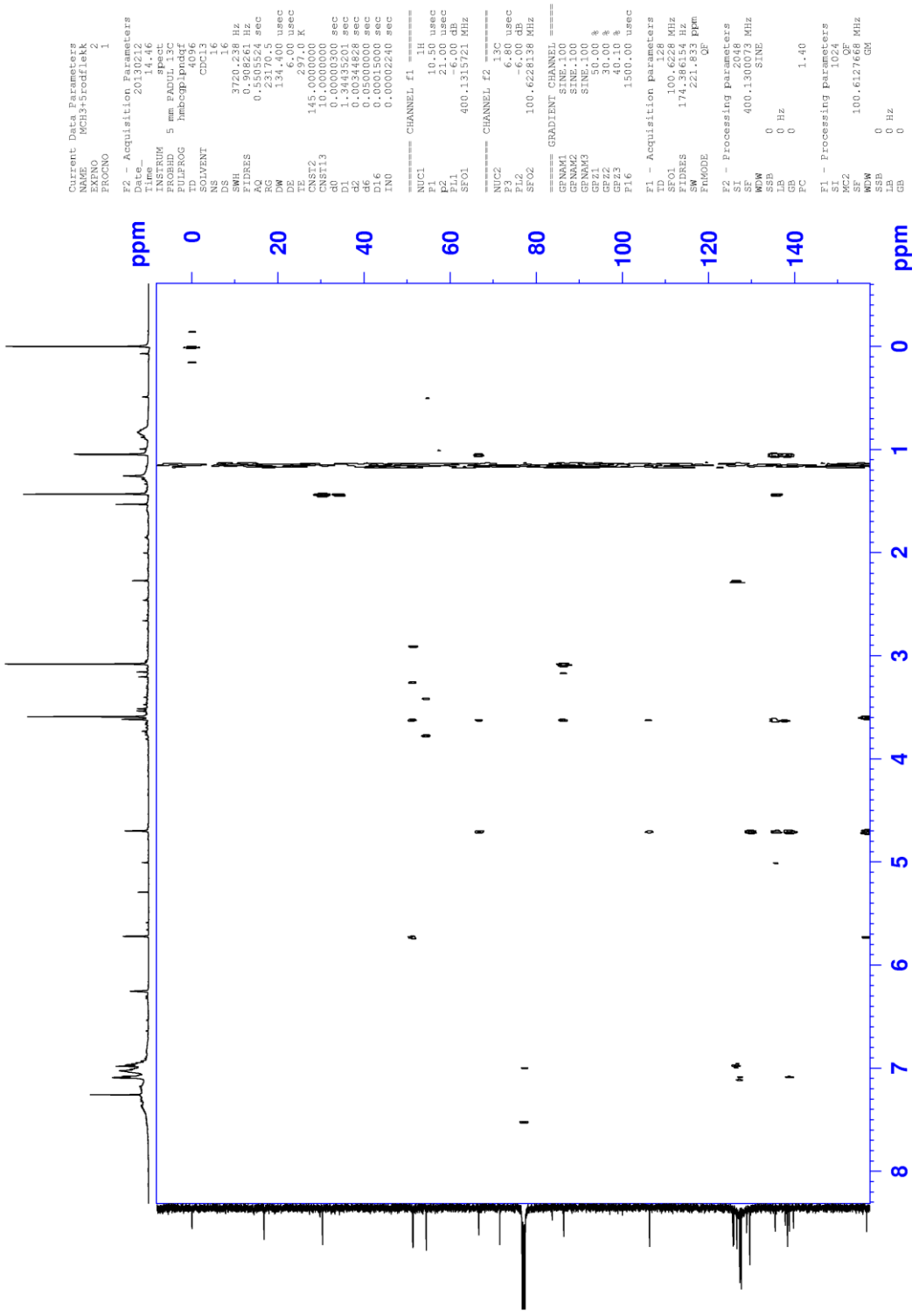

F-6 IR of cyclization product **7a**

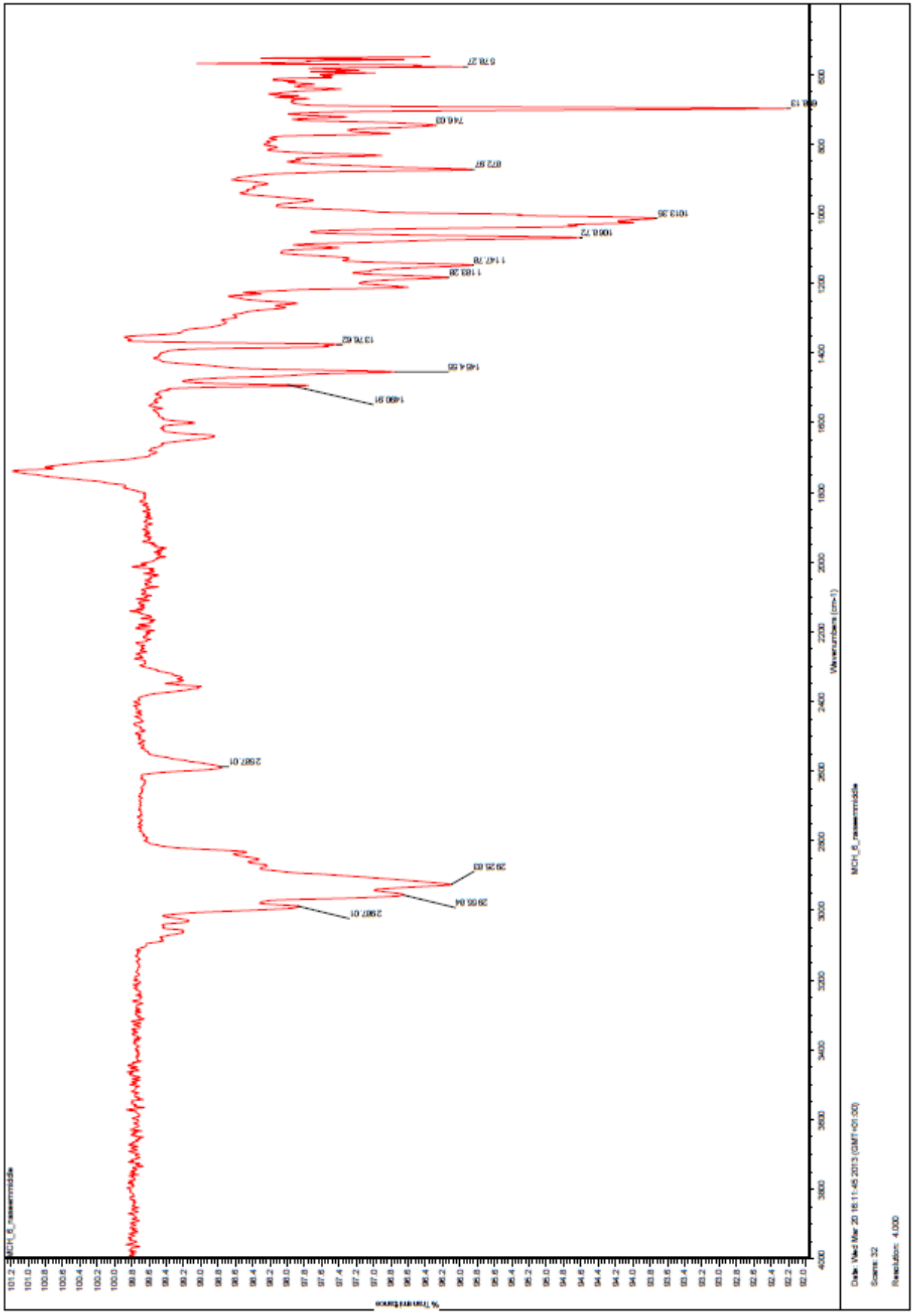

G Cyclization product 7b

G-1 ^{1}H NMR of cyclization product **7b**

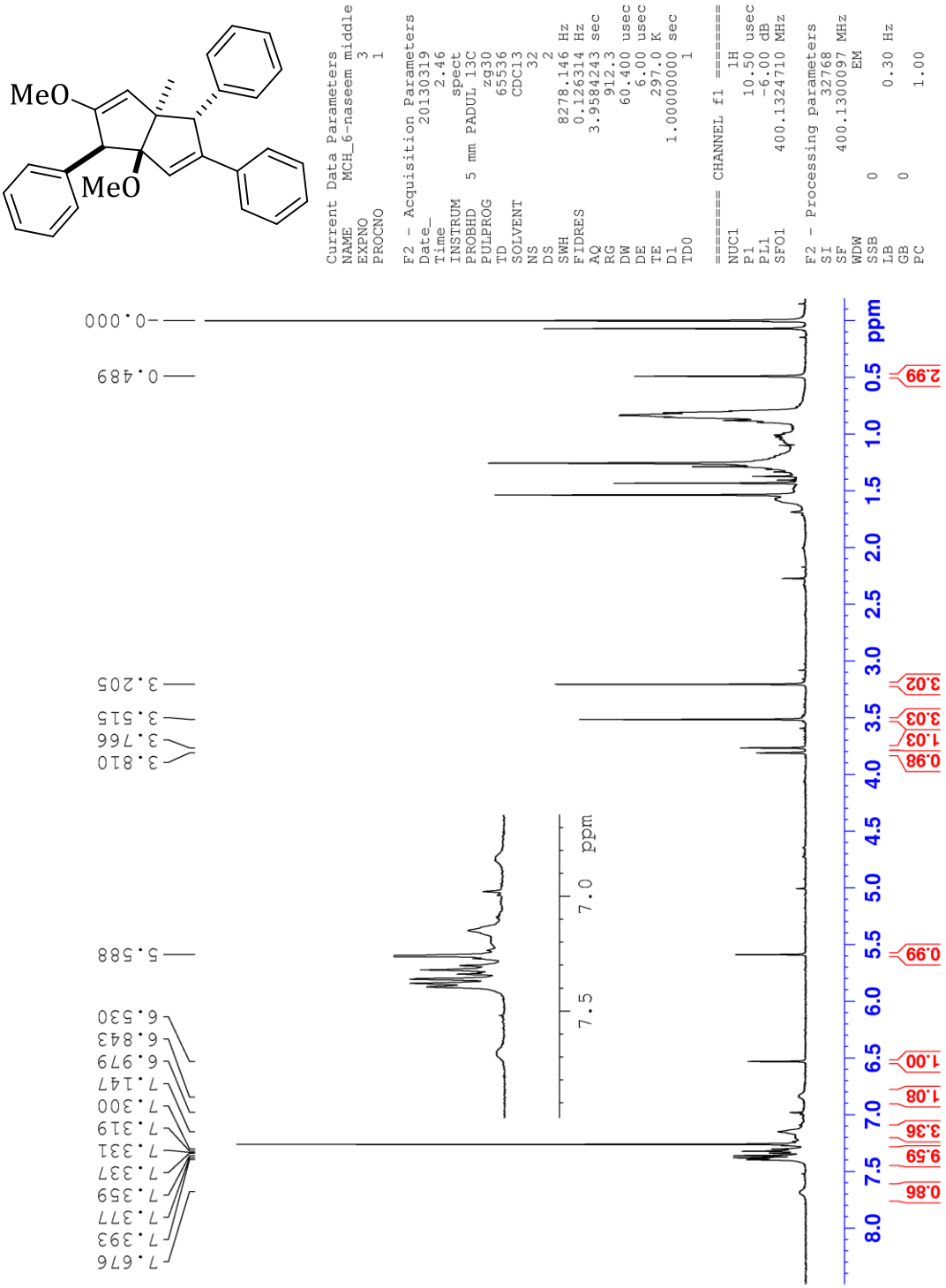

G-2 ^{13}C NMR of cyclization product **7b**

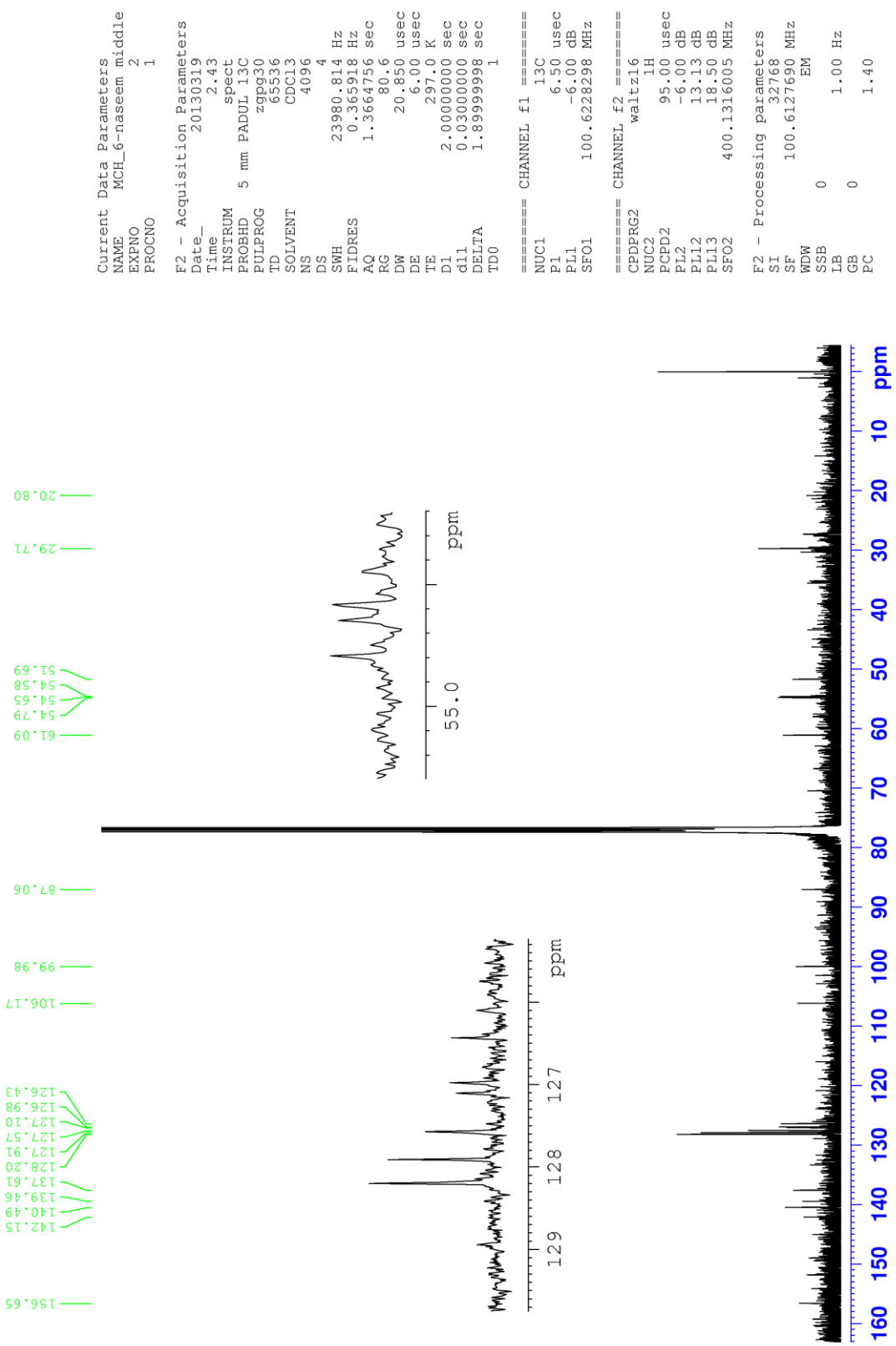

G-3 HSQC of cyclization product **7b**

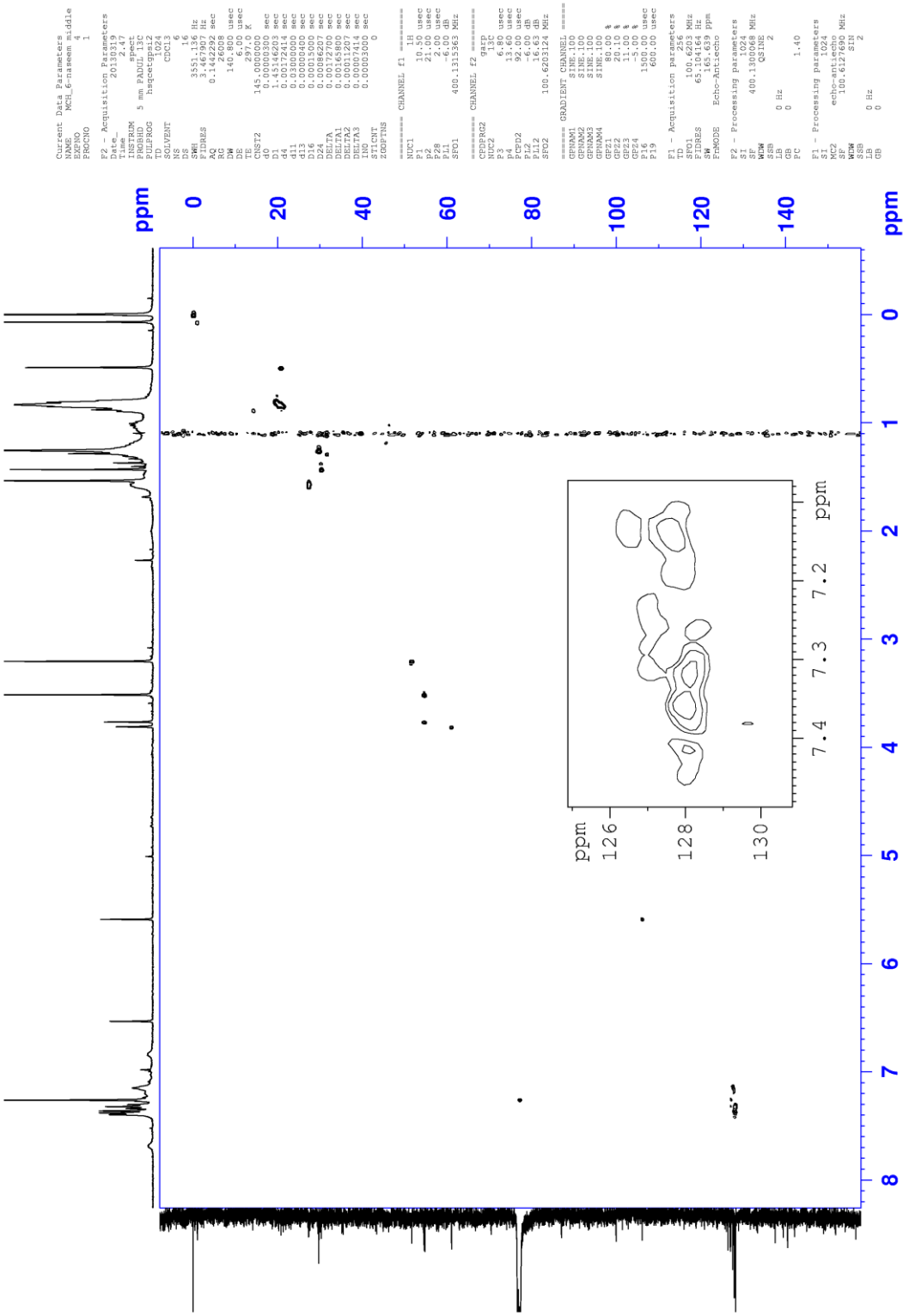

G-4 IR of cyclization product **7b**

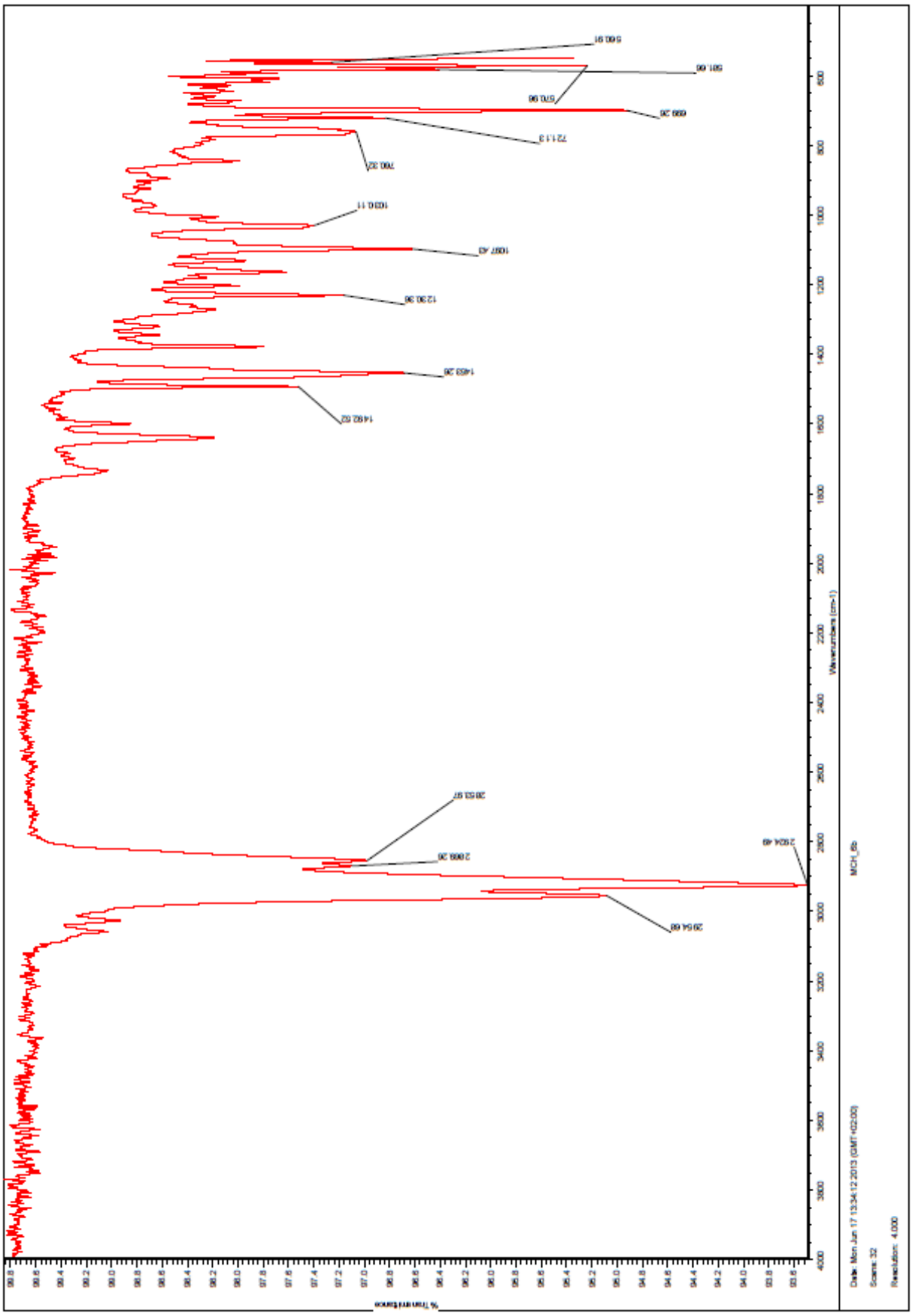

H Cyclization product 7c

H-1 ^{1}H NMR of cyclization product **7c**

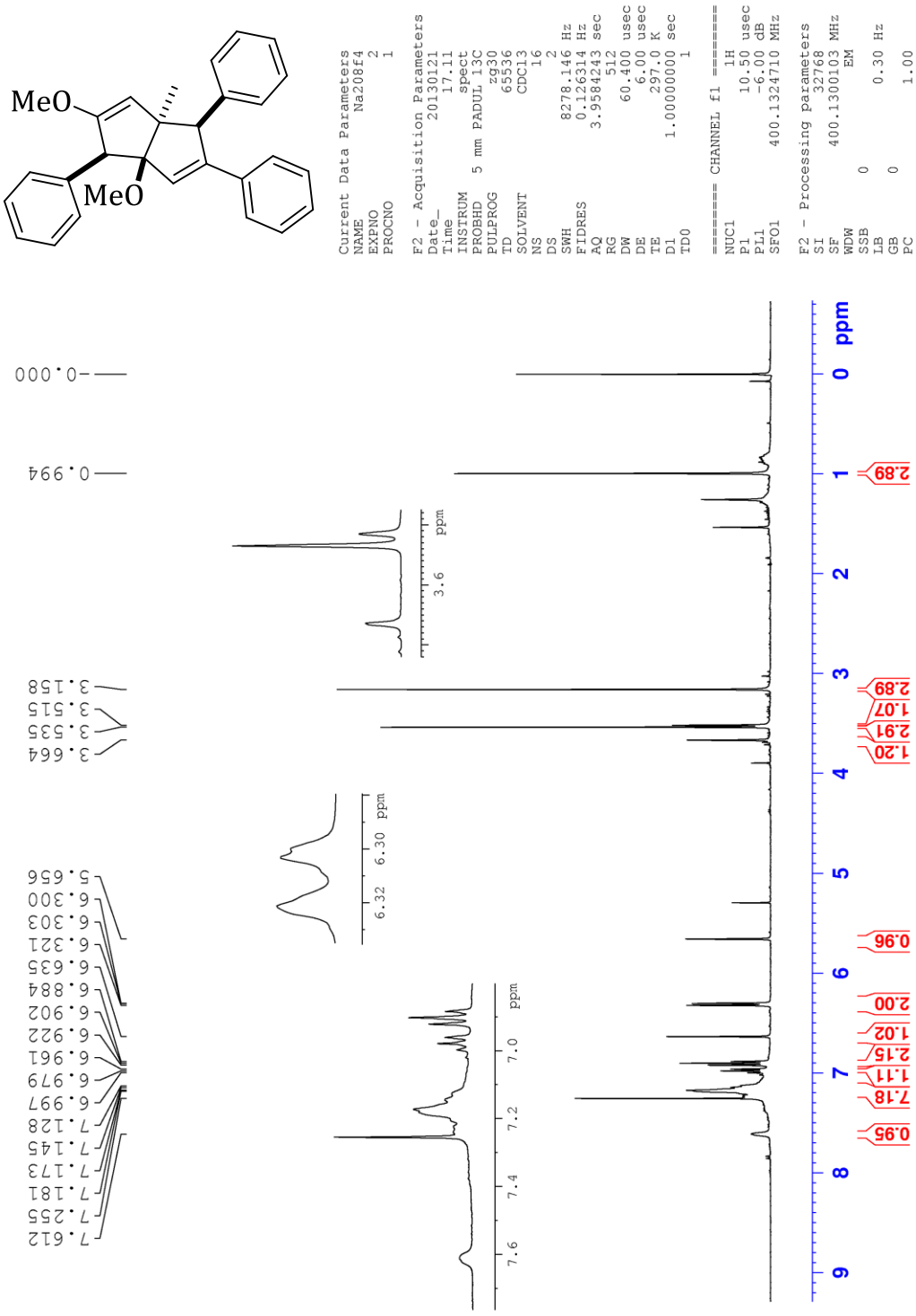

H-2 ^{13}C NMR of cyclization product **7c**

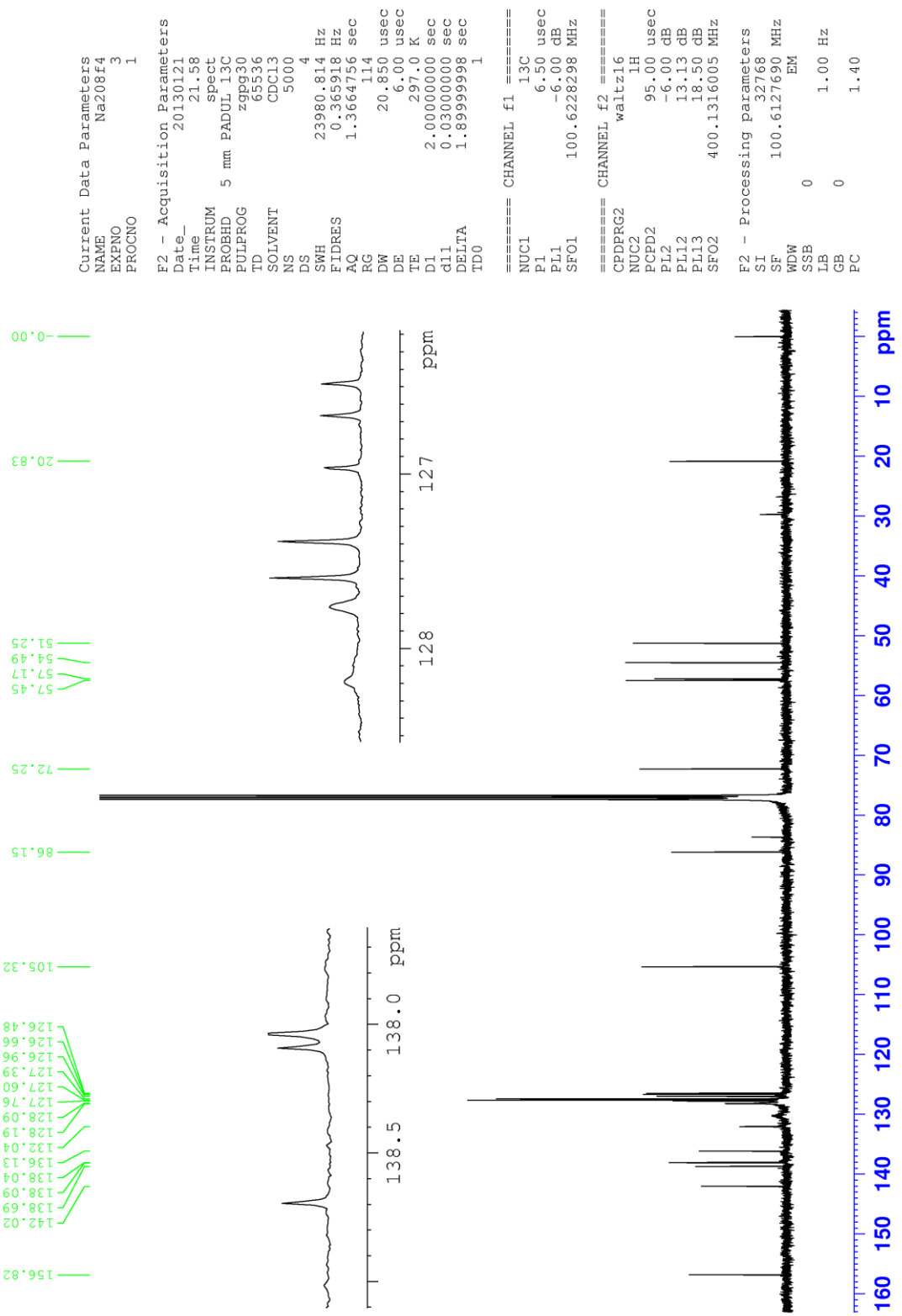

H-3 HSQC of cyclization product **7c**

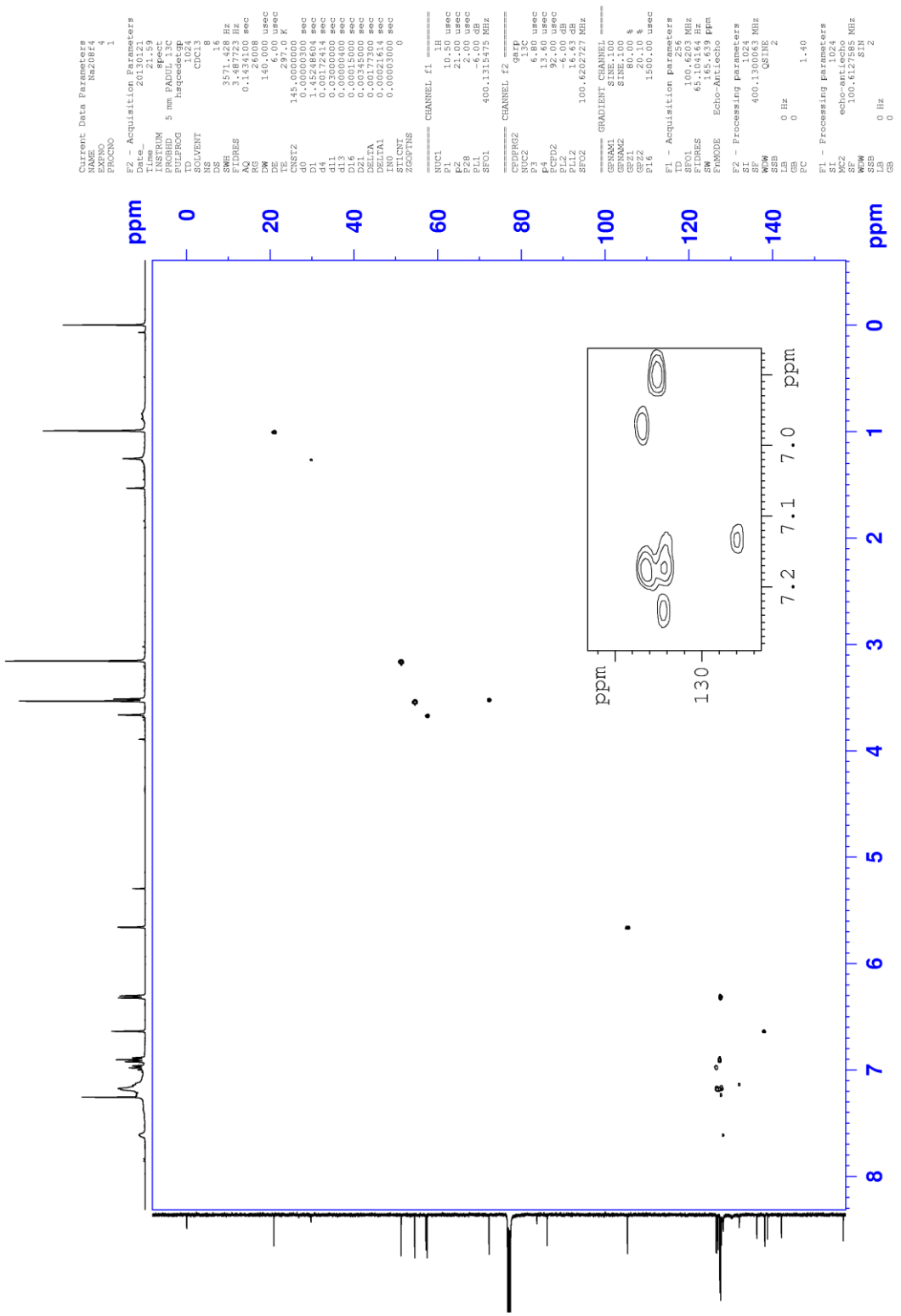

H-4 COSY of cyclization product **7c**

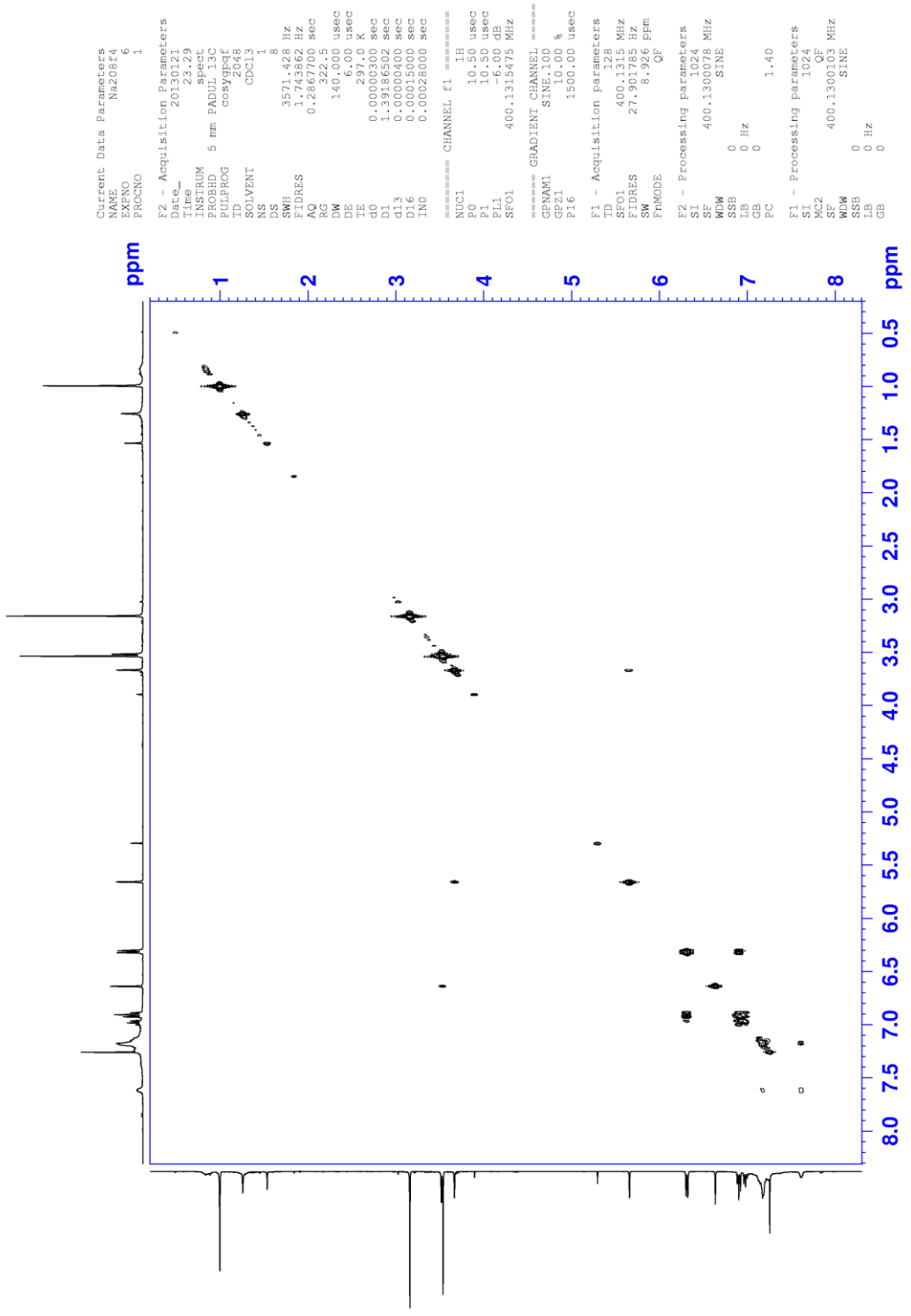

H-5 HMBC of cyclization product **7c**

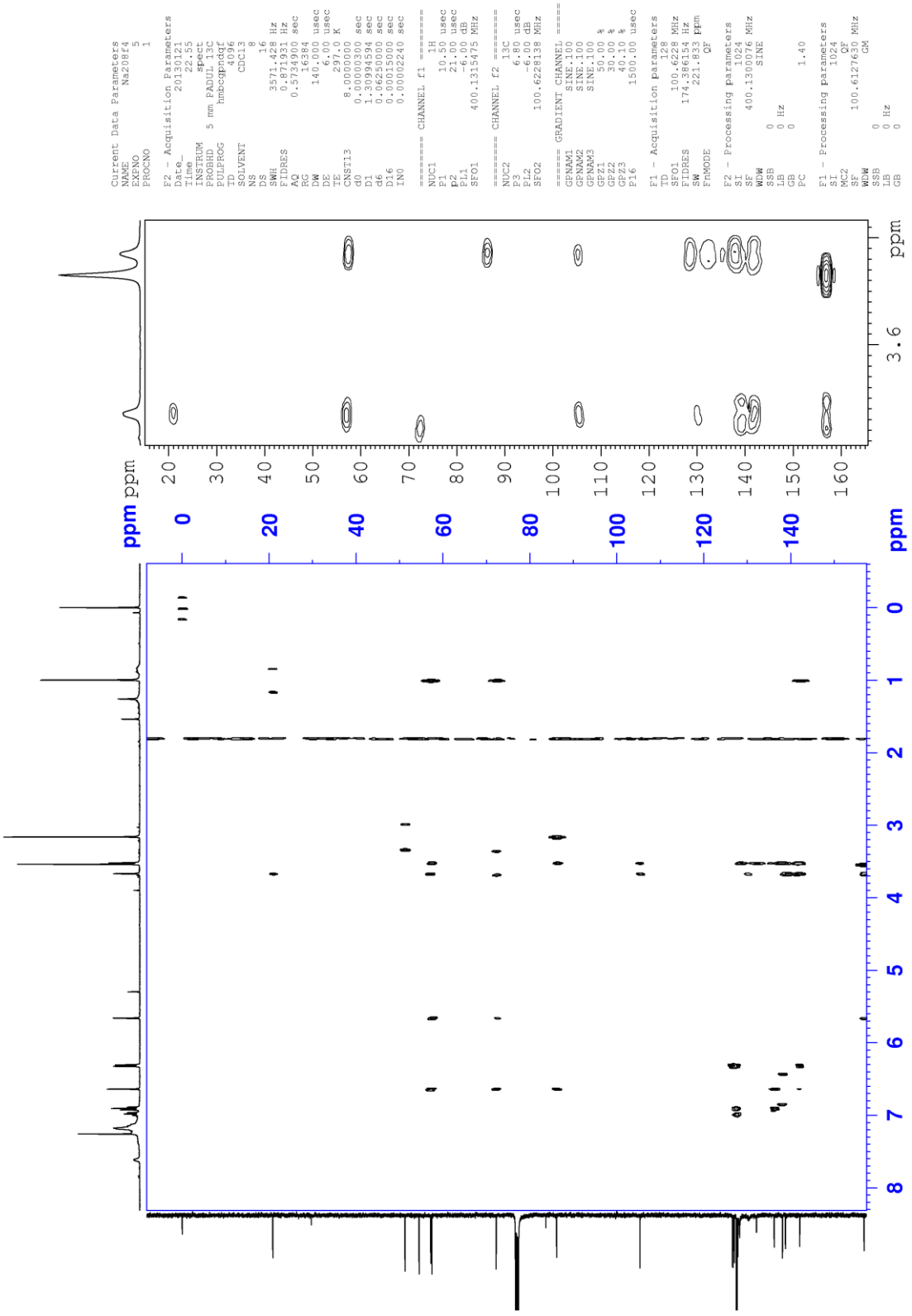

H-6 NOESY of cyclization product **7c**

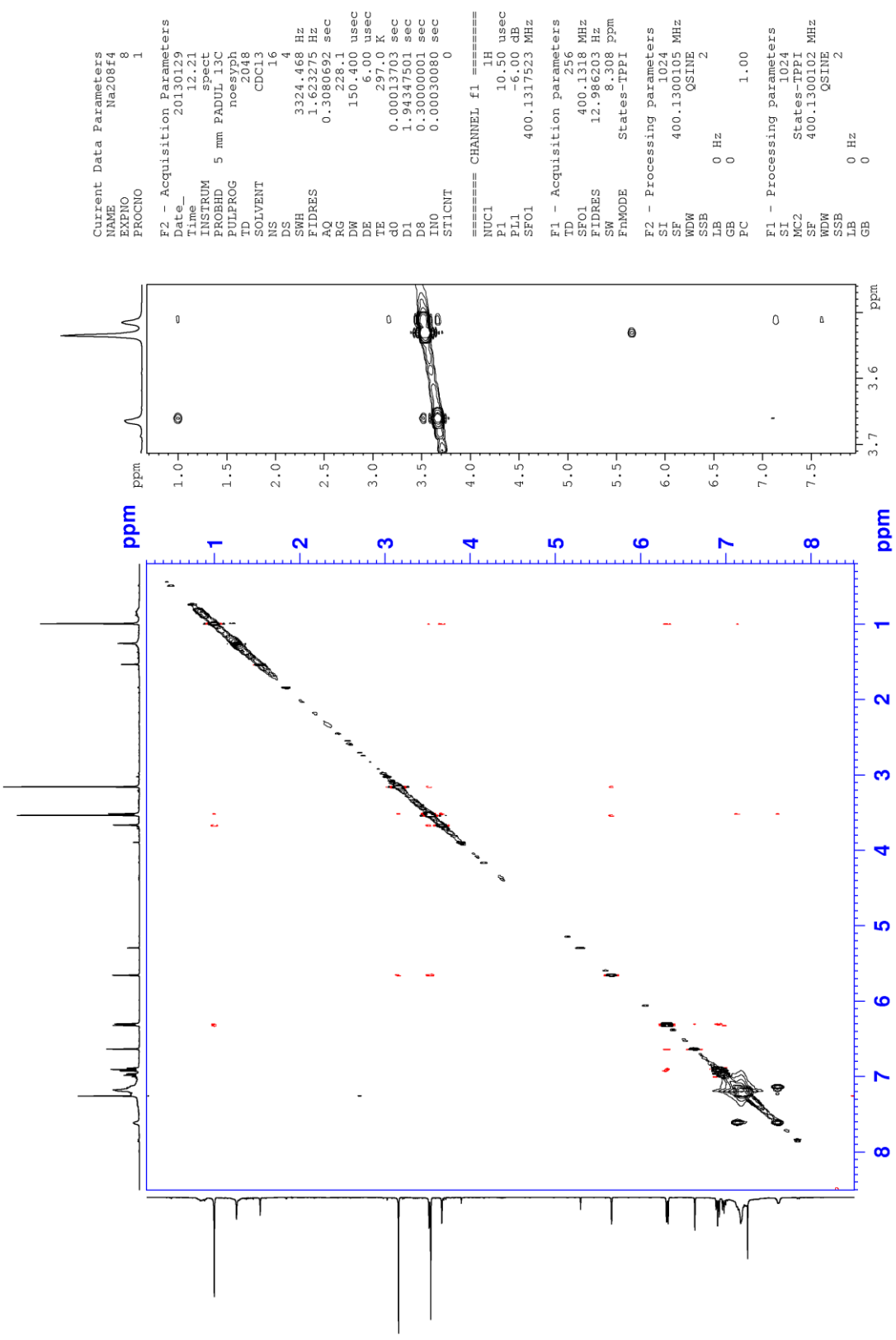

H-7a NOESY of cyclization products **7a-c**

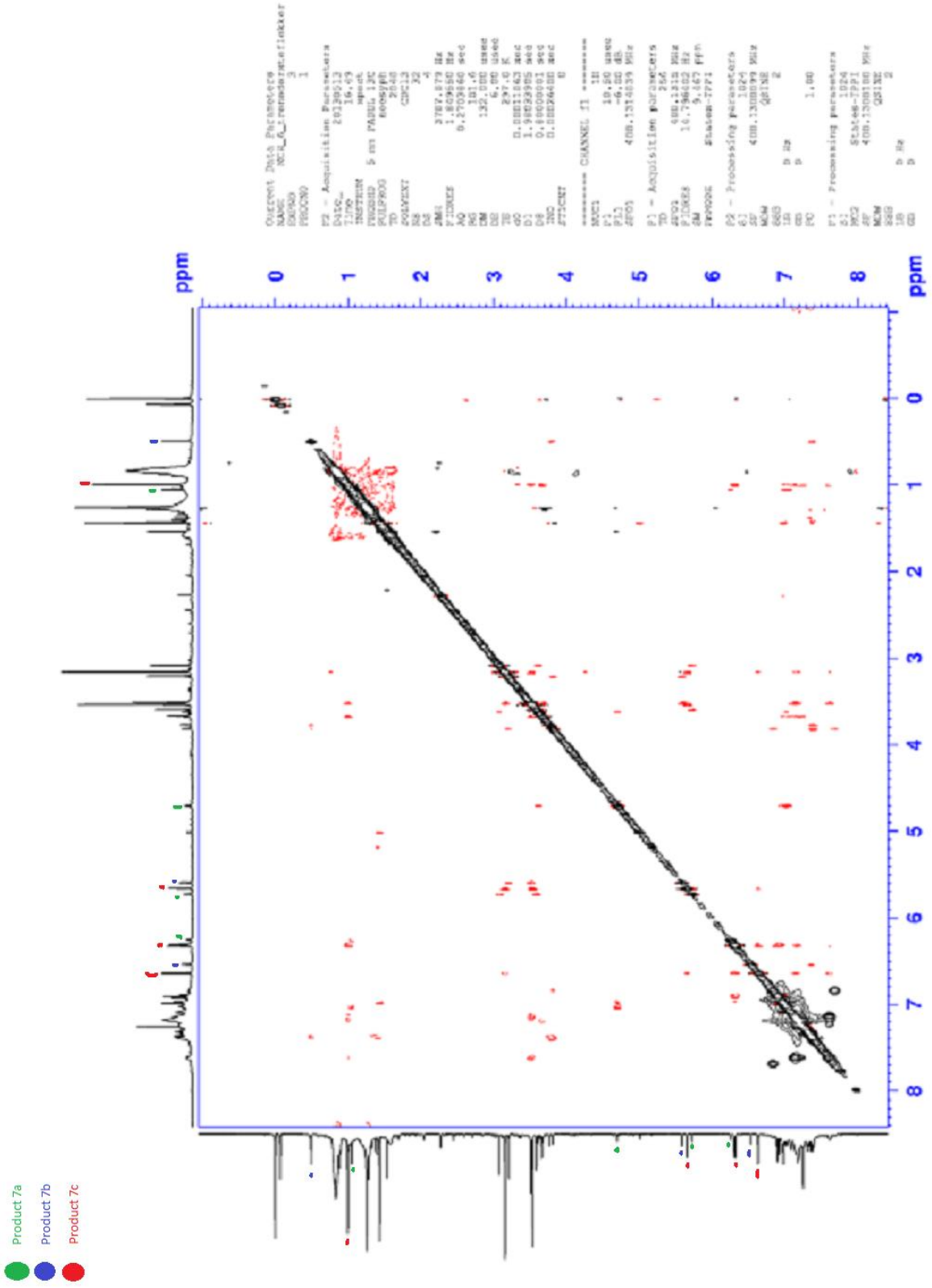

H-7b NOESY of cyclization products **7a-c**

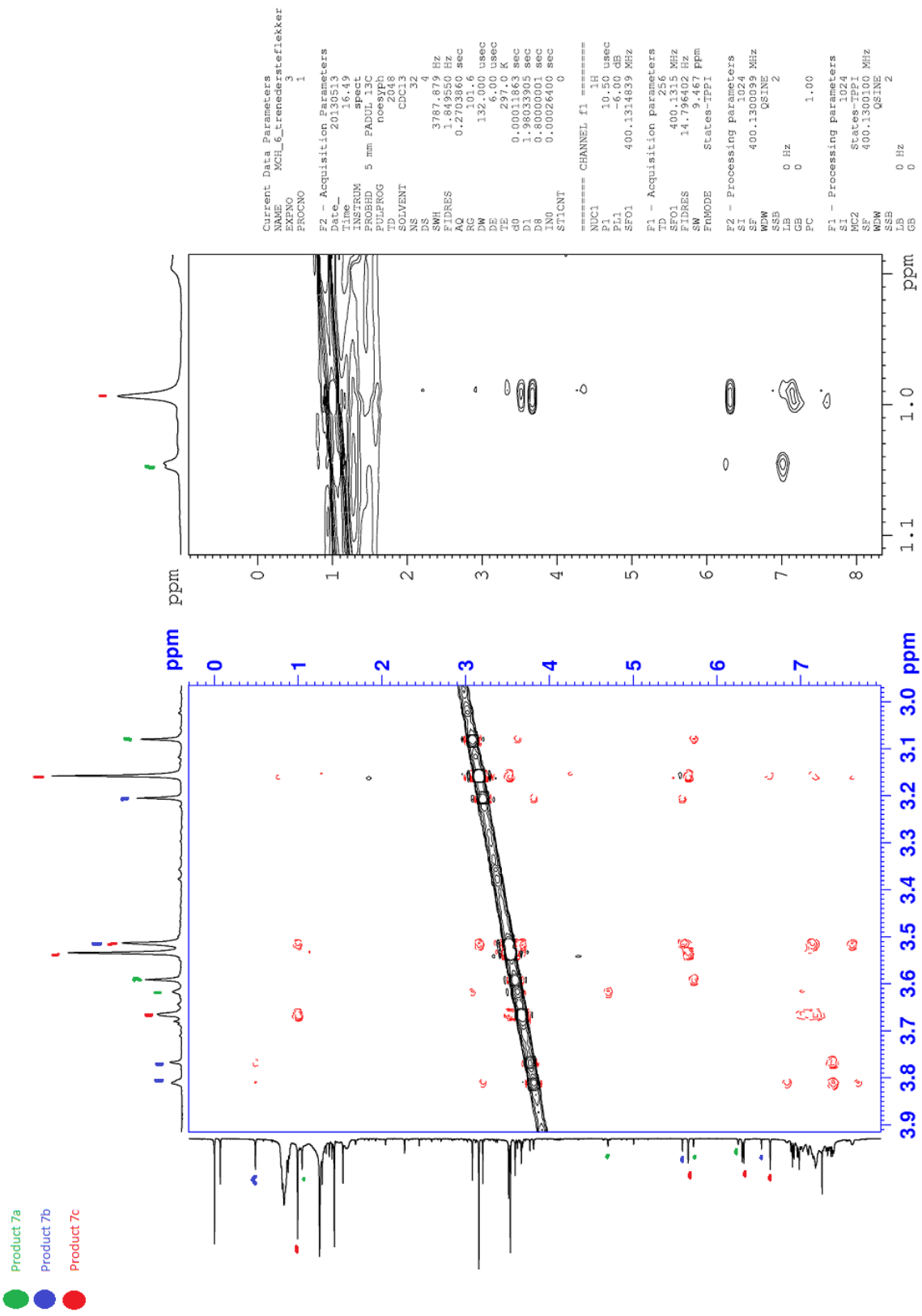

H-8 IR of cyclization product **7c**

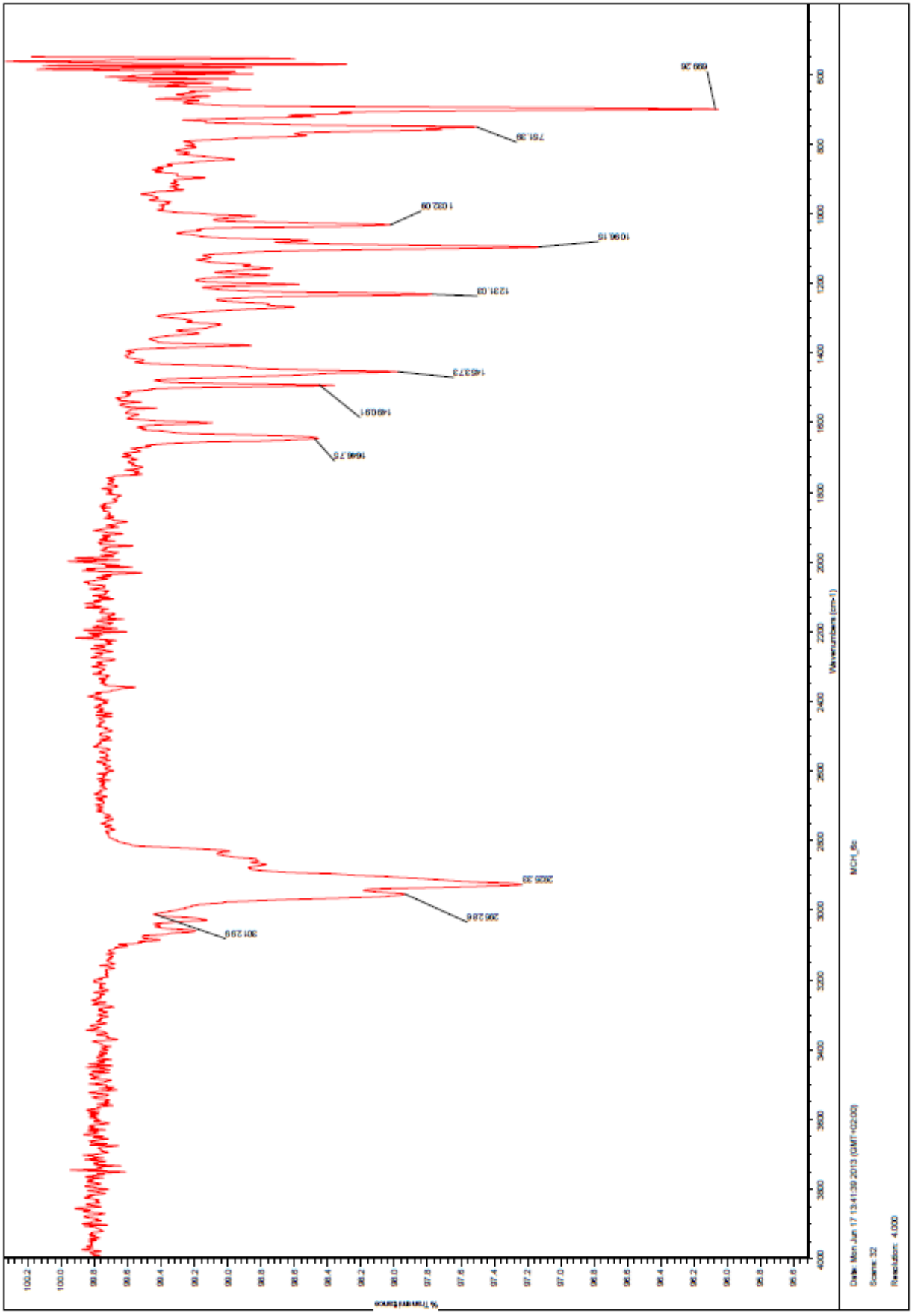

I Cyclization product 8a

I-1 ^{1}H NMR of cyclization product **8a**

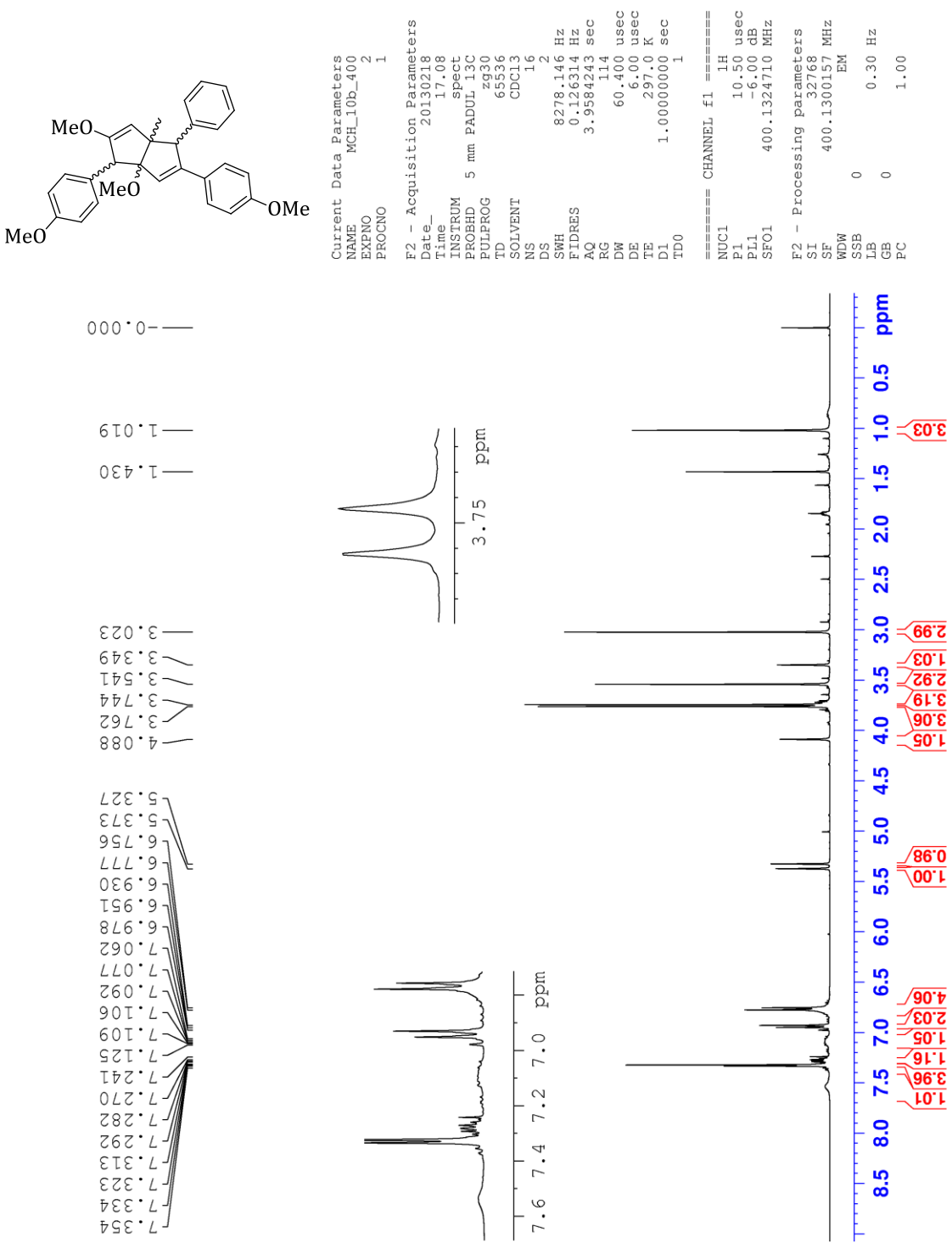

I-2 ^{13}C NMR of cyclization product **8a**

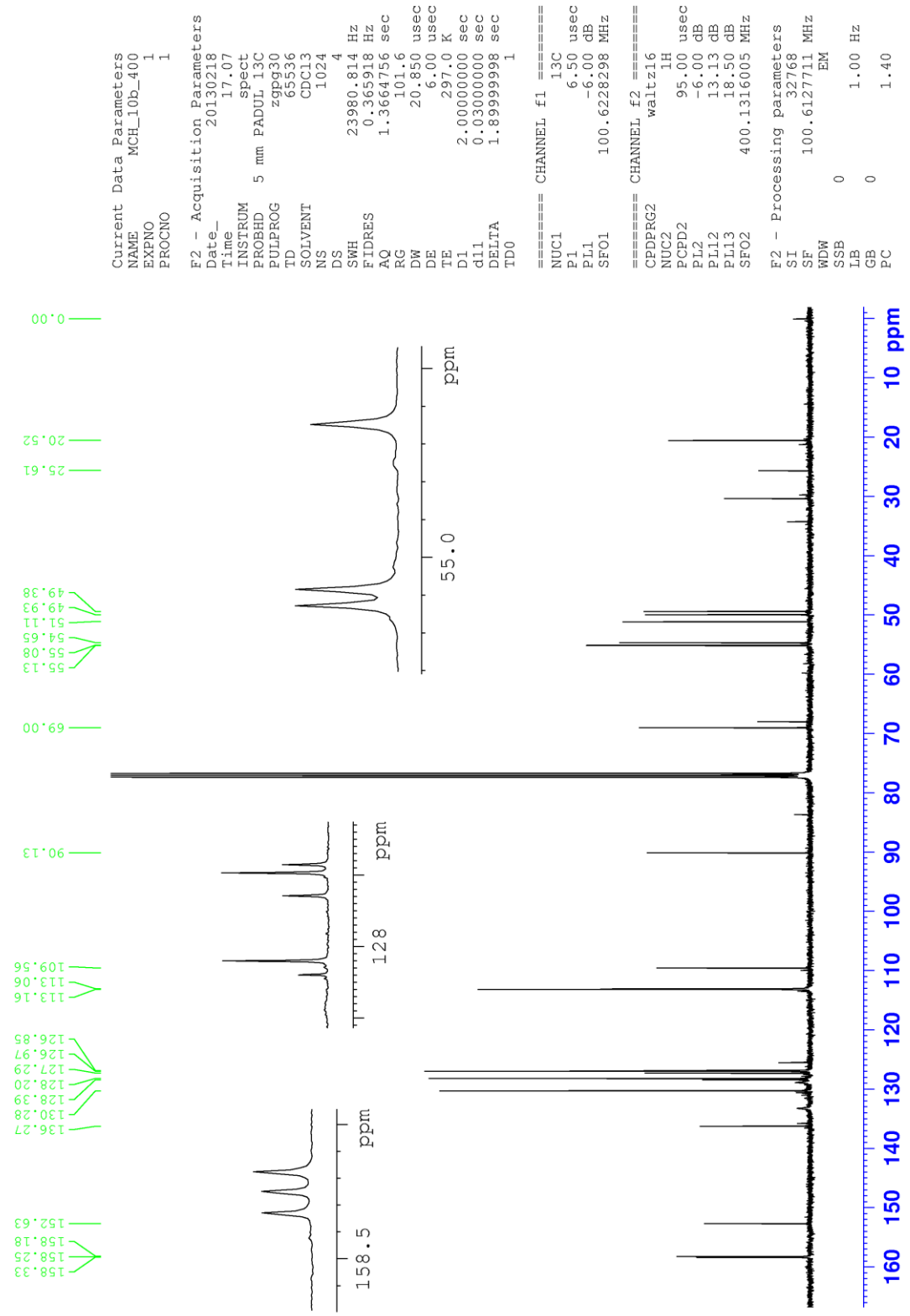

I-3 HSQC of cyclization product **8a**

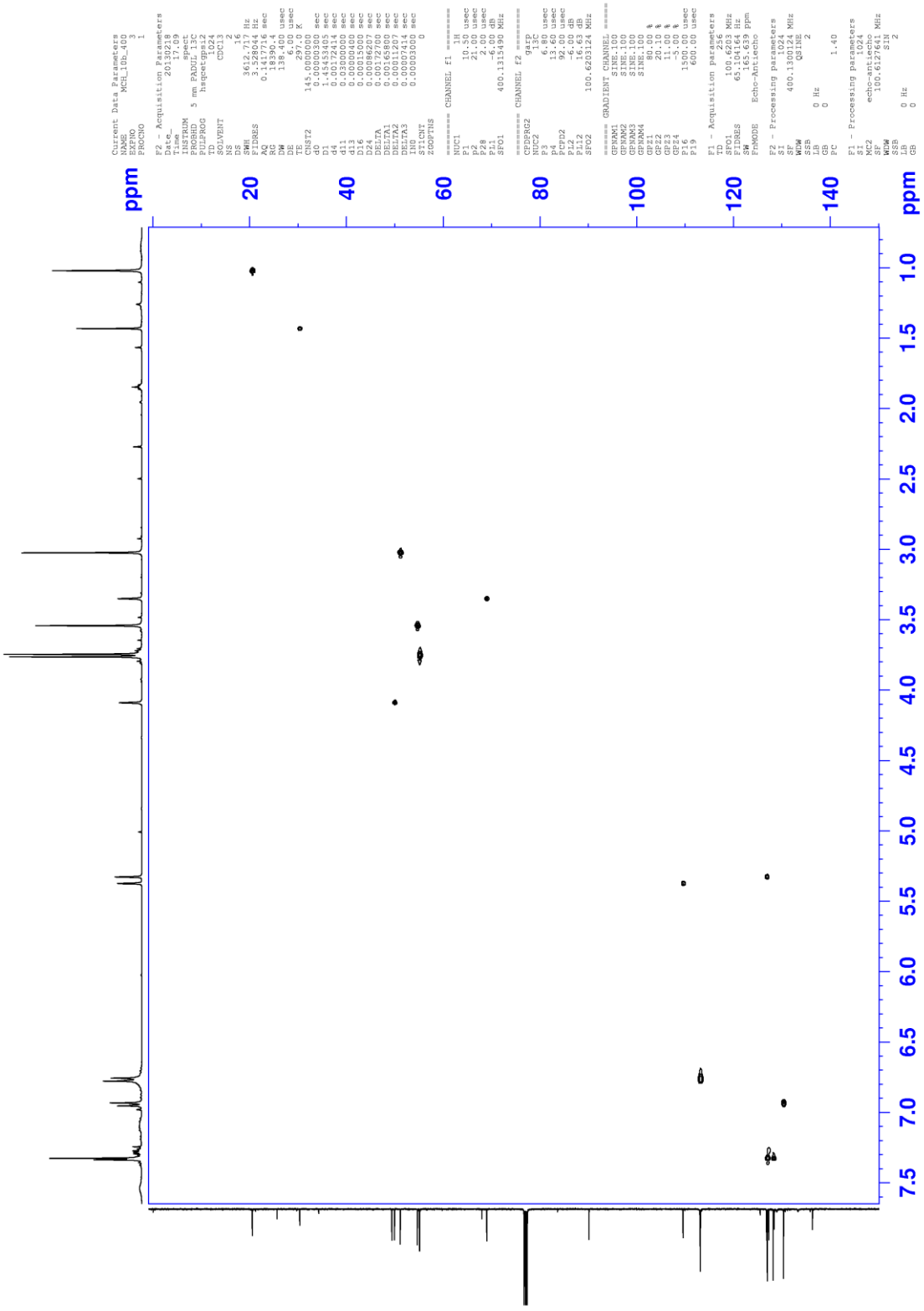

I-4 COSY of cyclization product **8a**

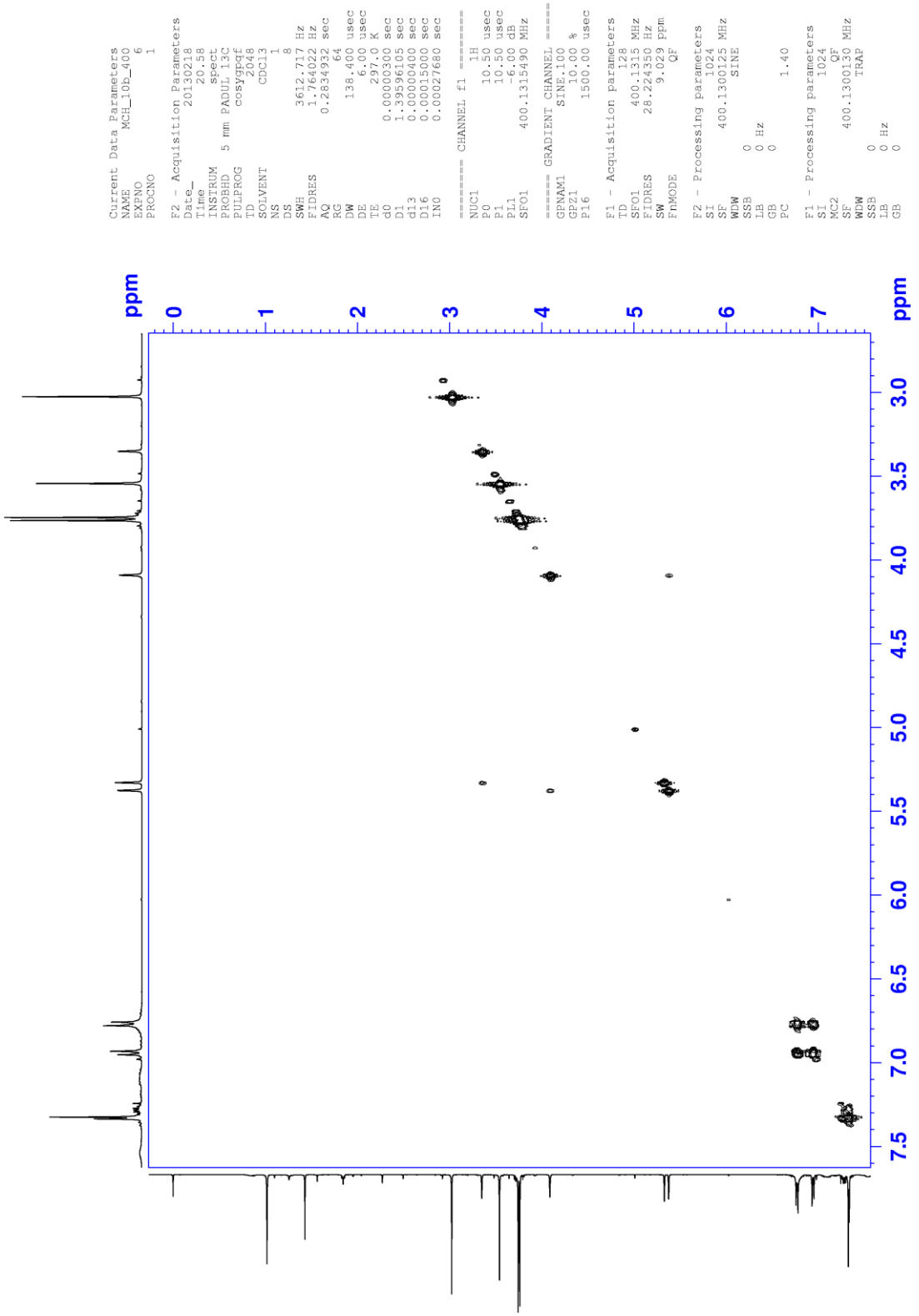

I-5 HMBC of cyclization product **8a**

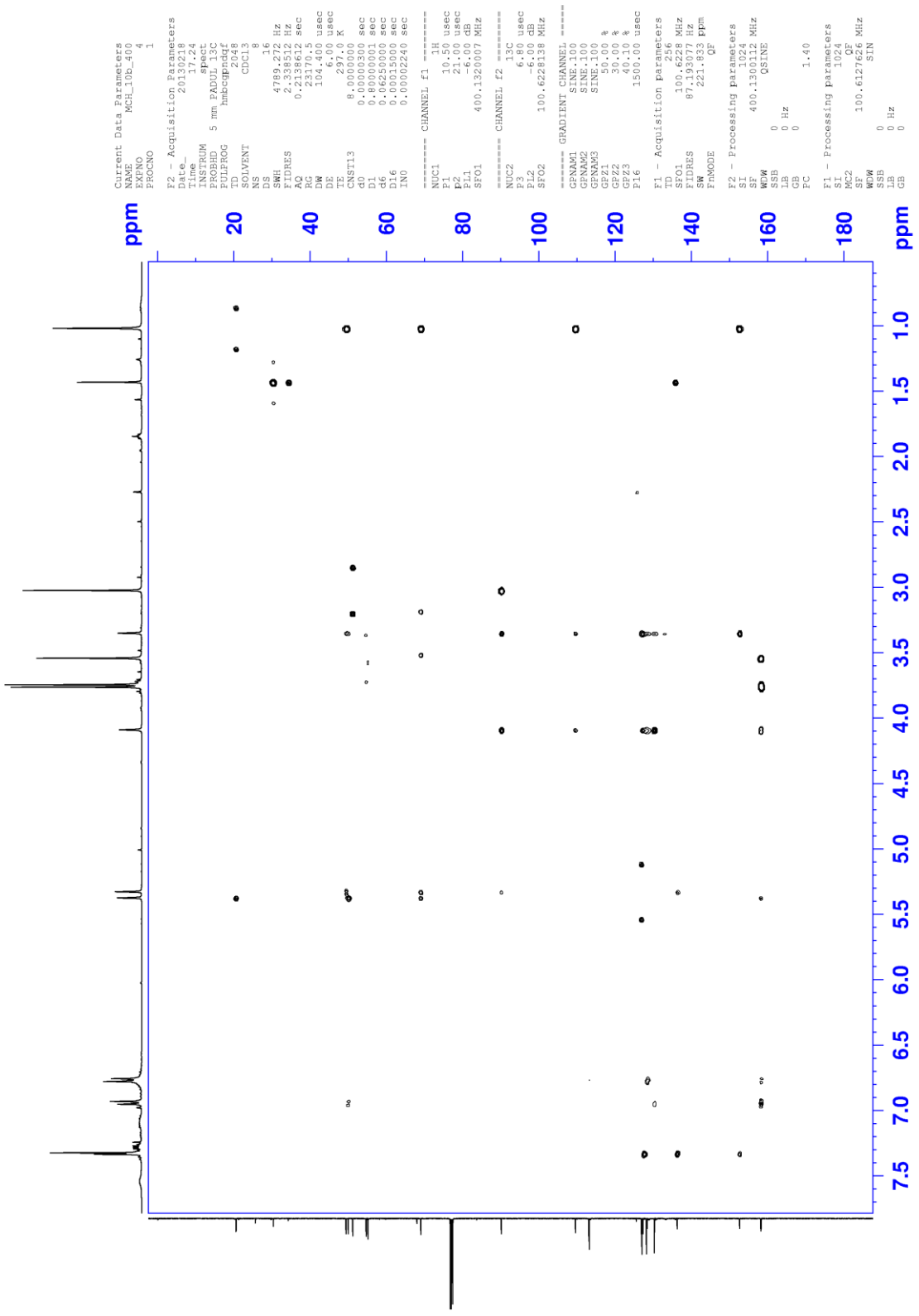

I-6 NOESY of cyclization product **8a**

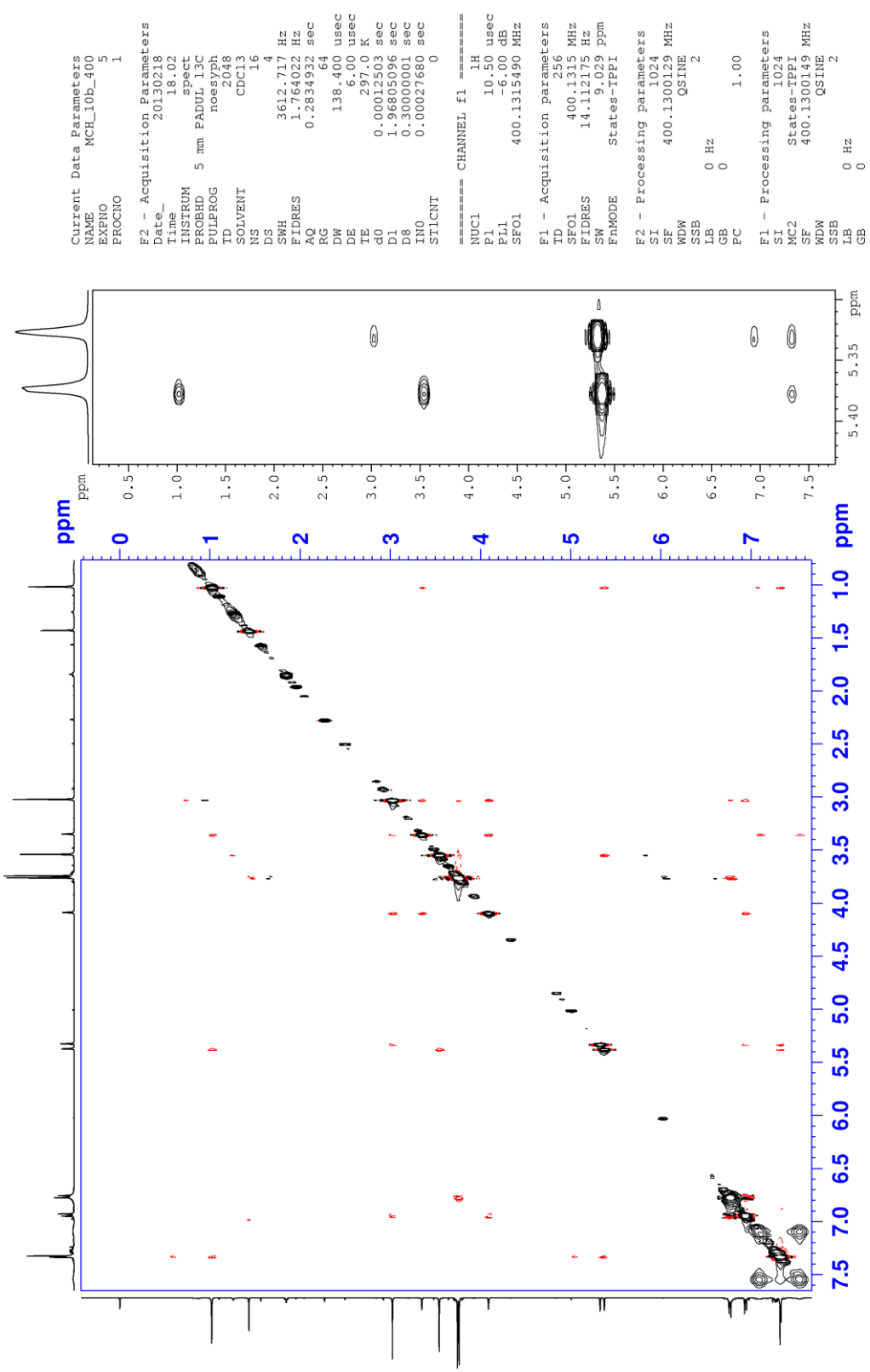

I-7 IR of cyclization product **8a**

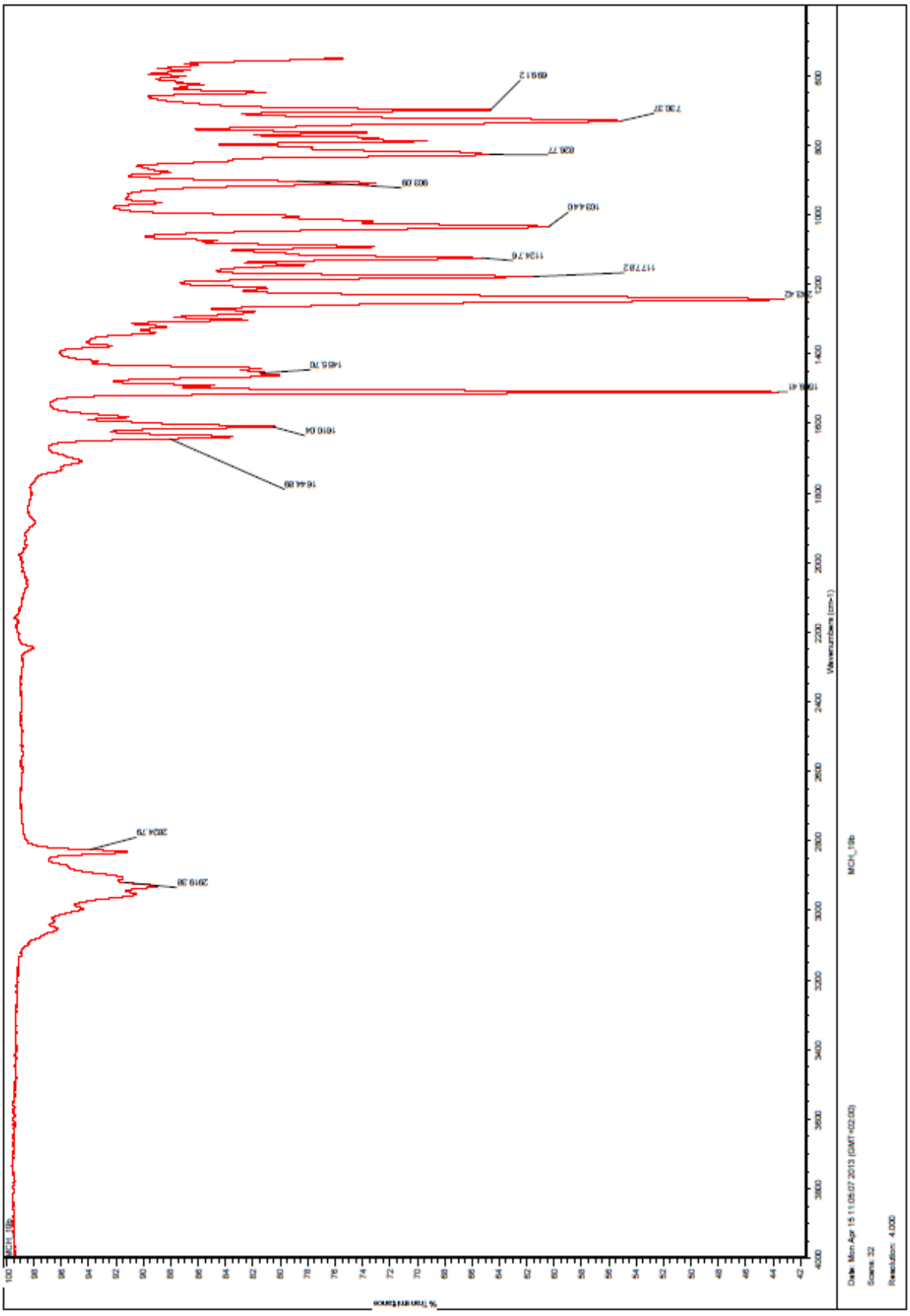

J Cyclization product 8b

J-1 ^{1}H NMR of cyclization product **8b**

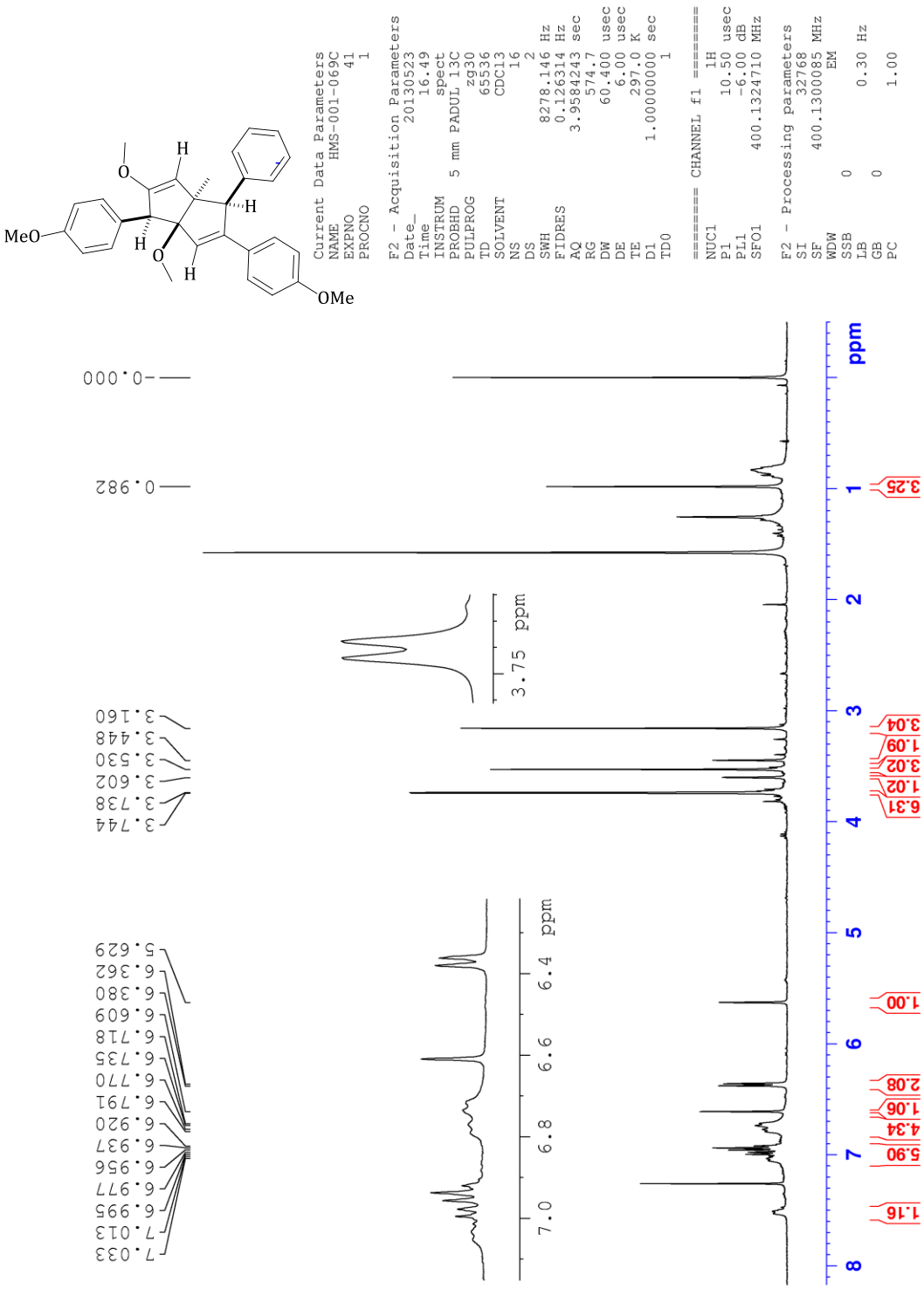

J-2 ^{13}C NMR of cyclization product **8b**

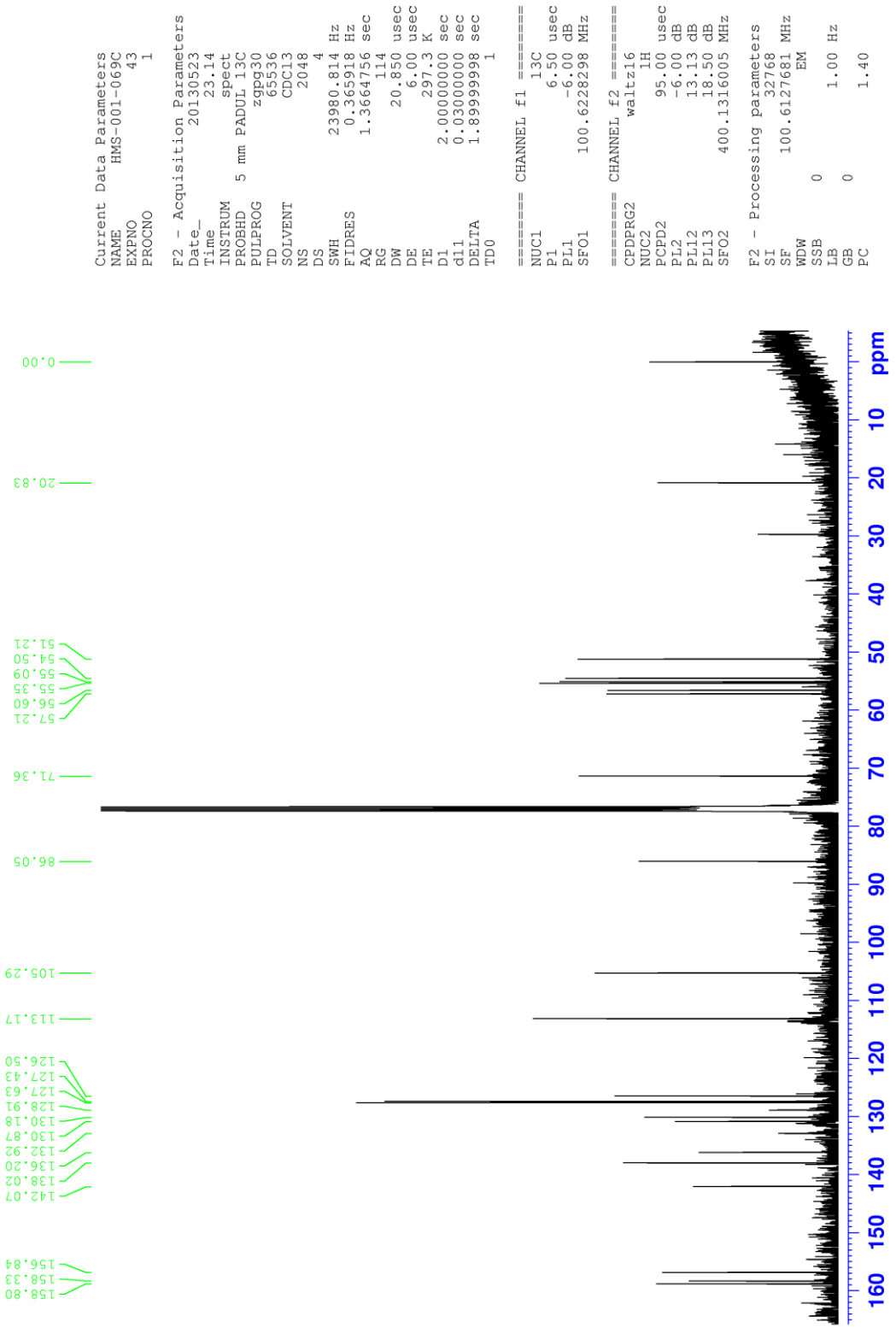

J-3 HSQC of cyclization product **8b**

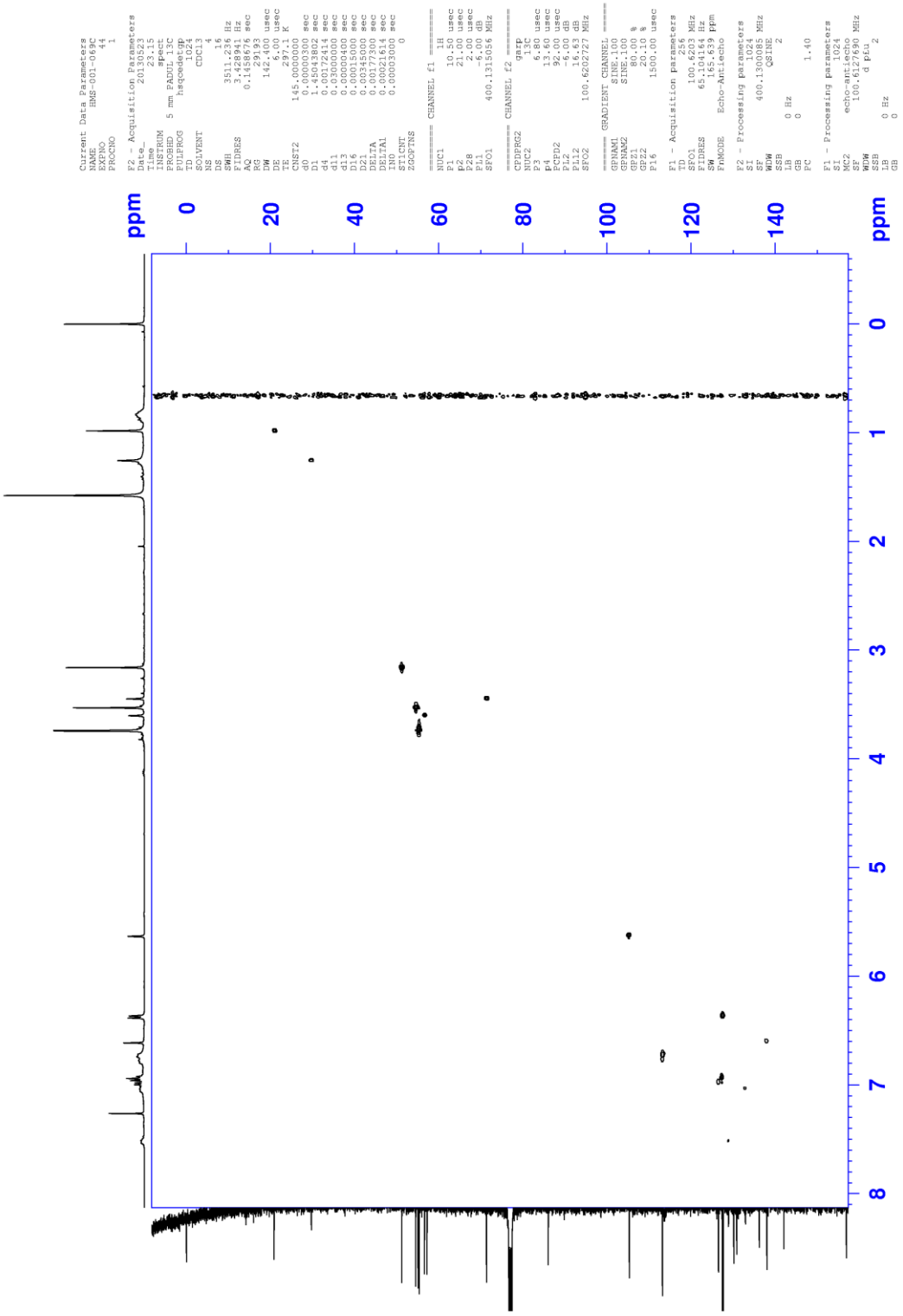

J-4 COSY of cyclization product **8b**

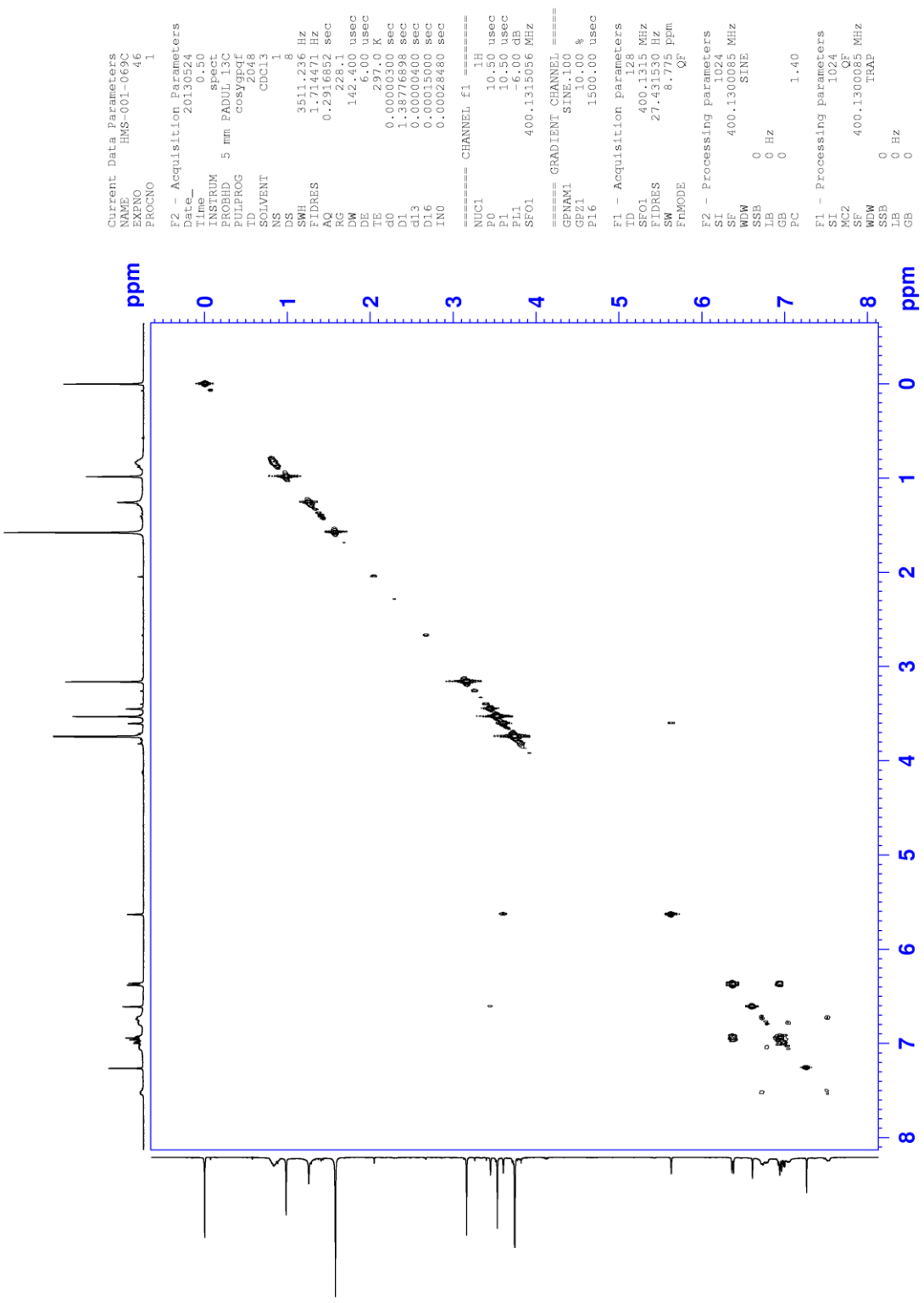

J-5 HMBC of cyclization product **8b**

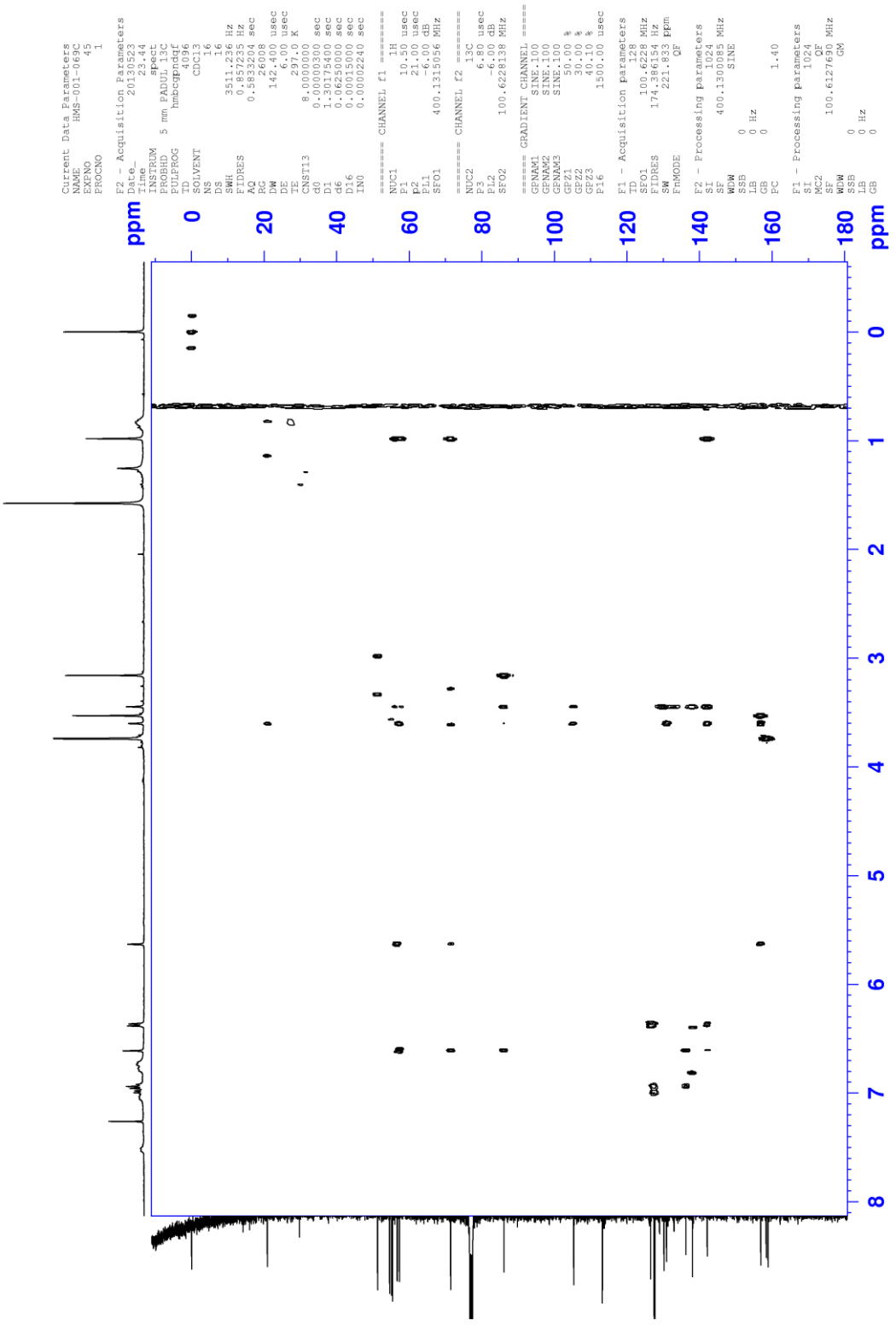

J-6 NOESY of cyclization product **8b**

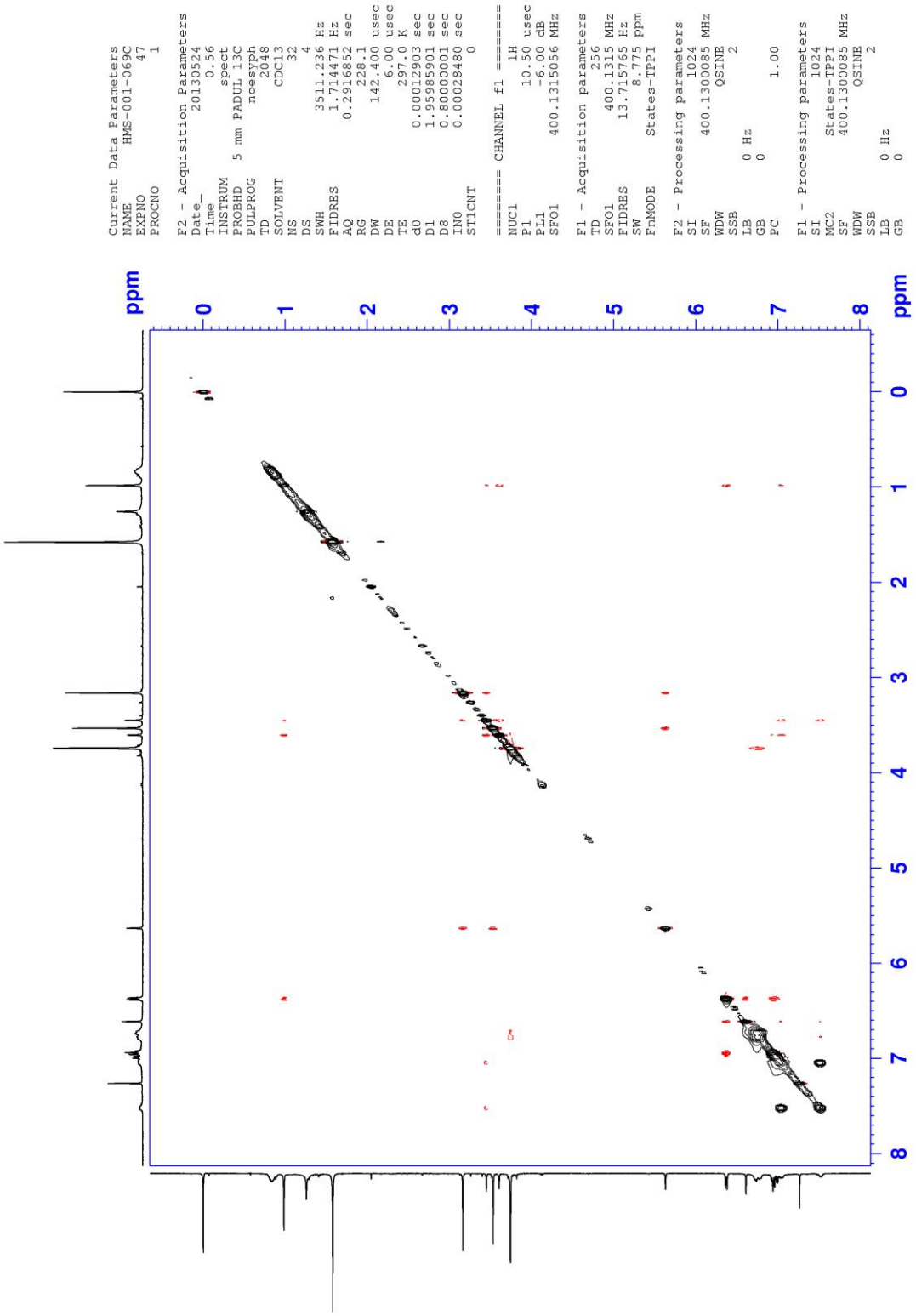

J-7 IR of cyclization product **8b**

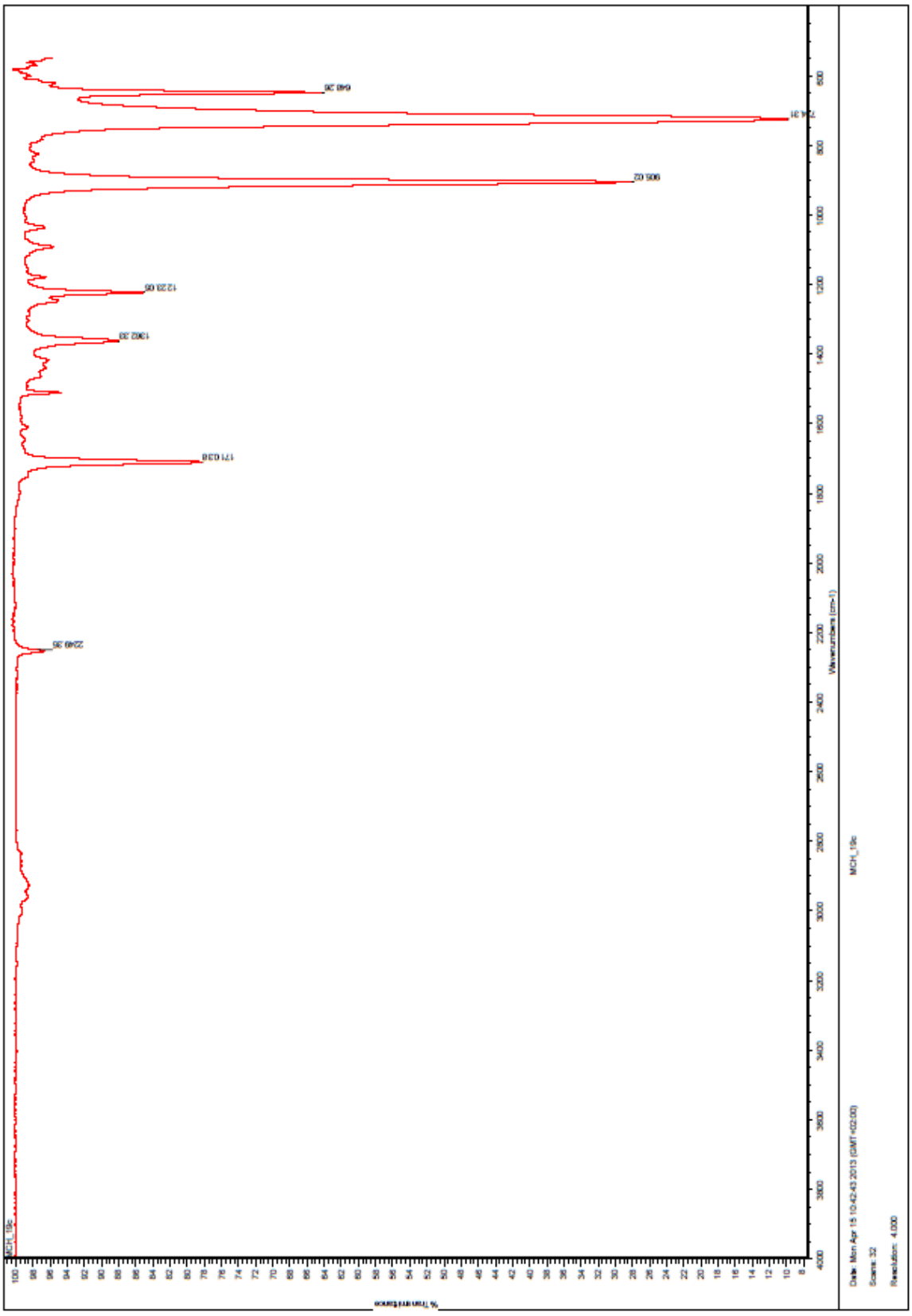

K Cyclization product 9

K-1 ^{1}H NMR of cyclization product **9**

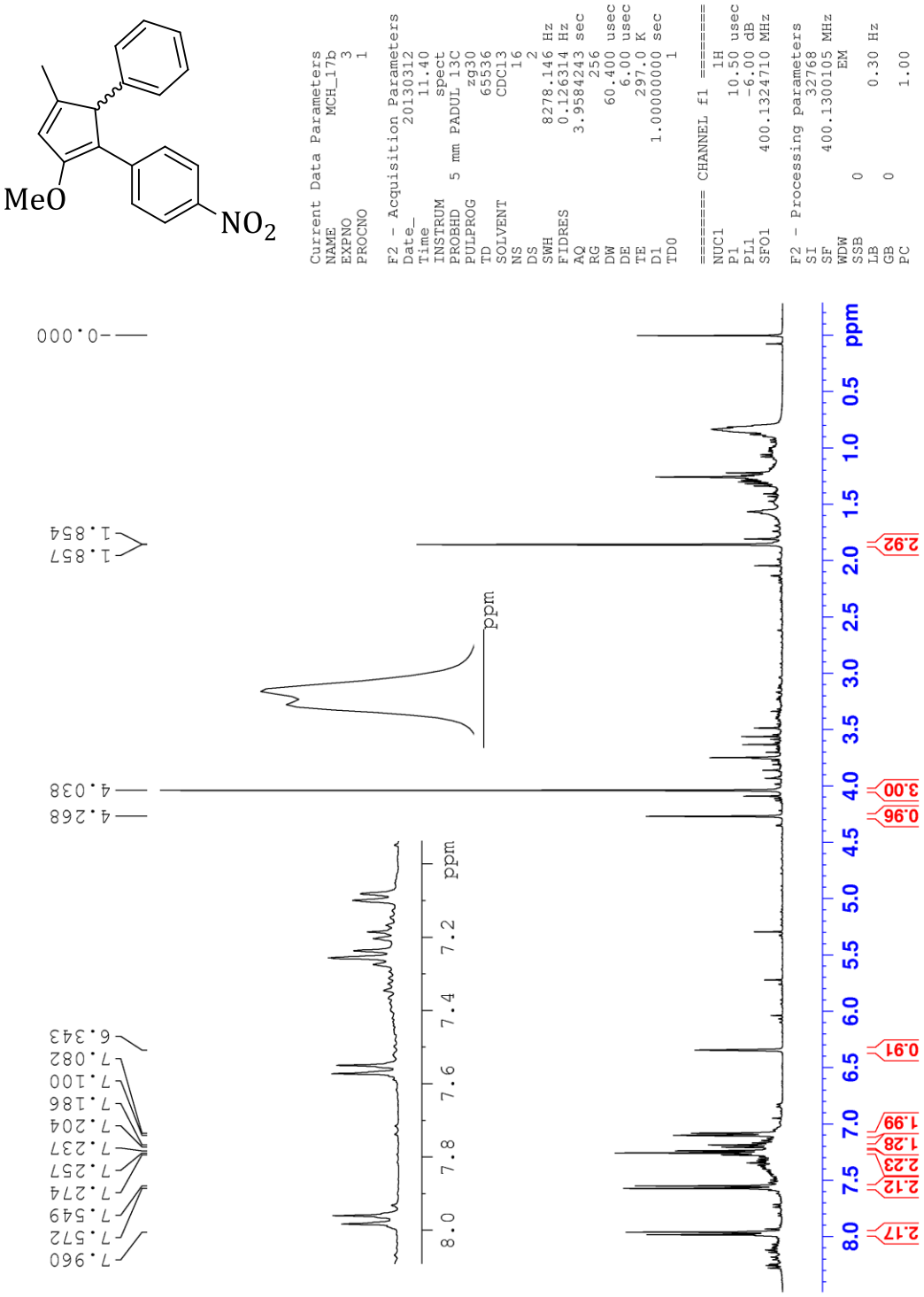

K-2 ^{13}C NMR of cyclization product **9**

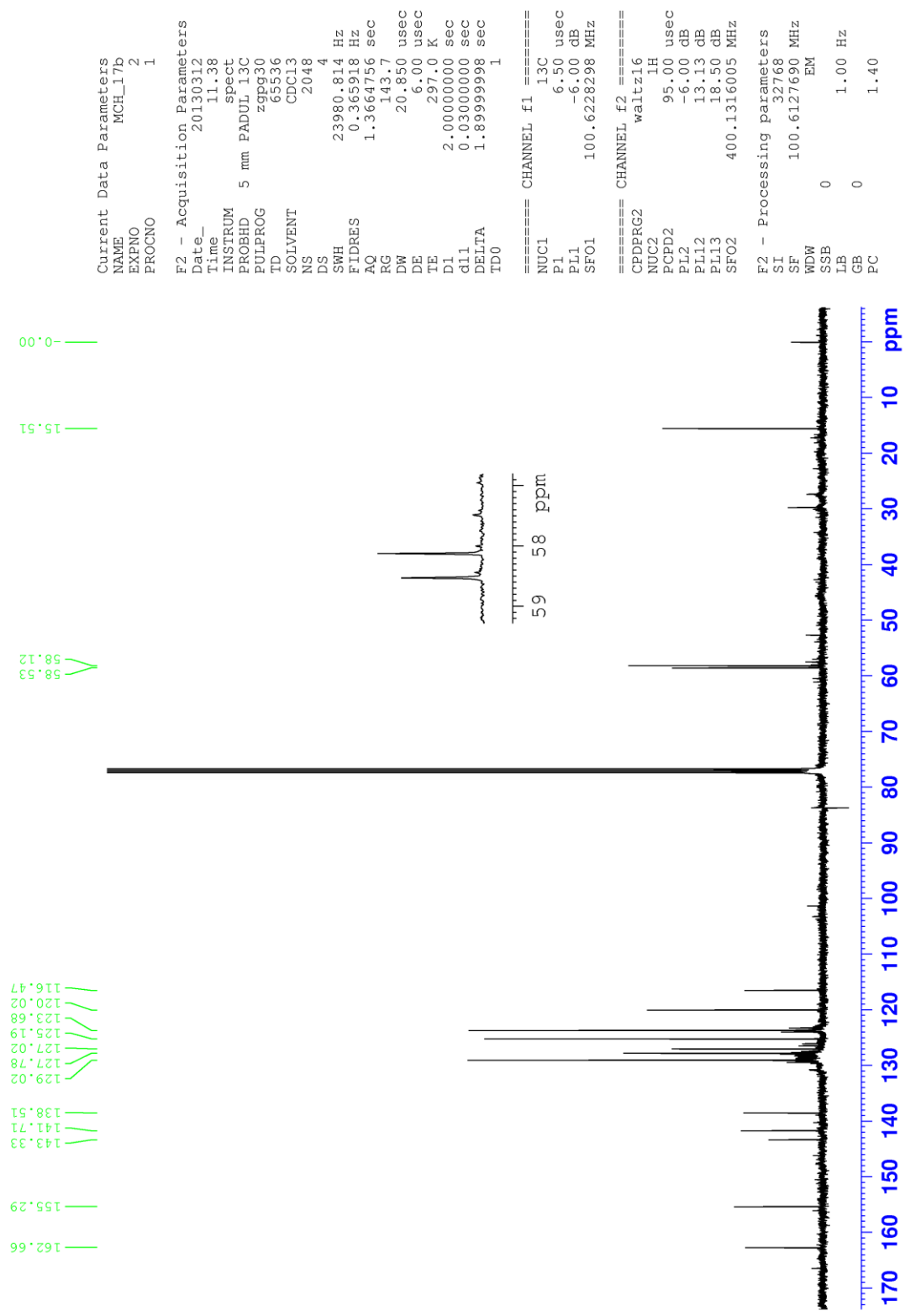

K-3 HSQC of cyclization product **9**

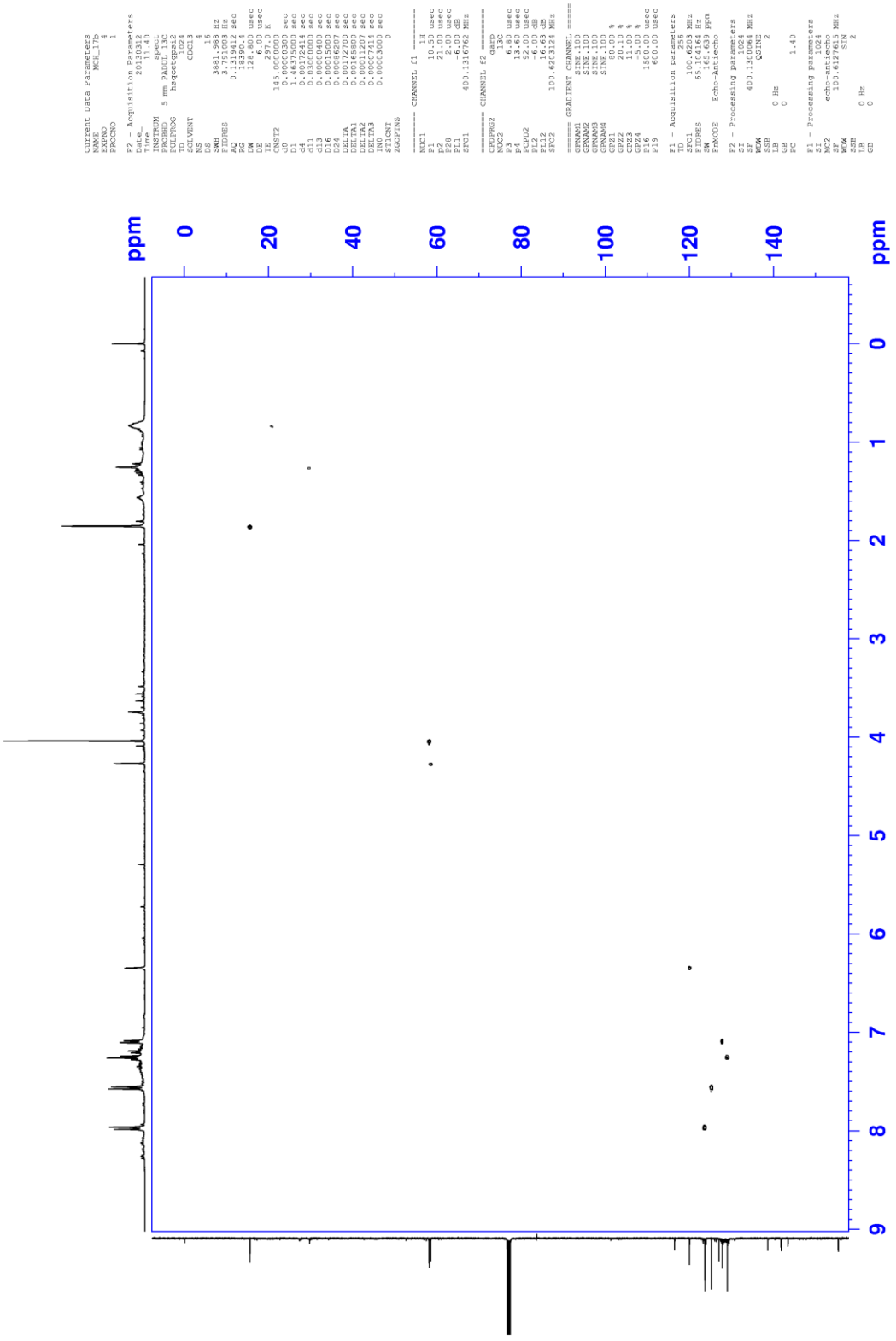

K-4 HMBC of cyclization product **9**

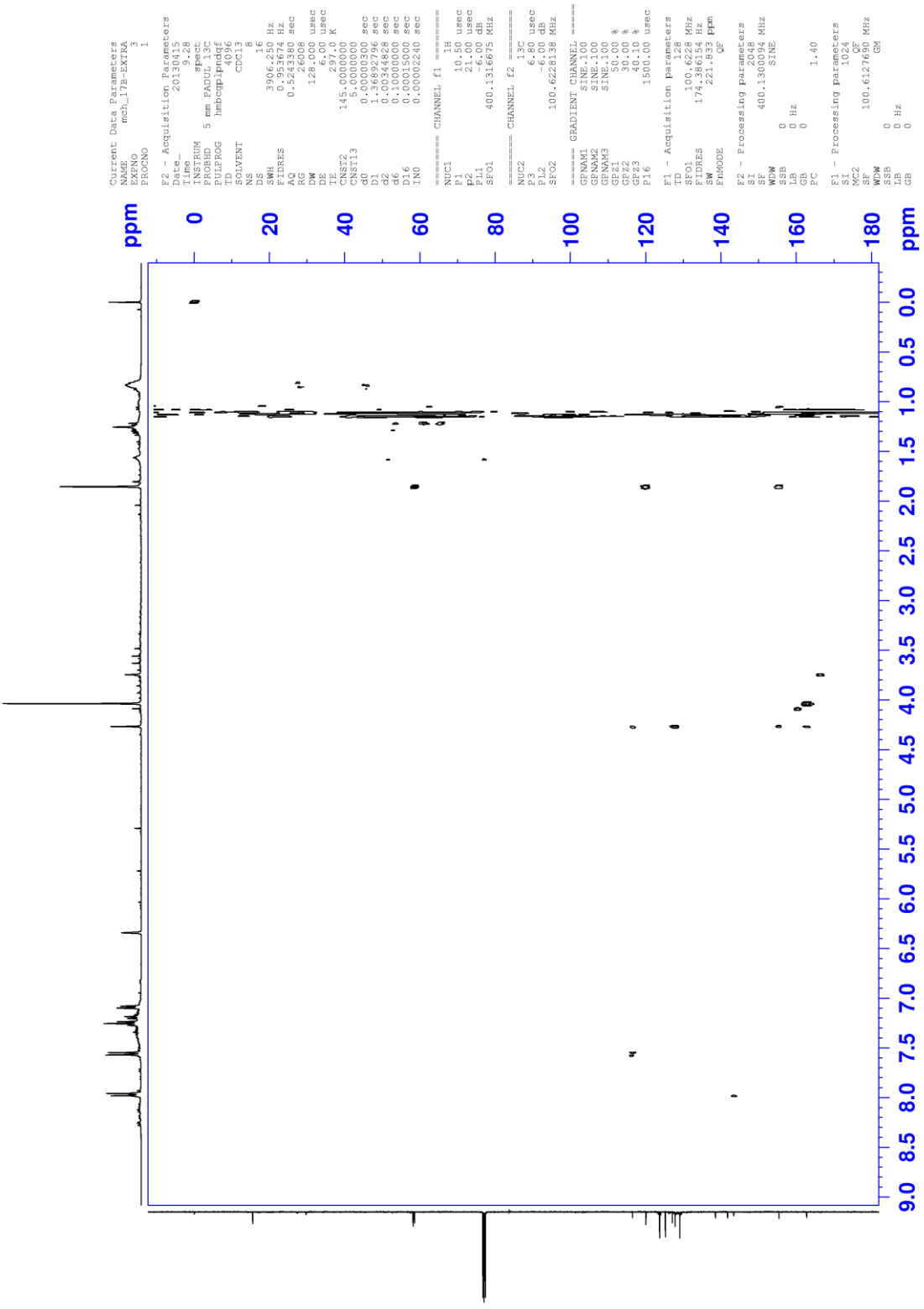

K-5 NOESY of cyclization product **9**

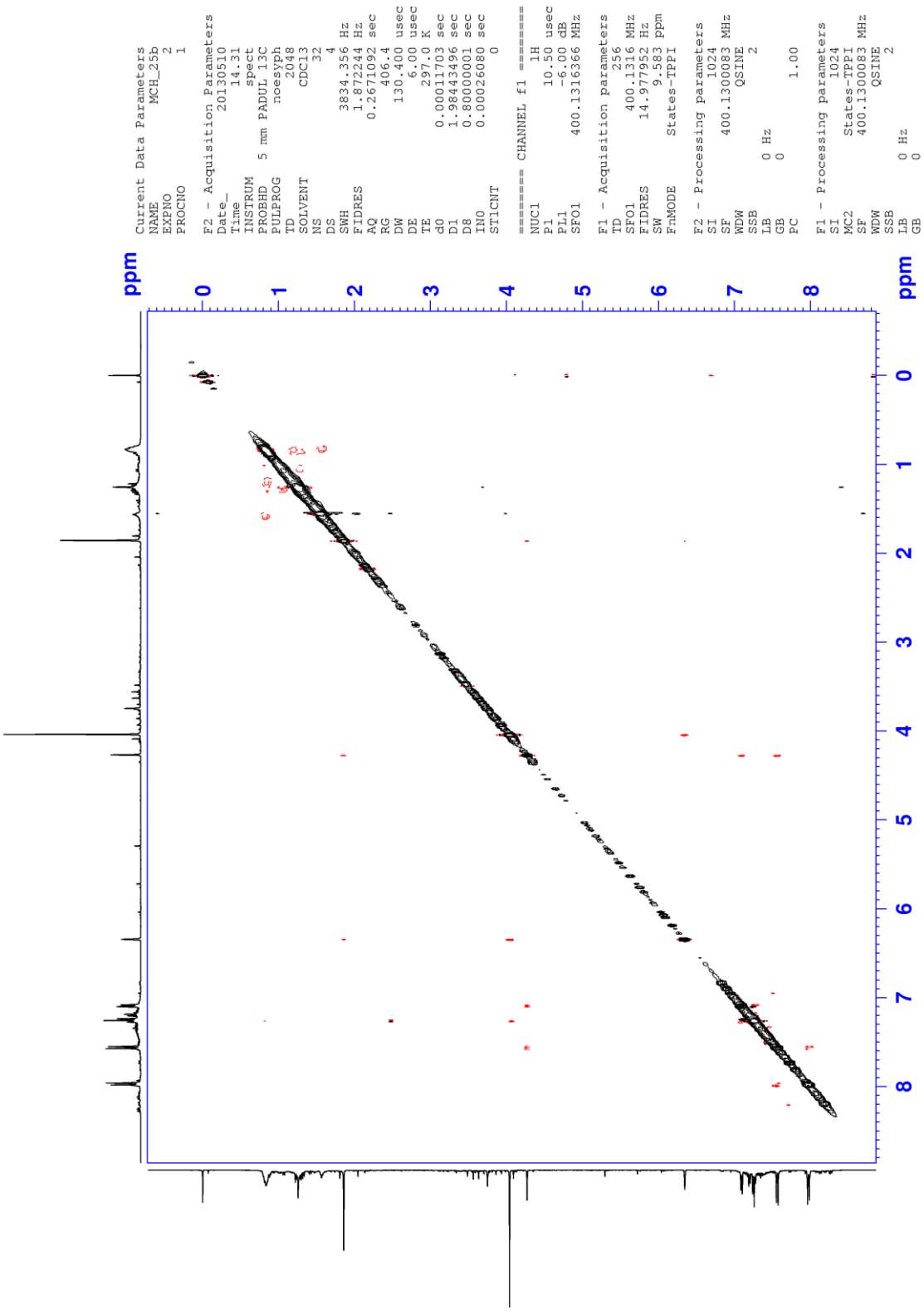

K-6 IR of cyclization product **9**

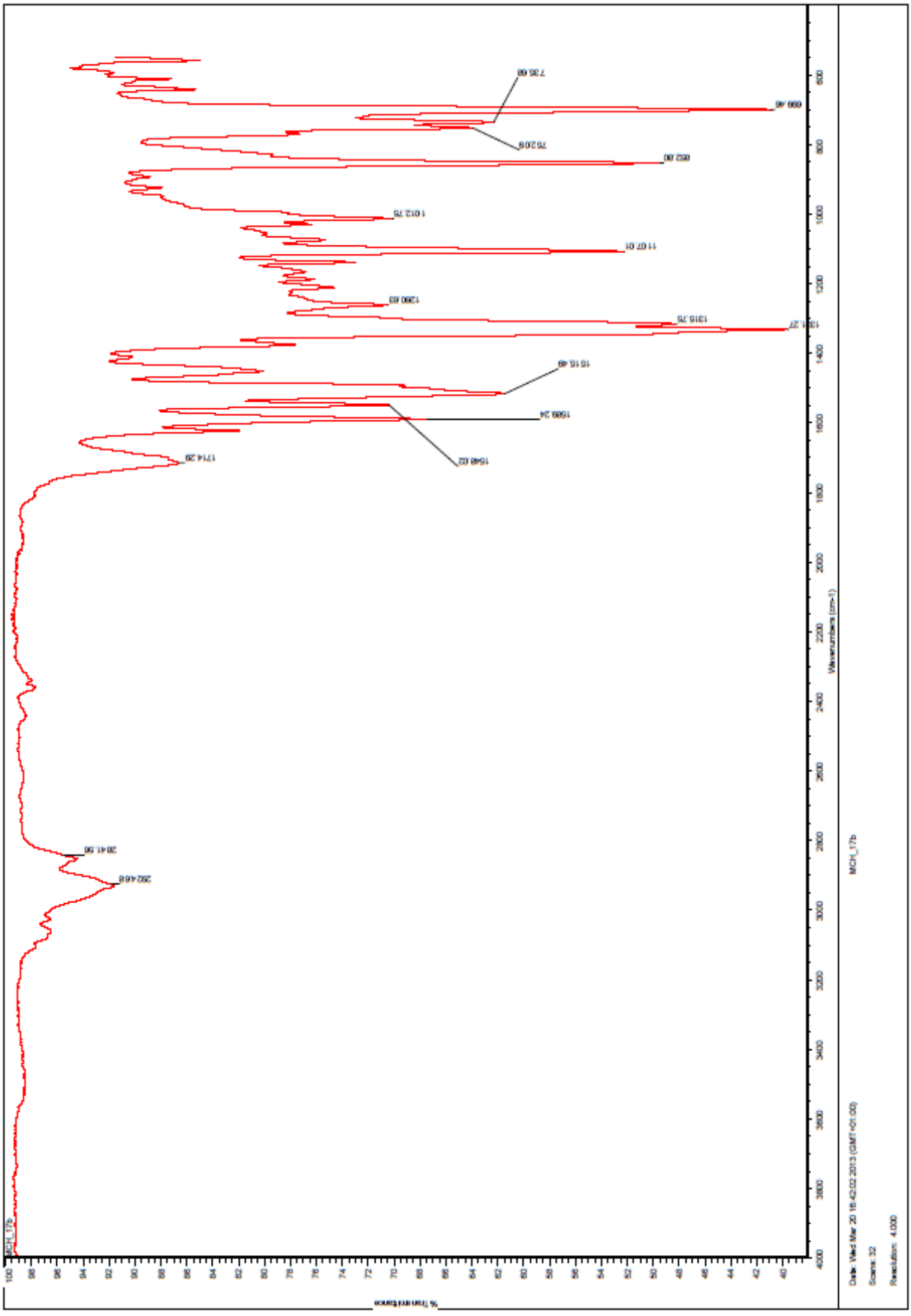

L Cyclization product 10a

L-1 ^{1}H NMR of cyclization product **10a**

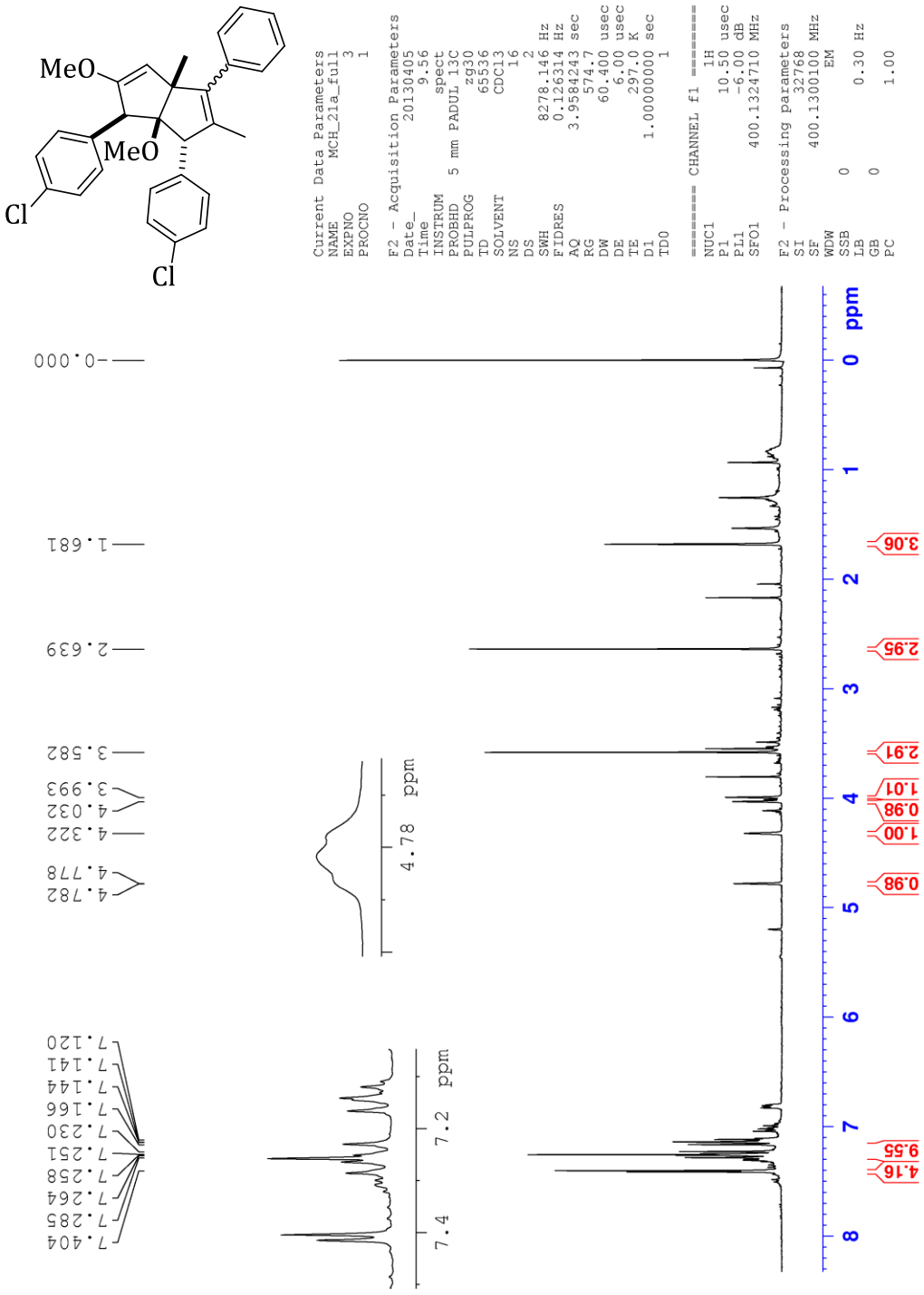

L-2 ^{13}C NMR of cyclization product **10a**

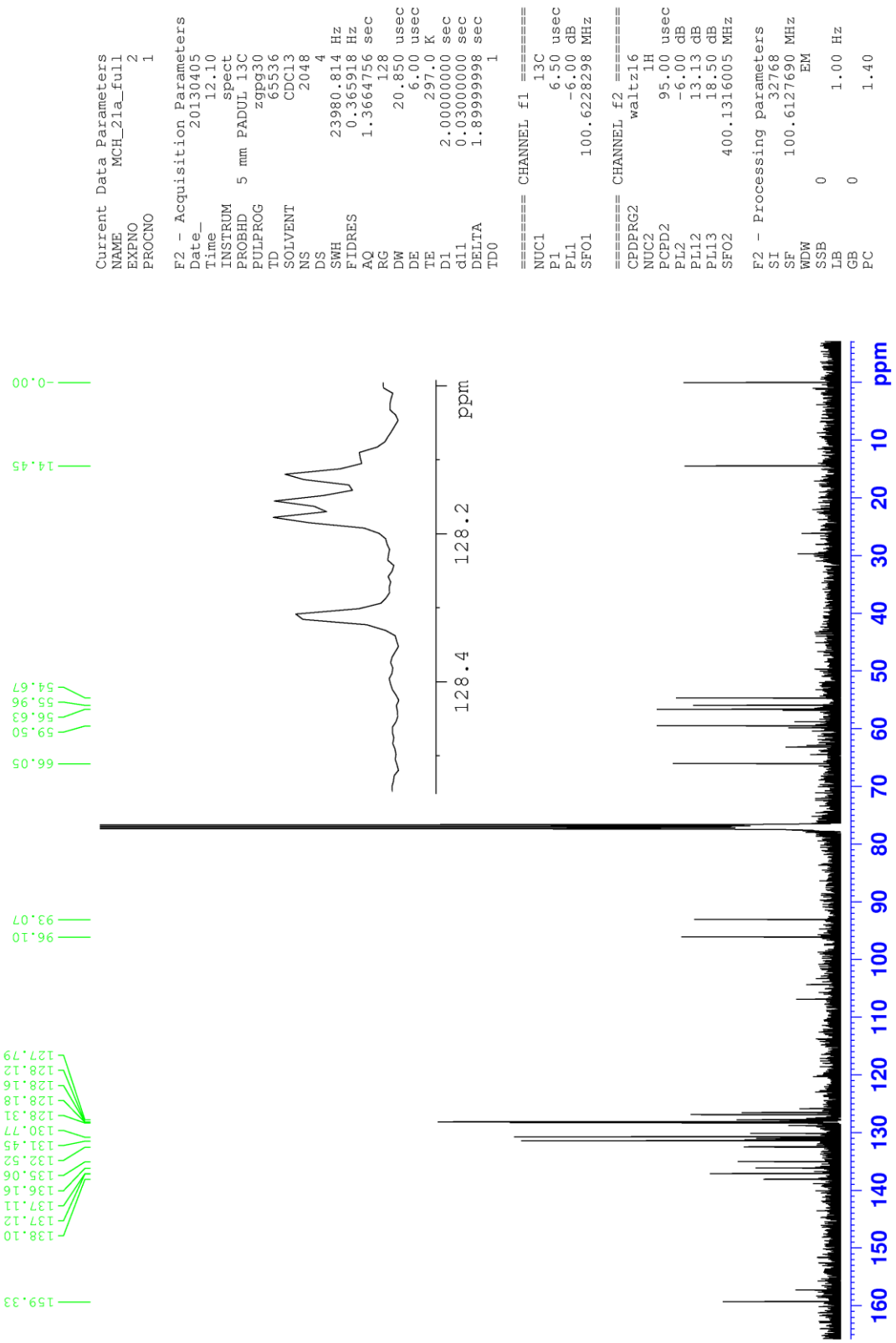

L-3 HSQC of cyclization product **10a**

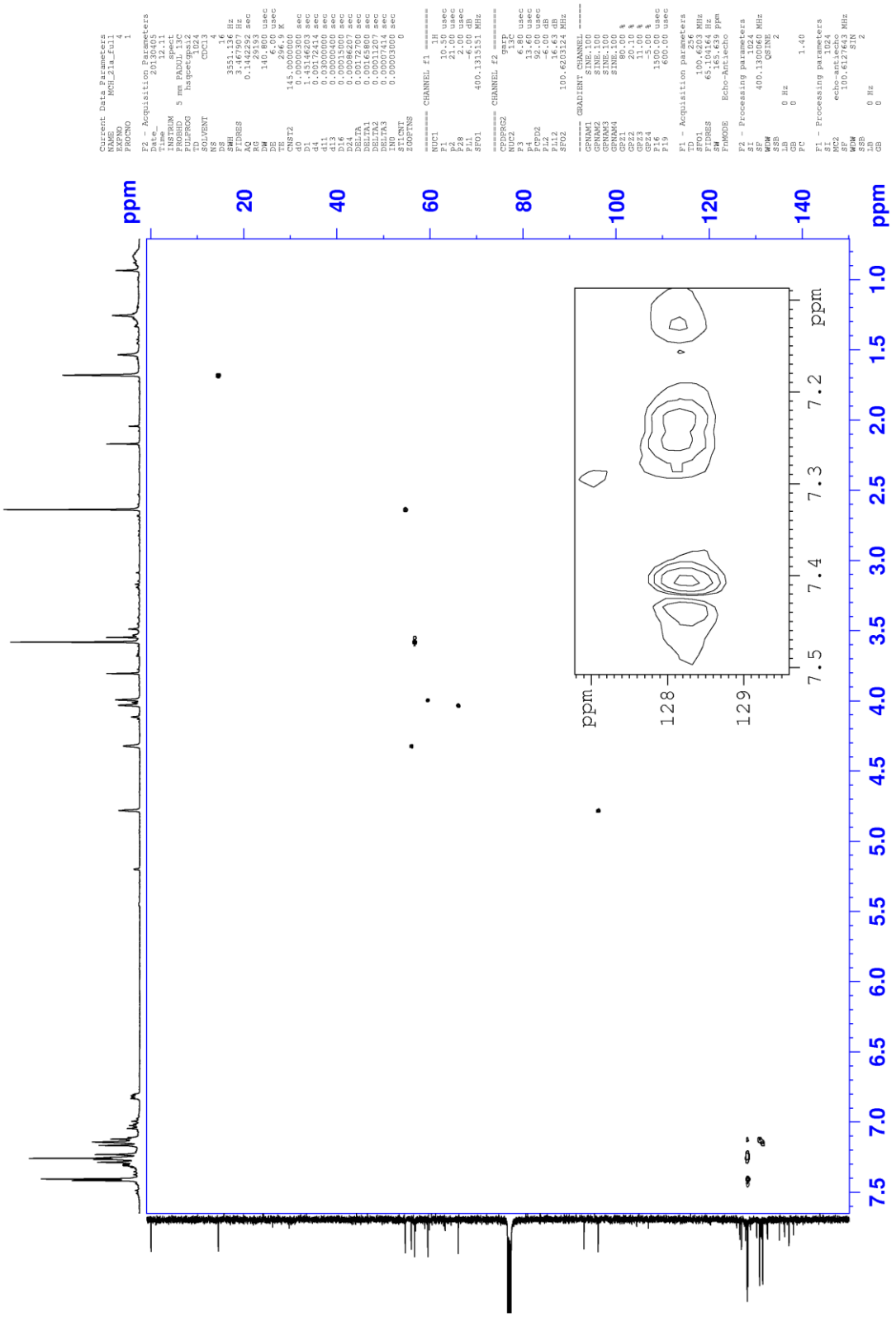

L-4 COSY of cyclization product **10a**

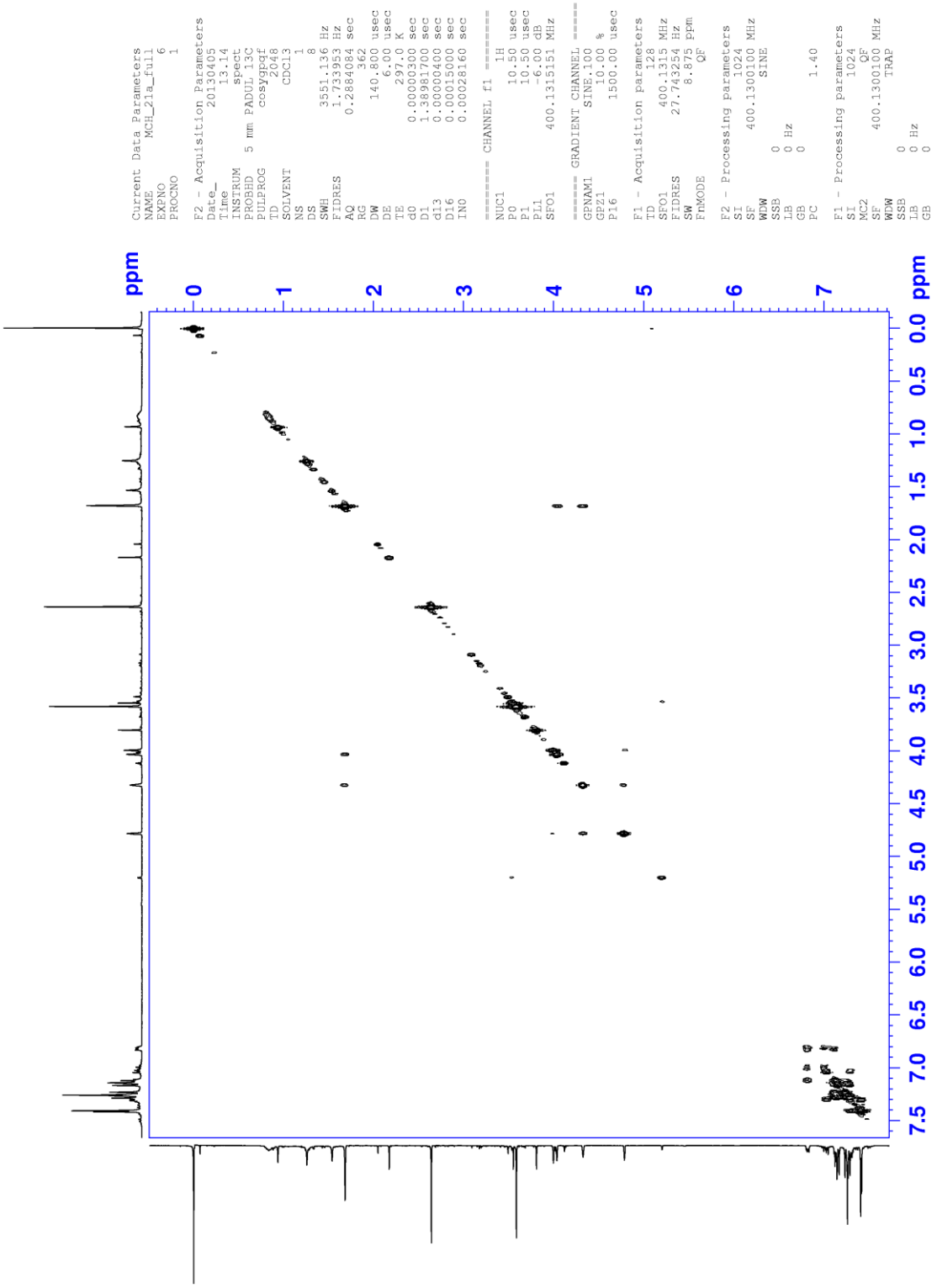

L-5 HMBC of cyclization product **10a**

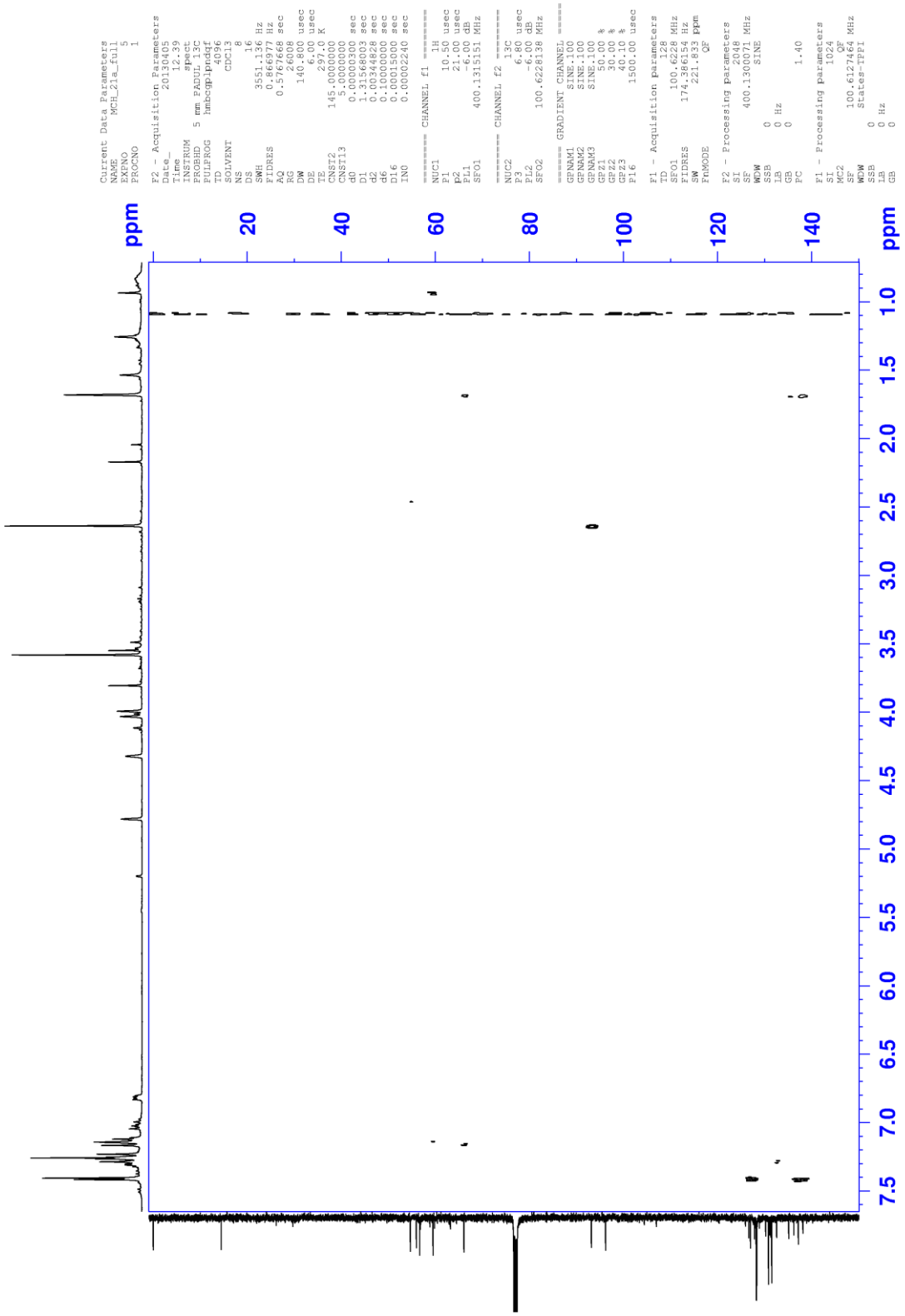

L-6 NOESY of cyclization product **10a**

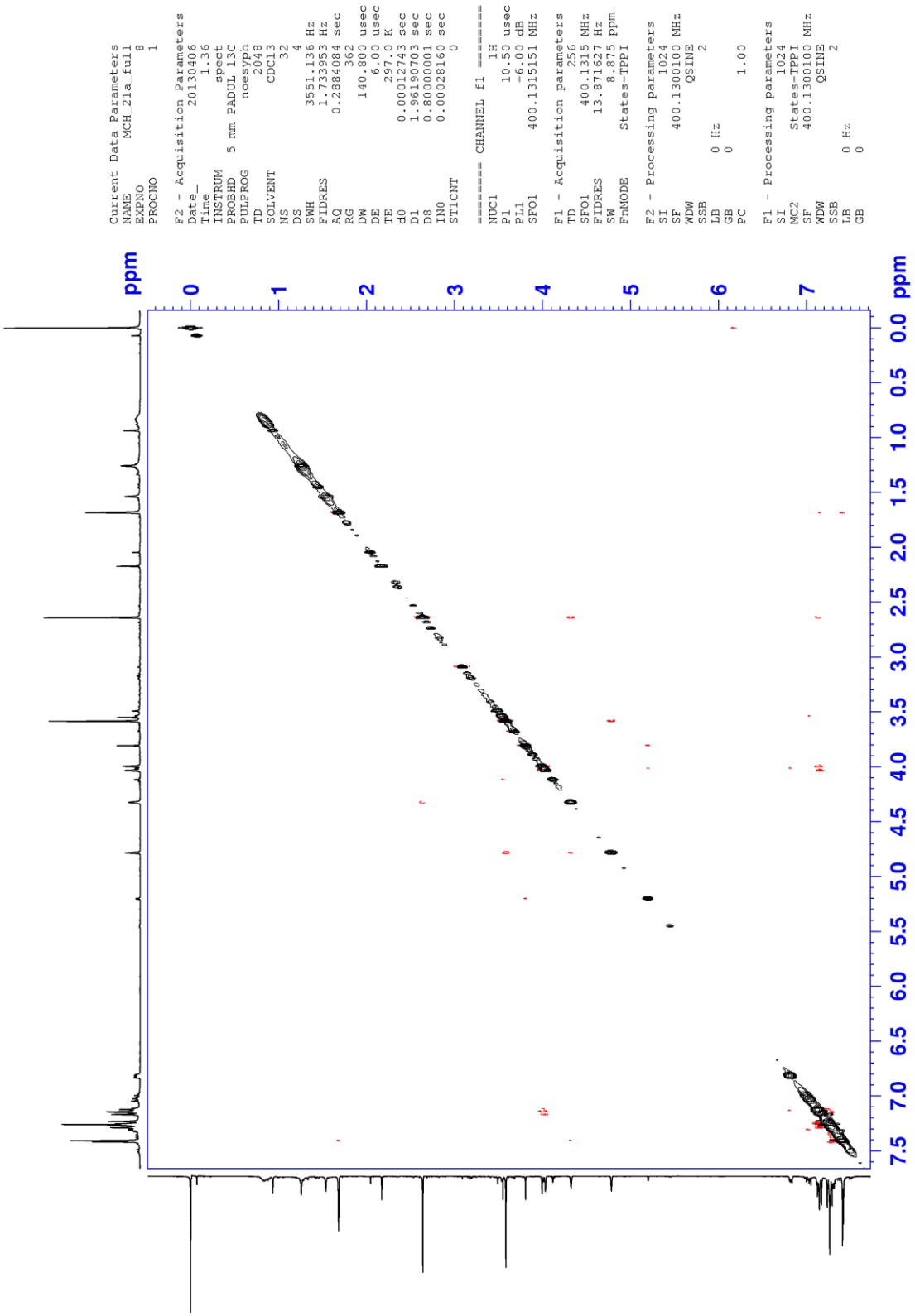

L-7 IR of cyclization product **10a**

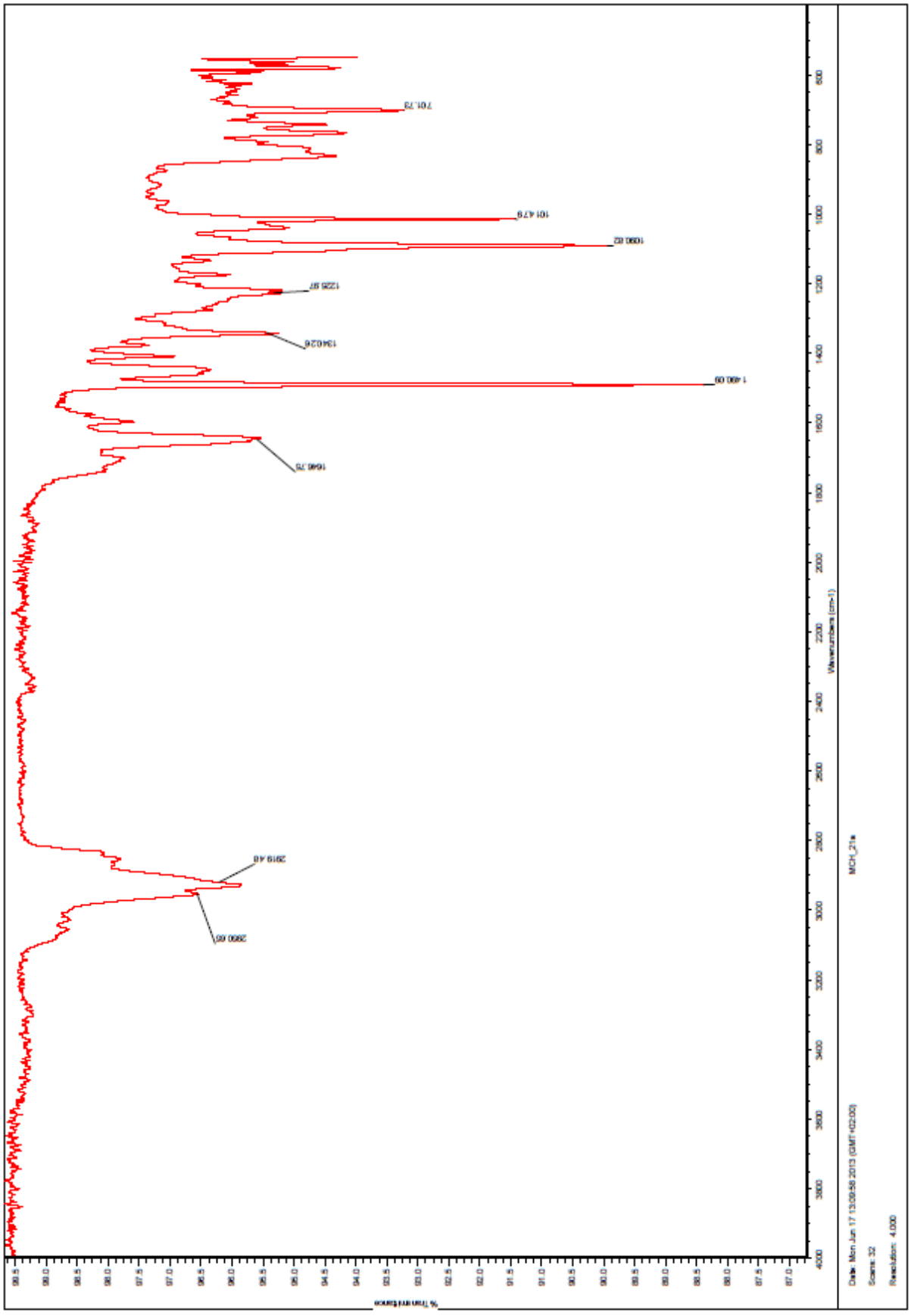

M Cyclization products 10b-c

M-1 ^{1}H NMR of cyclization products **10b-c**

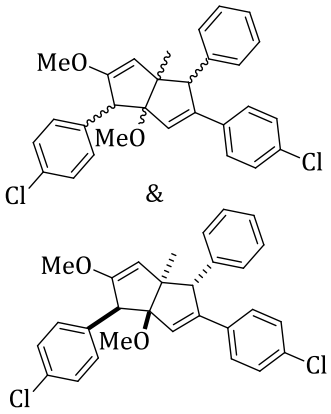

M-2 ^{13}C NMR of cyclization products **10b-c**

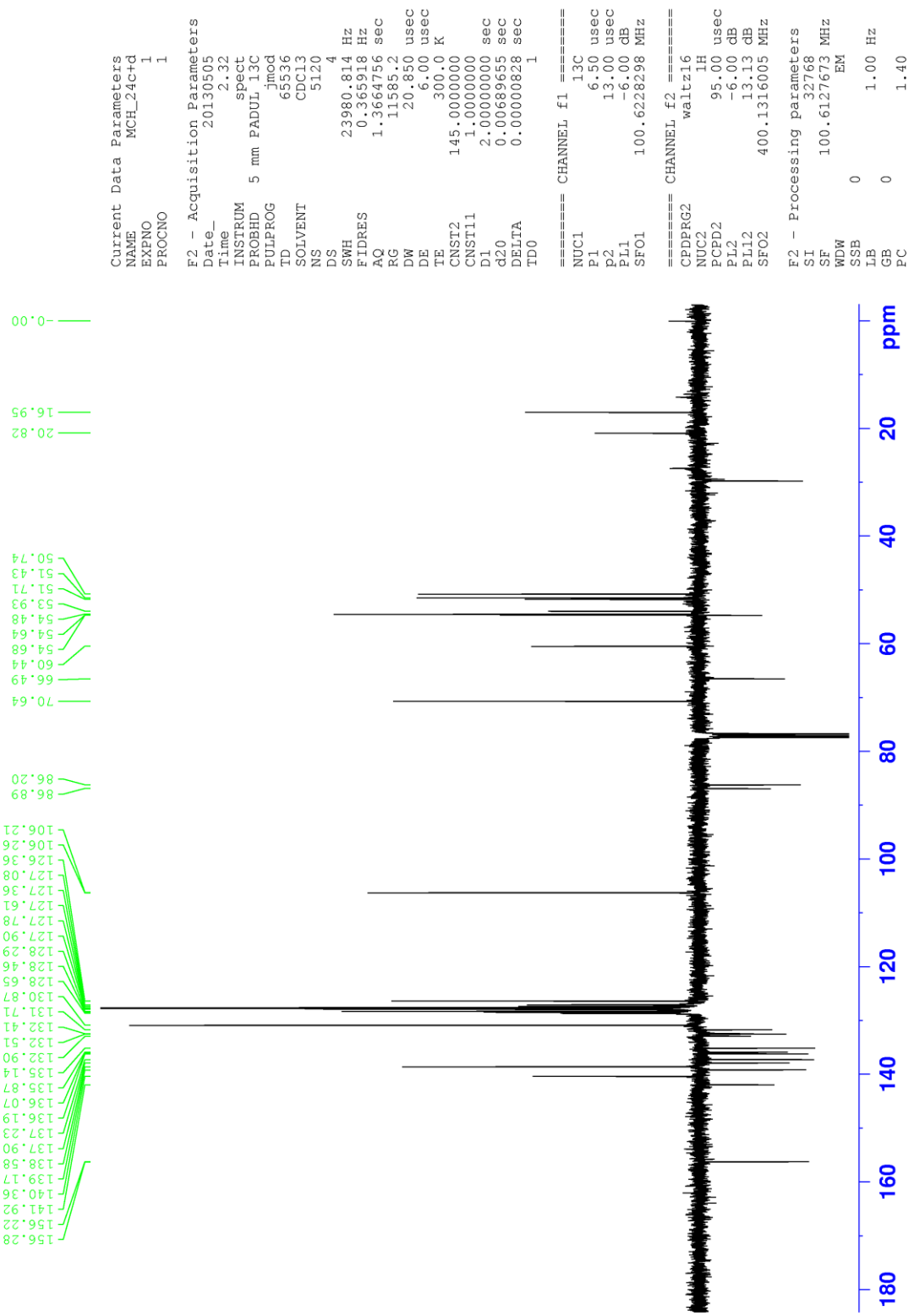

M-3 HSQC of cyclization products **10b-c**

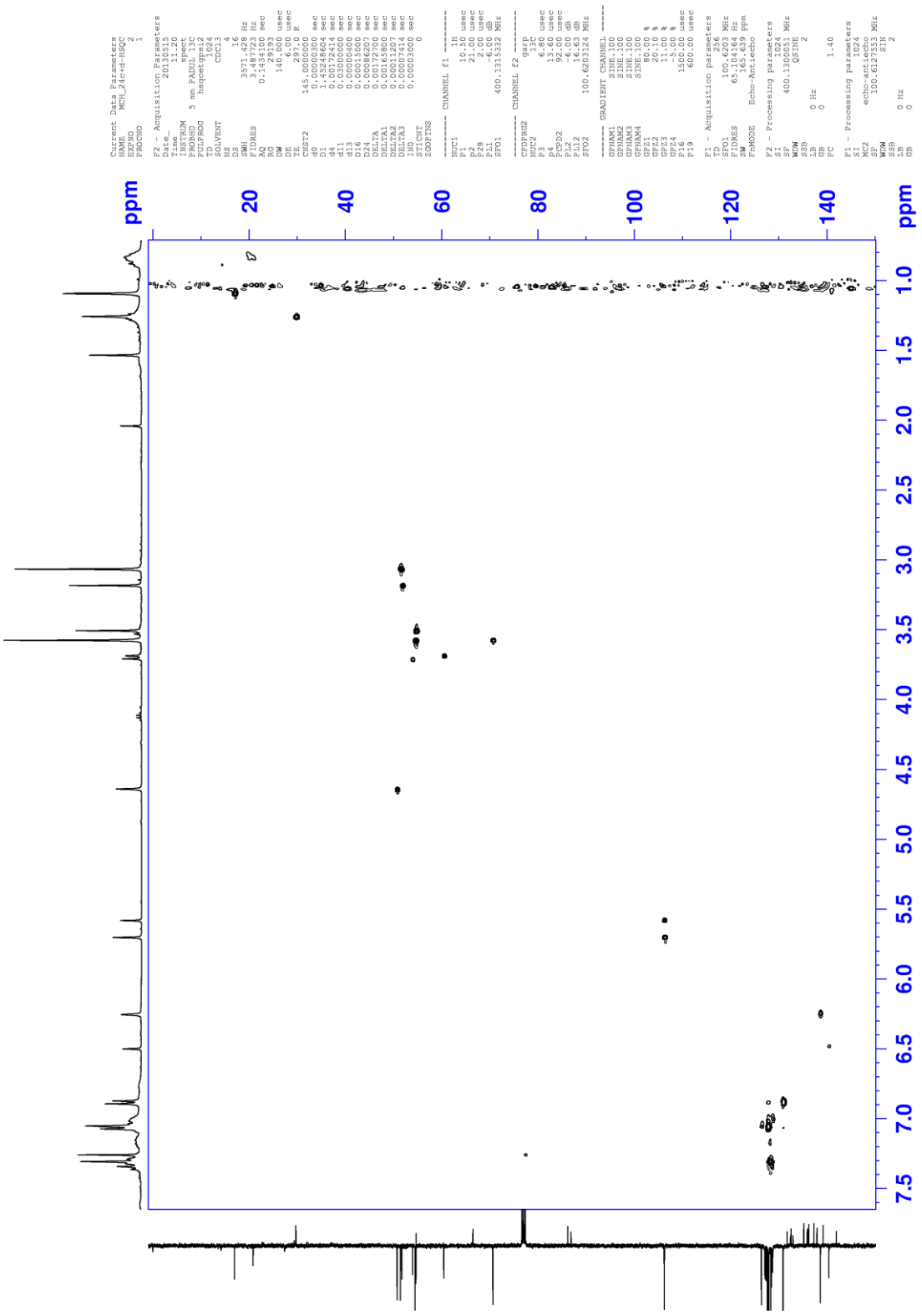

M-4 COSY of cyclization products **10b-c**

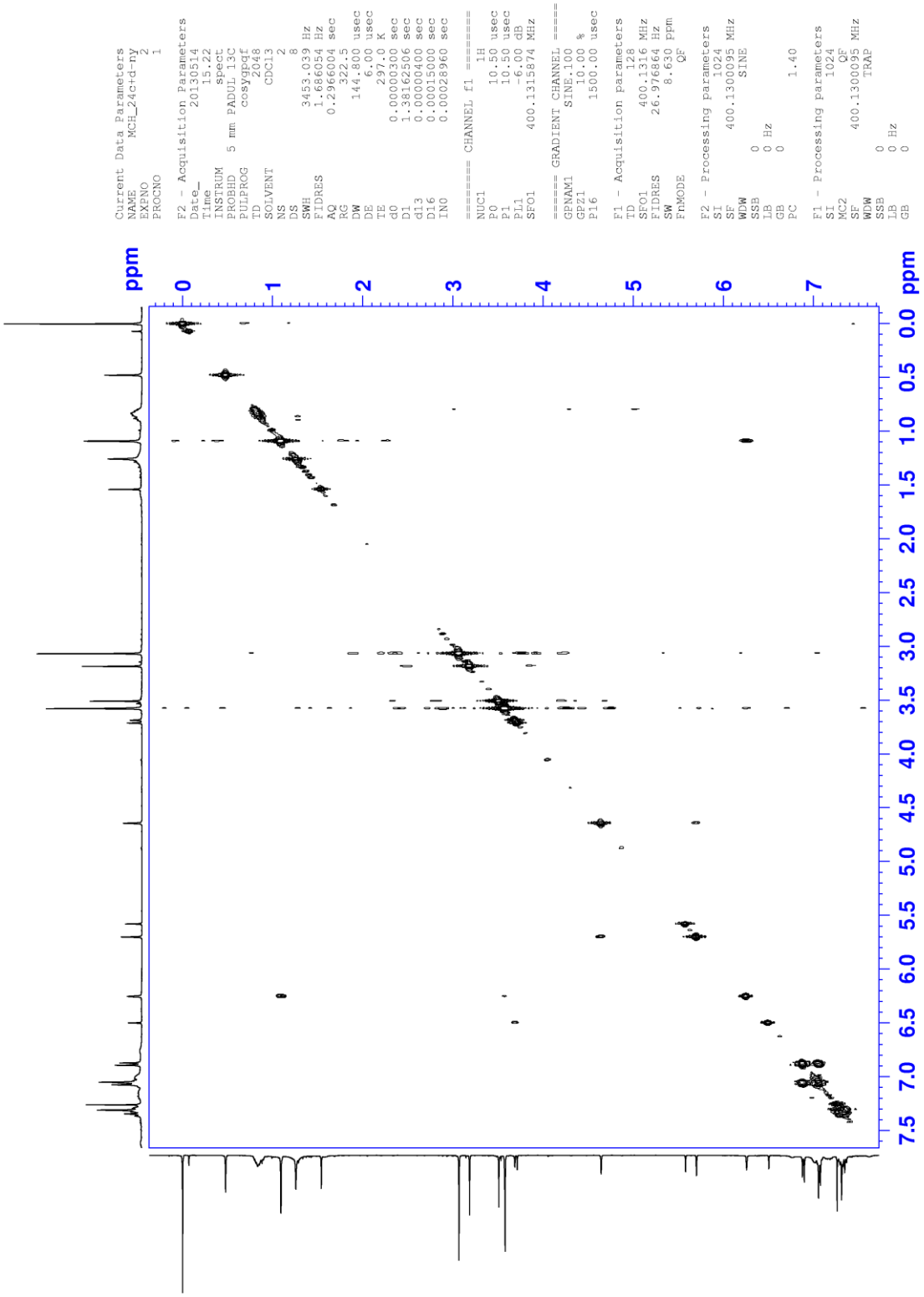

M-5 HMBC of cyclization products **10b-c**

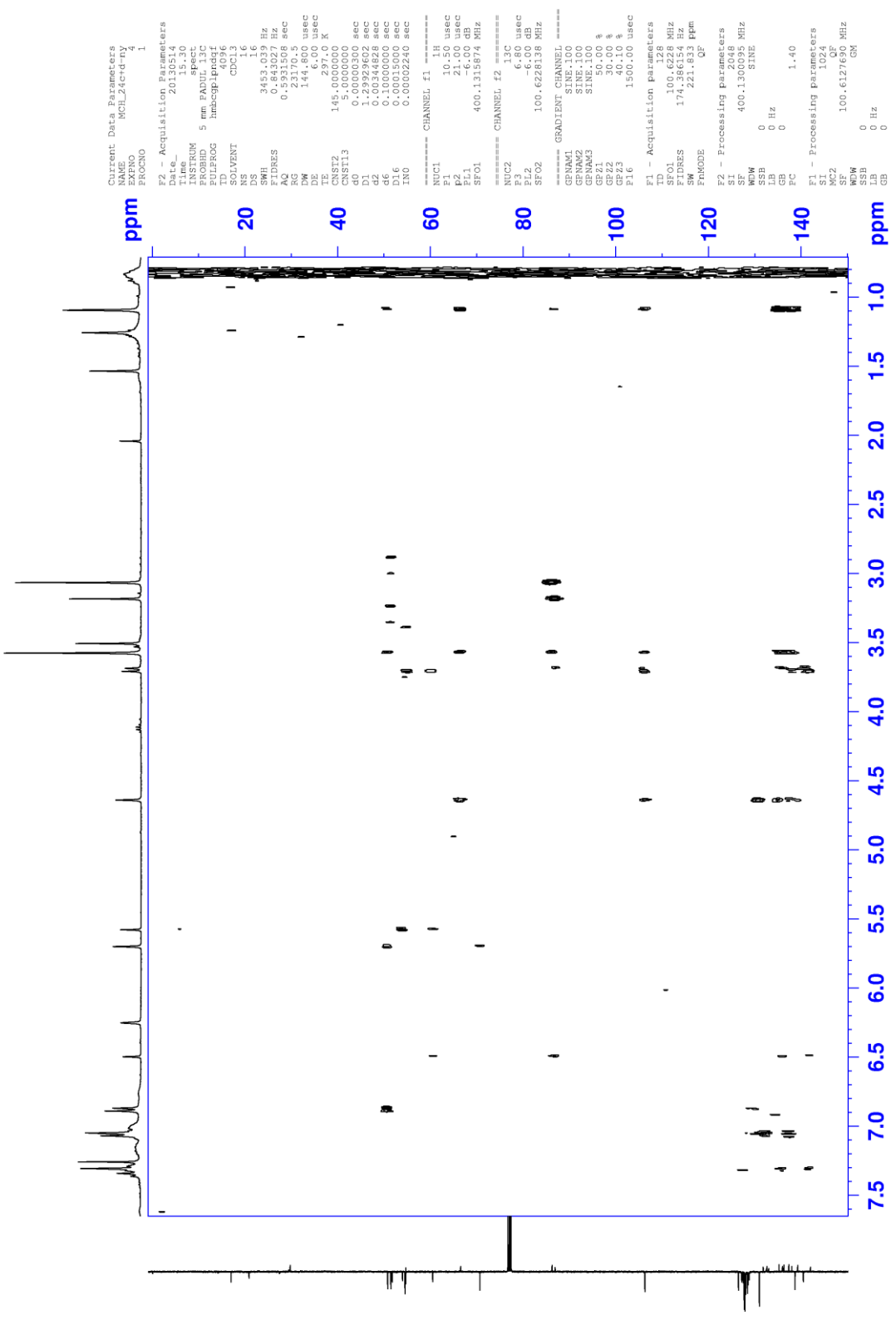

M-6 NOESY of cyclization products **10b-c**

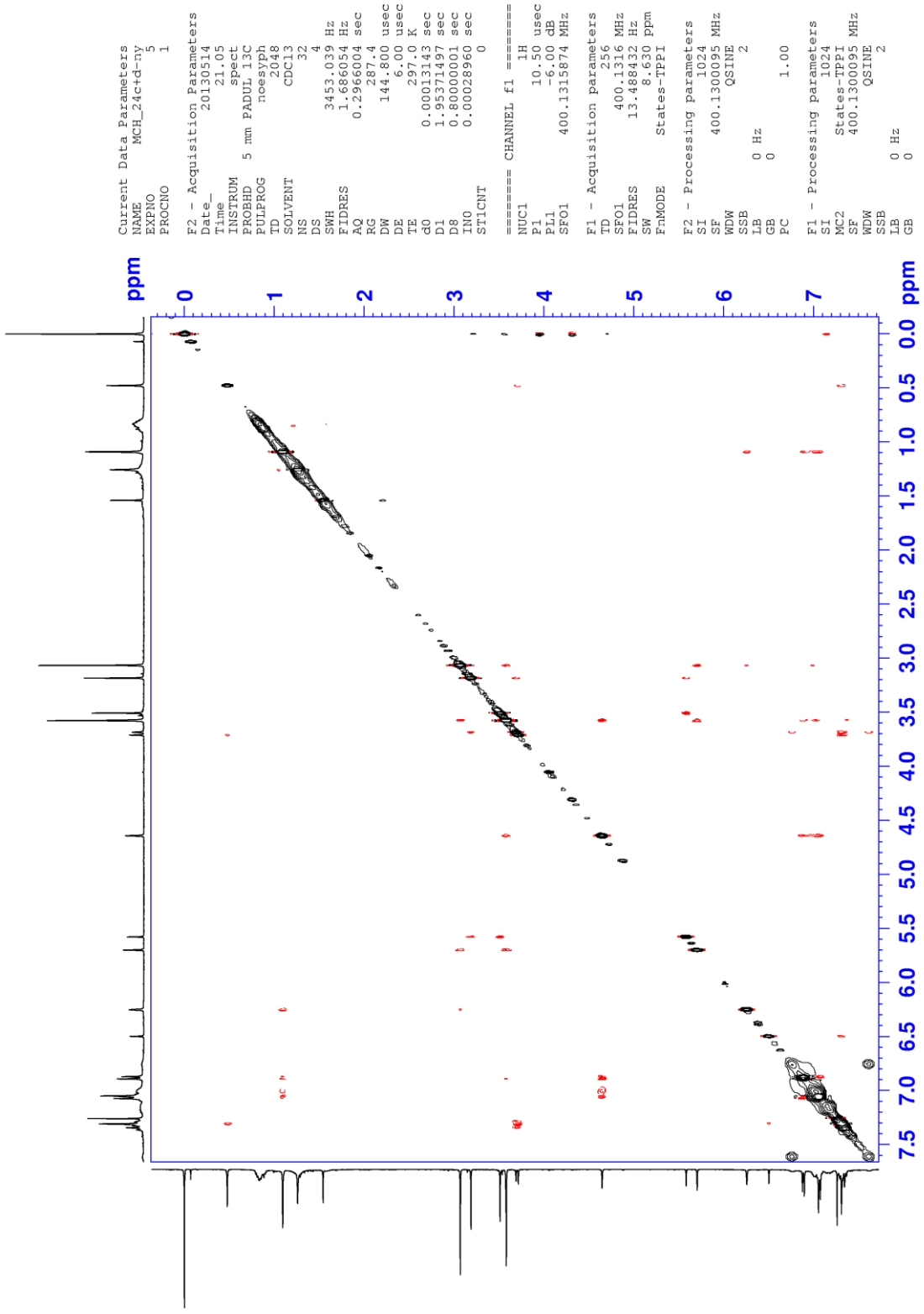

M-7 IR of cyclization products **10b-c**

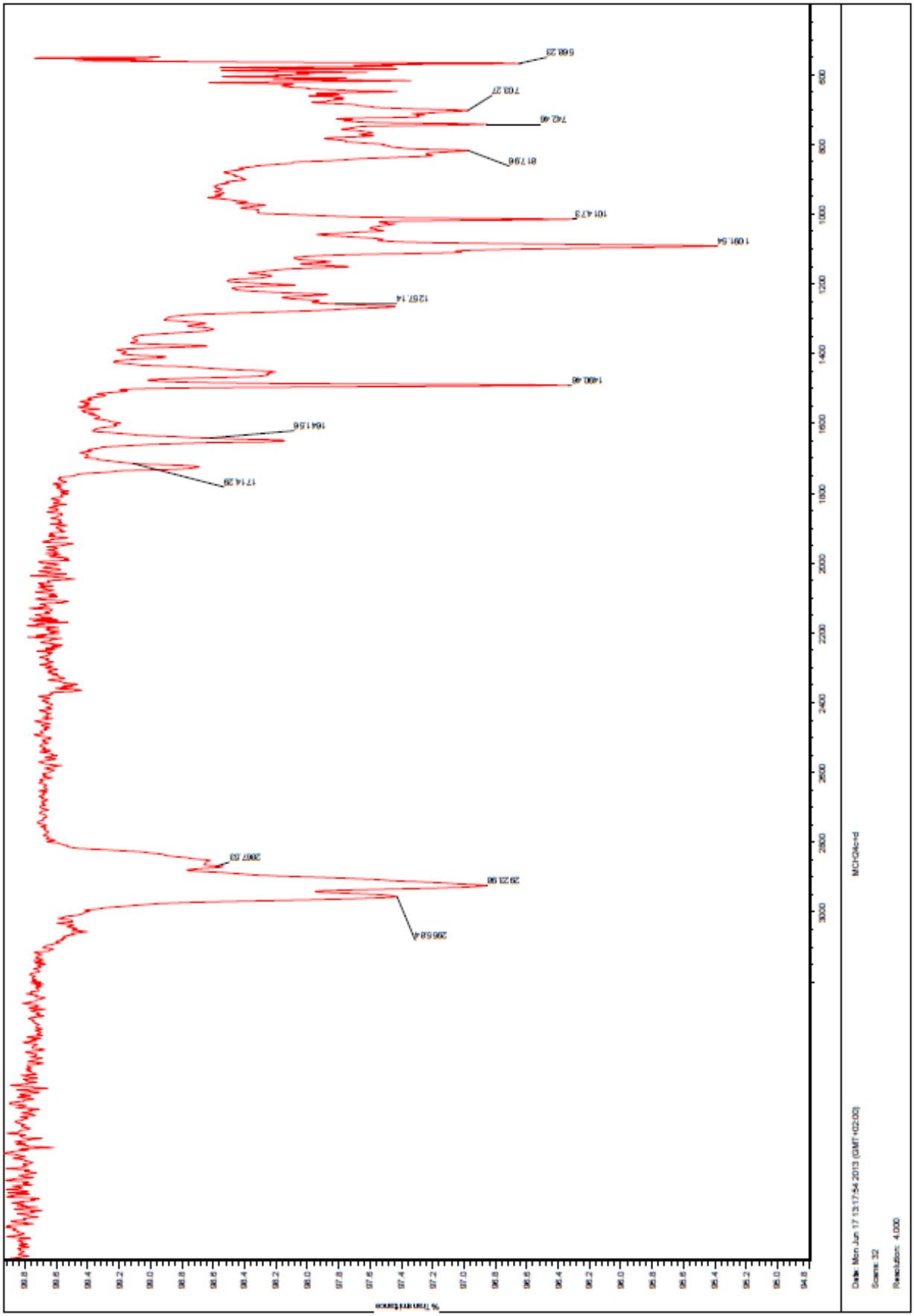

N Cyclization product 10b

N-1 ^{1}H NMR of cyclization product **10b**

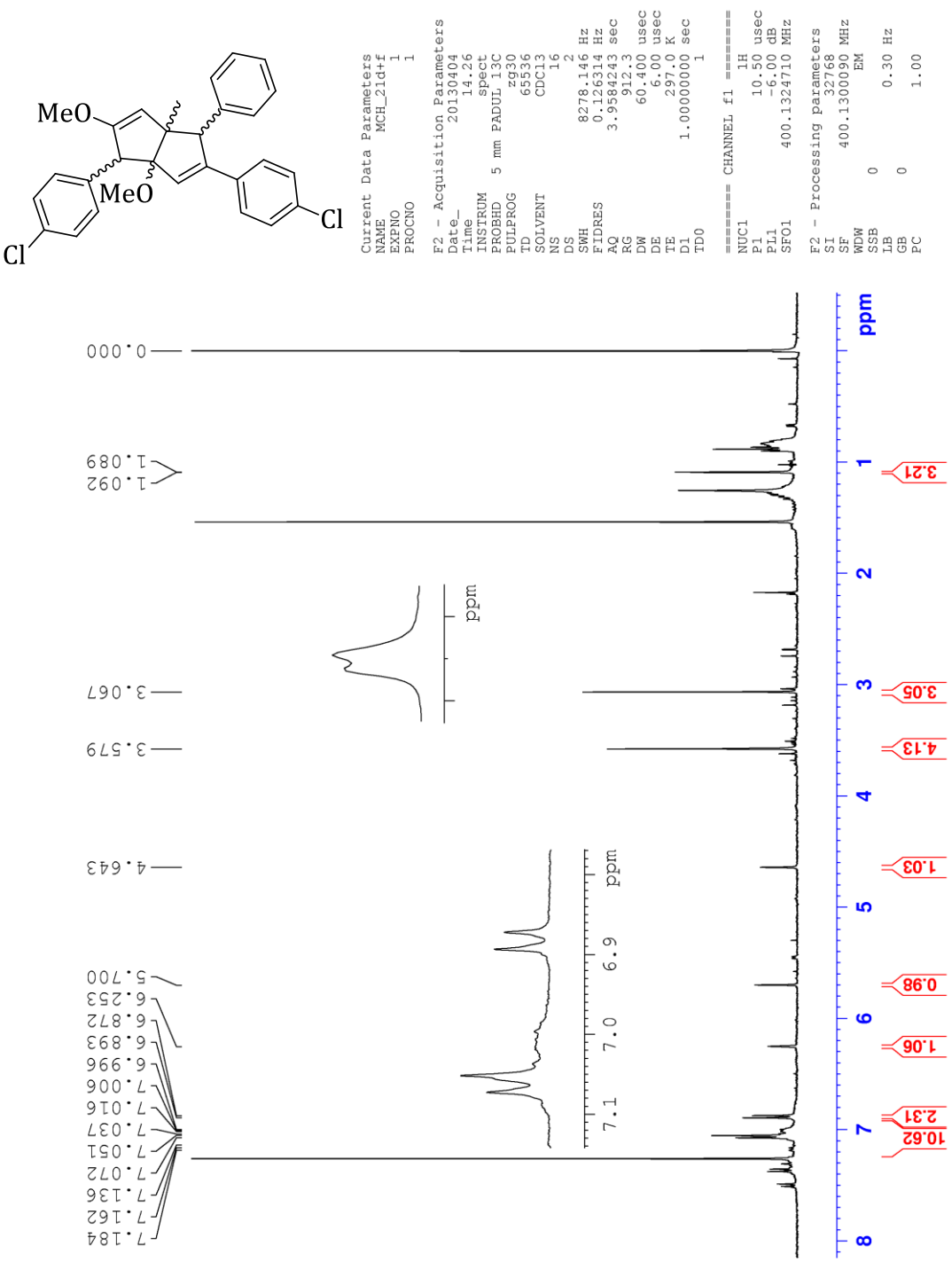

O Cyclization product 10d

O-1 ^{1}H NMR of cyclization product **10d**

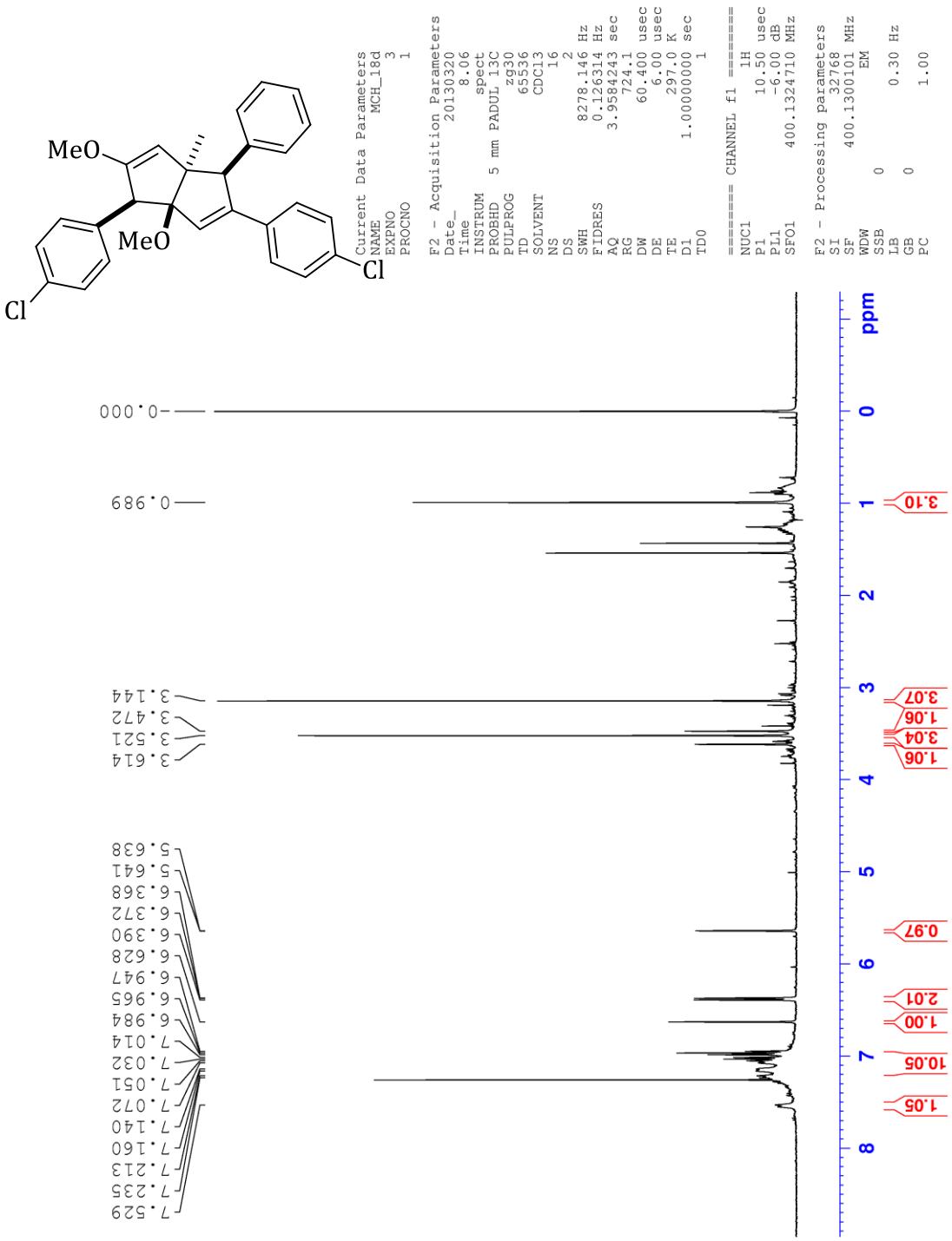

O-2 ^{13}C NMR of cyclization product **10d**

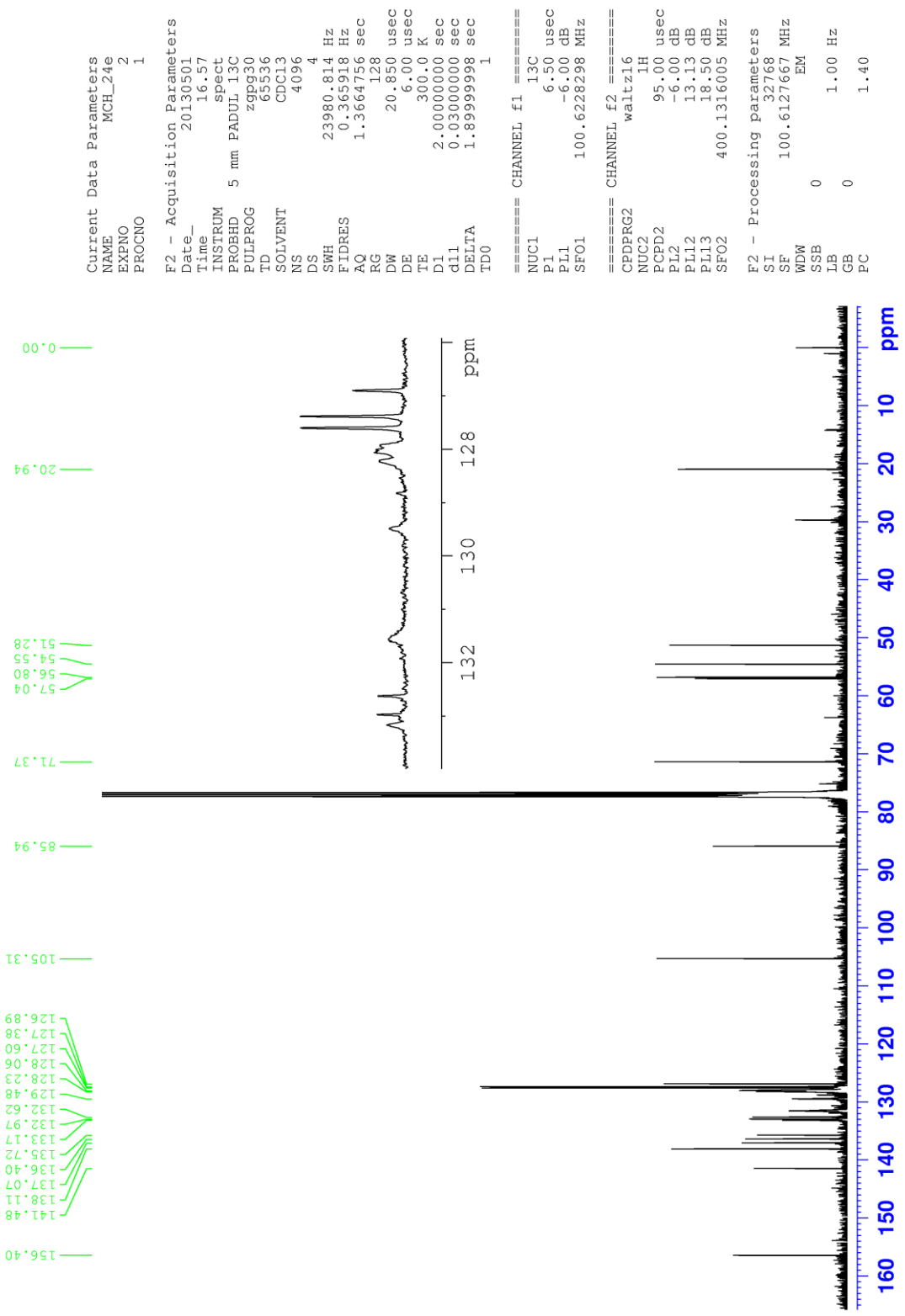

O-3 HSQC of cyclization product **10d**

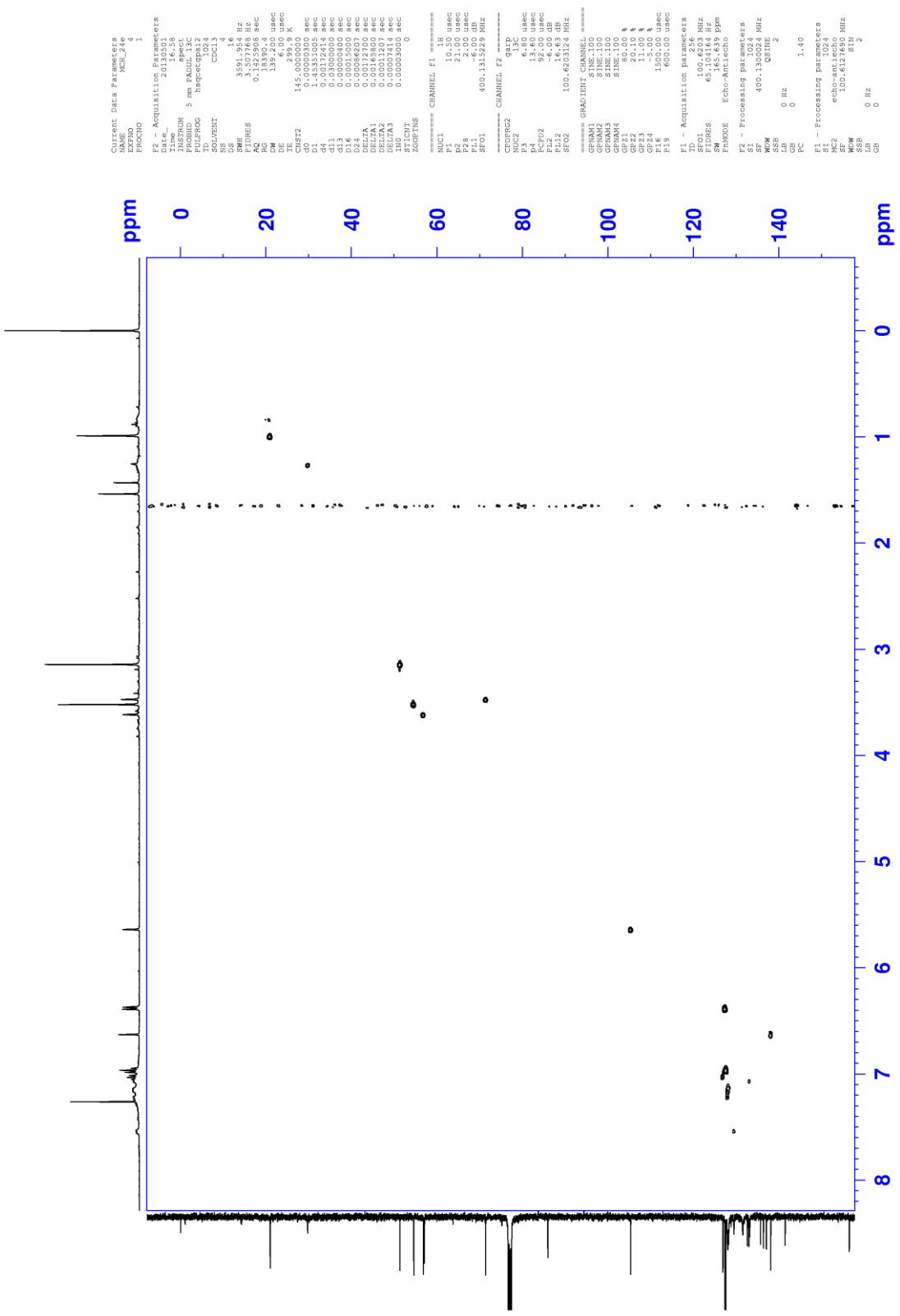

O-4 COSY of cyclization product **10d**

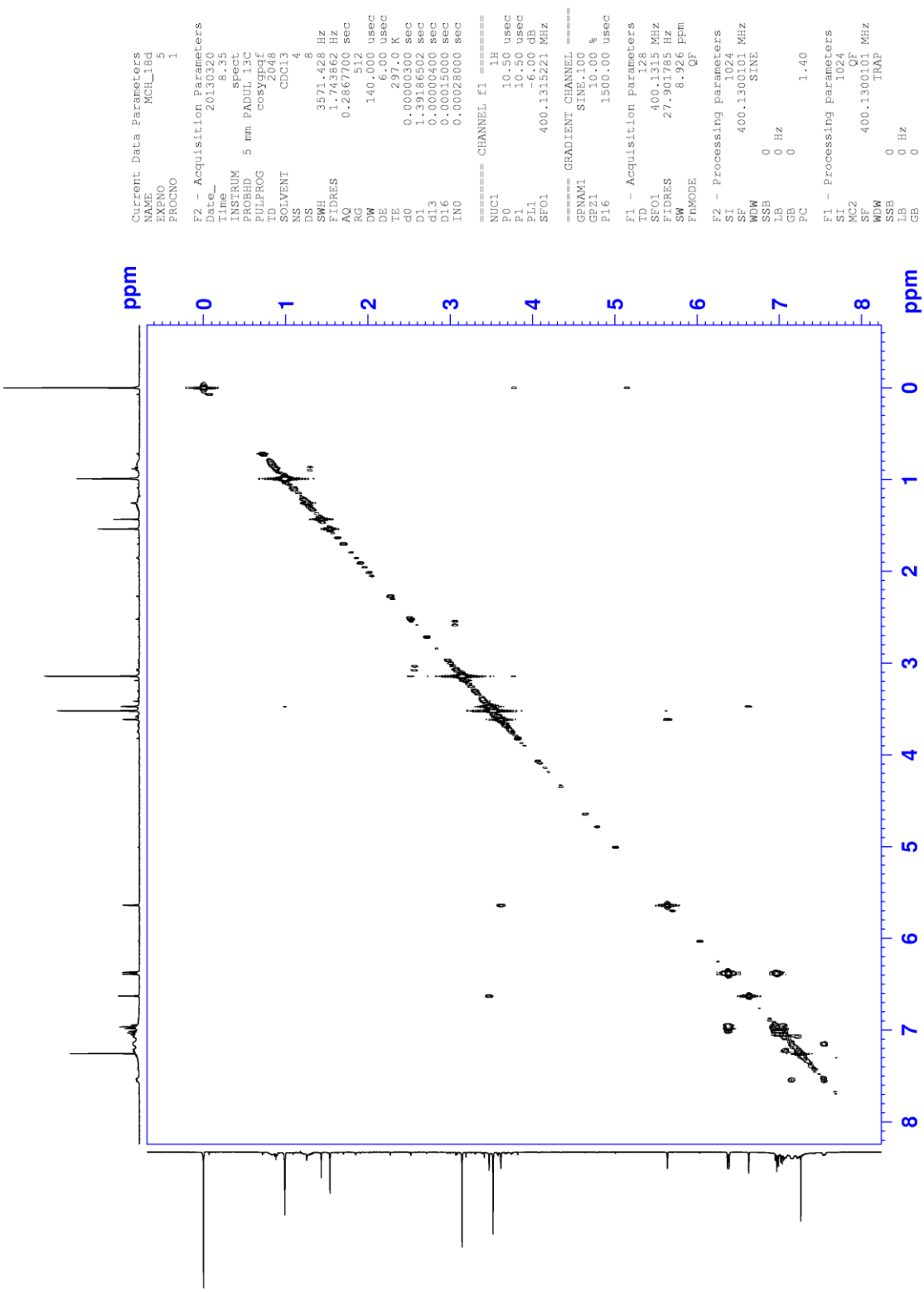

O-5 HMBC of cyclization product **10d**

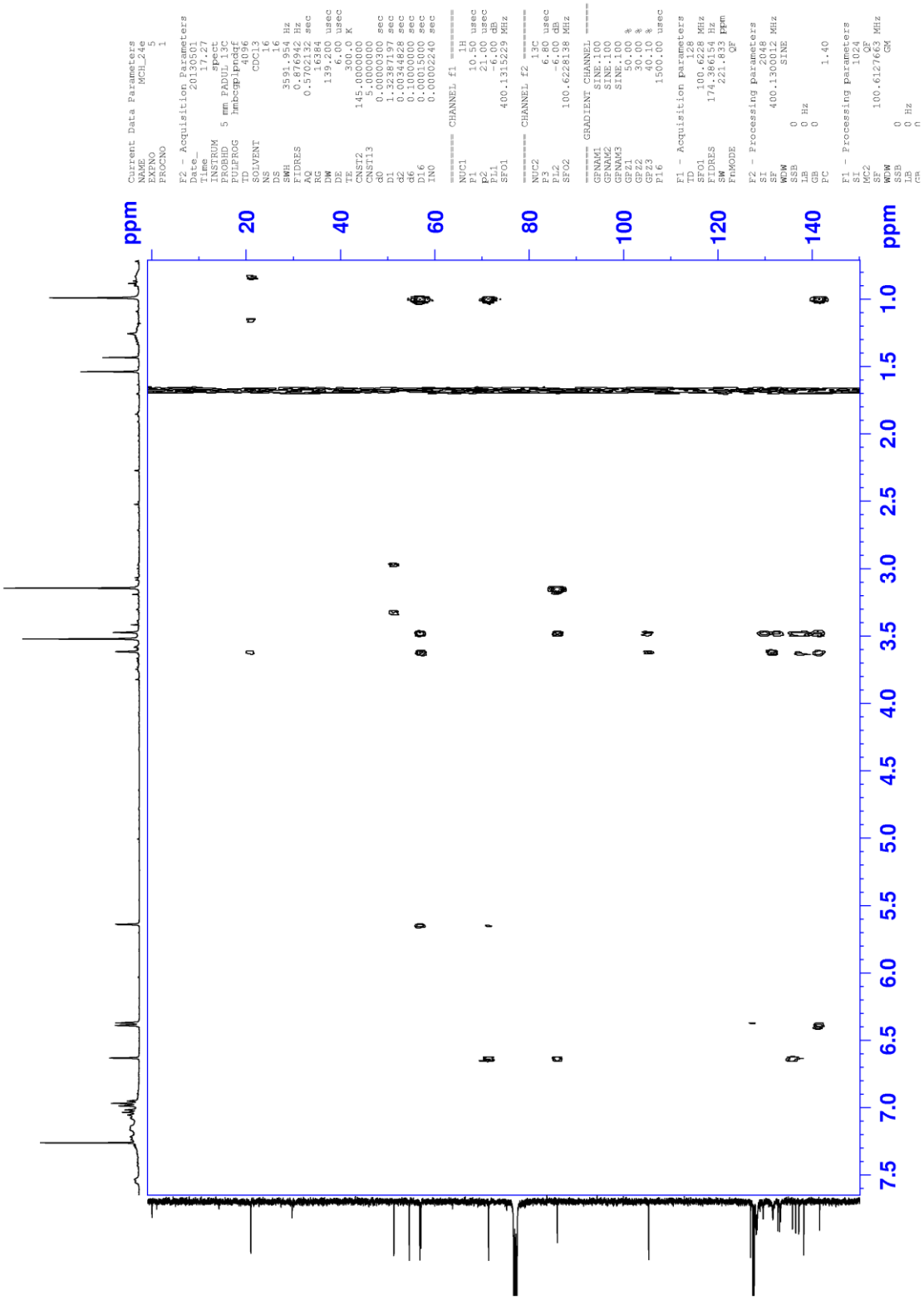

O-6 NOESY of cyclization product **10d**

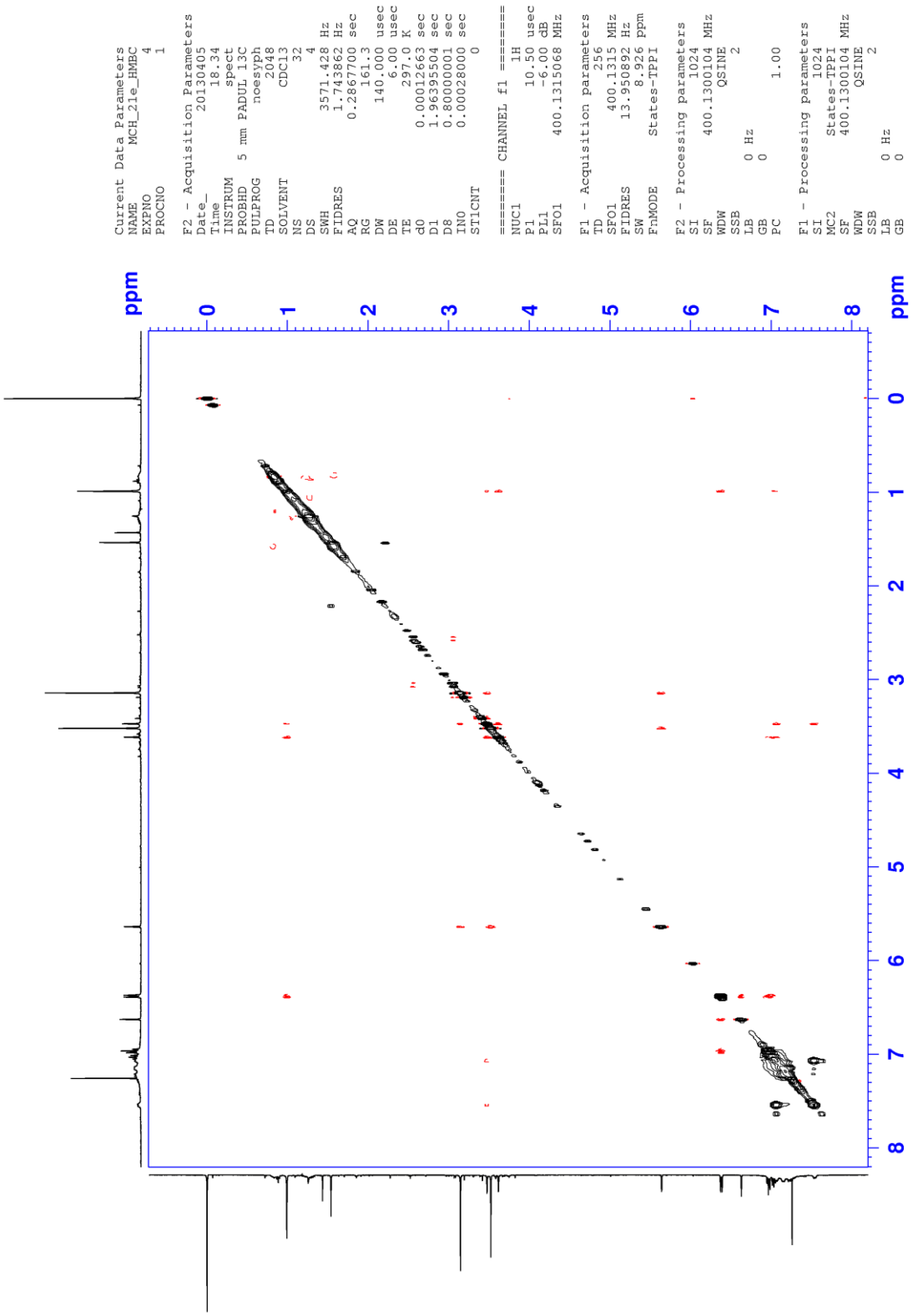

O-7 IR of cyclization product **10d**

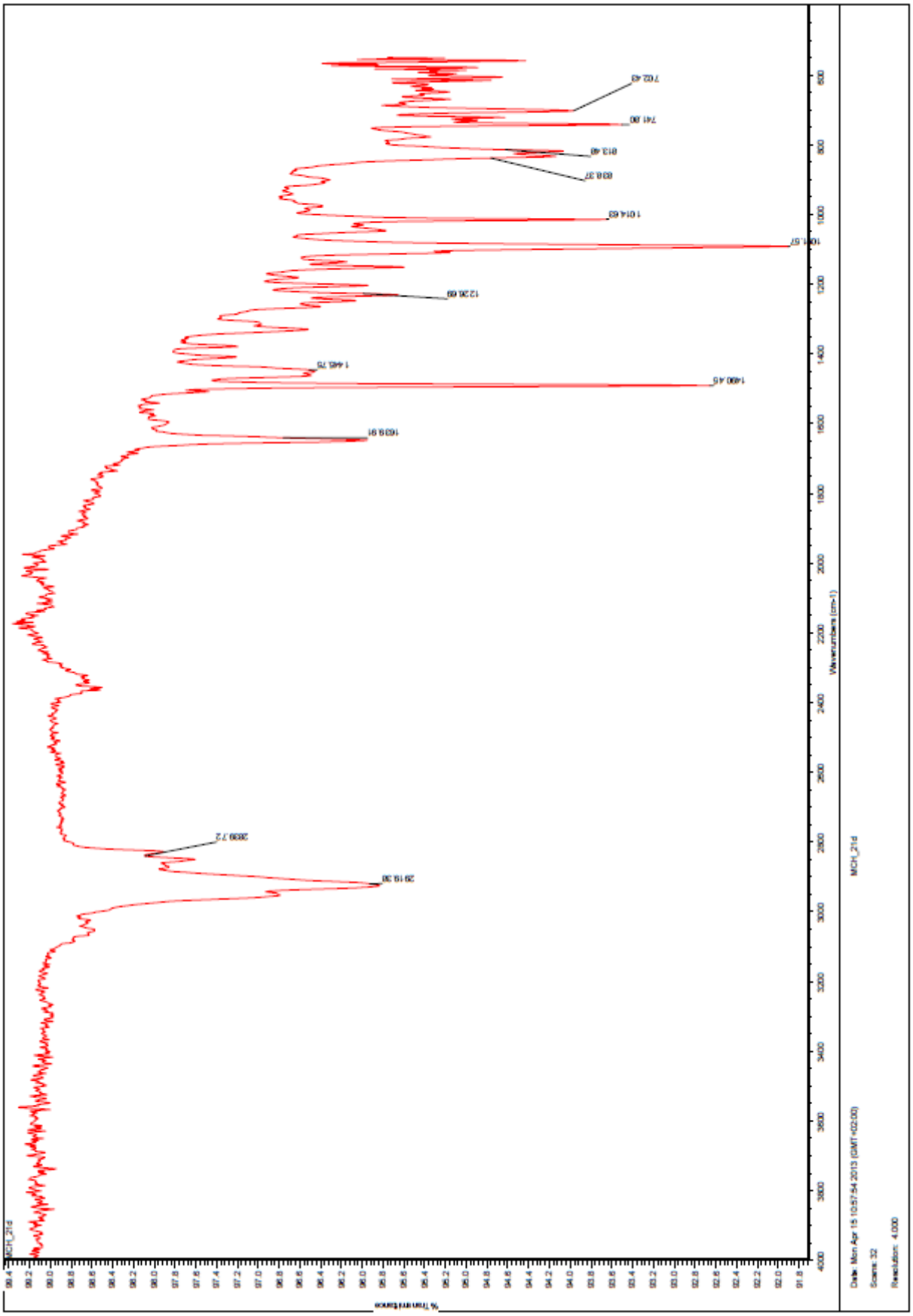

P Propargyl alcohols d-3a1-2

P-1 ^{1}H NMR of propargyl alcohols **d-3a1-2**

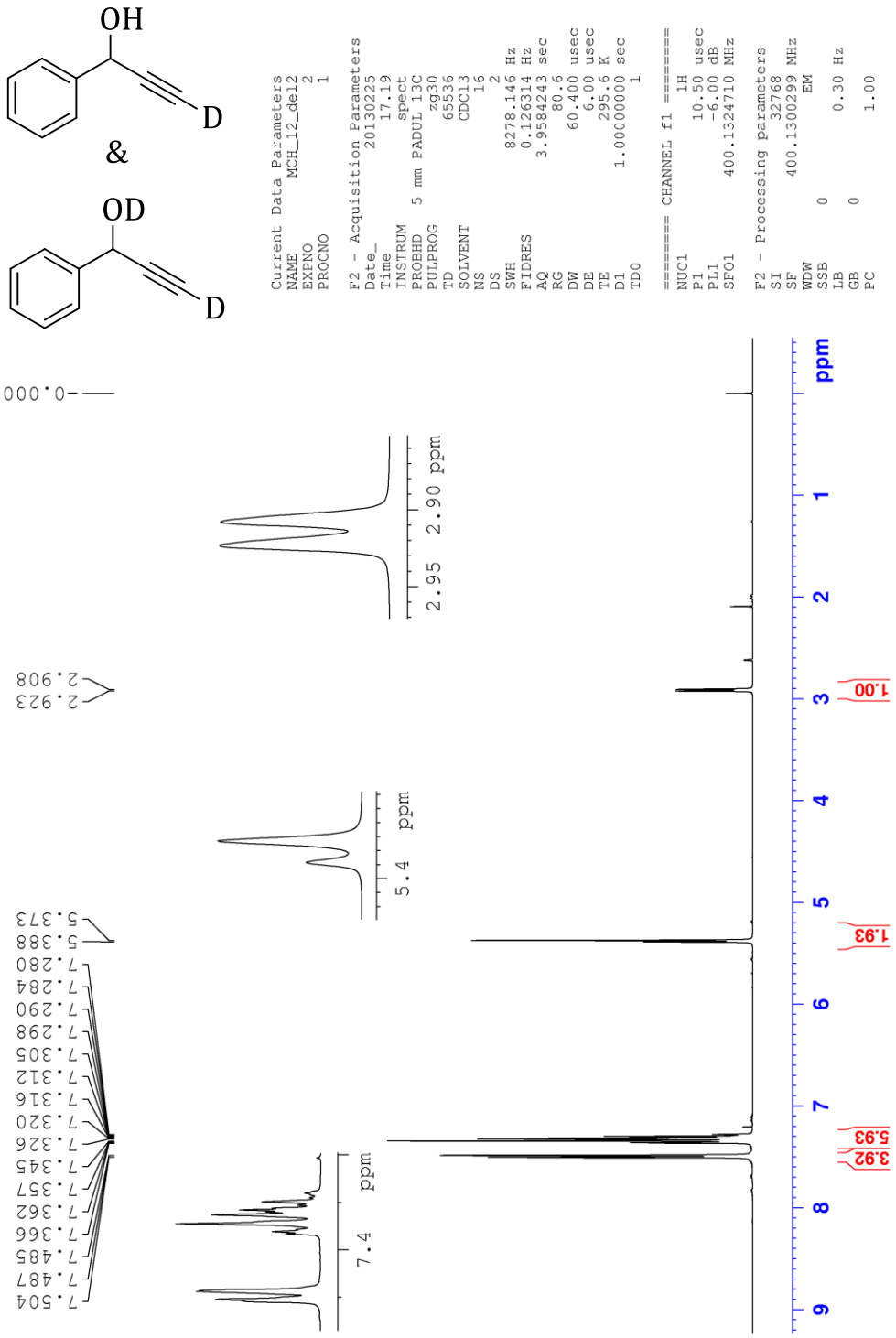

P-2 ^{13}C NMR of propargyl alcohols **d-3a1-2**

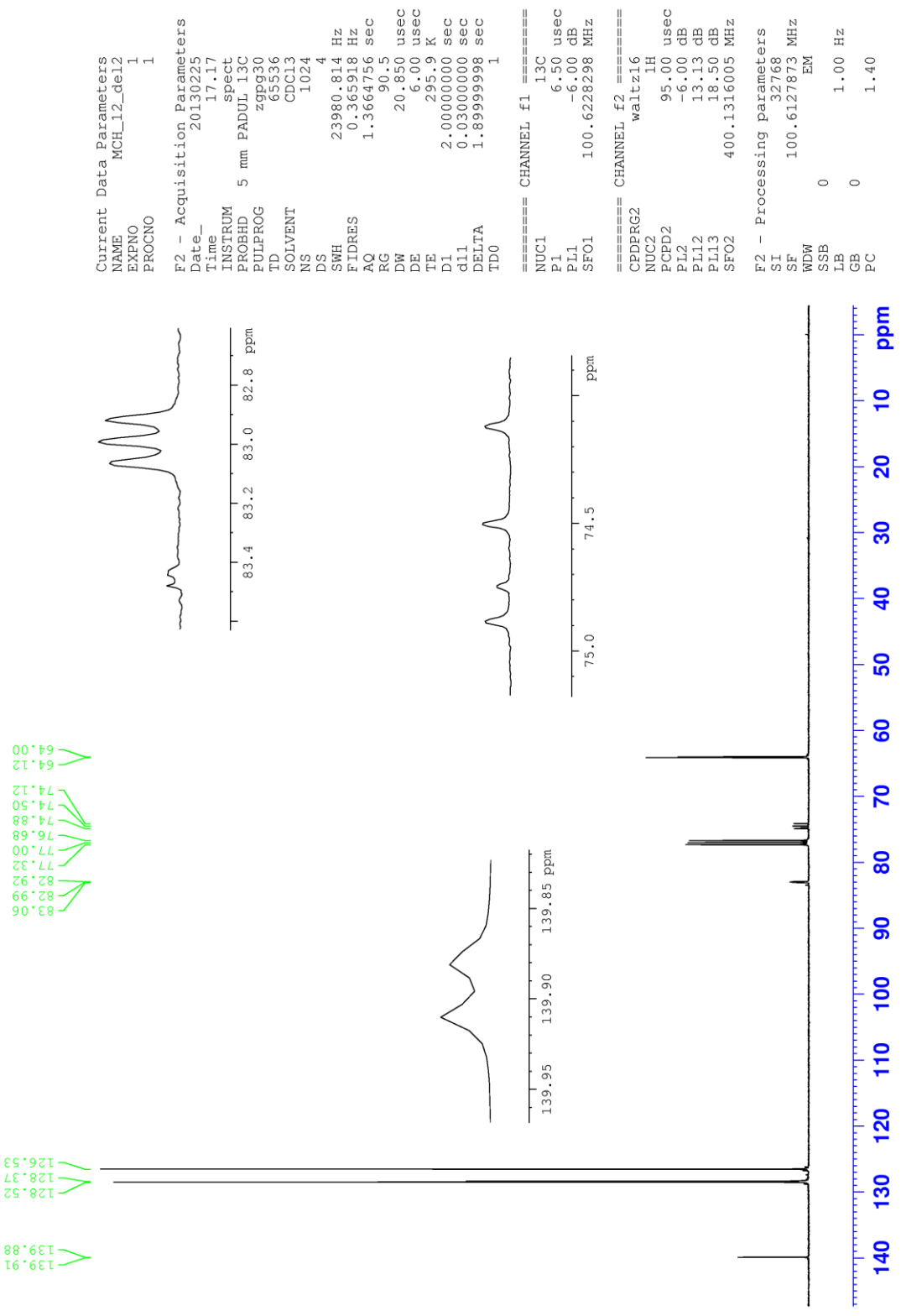

Q Propargyl acetal d-5a

Q-1 ^{1}H NMR of propargyl acetal **d-5a**

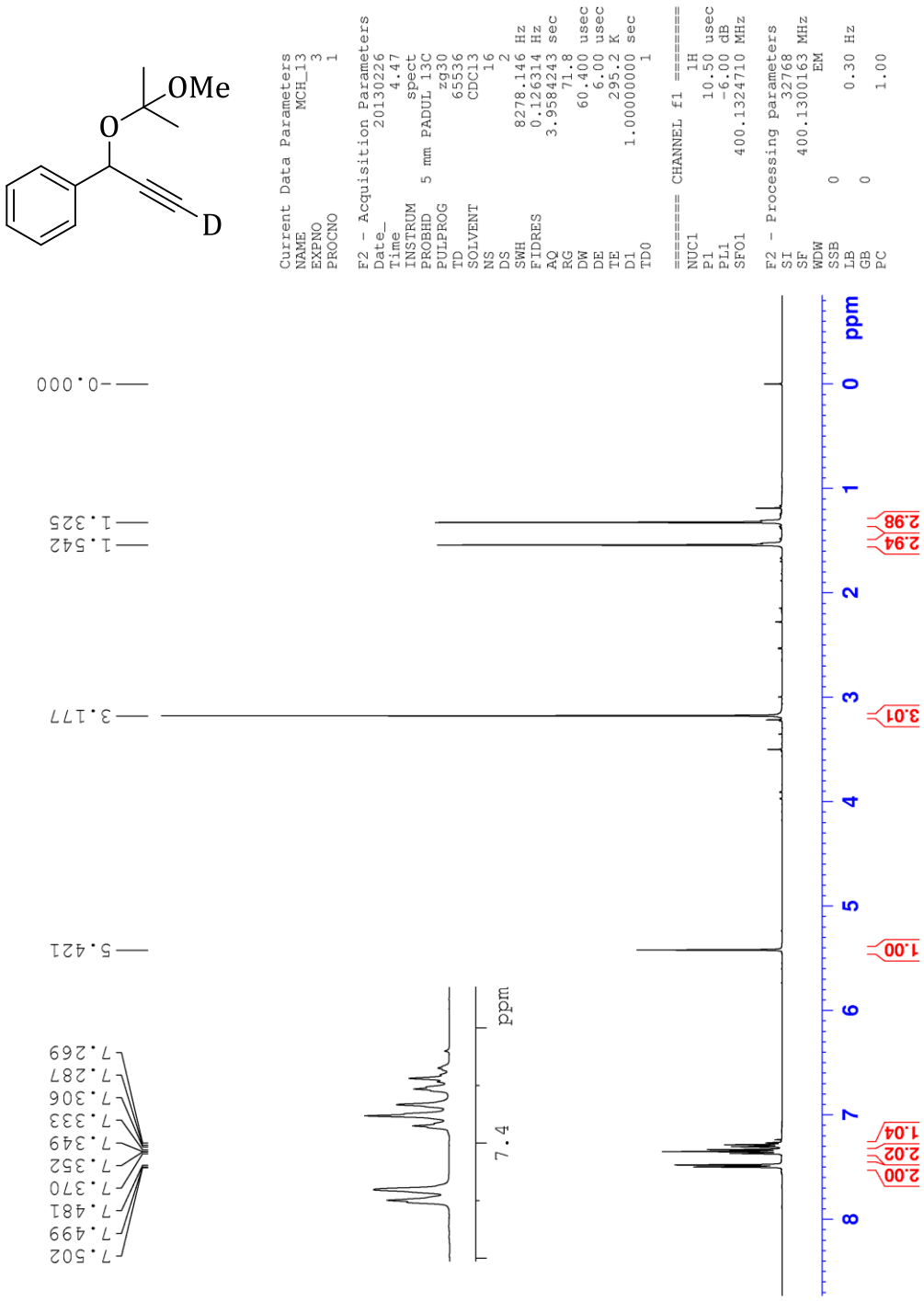

Q-2 ^{13}C NMR of propargyl acetal **d-5a**

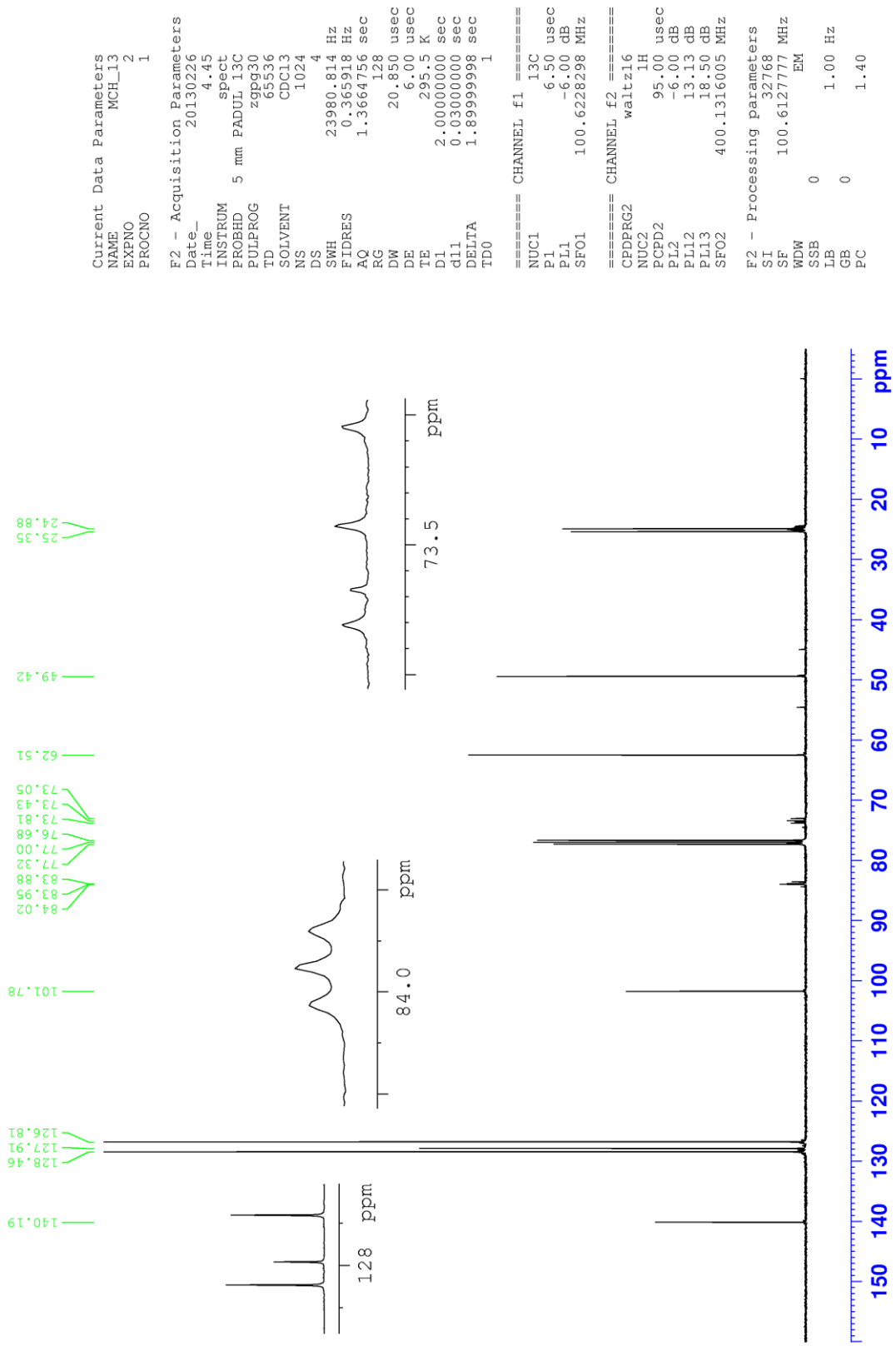

R Deuterated cyclization product d_2-7c

R-1 ^{1}H NMR of deuterated cyclization product **d_2-7c**